Final Report, March 16, 2009
Partially Satisfying Task 6.2

PROPOSAL FOR GRANT ACTIVITIES UNDER THE GRANT UMBRELLA FROM TCEQ TO THE UNIVERSITY OF TEXAS AT AUSTIN

Grant Activities No. 582-5-86245-FY08-01

Effects of Meteorology on Pollutant Trends

Tracking Number: (2008-20)

Prepared by
Dave Sullivan, Ph.D.
The University of Texas at Austin
Center for Energy and Environmental Resources
Building 133, MC R7100, 10100 Burnet Rd., Austin, TX 78758-4445
Phone: 512-471-7805, E-mail: sullivan231@mail.utexas.edu

1. Background

The primary goal of this project is to analyze trends in air pollutants in a manner that will allow an assessment of the effectiveness of emission controls. Pollutant concentrations are known to be random variables that are functions of weather and emissions. Furthermore, "weather" comprises local weather and meso- to synoptic-scale meteorology, which affects pollutant transport, and "emissions" comprises local emissions and distant upwind emissions.

The first phase of this project involved collecting as much data as practical to extend trends from 2007 to as far back in time as 1990, or as far back as practical, in all nonattainment and near nonattainment areas in the state of Texas. These nonattainment and near nonattainment areas include the Houston-Galveston-Brazoria area, the Dallas-Fort Worth area, the Beaumont-Port Arthur area, the Tyler-Longview-Marshall area, the San Antonio area, the Austin area, the Corpus Christi area, and the Victoria area. These data include one-hour ozone, eight-hour averaged ozone, nitrogen oxide (NO), nitrogen dioxide (NO_2), oxides of nitrogen (NO_X), non-methane hydrocarbons (NMHC), carbon monoxide (CO), all air toxics data including benzene, all pertinent and available meteorological data including upper level temperature, sea-level pressure gradients, surface wind speed, surface wind direction, upper level wind speed, and upper level wind direction.

The second phase involves data analysis for trends. Two general approaches are used. First, using a least squares linear regression with appropriate statistical tests, trends for pollutant data in all nonattainment and near nonattainment areas have been analyzed. Complicating this simple approach is the selection of the metrics to track. The report includes discussion of rationale for having selected specific time periods during the ozone season and hours of the day. Second, using more advanced methods, trends have been analyzed taking meteorology into account. For ozone, a generalized linear model (GLM) has been used to remove meteorological influences from the ozone trends. Less sophisticated efforts have been employed for primary pollutants.

Correlation and factor analysis methods have been applied to determine the most important meteorological variables and factors to employ in trend adjustments.

The vast majority of all analyses have been performed with SAS 9.1 software, although R, SPSS, and MS Excel have also been used to a small extent. The HYSPLIT desktop application has been used for back-trajectory generation and analysis. MS MapPoint 2004 and Golden Software Mapviewer 7 were use to create some maps.

2. Outline

The outline of this report is described below. In the electronic version of this document, titles are hot-linked to the appropriate section.

1. Background

2. Outline of report

3. History of this project

4. Data acquisition

5. Selection of trend indicators

6. Ozone (O3) trends
6.1 O_3 ordinary least squares trends
6.2 O_3 meteorologically-adjusted trends
- 6.2.1 Houston-Galveston-Brazoria conceptual model input
- 6.2.2. Assessing transport affecting the Houston region using HYSPLIT back-trajectories alone
- 6.2.3 Factor analysis to assess air-shed delineations
- 6.2.4 GLM development
- 6.2.5 Results

7. Oxides of nitrogen (NOx) trends
7.1 NO_x ordinary least squares trends

8. Carbon monoxide trends
8.1 CO ordinary least squares trends

9. Sulfur dioxide (SO_2) trends
9.1 SO_2 ordinary least squares trends

10. Hydrocarbon (HC) species trends (highly reactive volatile organic compounds (HRVOC), benzene, toluene, ethyl benzene, xylenes (BTEX) compounds, and significant alkane compounds)

10.1 HC ordinary least squares trends
10.2 HC meteorologically-adjusted trends

11. PM2.5 trends

12. Summary

3. History of This Project

June 2008 Monthly Report 1

- Acquisition of upper air dataset.
- Assessing ozone monitoring site longevity.
- Factor analysis to assess air shed delineations using data 1995-2007.

Conclusions: 63 EPA Regions 6 ozone sites have at least 12 years of data ending in 2007. If sites moved a short distance and reassigned a new AQS identity have their data combined with the older site, then 81 sites representing 43 counties have at least 12 years of data ending in 2007. Using the long time series of data, a multivariate analysis of ozone across Region 6 during summers from 1995 – 2007 reveals six geographical region factors.

An upper air meteorological dataset called METDAT was acquired. Several unit conversions were required on a year by year basis, as not all annual files had the same formats and data conventions.

July 2008 Monthly Report 2

- Assignments given to graduate student assistant.
- Revised Factor analysis to assess air-shed delineations using data 2005 – 2007.
- Some initial trend analysis.

Conclusions: Using more recent data (2005 – 2007) allowing more ozone sites representing 71 counties for analysis, a revised factor analysis for regional ozone patterns reveals seven regional factors.

August 2008 Monthly Report 3

- Detailed seasonality modeling for one site (AIRS=482010024, Houston Aldine).
- Correlation analysis of ozone with surface upper air meteorological data.
- EPA Region 6 trend analysis for ozone.

Conclusions: Ordinary least squares (OLS) regression of the average daily maximum 8-hour ozone averages (oz8hrpk) at the Aldine CAMS 8 site versus time shows a statistically significant downward slope in this measure from 1990 through 2007. There is evidence of a possible step down in concentrations beginning in 2001. A variety of SAS tools for transforming the variable and measuring the trend, the magnitude of seasonal effects, and the nature of the residual time series, found to be autoregressive order 1 (AR(1)), were used.

Correlations of the natural logarithm of oz8hrpk for 65 sites with 10 years of data with the METDAT variables reveals patterns of correlation of ozone with meteorological variables related to the seven factors derived in the July report.

An ordinary least squares regression of late summer (August – September) mean oz8hrpk shows 86 out of 97 sites show negative slopes, and Harris County sites have the largest decline. West Texas and New Mexico sites show positive trends.

September 2008 Monthly Report 4

- EPA trend analysis Web pages.
- Synoptic scale winds and regional trends.

Conclusions: An EPA Web site contains much of the information requested in this project, but with much less detail, at www.epa.gov/airtrends.

A regional East Texas trend analysis based on counting monitor-days with oz8hrpk >= 75 parts per billion (ppb) concentration for August – September, 1997 – 2007, using a fixed set of monitors with continuous data shows a significant downward trend. Severity of the ozone levels for August and September by year was qualitatively shown to be associated with the frequency of synoptic scales winds from northeast or from stagnant local wind patterns.

October 2008 Monthly Report 5

- EPA trend analysis Web pages and new ozone trend results.
- Some early generalized liner model (GLM) regression results.

Conclusions: A problem with the EPA trends at www.epa.gov/airtrends was identified. The research did not account for the changes in the number of ozone monitoring sites in metropolitan areas over time, which TCEQ has found to be a significant factor in trends. Using the core based statistical area (CBSA) geographic classifications used by EPA, a comparison of monthly average daily area maximum oz8hrpk using all sites versus only using sites with long-running data shows the selection of sites affects results in ordinary least squares regressions.

Using SAS generalized linear model (GLM) procedure to regress ln(oz8hrpk) from Aldine CAMS 8 on METDAT data from Bush International Airport shows a statistically significant relationship with a "pseudo-R^2" value of 81.6 percent.

November 2008 Monthly Report 6

- Discussion of choices in SAS for trend approaches
- Data quality assurance and HYSPLIT back-trajectories

Conclusions: It is not a trivial task converting the R code used by EPA researchers for met-adjusted trends to SAS code.
Missing values for some HYSPLIT back trajectory variables in METDAT were coded as "999" and this may have affected some earlier correlation and regression results, but this was found to have been only a minor issue.

December 2008 Draft Final Report and January 2009 Revised Draft Final Report

- Data acquisition summary
- Selection of trend indicators
- Revised O_3 ordinary least squares trends
- O_3 meteorologically-adjusted trends (correlation analysis)
- Revised NO, NO_2, NO_x ordinary least squares trends
- CO ordinary least squares trends
- SO_2 ordinary least squares trends
- Revised hydrocarbon (HC) species trends
- Initial discussion of meteorologically-adjusted trends for hydrocarbons (correlation analysis)

Conclusions: Combining data from several urban sites with similar diurnal pattern for oxides of nitrogen (NO_x), carbon monoxide (CO), and hydrocarbons (HC) led to the selection of hours 5 – 8 CST (5:00 – 8:59 am CST) to average measurements for a variable to represent a daily variable for these parameters. The study of diurnal patterns for sulfur dioxide (SO_2) was less definitive, so the daily one-hour maximum (so21hrpk) and daily average (so21hrav) were selected to represent daily variable. The daily variables were averaged across each year for each monitor with at least 10 years of data between 1990 and 2007 (1995-2007 for HCs). The independent variable in the OLS analysis was the number of years since 1990 (x = 0 … 17).

- All Houston area sites except Galveston CAMS 34 have negative slopes for NO, NO_2 and NO_x. Of the 24 regressions on NO_x, 17 were significant at p=0.05. Results from non-Houston area sites were graphed, but were not summarized for statistical significance at this point.
- For CO, of 17 sites around the state, only the Deer Park site is not statistically significant for a downward trend at a 0.05 level, but it is close (p=0.06).
- For SO_2, for 16 sites across the state, two variables per site, all had downward slopes, and 24 of 32 trends were significant at p=0.05 for downward trends.
- For HCs, the large majority of variables have downward slopes at the four sites with auto-GC data, but these were not summarized for statistical significance at this point.

4. Data Acquisition

An instance of the MOTHER data mart is in our possession. MOTHER includes surface meteorological and pollution data from 1972 – 2007 for EPA Region 6 states. We also have received a set of files from Mr. Erik Gribbin containing SAS data sets of aggregated national meteorological data from 1995 – 2007 from the Omnibus Meteorological Database[1] (METDAT). These data sets contain surface and upper air data, including summarized 24-hour HYSPLIT[2] back-trajectories.

The METDAT data come in files for individual calendar years. The data were provided in two different formats, and the files have been combined in a uniform format and filtered to include data for monitoring sites in EPA Region 6. SAS code is provided in Appendix 2 and as a separate electronic attachment (metdat.sas).

The METDAT SAS code sets up the data in three temporary files for manageability. The data for 2005 - 2007 are a slightly different format from earlier years' data. These three more recent yearly files

- contain quality control (QC) data,
- use different variable names for mixing height rate of change and for water vapor level,
- have different "date" information and formats, and
- have temperature values in K degrees instead of F.

The data are standardized by removing QC data, converting K to F, and by reformatting the date variable in the 2005-2007 data files, and by renaming two meteorological variables and dropping some unused date variables in the 1995-2004 data files.

The data set provided by Mr. Gribbin also includes location data for meteorological monitors. The data describing the monitoring locations within EPA Region 6 is imported in the SAS program and the key location data are merged with the combined meteorological data file. The resulting file can now be merged with a dataset containing ambient pollution data based on date and proximity (using a nearest neighbor method described below).

---

[1] See http://www.epa.gov/scram001/meteorology/omnibus_meteorological_data_set.pdf. Accessed March 2009.
[2] Draxler, R.R. and Rolph, G.D., 2003. HYSPLIT (HYbrid Single-Particle Lagrangian Integrated Trajectory) Model access via NOAA ARL READY Website (http://www.arl.noaa.gov/ready/hysplit4.html). NOAA Air Resources Laboratory, Silver Spring, MD.

Rolph, G.D., 2003. Real-time Environmental Applications and Display sYstem (READY) Website (http://www.arl.noaa.gov/ready/hysplit4.html). NOAA Air Resources Laboratory, Silver Spring, MD.

Table 4.1 Types of METDAT data elements

Morning and Afternoon average fractional cloud cover (tenths)
Average and maximum dew point temperature
Morning (~1200 UTC) 925 mb-surface temperature difference
Morning Height of 500 mb and 700mb surface (m)
Maximum mixing height (m)
Maximum water vapor mixing ratio
Rain, haze, relative humidity
Morning temperature at 700, 850, 925 mb
Average, minimum, maximum apparent temperature
Max temperature, morning, afternoon temperature, delta temperature
Transport distance, direction, u,v-components
Morning, afternoon, daily wind speed, direction, u,v -components

5. Selection of trend indicators

In Camalier et al.[3] the trend indicator for ozone is the annual average of the daily maximum urban-area eight-hour maxima. In our approach months May through October are used for meteorologically adjusted trends, in contrast to Camalier et al.'s use of May through September. Ozone issues in Texas persist later in the year than in northern states. In order to show the seasonality of ozone, ordinary least squares regression trends were run both on daily data, which have auto-correlation issues that degrade the quality of statistical tests, and on annual means.

For NO_x, CO, and hydrocarbons, the median diurnal patterns of the species data were examined to select a three or four hour period in the morning with the highest median concentrations. For NO_x, trends were run for nitric oxide (NO), nitrogen dioxide (NO_2), and total oxides of nitrogen (NO_x). For hydrocarbons, subsets were used from the following classes: highly reactive volatile organic species (ethylene, propylene, 1-butene), aromatics (benzene, toluene, ethyl benzene, o-xylene, m/p-xylene), and prominent alkanes (n-butane, isobutene, n-pentane, iso-pentane). For Sulfur dioxide (SO_2), an examination of diurnal patterns across the state failed to reveal a common diurnal pattern as was the case with other pollutants. SO_2 is principally a pollutant associated with coal burning, and in industrial areas to fugitive emissions from the sulfur removal process from feed stocks. Because of its lack of regular diurnal pattern, SO_2 trends were run on both daily 1-hour maxima and daily 24-hour averages.

A series of 72-hour HYSPLIT back-trajectories have been run from central Houston for all days with available data from May through October 1999 – 2007. The starting time was noon CST and from an altitude of 300 meters. A successful cluster analysis using HYSPLIT has also been run, showing six clusters. A preliminary examination shows the clusters are very similar to those run for two previous projects, centered in central eastern Texas. This corroboration suggests a robustness in the cluster analysis method over the East Texas area. These clusters have been

[3] Camalier, L., Cox, W., Dolwick, P., 2007. The effects of meteorology on ozone in urban areas and their use in assessing ozone trends. Atmospheric Environment 41, 7127-7137.

separately assessed as one form of meteorologically adjusted trend for ozone in support of Conceptual Model development in support of the SIP update.

6. Ozone Trends

6.1 Ordinary Least Squares Trends for Ozone

Below in Figures 6.1 – 6.8 we present comparisons between trends based on the 30-day moving average of daily ozone eight-hour maxima by CBSA using only the subset of monitors with nearly-continuous data during the period of study. The moving average time series are not appropriate for ordinary least squares (OLS) regression owing to the clear periodicity in the data and the high level of auto-correlations between observations. Nevertheless we have fit linear regression lines to the data for the purpose of showing simple qualitative trends plus the seasonal patterns. Below each graph we list the AQS site numbers used in the regression and the p-value for the regression, which may only serve as a rough guide for statistical significance. Special attention was given to only use monitors that had nearly continuous data collection over the 1990 – 2007 period. The importance of taking this approach rather than using all available monitoring data is that we have shown in the past that the number of monitors active in a monitoring network affects the extreme value statistics such as maximum observed value and number of ozone exceedance days.[4]

Figure 6.1 Austin 8-hr max 30-day moving average with regression line using only long-running sites' data

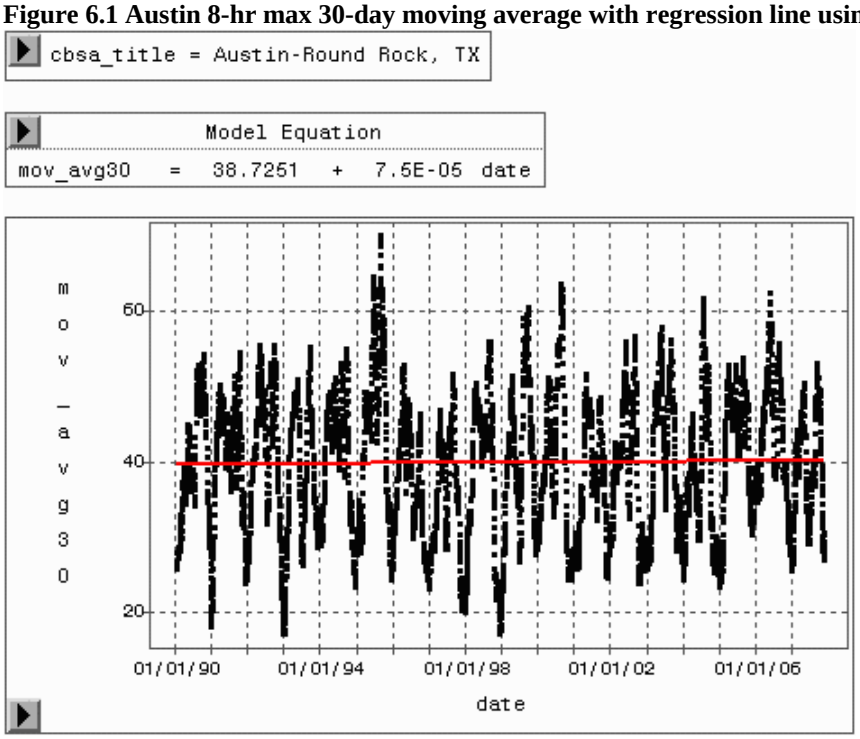

Sites used: 484530014; p = 0.22

[4] D.W. Sullivan and Z. Fang, "Design Value as a Preferred Indicator over Exceedance Day Counts," TCEQ Trade Fair, 2004.

Figure 6.2 BPA 8-hr max 30-day moving average with regression line using only long-running sites' data

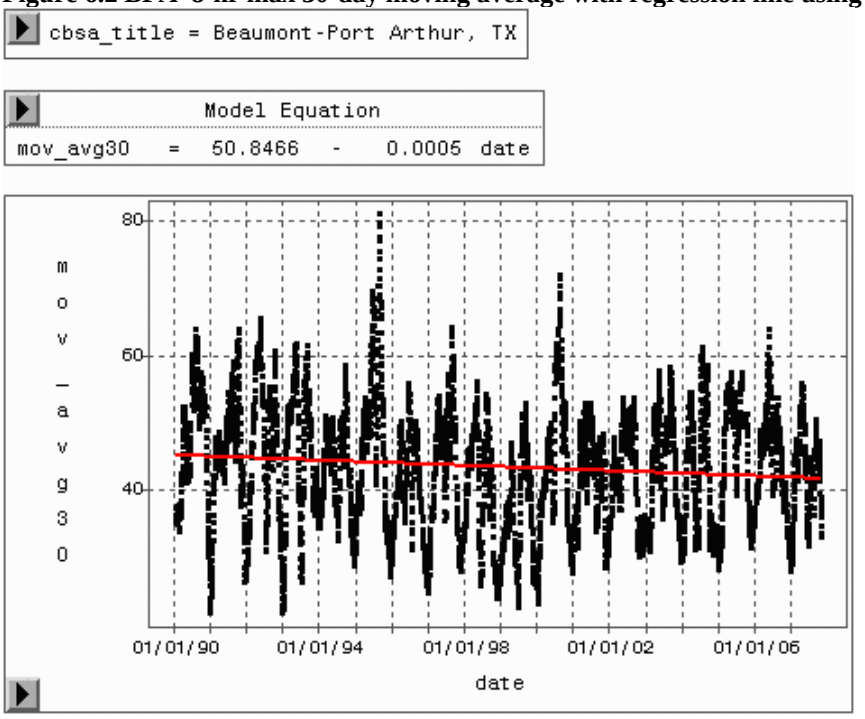

Sites used: 482450009, 482450011, 483611001; $p < 0.0001$

Figure 6.3 DFW 8-hr max 30-day moving average with regression line using only long-running sites' data

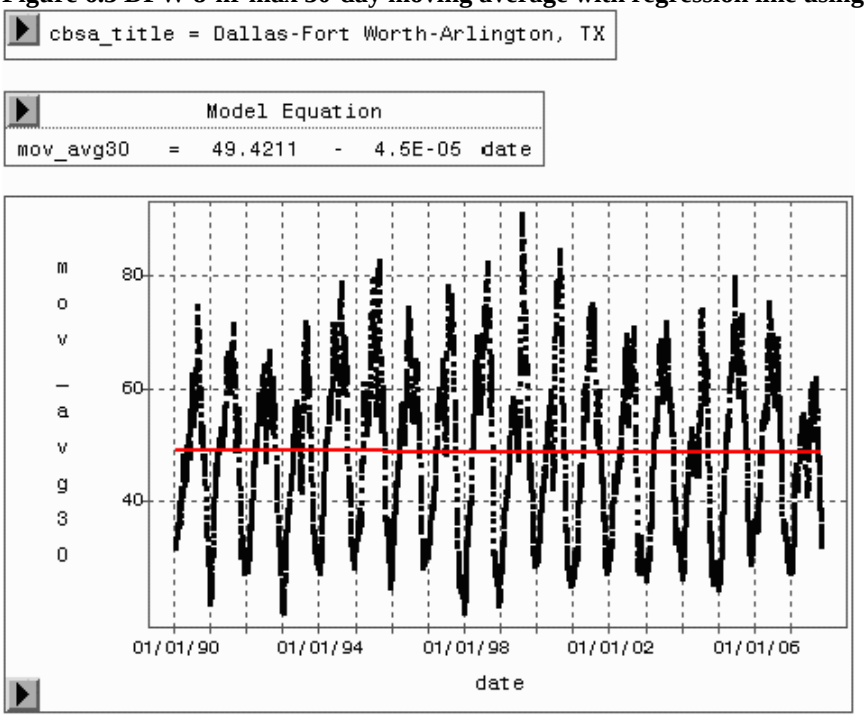

Sites used: 480850005, 481130069, 481130075, 484391002, 484392003; $p = 0.64$

Figure 6.4 El Paso 8-hr max 30-day moving average with regression line using only long-running sites' data

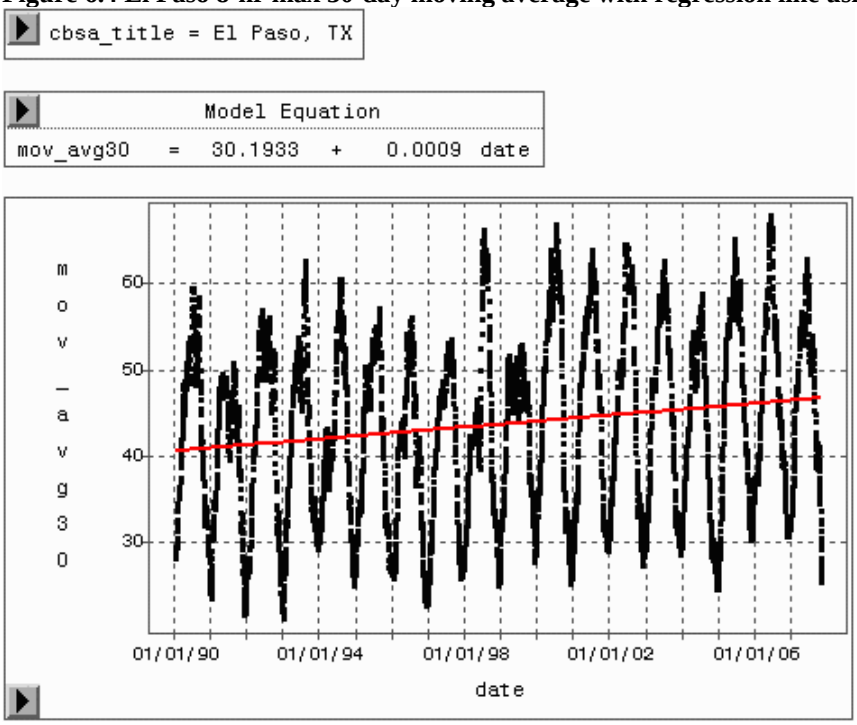

Sites used: 481410037, 481410044, 481410055; $p < 0.0001$

Figure 6.5 HGB 8-hr max 30-day moving average with regression line using only long-running sites' data

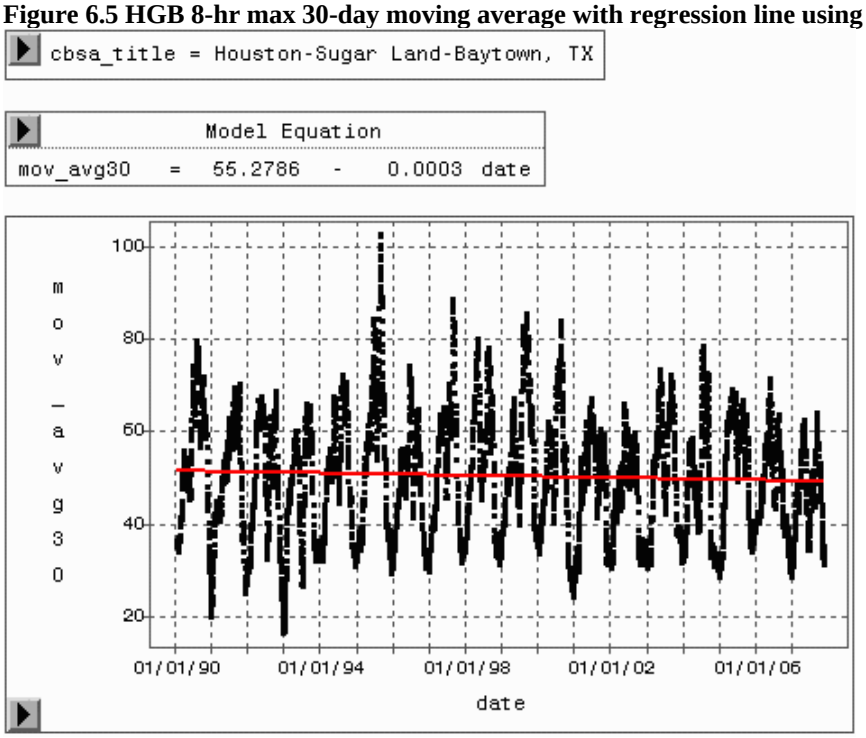

Sites used: 480391016, 482010024, 482010029, 482010046, 482010047, 482010051, 482010062, 482010075, 482011034, 482011035, 482011039; $p < 0.0001$

Figure 6.6 SAN 8-hr max 30-day moving average with regression line using only long-running sites' data

cbsa_title = San Antonio, TX

Model Equation
mov_avg30 = 18.7447 + 0.0015 date

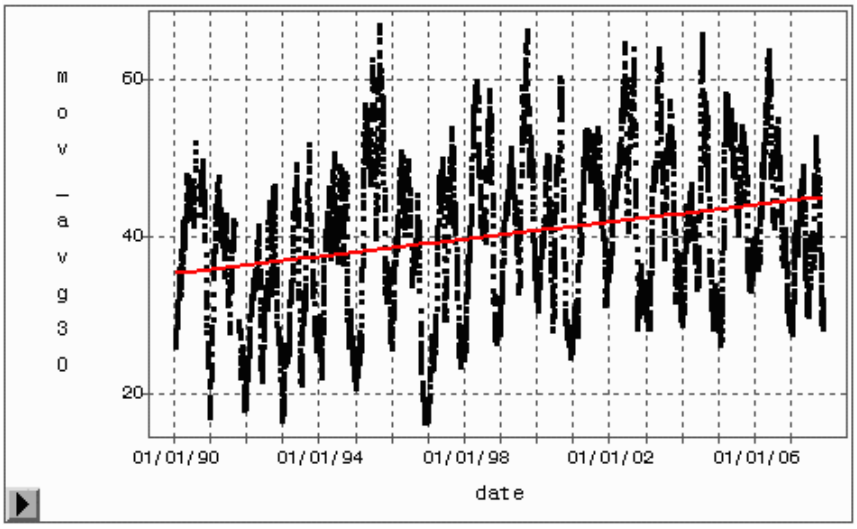

Sites used: 480290032, 480290052; $p < 0.0001$

Figure 6.7 CC 8-hr max 30-day moving average with regression line using only long-running sites' data

cbsa_title = Corpus Christi, TX

mov_avg30 = date
Response Distribution: Normal
Link Function: Identity

Model Equation
mov_avg30 = 41.0181 - 0.0002 date

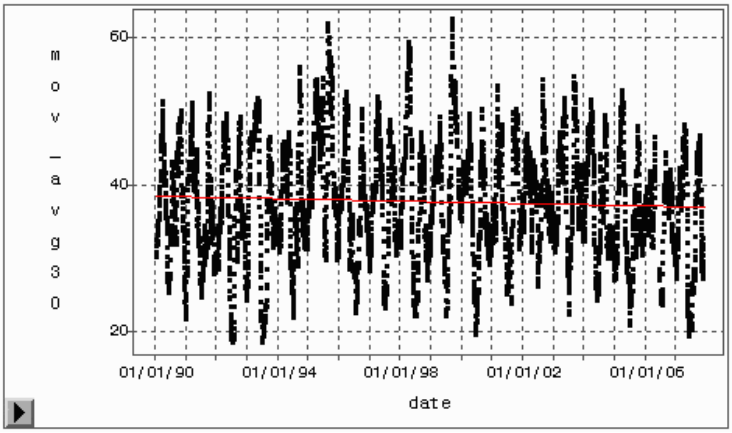

Sites used: 483550025, 483550026; $p < 0.0001$

Figure 6.8 CC 8-hr max 30-day moving average with regression line using only long-running sites' data

cbsa_title = Longview, TX

mov_avg30	=	date
Response Distribution:	Normal	
Link Function:	Identity	

Model Equation
mov_avg30 = 48.4776 - 0.0003 date

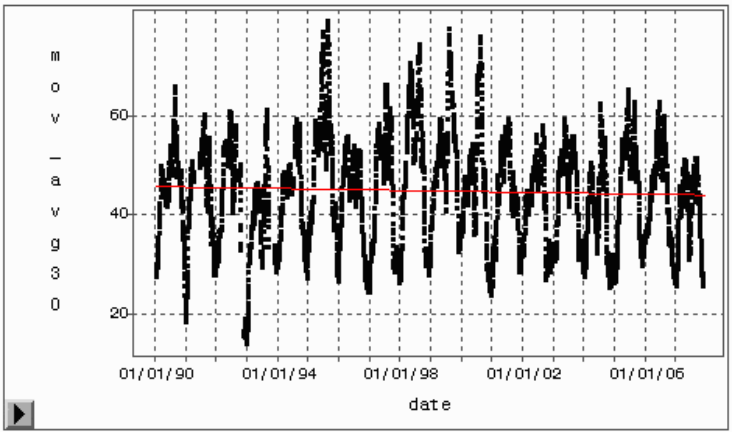

Sites used 481810001; p = 0.0004

1. SAS code to determine long-running ozone sites and extend time series by merging nearby "early" and "later" sites (filename get *ozone longterm data.sas*:

```
libname cams2 "D:\cams2"; run;
libname other "C:\Documents and Settings\Sully\My Documents\mother\OTHERDATA"; run;

* This program prepares data for merger with the meteorological data sets provided by Erik Gribbin;

* Read in all the data from 1990-2007 from MOTHER;
* An earlier assessment (shown at bottom of program and using Excel) suggested that
  time series for some monitors could be concatenated because of close proximity
  and one having ended shortly before the other began (i.e., the site moved).;
data ozone_sites0;
  set cams2.oz_1990 cams2.oz_1991 cams2.oz_1992 cams2.oz_1993 cams2.oz_1994
      cams2.oz_1995 cams2.oz_1996 cams2.oz_1997 cams2.oz_1998 cams2.oz_1999
      cams2.oz_2000 cams2.oz_2001 cams2.oz_2002 cams2.oz_2003 cams2.oz_2004
      cams2.oz_2005z cams2.oz_2006 cams2.oz_2007;
        if airs = "481210033"  then airs =  "481210034" ;
        if airs = "481130045"  then airs =  "481130075" ;
      if airs = "483390089"  then airs =  "483390078" ;
      if airs = "481410028"  then airs =  "481410055" ;
      if airs = "401430127"  then airs =  "401431127" ;
      if airs = "482011003"  then airs =  "482011039" ;
      if airs = "481670014"  then airs =  "481671034" ;
      if airs = "051191005"  then airs =  "051191008" ;
      if airs = "482011037"  then airs =  "482010075" ;
      if airs = "350431002"  then airs =  "350431003" ;
      if airs = "482011041"  then airs =  "482011015" ;
      if airs = "484230004"  then airs =  "484230007" ;
      if airs = "220470002"  then airs =  "220470012" ;
      if airs = "350011003"  then airs =  "350010029" ;
      if airs = "220730002"  then airs =  "220730004" ;
      if airs = "350131012"  then airs =  "350130023" ;
      if airs = "482450102"  then airs =  "482451035" ;
      if airs = "350010028"  then airs =  "350010024" ;
      if airs = "220570002"  then airs =  "220570004" ;
      if airs = "484390057"  then airs =  "484393011" ;
      if airs = "220870002"  then airs =  "220870009" ;
      if airs = "480391003"  then airs =  "480391016" ;
      if airs = "400870073"  then airs =  "400871073" ;
```

```
      if airs = "400310647"  then airs =  "400310649" ;
      if airs = "480290036"  then airs =  "480290052" ;
/*  if airs in ("481210034" "481130075" "483390078" "481410055" "401431127" "482011039" "481671034"*/
/*              "051191008" "482010075" "350431003" "482011015" "484230007" "220470012" "350010029"*/
/*              "220730004" "350130023" "482451035" "350010024" "220570004" "484393011" "220870009"*/
/*              "480391016" "400871073" "400310649" "480290052") ;*/
  keep airs date oz8hrpk oz1hrpk oz1hrav oz1hrvh oz1hrvd oz8hrvd;
run;

* Figure out the length of the time series for each site;
proc sort data=ozone_sites0; by airs date; run;
data ozone_sites; set ozone_sites0; by airs date; if first.airs or last.airs; run;
proc sort data=ozone_sites; by airs date; run;
proc transpose data=ozone_sites out=ozone_sites; by airs; var date; run;
data ozone_sites;
  set ozone_sites;
  early = col1; late = col2; drop col1 col2; format early late mmddyy8.;
  duration = (late - early)/365.25;
run;

* Get geographic data for sites, including 9 not in MOTHER;
proc import datafile="C:\Documents and Settings\Sully\Desktop\Kasey's O3 trend project\9_o3_sites.xls"
  out=nine_sites dbms=XLS; run;
data site_info;
  set other.siteinfo_newx2 nine_sites;
  if site_description = "" then do;
    if city ^= "" then
      site_description = substr(city,1,8)||" "||substr(county,1,8)||" "||substr(site_address,1,8);
    else
      site_description = substr(county,1,8)||" "||substr(site_address,1,8);
  end;
run;
proc sort data=site_info; by airs; run;

data ozone_sites;
  merge ozone_sites (in=in_o3) site_info;
  by airs;
  if in_o3;
  keep airs early late duration latitude longitude;
run;
```

```
/*proc export data=ozone_sites outfile="C:\Documents and Settings\Sully\Desktop\190_o3_sites.xls" dbms=XLS
replace; run;*/

* which sites have > 15 years of data?;
data ozone_sites_long;
  set ozone_sites;
  if duration >= 15;
run;
```

****

2. Compute moving averages for daily maxima ozone by urban area (CBSA) (filename *sites over time2.sas*)

```
libname other "C:\Documents and Settings\Sully\My Documents\mother\OTHERDATA";
libname cams2 "D:\cams2";
data oz;
  set cams2.oz_1990 cams2.oz_1991 cams2.oz_1992 cams2.oz_1993 cams2.oz_1994
      cams2.oz_1995 cams2.oz_1996 cams2.oz_1997 cams2.oz_1998 cams2.oz_1999
      cams2.oz_2000 cams2.oz_2001 cams2.oz_2002 cams2.oz_2003 cams2.oz_2004
      cams2.oz_2005z cams2.oz_2006 cams2.oz_2007;
        keep airs date oz8hrpk;
run;

proc sort data=oz; by airs; run;
proc sort data=ozone_sites_long; by airs; run;

data oz;
  merge oz ozone_sites_long (in=inlong);
  by airs;
  if inlong;
run;

data site_cbsa;
  set other.Siteinfo_newx2;
  keep airs cbsa_code cbsa_title state;
run;

proc sort data=site_cbsa; by airs; run;

data oz_cbsa;
```

```
  merge site_cbsa oz (in=inoz);
  by airs;
  if inoz;
  if cbsa_code;
run;

proc sort data=oz_cbsa; by date state cbsa_title; run;
proc means data=oz_cbsa noprint;
  by date state cbsa_title;
  output out=oz_cbsa_stats max(oz8hrpk)=oz8hrmax n(oz8hrpk)=num_sites;
run;


data tx_oz_cbsa_stats;
  set oz_cbsa_stats;
  if state = "TX";
  drop state _TYPE_ _FREQ_;
  if substr(cbsa_title,1,2) in ("Au" "Be" "Da" "El" "Ho" "Sa" “Co” “Lo”);
run;
proc sort data=tx_oz_cbsa_stats; by date; run;


data days;
  format date mmddyy8.;
  format cbsa_title $50.;
  date = mdy(1,1,1990);
  do while (date <= mdy(12,31,2007));
    cbsa_title = "Austin-Round Rock, TX";  output;
    cbsa_title = "Beaumont-Port Arthur, TX";  output;
    cbsa_title = "Dallas-Fort Worth-Arlington, TX";  output;
    cbsa_title = "El Paso, TX";  output;
    cbsa_title = "Houston-Sugar Land-Baytown, TX";  output;
    cbsa_title = "San Antonio, TX";  output;
    cbsa_title = "Corpus Christi, TX";  output;
    cbsa_title = "Longview, TX";  output;
      date = date + 1;
  end;
run;
proc sort data=days; by date cbsa_title; run;
```

```
data tx_oz_cbsa_days;
  merge days tx_oz_cbsa_stats;
  by date cbsa_title;
  if num_sites = . then num_sites = 0;
run;

* moving averages ;

proc sort data=tx_oz_cbsa_days; by cbsa_title date; run;
data tx_oz_cbsa_days2;
  set tx_oz_cbsa_days;
  format last_cbsa $50.;
  last_cbsa = lag29(cbsa_title);
    oz8_lag_29 = lag29(oz8hrmax);
    oz8_lag_28 = lag28(oz8hrmax);
    oz8_lag_27 = lag27(oz8hrmax);
    oz8_lag_26 = lag26(oz8hrmax);
    oz8_lag_25 = lag25(oz8hrmax);
    oz8_lag_24 = lag24(oz8hrmax);
    oz8_lag_23 = lag23(oz8hrmax);
    oz8_lag_22 = lag22(oz8hrmax);
    oz8_lag_21 = lag21(oz8hrmax);
    oz8_lag_20 = lag20(oz8hrmax);
    oz8_lag_19 = lag19(oz8hrmax);
    oz8_lag_18 = lag18(oz8hrmax);
    oz8_lag_17 = lag17(oz8hrmax);
    oz8_lag_16 = lag16(oz8hrmax);
    oz8_lag_15 = lag15(oz8hrmax);
    oz8_lag_14 = lag14(oz8hrmax);
    oz8_lag_13 = lag13(oz8hrmax);
    oz8_lag_12 = lag12(oz8hrmax);
    oz8_lag_11 = lag11(oz8hrmax);
    oz8_lag_10 = lag10(oz8hrmax);
    oz8_lag_9 = lag9(oz8hrmax);
    oz8_lag_8 = lag8(oz8hrmax);
    oz8_lag_7 = lag7(oz8hrmax);
    oz8_lag_6 = lag6(oz8hrmax);
    oz8_lag_5 = lag5(oz8hrmax);
    oz8_lag_4 = lag4(oz8hrmax);
    oz8_lag_3 = lag3(oz8hrmax);
    oz8_lag_2 = lag2(oz8hrmax);
```

```
  oz8_lag_1 = lag(oz8hrmax);
  oz8_lag_0 = oz8hrmax;
if ( last_cbsa = cbsa_title ) then do;
  mov_avg30 = mean( of oz8_lag_0-oz8_lag_29 );
  num_days = n( of oz8_lag_0-oz8_lag_29 );
    if num_days <= 20 then mov_avg30 = .;
end;
else do;
  mov_avg30 = .; num_days = .;
end;
run;
```

3. Open SAS Interactive Analysis, select the *tx_oz_cbsa_days2* dataset and fit variables *mov_avg30* vs *date* by *cbsa_title*

.

6.2 Meteorologically-adjusted Trends for Ozone

6.2.1 Houston-Galveston-Brazoria Conceptual Model Input

In comparing the surface and upper air meteorological Omnibus Meteorological Database (METDAT) maintained by U.S. EPA with surface ozone measurements, some clear relationships can be observed. As is common in many air pollution research applications, the ozone variable of concern – the daily area 8-hour maximum concentration – has been transformed to create a "better behaved" variable in the sense that the distribution of the variable is closer to a normal distribution. Thus, the natural logarithm of the daily area maximum is used throughout much of the ensuing analysis. In addition, care has been maintained in using a consistent set of ozone monitors in the analysis, as prior research has shown that the number of monitors affects the maximum measured concentration daily. The ozone monitors used are listed in Table 6.1. All of these sites have nearly complete data for the 1990 – 2007 period.

Table 6.1 Houston Area Ozone Monitoring Sites with Long-run Data

AQS Ident	Site name	Latitude	Longitude
482011039	Deer Park C35	29.670	-95.128
482011035	Clinton C403	29.734	-95.258
482011034	East C1	29.768	-95.221
482010075	Texas Avenue C411	29.753	-95.350
482010062	Monroe C406	29.626	-95.267
482010051	Croquet C409	29.624	-95.474
482010047	Lang C408	29.834	-95.489
482010046	North Wayside C405	29.828	-95.284
482010029	Northwest Harris Co. C26	30.039	-95.674
482010024	Aldine C8	29.901	-95.326
480391016	Lake Jackson C1016 (and Clute C11)	29.044	-95.473

The data at the deactivated Clute site in Brazoria County were connected with the time series of data at the currently active Lake Jackson site because of the close proximity between sites and the fact that an examination of the concatenated time series showed a good match.

A histogram showing the counts for the number of times that each site produced the daily area 8-hour ozone maximum over the 1995 – 2007 period is shown in Figure 6.9.

Figure 6.9 Count of days for which each site presented the area maximum daily 8-hour maximum, May-Oct. 1995-2007

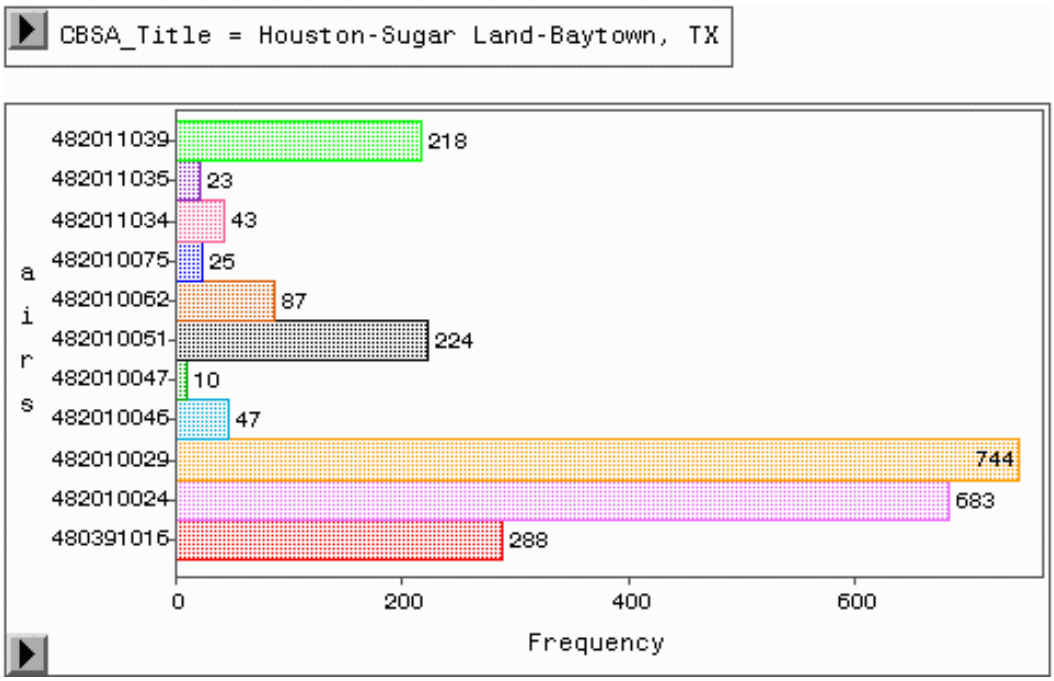

Generally the sites with the lowest frequency in Figure 6.9 are in the areas with highest NO emissions, and the sites with the highest frequency tend to be in downwind suburban or rural areas.

As was mentioned earlier, the transformed ozone variable employed in subsequent analysis is the natural logarithm of the area 8-hour maximum, which is referred to as "*l_oz8*". Only data from May through October (seven months) for the years 1995 – 2007 (13 years) were used to match the available METDAT data.

The variables in the METDAT database are described in Table 6.2. The ozone data from each urban area were merged with the corresponding day's METDAT data from the nearest upper air monitoring location. In most cases the associated upper air site was located within or adjacent to is nearest urban area. The exception is Austin, which is just under 50 miles from the upper air site at Fort Hood. This may in part explain why Austin correlations are weaker than average among the eight areas considered. The Pearson correlations of *l_oz8* with the METDAT variables for each large metropolitan area in Texas are shown in Table 6.3. The correlations for Houston and Dallas/Fort Worth are among the best. The correlation values are color coded to highlight the best relationships. The color-coding is blue for less than -0.3 and orange for greater than 0.3. The black-bolded rows correspond to the variables used in the Camalier, Cox, and Dolwick analysis[5]. Because El Paso is located above the typical 925 mb altitude, some METDAT parameters are missing. The columns in Table 6.3 are grouped based on a separate factor analysis of the behavior of regional ozone concentrations in Texas and on the common

[5] Camalier, L., Cox, W., Dolwick, P., 2007. The effects of meteorology on ozone in urban areas and their use in assessing ozone trends. Atmospheric Environment 41, 7127-7137.

behavior of the correlations within this table. Thus, South Texas areas are grouped, Central and Upper Gulf Coast areas are grouped, and Dallas/Fort Worth and El Paso stand alone. It should be noted that many lower correlations not highlighted may be statistically significant because of the large number of available observations.

Examples of the behavior of the relationships for three of the highest absolute value correlations for the Houston area are shown in Figures 6.10, 6.11, and 6.12. Figure 6.10 shows that the ozone maximum is negatively related to the distance the large scale air mass has moved during the preceding 24 hours, supporting the well-known relationship between stagnation and pollutant accumulation. Figure 6.11 shows the important fact that the drier an air mass, the higher the ozone concentration. Caution must be used in assessing this relationship, as "Gulf" air is generally cleaner and more humid than "Continental" air, so "*humidity*" may be related to "*transport*" variables. However, the same relative humidity variable is negative and significant in Dallas and El Paso, the two regions farthest from the Gulf. Figure 6.12 shows that the difference between the maximum and minimum temperature is strongly positively related to the maximum area ozone, and this variable is a better predictor for ozone than maximum temperature alone (see Table 6.3 on a following page). One hypothesis may be that a bigger swing in temperatures over the course of a day may increase evaporation of hydrocarbons.

For the Houston-Galveston-Brazoria region, an ordinary least squares regression analysis of *l_oz8* on up to 51 of the variables in the METDAT list explains 73 percent in the variance for daily area maximum ozone. Using a more parsimonious model with only the best set of 10 largely independent variables reduces the R^2 to 47 percent. Implementing a more complicated parsimonious general linear model (GLM) with spline functions to reduce short-term random variations and to accommodate nonlinear relationships and including a circular spline function for the TRANDIR (net direction of HYSPLIT back-trajectory) variable plus including a set of dummy variables for "*year*", the R^2 improves to 67 percent. This GLM regression approach shows no day-of-the week effect, but does show a statistically significant decline in meteorologically-adjusted ozone levels from 1995 – 2007. More details on the GLM regression approach are provided in sections 6.2.4 and 6.2.5 of this report.

Table 6.2 Variables from the METDAT Database

ID	NAME	UNIT	DURATION	PARM
1	Maximum surface temperature	C	24-hr calc	TMAX
2	Morning (7-10 a.m. LST) average temperature	C	4-hr calc	TAVGAM
3	Afternoon (1-4 p.m. LST) average temperature	C	4-hr calc	TAVGPM
4	Diurnal temperature change	C	24-hr calc	TDELTA
5	Average daily wind U vector (m/s)	m/s	24-hr calc	UAVG
6	Average daily wind V vector (m/s)	m/s	24-hr calc	VAVG
7	Average daily wind speed (m/s)	m/s	24-hr calc	WSAVG
8	Average daily wind direction (deg)	deg	24-hr calc	WDAVG
9	Average morning (7-10 a.m. LST) wind U vector (m/s)	m/s	4-hr calc	UAVGAM
10	Average morning (7-10 a.m. LST) wind V vector (m/s)	m/s	4-hr calc	VAVGAM
11	Average morning (7-10 a.m. LST) wind speed (m/s)	m/s	4-hr calc	WSAVGAM
12	Average morning (7-10 a.m. LST) wind direction (deg)	deg	4-hr calc	WDAVGAM
13	Average afternoon (1-4 p.m. LST) wind U vector (m/s)	m/s	4-hr calc	UAVGPM
14	Average afternoon (1-4 p.m. LST) wind V vector (m/s)	m/s	4-hr calc	VAVGPM
15	Average afternoon (1-4 p.m. LST) wind speed (m/s)	m/s	4-hr calc	WSAVGPM
16	Average afternoon (1-4 p.m. LST) wind direction (deg)	deg	4-hr calc	WDAVGPM
17	Average daily relative humidity (%)	%	24-hr calc	RHAVG
18	Midday (10 a.m.-4 p.m. LST) average relative humidity (%)	%	7-hr calc	RHAVGMID
19	Nighttime (8 p.m.-7 a.m. LST) average relative humidity (%)	%	12-hr calc	RHAVGNIGHT
20	Average dew point temperature	C	24-hr calc	DPAVG
21	Maximum dew point temperature	C	24-hr calc	DPMAX
22	Maximum water vapor mixing ratio (g/kg)	g/kg	24-hr calc	MRMAX
23	Average Sea level pressure (mb)	mb	24-hr calc	SLPAVG
24	Average Station pressure (mb)	mb	24-hr calc	STPAVG
25	Minimum apparent temperature	C	24-hr calc	TAMIN
26	Average apparent temperature	C	24-hr calc	TAAVG
27	Maximum apparent temperature	C	24-hr calc	TAMAX
28	Morning (7-10 a.m. LST) average fractional cloud cover (tenths)	tenths	4-hr calc	CCAVTAM
29	Afternoon (1-4 p.m. LST) average fractional cloud cover (tenths)	tenths	4-hr calc	CCAVGPM
30	Total precipitation (inches)	in	24-hr calc	PRECIP
31	Occurrence of rain (hours)	hrs	24-hr calc	RAINHRS
32	Occurrence of haze (hours)	hrs	24-hr calc	HAZEHRS
33	Occurrence of fog (hours)	hrs	24-hr calc	FOGHRS
34	Morning (~1200 UTC) Height of 500 mb surface (m)	m	1-hr obs	H500
35	Morning (~1200 UTC) Height of 700 mb surface (m)	m	1-hr obs	H700
36	Morning (~1200 UTC) Height of 850 mb surface (m)	m	1-hr obs	H850
37	Morning (~1200 UTC) Temperature at 925 mb	C	1-hr obs	T925
38	Morning (~1200 UTC) Temperature at 850 mb	C	1-hr obs	T850
39	Morning (~1200 UTC) Temperature at 700 mb	C	1-hr obs	T700
40	Morning (~1200 UTC) Temperature at 500 mb	C	1-hr obs	T500
41	Morning (~1200 UTC) Dewpoint Temperature at 850 mb	C	1-hr obs	TD850
42	Morning (~1200 UTC) 925 mb-surface temperature difference	C	1-hr calc	DT925
43	Morning (~1200 UTC) 850 mb-surface temperature difference	C	1-hr calc	DT850
44	Morning (~1200 UTC) 700 mb-surface temperature difference	C	1-hr calc	DT700
45	Maximum rate of mixing height increase (m/hr) 6am-12pm LST	m/hr	7-hr calc	MRMHI
46	Maximum mixing height (m) 4am-4pm LST	m	13-hr calc	MHMAX
47	24-hr Transport Direction	deg	24-hr calc	TRANDIR
48	24-hr Transport Distance	km	24-hr calc	TRANDIS
49	X-component of the 24-hr Transport Vector	km	24-hr calc	TRANU
50	Y-component of the 24-hr Transport Vector	km	24-hr calc	TRANV
51	Z-component of the 24-hr Transport Vector	km	24-hr calc	TRANW
52	24-hr Scalar Wind Run	km	24-hr calc	WNDRUN
53	24-hr Change in Morning (~1200 UTC) Temperature at 850 mb	C	1-hr calc	D24T850
54	24-hr Change in Morning (~1200 UTC) Dewpoint Temperature at 850 mb	C	1-hr calc	D24TD850
55	Deviation in Morning (~1200 UTC) Temperature at 850 mb from 10-yr monthly mean	C	1-hr calc	DEVT850
56	Deviation in Morning (~1200 UTC) Temperature at 700 mb from 10-yr monthly mean	C	1-hr calc	DEVT700
57	Deviation in Morning (~1200 UTC) Temperature at 500 mb from 10-yr monthly mean	C	1-hr calc	DEVT500
58	Deviation in Morning (~1200 UTC) Height of 850 mb surface (m) from 10-yr monthly mean	m	1-hr calc	DEVH850
59	Deviation in Morning (~1200 UTC) Height of 700 mb surface (m) from 10-yr monthly mean	m	1-hr calc	DEVH700
60	Deviation in Morning (~1200 UTC) Height of 500 mb surface (m) from 10-yr monthly mean	m	1-hr calc	DEVH500

Table 6.3 Correlations of l_oz8 with METDAT variables, May-Oct. 1995 - 2007

ln(area oz8hrpk)	Austin	BPA	HGB	San Antonio	DFW	Victoria	CC	El Paso
Num obs	2,336	2,379	2,387	2,381	2,392	2,222	2,343	2,391
NOx			0.21		0.24			-0.17
Isoprene			0.31		0.42			0.00
HRVOC			0.08		0.19			-0.08
Alkanes			0.03		0.18			-0.04
BTEX			0.17		0.24			-0.04
CCAVGPM	-0.37	-0.35	-0.42	-0.36	-0.42	-0.17	-0.07	-0.13
CCAVTAM	-0.46	-0.51	-0.50	-0.51	-0.53	-0.36	-0.21	-0.21
D24T850	0.04	-0.04	-0.04	0.00	0.08	-0.05	-0.08	0.09
D24TD850	-0.07	-0.03	-0.04	-0.05	0.00	-0.05	-0.04	-0.02
DEVH500	0.04	-0.13	-0.09	-0.04	0.17	-0.10	-0.15	0.18
DEVH700	0.11	-0.06	-0.06	0.04	0.21	0.03	-0.03	0.20
DEVH850	0.17	0.05	0.02	0.10	0.20	0.16	0.11	0.11
DEVT500	-0.06	-0.09	-0.04	-0.06	0.04	-0.11	-0.11	0.00
DEVT700	-0.09	-0.15	-0.08	-0.11	0.02	-0.24	-0.24	0.16
DEVT850	**-0.02**	**-0.20**	**-0.14**	**-0.06**	**0.10**	**-0.20**	**-0.23**	**0.14**
DPAVG	-0.36	-0.28	-0.23	-0.31	0.02	-0.48	-0.53	0.04
DPMAX	-0.33	-0.24	-0.20	-0.25	0.03	-0.45	-0.50	0.06
FOGHRS	-0.12	0.07	-0.04	-0.11	-0.22	0.14	0.19	-0.15
HAZEHRS	-0.18	0.18	0.01	-0.03	-0.09	0.18	0.20	-0.06
MRMAX	-0.37	-0.26	-0.23	-0.28	-0.01	-0.49	-0.54	0.06
RAINHRS	-0.39	-0.32	-0.41	-0.40	-0.41	-0.25	-0.10	-0.16
RHAVG	-0.56	-0.45	-0.46	-0.55	-0.56	-0.42	-0.33	-0.27
RHAVGMID	**-0.53**	**-0.56**	**-0.54**	**-0.55**	**-0.59**	**-0.45**	**-0.28**	**-0.33**
RHAVGNIGHT	-0.48	-0.17	-0.23	-0.40	-0.45	-0.26	-0.25	-0.23
SLPAVG	0.06	0.09	0.09	0.03	-0.01	0.10	0.12	-0.13
STPAVG	0.08	0.09	0.15	0.05	-0.07	0.10	0.12	0.06
TAAVG	0.00	-0.12	-0.03	0.01	0.36	-0.34	-0.47	0.44
TAMAX	0.11	0.04	0.09	0.13	0.44	-0.18	-0.37	0.49
TAMIN	-0.15	-0.25	-0.15	-0.17	0.23	-0.46	-0.52	0.31
TAVGAM	0.15	0.02	0.04	0.14	0.45	-0.24	-0.39	0.43
TAVGPM	0.24	0.26	0.32	0.30	0.56	0.03	-0.20	0.52
TDELTA	0.49	0.59	0.48	0.46	0.47	0.52	0.30	0.29
TMAX	**0.22**	**0.23**	**0.23**	**0.25**	**0.52**	**-0.02**	**-0.24**	**0.51**
TRANDIS	**-0.47**	**-0.40**	**-0.45**	**-0.41**	**-0.49**	**-0.32**	**-0.21**	**-0.20**
TRANU	0.20	0.19	0.19	0.20	0.07	0.14	0.09	-0.12
TRANV	-0.39	-0.48	-0.44	-0.32	-0.17	-0.53	-0.58	-0.08
TRANW	0.25	0.23	0.20	0.12	0.09	0.24	0.21	0.17
UAVG	0.07	0.03	0.07	0.15	-0.12	0.04	0.08	-0.13
UAVGAM	0.11	-0.08	0.00	0.09	-0.01	-0.12	-0.05	-0.11
UAVGPM	-0.10	-0.05	-0.09	-0.03	-0.18	-0.06	0.02	-0.10
VAVG	-0.28	-0.37	-0.27	-0.19	-0.07	-0.45	-0.50	-0.01
VAVGAM	-0.27	-0.44	-0.39	-0.24	-0.09	-0.50	-0.56	0.02
VAVGPM	-0.29	-0.28	-0.20	-0.13	-0.05	-0.43	-0.46	-0.05
WNDRUN	-0.44	-0.39	-0.44	-0.38	-0.47	-0.28	-0.17	-0.20
WSAVG	-0.37	-0.35	-0.34	-0.36	-0.39	-0.31	-0.24	-0.24
WSAVGAM	**-0.33**	**-0.29**	**-0.32**	**-0.36**	**-0.42**	**-0.24**	**-0.20**	**-0.27**
WSAVGPM	**-0.30**	**-0.35**	**-0.25**	**-0.26**	**-0.31**	**-0.35**	**-0.31**	**-0.30**
DT925	**0.19**	**0.36**	**0.21**		**0.16**	**0.30**	**0.29**	

Figure 6.10 Scatterplot l_oz8 vs TRANDIS (distance from HGB to last endpoint in 24-hr HYSPLIT back-traj), r=-0.45

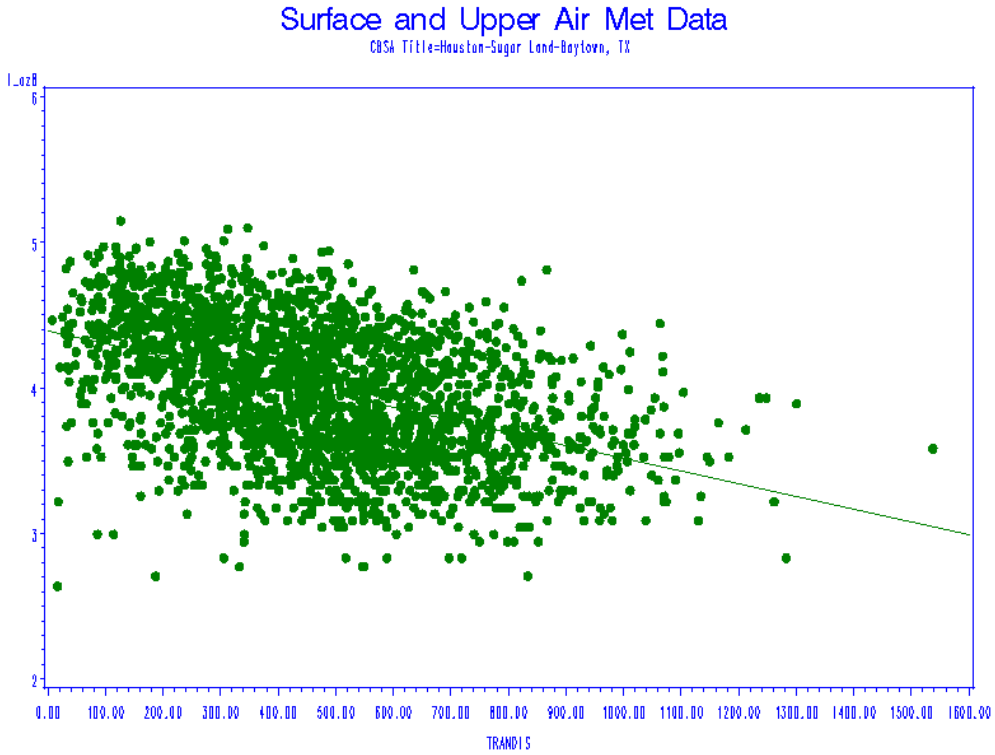

Figure 6.11 Scatterplot l_oz8 vs RHAVMID (mid-day relative humidity, %), r=-0.54

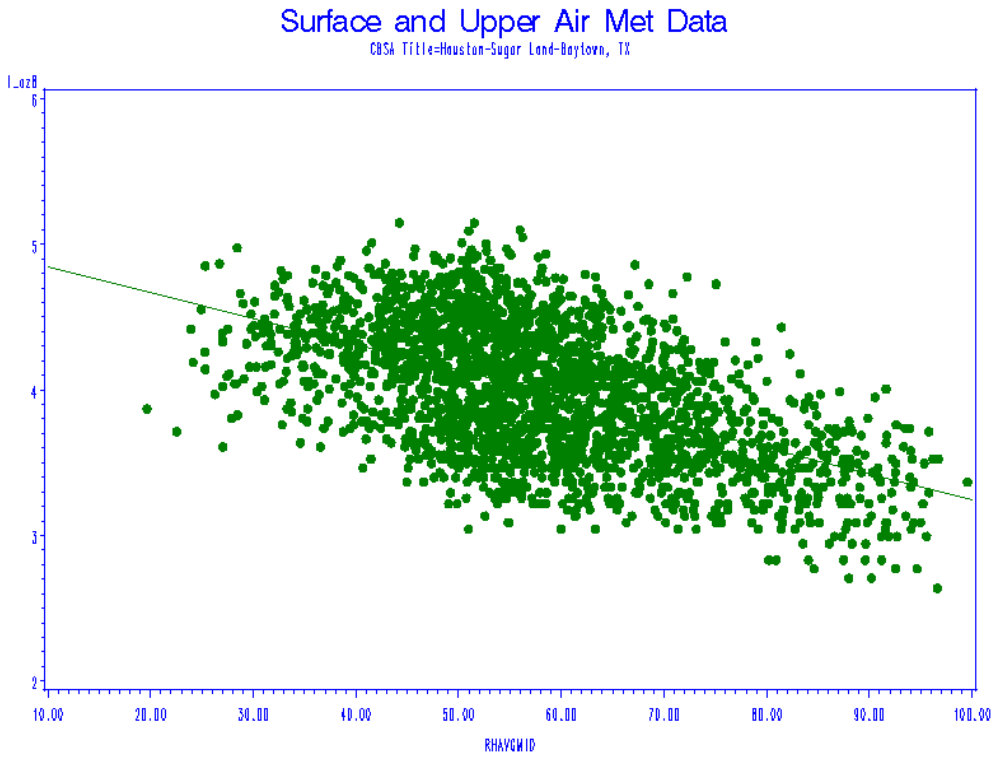

Figure 6.12 Scatterplot l_oz8 vs TDelta (daily maximum minus minimum temperature °C), r=0.48

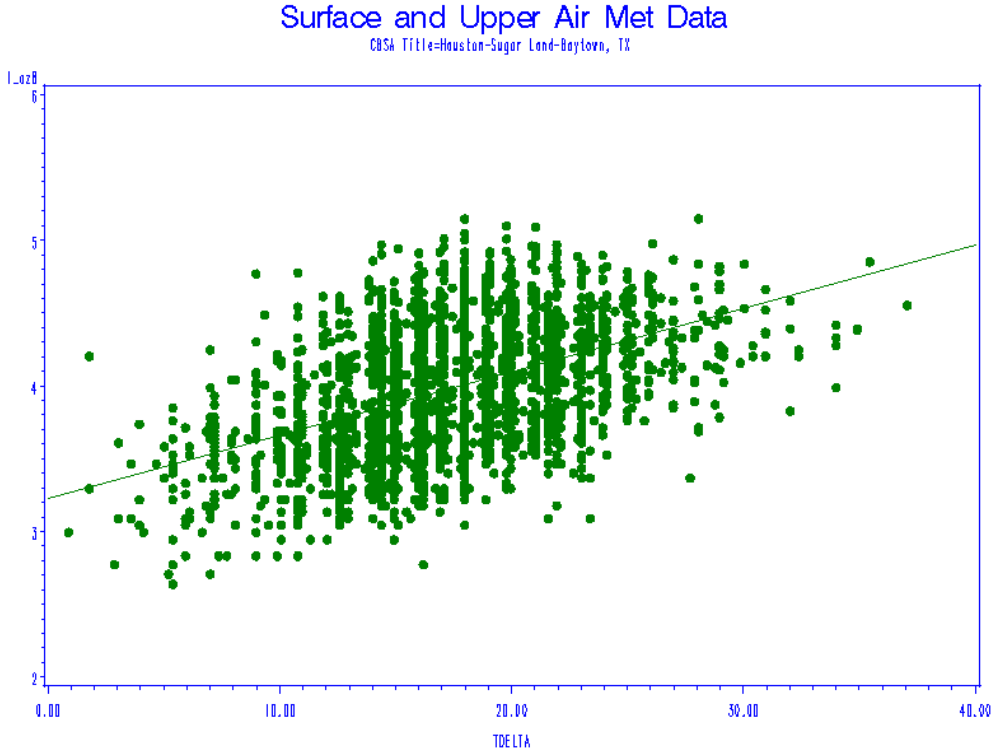

6.2.2. Assessing Transport Affecting the Houston Region Using HYSPLIT Back-trajectories Alone

The National Oceanic and Atmospheric Administration (NOAA) Air Resource Laboratory (ARL) maintains software, data files, and documentation useful in assessing pollution transport. The HYSPLIT 4.8[6] desktop computer application was used with Eta Data Assimilation System (EDAS) datasets to assess the year to year variability of regional and continental scale winds, and the relationship of the winds to surface level ozone concentrations in Houston.

Back-trajectories were run for all days with available data from May 1 and October 31, 2000 – 2007. The common starting point for all runs was in central Houston, TX (29.76° north latitude, 95.36° west longitude), 300 meters above ground level. Trajectories were started at 18 Coordinated Universal Time (UTC), which equals noon, Central Standard Time (CST), and were run backwards in time for 72 hours (three days). The location of the starting point appears in Figure 6.13 on a local scale and Figure 6.14 on a continental scale.

An individual back-trajectory is an idealized hypothetical center-line for the broad path that incoming air *likely* took in moving into an area. Upwind pollution sources could be near or faraway along that path, and relatively far from that modeled centerline. However, when multiple monitors spread over a larger area are used – such as a county, a metropolitan area (MSA), or an air quality control region (AQCR) – and assuming these monitors are historically well correlated and all are measuring similar concentration levels on a given day, then the associated back-trajectory is more meaningful in suggesting that the pollution has been transported into the area from a location relatively near the modeled centerline. Furthermore, when many trajectories are used and a correlation is established between concentrations and particular trajectory directions, shapes, and lengths, then one can conclude that some upwind source areas and/or pathways have a causative relation with higher than average concentrations, and some other areas/paths are associated with cleaner air and lower concentrations.

---

[6] Draxler, R.R. and Rolph, G.D., 2003. HYSPLIT (HYbrid Single-Particle Lagrangian Integrated Trajectory) Model access via NOAA ARL READY Website (http://www.arl.noaa.gov/ready/hysplit4.html). NOAA Air Resources Laboratory, Silver Spring, MD.

Rolph, G.D., 2003. Real-time Environmental Applications and Display sYstem (READY) Website (http://www.arl.noaa.gov/ready/hysplit4.html). NOAA Air Resources Laboratory, Silver Spring, MD.
.

Figure 6.13 Starting point for HYPLIT 72-hour back-trajectories from 300 m AGL, 18 UTC, meso-scale

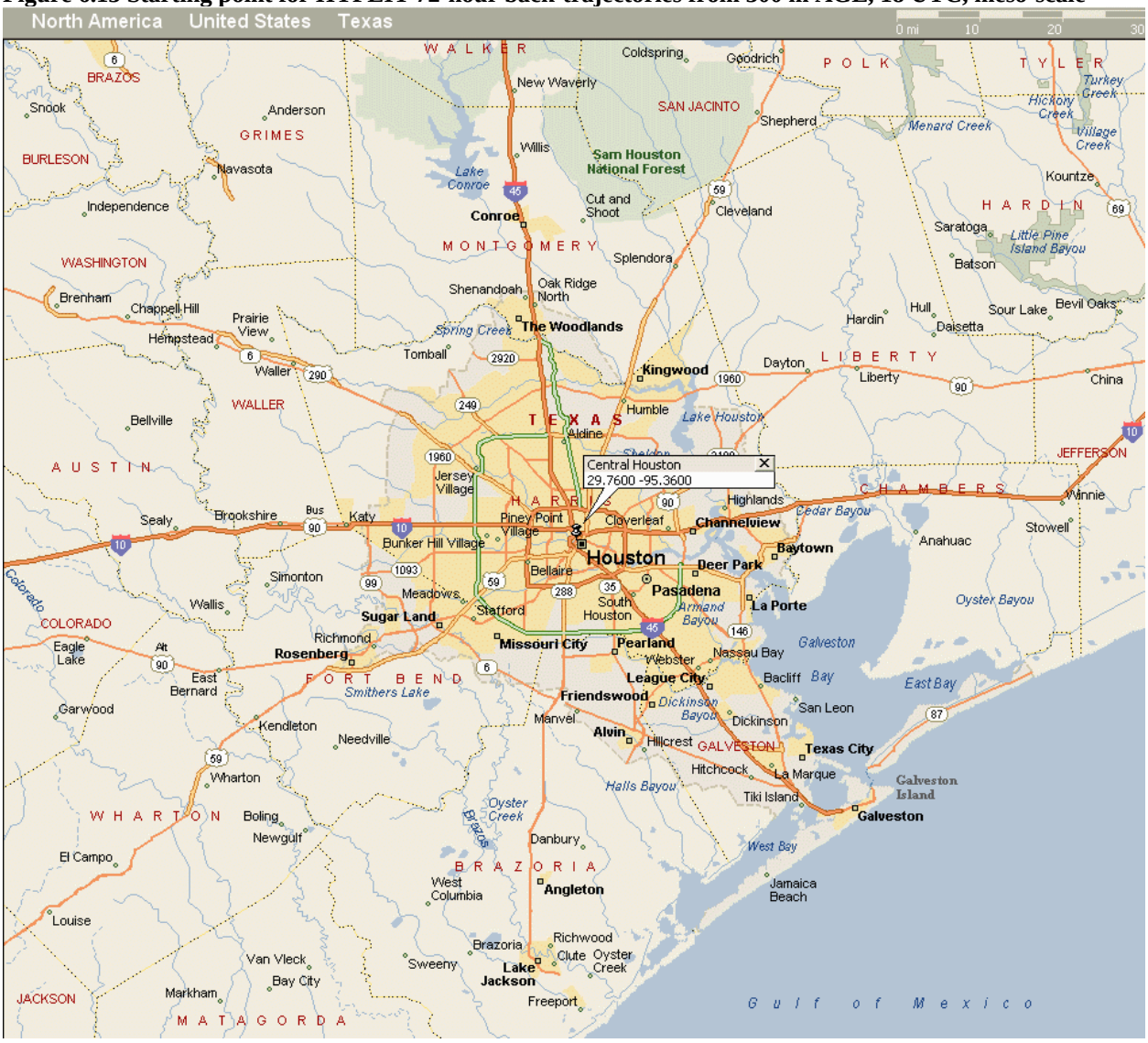

Figure 6.14 Starting point for HYPLIT 72-hour back-trajectories from 300 m AGL, 18 UTC, synoptic scale

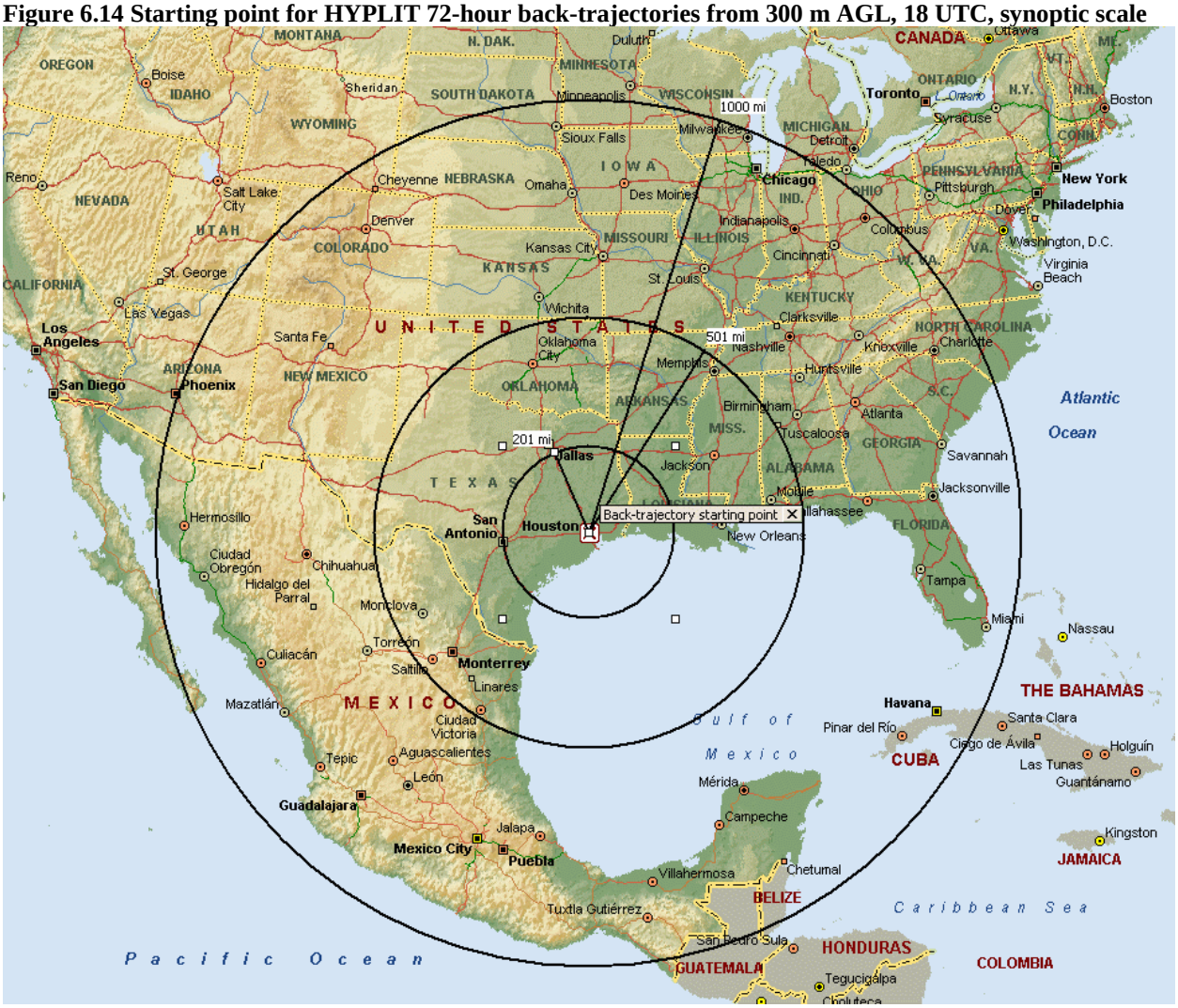

In this particular application, three major steps were taken.

- First, as was mentioned above, daily synoptic-scale back-trajectories were created.
- Second, a clustering algorithm built into HYPSLIT was used to sequester individual back-trajectories into a relatively small set of classes based on shape and direction. (Details on the clustering algorithm originally composed for an earlier contract report appears below.) The mean centerlines for the six identified clusters appears in Figure 6.15. The clusters of trajectories appear in Figures 6.17 – 6.22. Figure 6.16 shows a set of trajectories which were not contained in any cluster, and have been assigned cluster 0. All but one of these cluster 0 trajectories run to the south and would go beyond the modeling domain for the EDAS data, so they do represent a meaningful cluster to themselves with one outlier. Figure 6.23 shows a histogram summarizing the number of trajectories per cluster.
- In a separate process, the ozone data were analyzed to select a set of monitors with a nearly continuous record of operation over the 2000 – 2007 period. Using 12 such sites selected to give good regional coverage, the daily area-wide maximum and daily area-wide minimum 8-hour ozone maximum by site (oz8hrpk) were collected. The max was

identified as the "oz_area_max" and the min was identified as the "background". The 12 ozone sites are depicted in Figure 6.24.

- Next, the file with the variable identifying the cluster classification for each day was merged with a file containing the ozone data for each day.
- Lastly, the statistics for mean "oz_area_max" and "background" and the daily difference between them – "difference" – were calculated as functions of the trajectory classification.

The results show conclusively that trajectory cluster has a highly significant affect on local "oz_area_max" and "background" values. These results are summarized later in this section.

Figure 6.15 Means of seven 60-hour back-trajectory clusters, May-October 2000 – 2007, Houston origin 300 m AGL, 18 UTC: 0. (not shown) far southerly fetch; 1. red, SE fetch; 2. blue, SSE fetch; 3. green, northerly fetch; 4. cyan, short fetch; 5. magenta, NE fetch; 6. yellow, easterly fetch

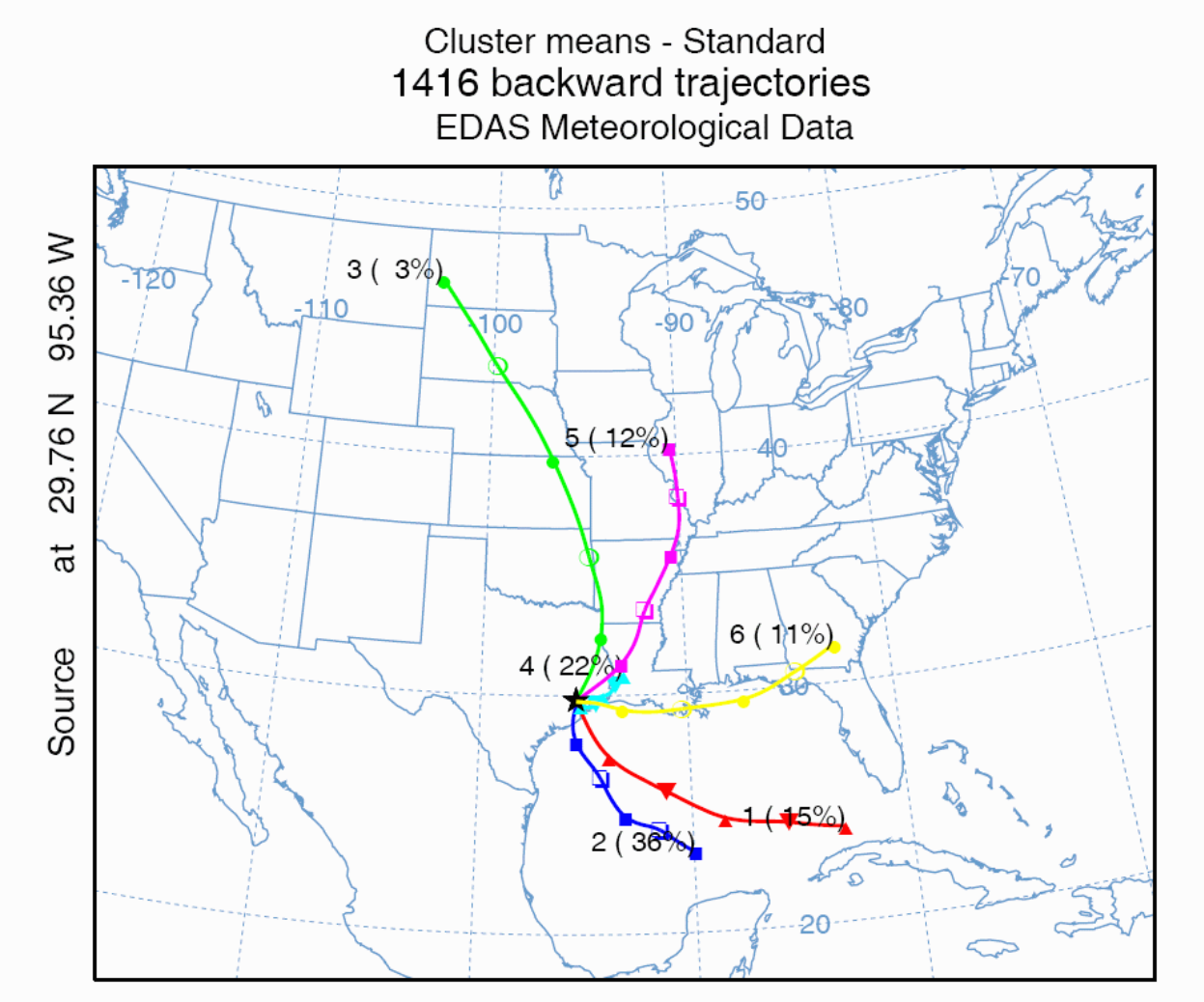

Figure 6.16 Cluster 0 72-hour back-trajectories from Houston

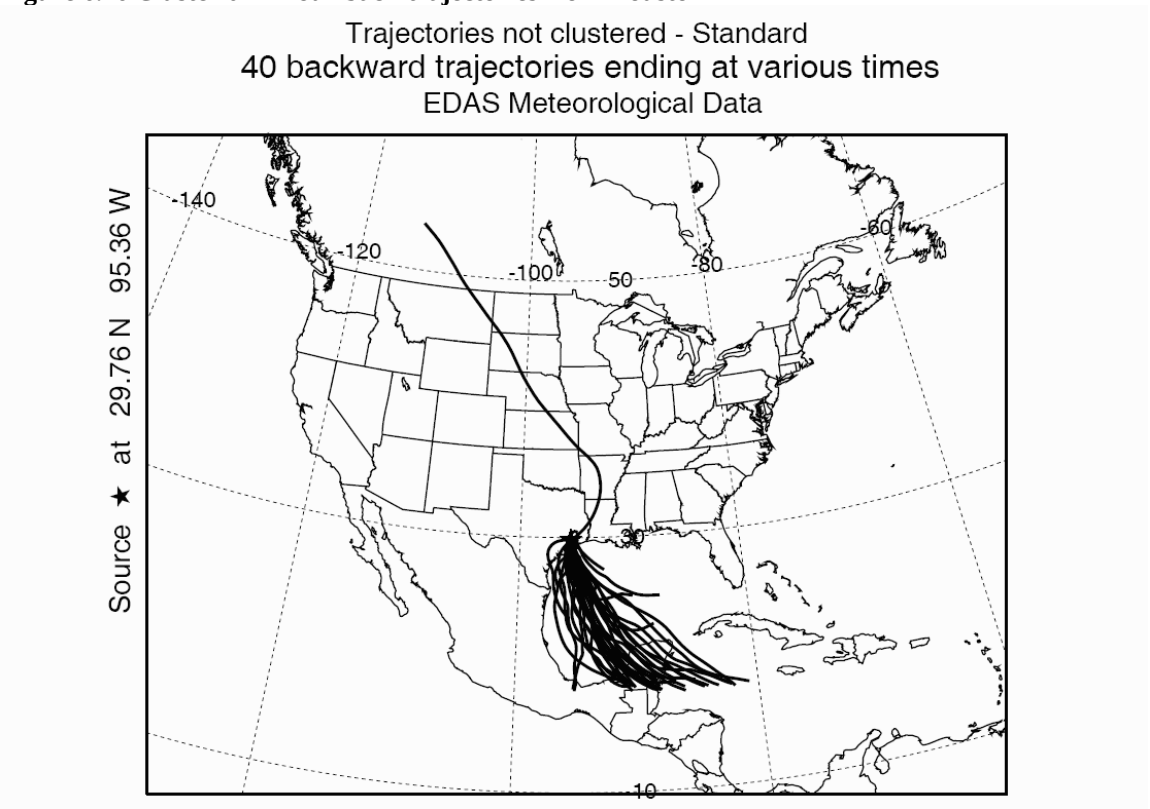

Figure 6.17 Cluster 1 72-hour back-trajectories from Houston

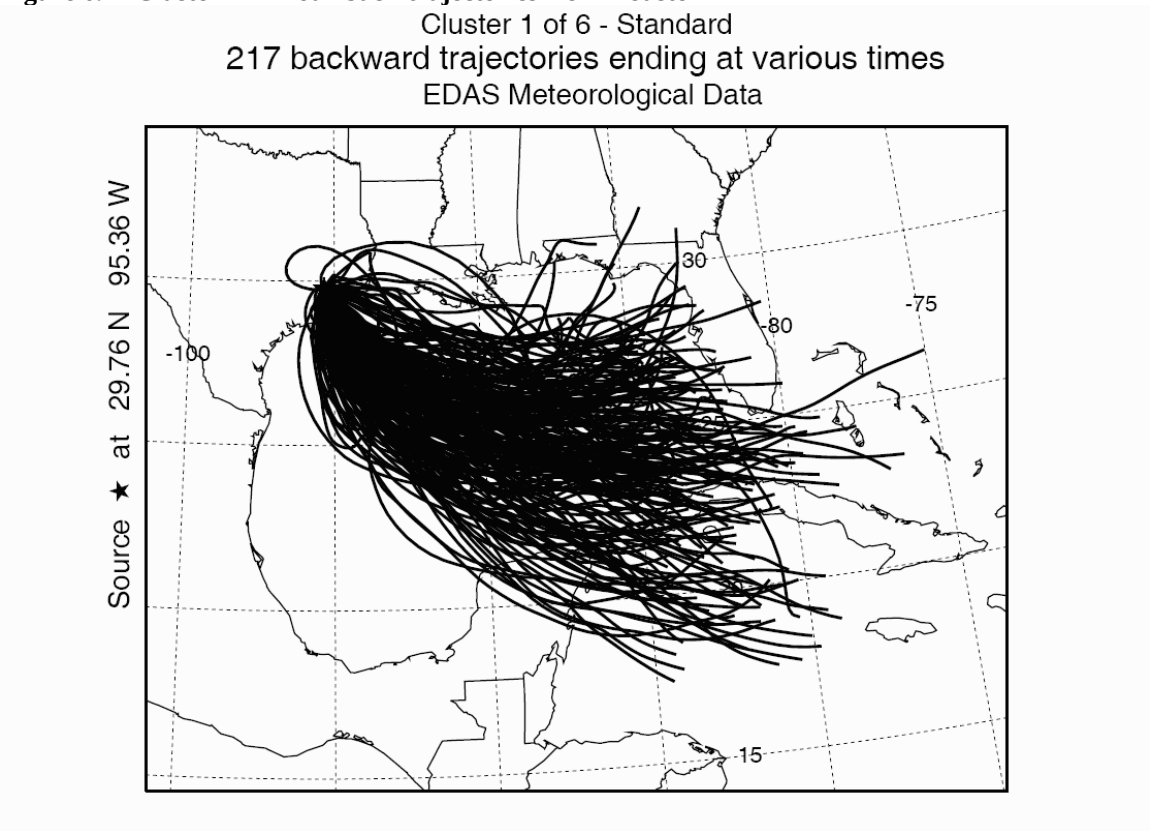

Figure 6.18 Cluster 2 72-hour back-trajectories from Houston

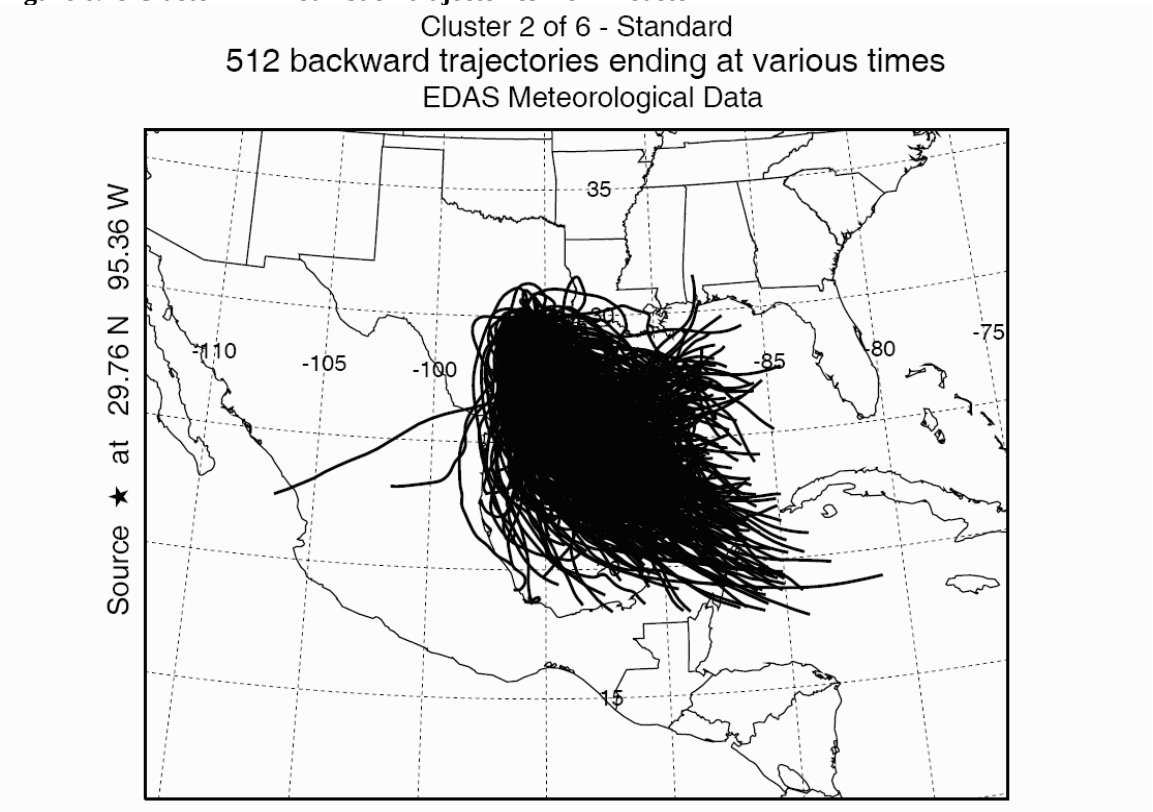

Figure 6.19 Cluster 3 72-hour back-trajectories from Houston

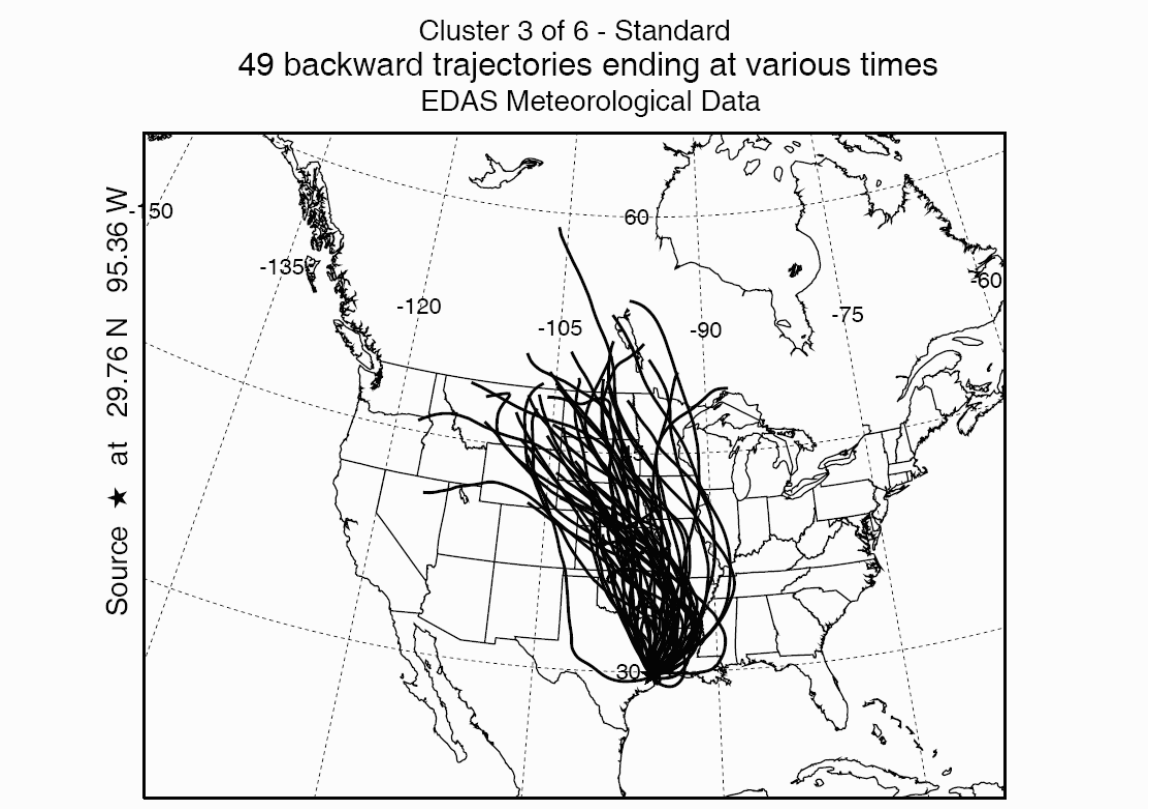

Figure 6.20 Cluster 4 72-hour back-trajectories from Houston

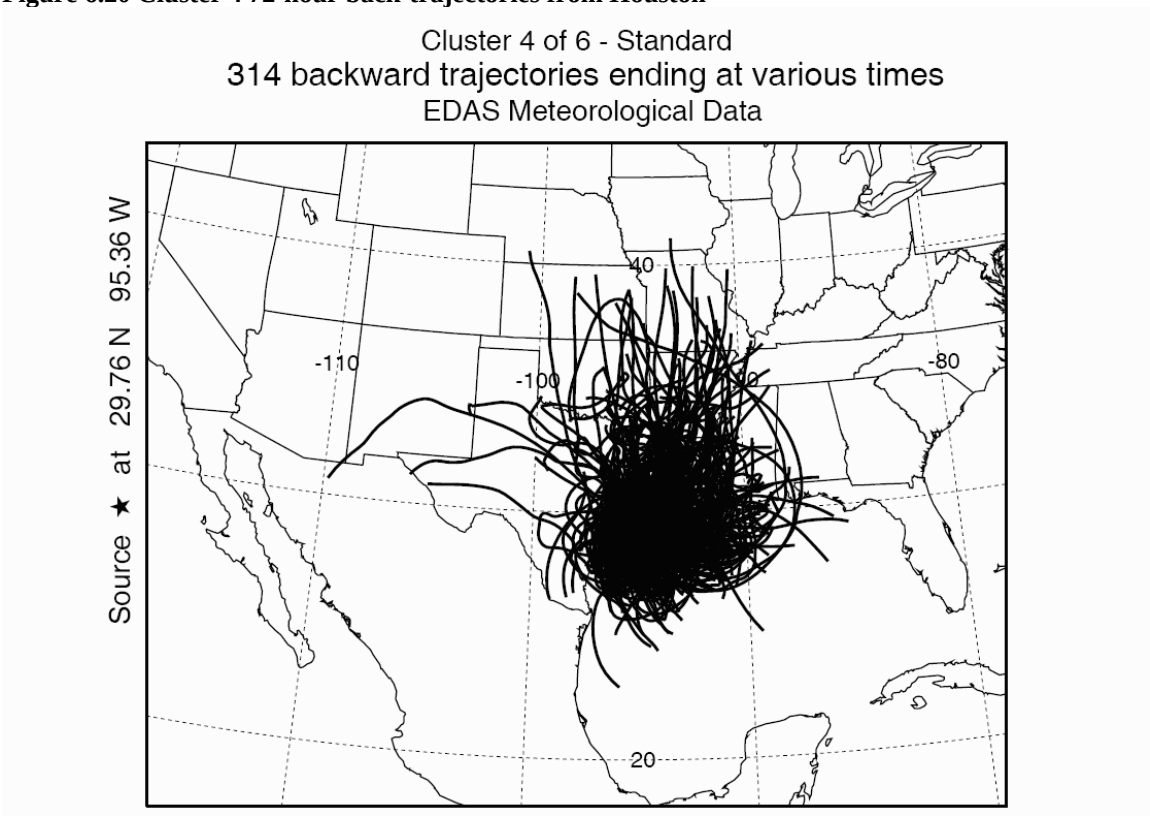

Figure 6.21 Cluster 5 72-hour back-trajectories from Houston

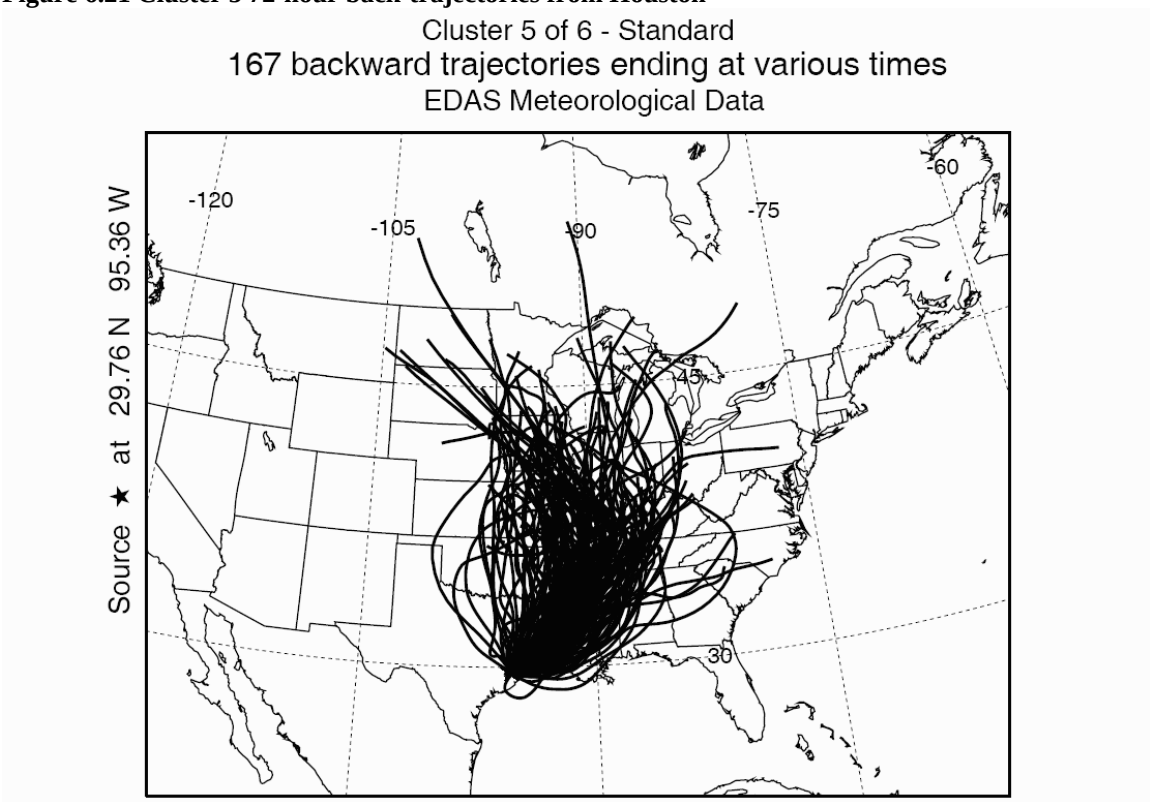

Figure 6.22 Cluster 6 72-hour back-trajectories from Houston

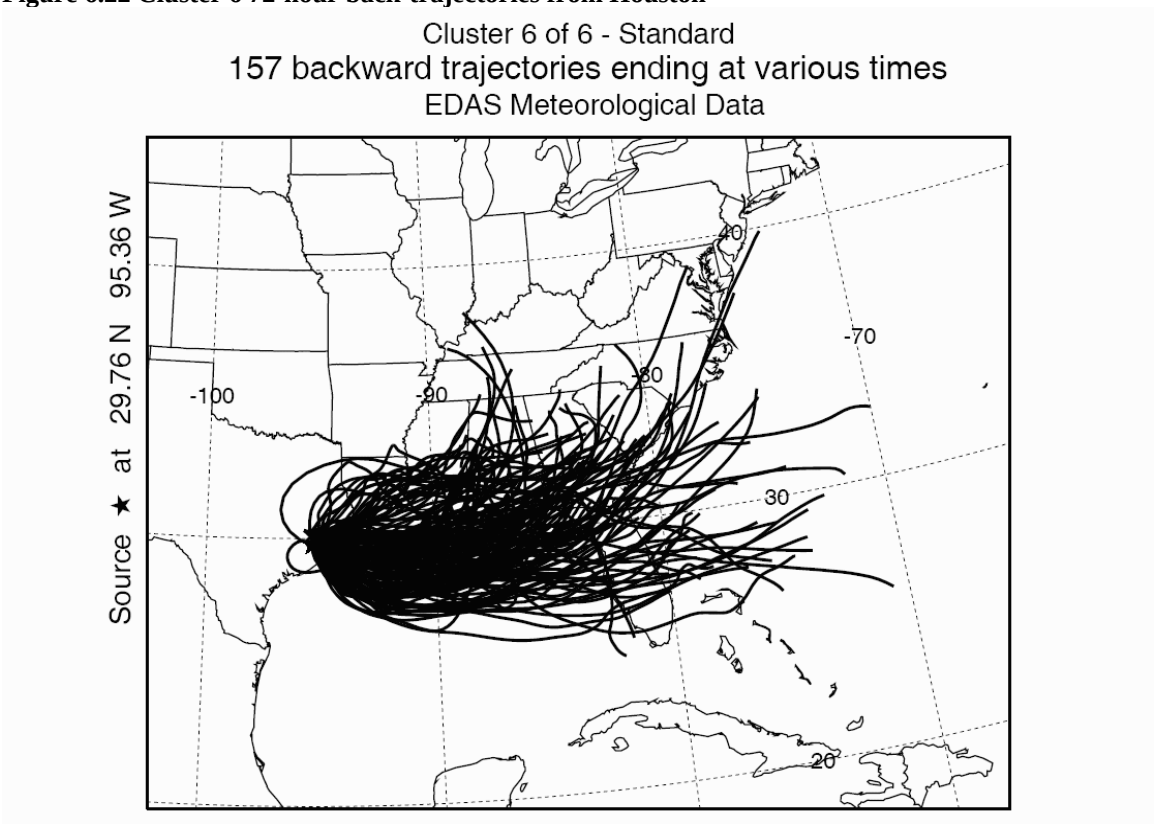

Figure 6.23 Histogram on number of trajectories in each cluster

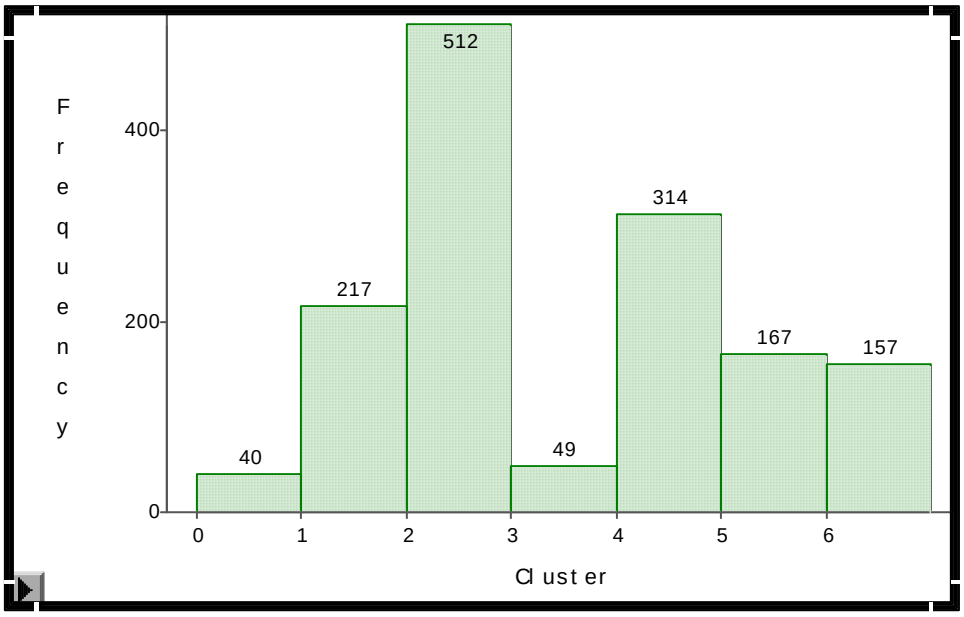

Figure 6.24 Sites used in ozone area max and background determination

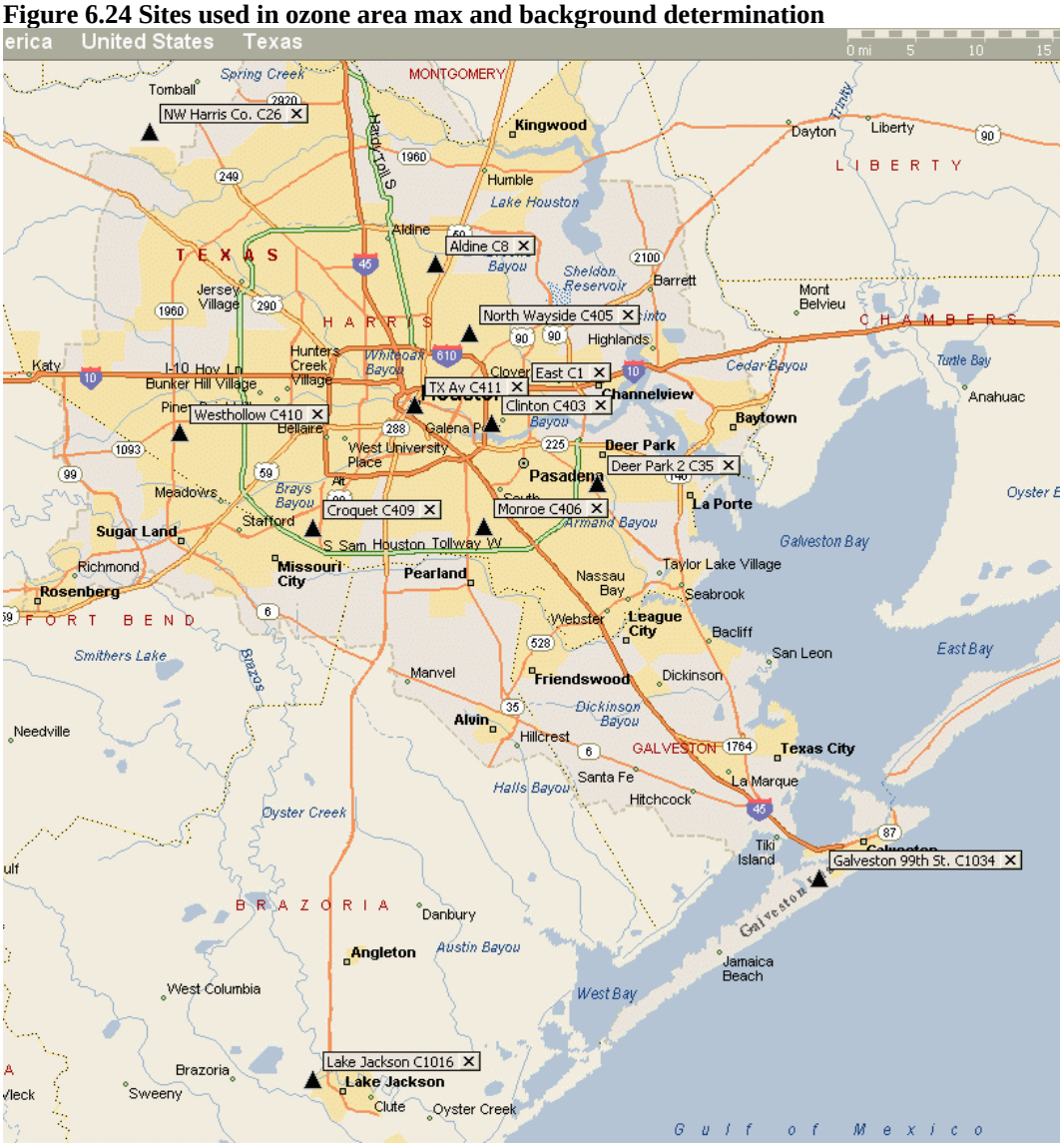

How Trajectory Clustering Works

(This text first appeared in a report under another contract in 2007.) Clustering works by successively combining smaller clusters into larger ones based on some criteria. Initially, all elements (trajectories, in this case) are their own clusters[7]. An individual trajectory has zero "spatial variance." A distance measure between pairs of trajectories is calculated, and the pair closest together according to the distance measure is joined as a cluster, represented by a cluster mean. The process is repeated merging individual trajectories or clusters based on minimizing each step's effect on increasing the total spatial variance (TSV) within all clusters. In the early steps of clustering, the TSV may increase as each new small cluster has variability within it that individual trajectories do not have. At some point the number of clusters will have grown and the change in TSV from step to step becomes small and steady. However, eventually there is a

[7] Stunder, B.J., 1996, "An Assessment of the Quality of Forecast Trajectories," J. Appl. Meteor., 35, 1319–1331.

relatively large jump in TSV, as two dissimilar clusters are joined. Thus, the number of clusters just before the jump is a good choice for total number of factors. In Figure 6.25, a jump occurs from six to five clusters, with another sharp jump from four to three clusters. An examination of the six-cluster results suggests this choice is best at reflecting the diversity of air flows that vary in both direction and length of fetch.

Figure 6.25 Change in total spatial variance by step in cluster process

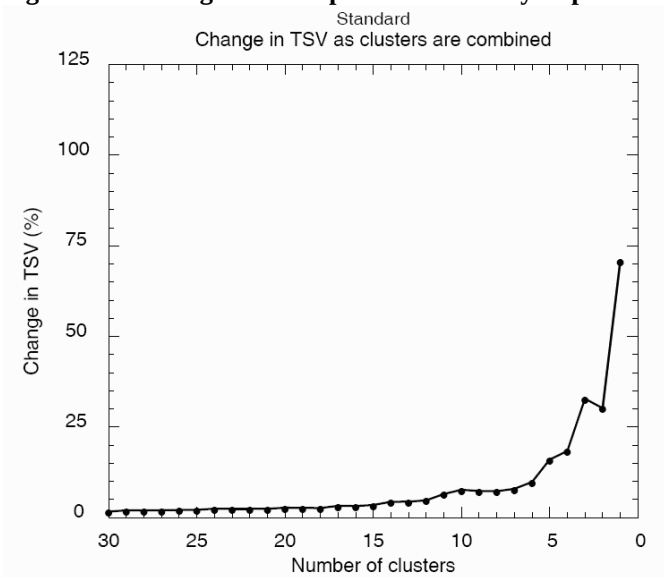

Final Results from Relating HYSPLIT Back-trajectories to Ozone in Houston

Table 6.4 is the statistical summary for the "oz_area_max" and "background" ozone for each day by cluster. The table shows that clusters 4 for "short fetch" and 5 for "northeast fetch" have the highest values for both oz_area_max and background. The average difference between the daily oz_area_max and background data is shown in the "difference mean" column, and the ratio between the difference and the average of oz_area_max and background is shown in the "difference %" column. Although clusters 4 and 5 also have the highest "difference mean", they are in the mid-to-low range in terms of "difference %".

Table 6.4 Statistics for mean area max / min oz8hrpk by HYSPLIT back-trajectory cluster, 2000-2007 data

Cluster	Fetch far	Count	oz_area_max mean	background mean	difference mean	difference %
0	SE	40	45.0	23.8	21.1	61%
1	ESE	217	40.6	21.4	19.1	62%
2	SE	506	48.5	24.8	23.7	65%
3	North	49	59.1	37.2	21.9	45%
4	Short	312	71.6	40.8	30.8	55%
5	NE	166	73.3	45.1	28.1	48%
6	East	151	61.1	35.6	25.5	53%

Table 6.5 shows the results of calculating approximate 95 percent confidence intervals on the mean of area max by cluster. A simple approach was used in selecting two standard errors for the confidence intervals in each row. The table shows the differences between means is statistically significant in most pair-wise comparisons.

Table 6.5 Mean area max approx. 95% confidence intervals, generally not overlapping beyond one or two rows

Cluster ranked by max mean	Fetch	Count	oz8hr_max mean	mean max + 2se	mean max - 2se
1	ESE	217	40.6	42.7	38.5
0	far SE	40	45.0	51.5	38.4
2	SE	506	48.5	50.3	46.6
3	North	49	59.1	65.2	53.0
6	East	151	61.1	64.5	57.8
4	Short	312	71.6	74.3	68.9
5	NE	166	73.3	76.7	69.8

Care was taken in selecting the 12 ozone monitoring sites used in the assessment to maximize the inclusion of clear upwind and downwind monitoring sites. The Harris NW CAMS 26, the Lake Jackson / Clute combined site pair, and the Galveston Airport / 99th St combined site pair generally represent the background sites, with sites on the downwind side of the urban core and ship channel generally representing the area max sites. However, the true "background" ozone may be farther away in a more rural area on many days, and true area max may be underestimated. Nevertheless, the large number of observations used in this assessment makes clear that both the observed area max and observed area min are affected by the back-trajectories. Figure 6.26 shows that the relationship between area min and max by cluster is linear and significant ($p<0.01$). This suggests that the trajectory cluster is a factor in severity for <u>both</u> the area max and the area background.

Figure 6.26 also shows that the difference between area max and min is also roughly linear with area max, but with a lower slope and overall statistical significance ($p=0.03$). This second graph on difference may suggest the local contribution may also be related to back trajectories. An explanation for this is that the slower air movement of the "short" cluster 4 allows greater accumulation in the area under lower local surface wind speeds. Another explanation for "east" cluster 6 and "NE" cluster 5 is that winds from these directions help to move surface air along the ship channel region and across the central city, an alignment of winds and sources shown in the TexAQS II Rapid Science Synthesis (RSS) report to lead to very high ozone readings.

The bottom line is that variation in synoptic scale back trajectories can account for around 24 ppb of variation in background concentrations and around 33 ppb in area max on average (comparing Cluster 1 and Cluster 5 results).

Figure 6.26 Relationship between mean max and mean min (background) by cluster, and relationship between "local contribution" (difference max – min) by cluster

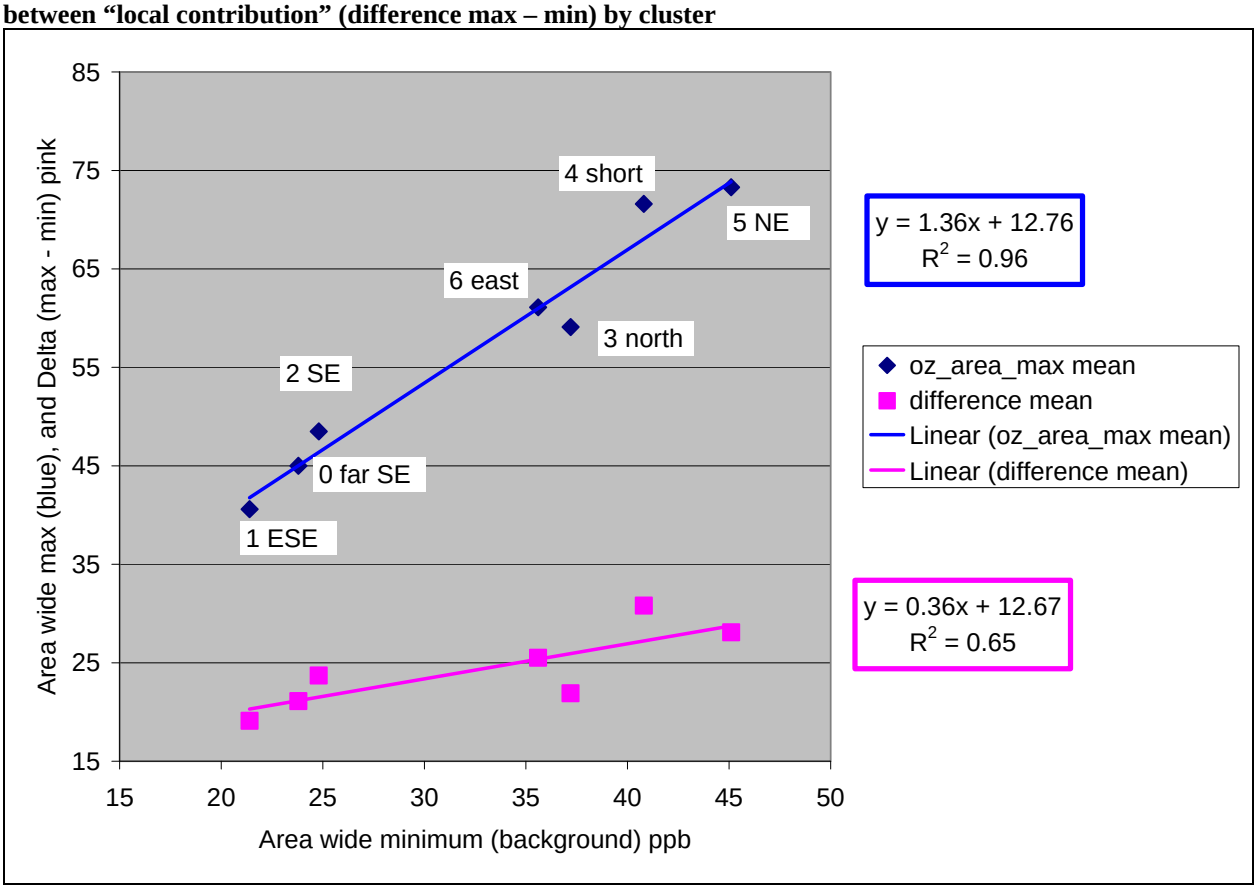

6.2.3 Factor Analysis to Assess Air-shed Delineations

In an early report on this project, a factor analysis using historical ozone data (1995-2007) was used to delineate geographic areas with distinct ozone concentration behavior. Later this analysis re-done using data from 2005-2007. As was the case in the earlier model, only data from May through October were used. The total number of days available over the three year period is 552. The number of days that could be used based on the data completeness thresholds tests was 306. The long-term (1995-2007) data provided for 43 counties to contribute to the factor analysis. In the more recent data model, 71 counties provide data. These include relatively new monitoring in counties surrounding the Dallas-Fort Worth urban core, monitors sited for the TexAQS II study, relatively new monitors in other Region 6 states, and the Big Bend site in West Texas. Some TexAQS II sites were excluded for low data counts.

The 2005-2007 analysis suggests seven factors

- West Texas/ Southern New Mexico
- Northern New Mexico
- Oklahoma
- Arkansas
- Southern Louisiana and southeast Texas
- South Texas
- East Texas.

The best results were reached with an oblique "quartimin" rotation. A table of the rotated factor loadings with geographic labels appears in Table 6.6. The table is organized to group counties with similar loadings on a given factor. Cells are color-coded by loading – yellow for 0.30-0.50, orange for 0.50-0.70, and red for greater than 0.70. As should be expected, significant overlap exists, and some counties (e.g., Montgomery-48339 and Harris-48201) clearly settle in two or three. A map of EPA Region 6 illustrating the counties listed above with the clusters of factors found appears in Figure 6.27. Ovals are drawn to represent the large uncertainty in actual air shed boundaries and the considerable overlap across factors for many counties as seen in the factor loadings in Table 6.6.

Table 6.6 Rotated factor loadings for EPA R6 counties

Region ->	S. LA - SE TX	OK	S. TX	E. TX	AR	S. NM	N. NM	Color
County	Factor 1	Factor 2	Factor 3	Factor 4	Factor 5	Factor 6	Factor 7	
_22095	0.95	0.19	0.34	0.30	0.39	0.06	0.00	
_22063	0.94	0.18	0.28	0.24	0.39	0.08	-0.02	
_22033	0.94	0.19	0.26	0.21	0.44	0.13	-0.03	
_22093	0.94	0.23	0.43	0.35	0.39	0.04	-0.07	
_22047	0.94	0.23	0.42	0.38	0.46	0.04	-0.08	
_22057	0.93	0.20	0.46	0.37	0.40	0.01	-0.08	
_22121	0.93	0.21	0.26	0.22	0.44	0.13	-0.05	
_22055	0.90	0.35	0.48	0.50	0.52	0.14	-0.08	
_22005	0.90	0.16	0.21	0.24	0.35	0.03	0.02	
_22089	0.90	0.13	0.37	0.31	0.35	0.01	0.03	
_22077	0.89	0.18	0.28	0.17	0.42	0.10	-0.05	
_22051	0.88	0.13	0.33	0.25	0.34	0.03	-0.06	
_22019	0.82	0.33	0.60	0.57	0.52	0.11	-0.10	
_48361	0.81	0.29	0.58	0.59	0.49	0.07	-0.07	
_22073	0.76	0.44	0.32	0.51	0.70	0.17	-0.08	
_48245	0.74	0.33	0.68	0.65	0.46	0.02	-0.06	
_48339	0.67	0.32	0.51	0.49	0.34	0.19	-0.12	
_40109	0.30	0.95	0.36	0.52	0.53	0.24	0.07	
_40017	0.28	0.93	0.37	0.55	0.48	0.20	0.07	
_40027	0.29	0.93	0.37	0.54	0.46	0.26	0.06	
_40087	0.24	0.92	0.34	0.56	0.42	0.21	0.05	
_40143	0.25	0.92	0.29	0.48	0.68	0.21	0.10	
_40071	0.32	0.89	0.29	0.43	0.59	0.28	0.04	
_40037	0.23	0.87	0.27	0.45	0.60	0.08	0.00	
_40031	0.24	0.86	0.36	0.66	0.38	0.34	0.13	
_40043	0.25	0.85	0.37	0.49	0.40	0.38	0.12	
_40021	0.31	0.83	0.28	0.39	0.79	0.25	0.08	
_40097	0.29	0.83	0.27	0.37	0.74	0.26	0.04	
_40121	0.38	0.83	0.34	0.52	0.72	0.13	-0.01	
_40115	0.31	0.82	0.26	0.37	0.74	0.27	0.10	
_48121	0.38	0.78	0.32	0.79	0.58	0.27	0.01	
_48367	0.29	0.76	0.53	0.79	0.43	0.27	-0.01	
_48439	0.32	0.75	0.44	0.87	0.51	0.22	-0.01	
_48113	0.36	0.74	0.45	0.88	0.54	0.24	-0.02	
_48397	0.42	0.74	0.46	0.83	0.60	0.23	-0.07	
_48085	0.41	0.73	0.33	0.78	0.62	0.21	-0.02	
_48231	0.42	0.73	0.41	0.81	0.64	0.18	-0.15	
_48221	0.31	0.70	0.61	0.82	0.39	0.24	-0.03	
_48139	0.37	0.69	0.54	0.88	0.47	0.22	-0.04	
_48251	0.31	0.68	0.52	0.84	0.42	0.20	-0.04	
_48257	0.45	0.68	0.53	0.82	0.60	0.17	-0.06	
_48423	0.50	0.62	0.54	0.82	0.63	0.08	-0.15	
_48183	0.58	0.60	0.46	0.77	0.71	0.16	-0.08	
_48201	0.63	0.40	0.69	0.75	0.44	0.03	-0.08	
_48355	0.34	0.27	0.93	0.42	0.16	-0.03	-0.15	
_48215	0.36	0.28	0.93	0.34	0.21	0.16	-0.10	
_48469	0.44	0.39	0.93	0.58	0.28	0.08	-0.15	
_48061	0.33	0.21	0.90	0.21	0.13	0.07	-0.11	
_48479	0.29	0.30	0.89	0.27	0.13	0.24	-0.07	
_48029	0.39	0.49	0.87	0.60	0.28	0.17	-0.12	
_48209	0.43	0.50	0.83	0.69	0.32	0.14	-0.15	
_48453	0.42	0.52	0.80	0.71	0.37	0.13	-0.12	
_48039	0.55	0.36	0.80	0.69	0.36	-0.02	-0.11	
_48167	0.58	0.28	0.73	0.63	0.34	-0.06	-0.06	
_22015	0.68	0.49	0.35	0.58	0.79	0.18	-0.07	
_40001	0.35	0.79	0.34	0.41	0.82	0.20	-0.01	
_22017	0.58	0.48	0.29	0.56	0.80	0.12	-0.17	
_48203	0.62	0.54	0.29	0.61	0.78	0.14	-0.14	
_05101	0.36	0.47	0.28	0.28	0.84	0.07	-0.04	
_05119	0.53	0.54	0.21	0.45	0.87	0.21	0.11	
_05113	0.34	0.54	0.16	0.43	0.77	0.11	-0.07	
05035	0.52	0.39	0.12	0.24	0.77	0.25	0.21	
_35015	0.01	0.22	0.07	0.06	0.08	0.87	0.42	
_35013	0.05	0.14	0.10	0.10	0.07	0.85	0.50	
_35025	0.11	0.36	0.08	0.15	0.16	0.83	0.32	
_48141	0.01	0.05	0.00	0.01	0.09	0.81	0.47	
_35017	0.11	0.15	0.14	0.09	0.04	0.77	0.57	
_48043	0.23	0.22	0.50	0.07	0.16	0.64	0.27	
_35043	0.01	0.23	-0.04	0.07	0.05	0.59	0.91	
_35001	-0.07	0.18	-0.12	0.00	0.02	0.59	0.90	
_35045	-0.01	0.10	-0.09	-0.07	0.08	0.38	0.90	

Figure 6.27 EPA R6 regional ozone factors 2005-2007 data

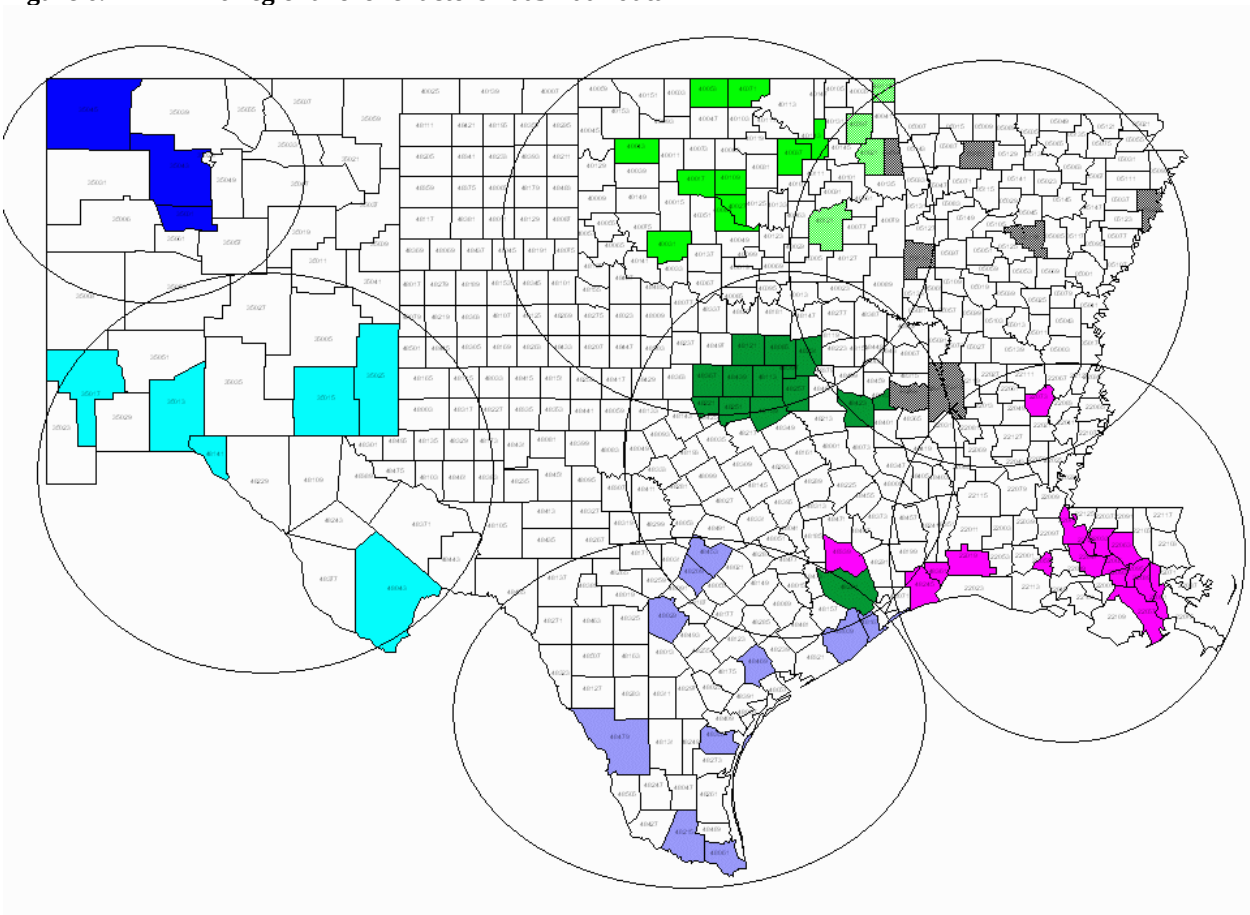

6.2.4 GLM Development

The first step in the development of the model following the EPA Camalier et al. method is to examine the relationship between the chosen ozone variable and the meteorological data. The correlations were discussed in section 6.2.1. Recalling the graphs in Figures 6.8 – 6.10 that showed "l_oz8" versus "trandis", rhavgmid", and "tdelta". In each of these, a linear fit was applied. A "linear" fit is one instance of a model that is a smooth and connected curve. Many data analysts are familiar with other examples of fitting models; e.g., quadratic fits. A more general method of modeling is to use splines. Splines in general are collections of functions, usually polynomials, fit to segments of the data and connected such that the y-value and first and second derivatives of the conjoining functions are equal. One example of this approach appears in Figure 6.28. In selecting a spline model, a user must consider trade-offs between smoothness and the model fit. The number and location of "knots" that are the endpoints of the connected model segments are user controlled. SAS spline calculations are predicated on balancing the improved fit against the increased roughness in the curve using a penalty function incorporated into the ordinary least squares objective function.

Figure 6.28 Generic example of a spline model fit to data

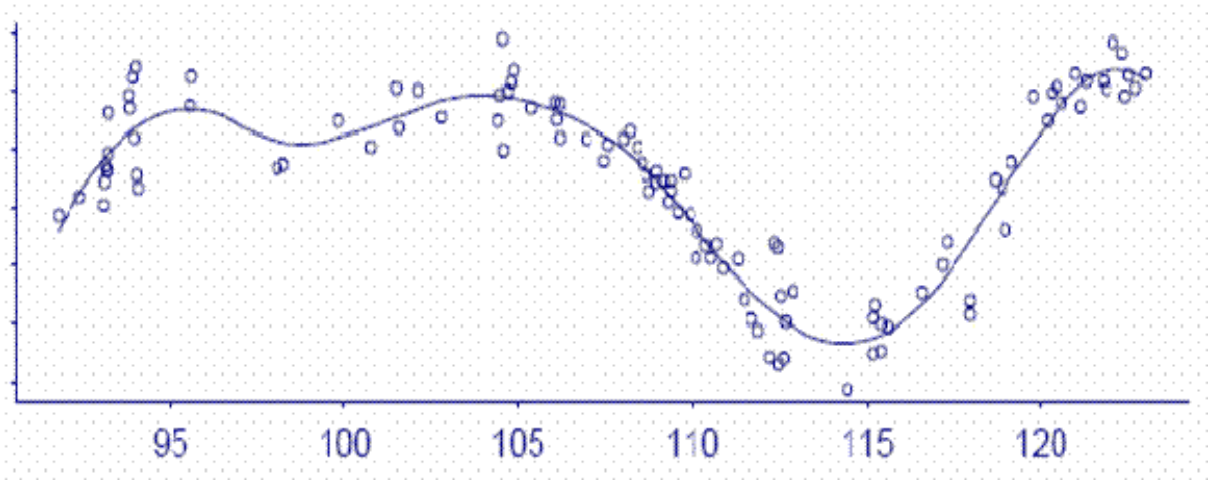

The approach we follow in this project is a general linear model in the sense that we assume a log-link function for ozone and do not assume normality for the independent variables. The implementation in SAS is via PROC TRANSREG (transformation regression). This procedure fits linear models, optionally with spline and other nonlinear transformations, in "simple, multiple, and multivariate regression with variable transformations."[8] More details on the approach we use will be provided in the training class, and a more detailed written element can be added upon request.

[8] SAS 9.1 PROC TRANSREG documentation.

6.2.5 Results

The GLM model used by Camalier, Cox, and Dolwick and found on the EPA Trend Website coded in the R programming language was approximately recoded in SAS. Only an approximate match was achieved with the Cincinnati, OH test data on the EPA Trends Website, but it was judged to be acceptable. A comparison based on using data posted on the EPA Tend Web site for Cincinnati, OH appears in Figure 6.29.

Figure 6.29 PROC TRANSREG results for EPA Trend Website Cincinnati, OH data compared with R-code results

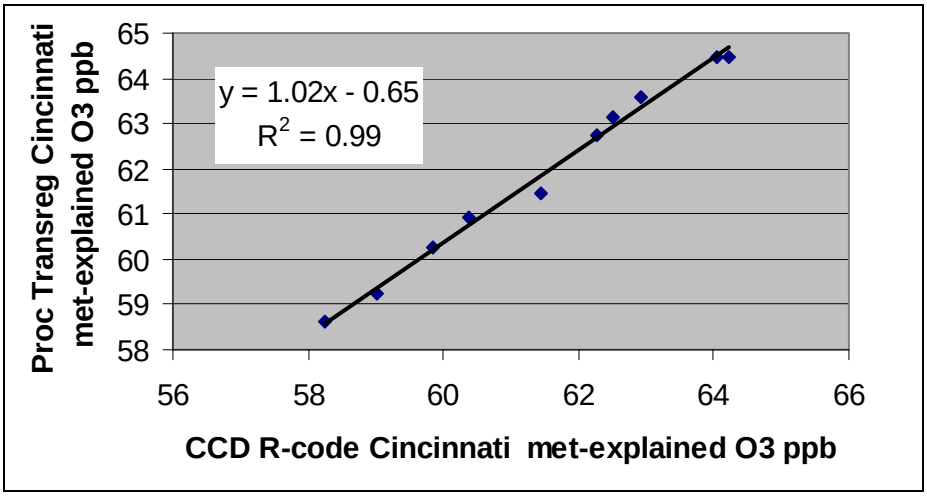

The exact nature of the GLM procedure in R and the algorithmic match in SAS was investigated by examining documentation on PROCs TRANSREG, GLM, GAM (experimental), and GLIMIX (experimental). Accuracy of results and ease of use argued for TRANSREG.

The graphs showing the annual time series for annual mean 8-hour daily max and annual mean ozone as a function of meteorology appear in even-numbered Figures 6.30 – 6.44. The odd-numbered Figures 6.31 – 6.45 show the result of subtracting the meteorologically-produced ozone from the actual ozone. This, we posit, is the sum of anthropogenic factors, model error, and undiagnosed meteorological factors. If we assume the model error and undiagnosed meteorological factors are relatively constant over time, then the trends in the odd-numbered figures represent the effect of chemical emissions reductions.

The statistical results are summarized in Table 6.7 following the graphs**. The bottom line is that after adjusting for meteorology, concentrations of ozone have declined significantly in the Dallas-Fort Worth and Houston areas. All else held equal, one would expect from around 6 ppb lower 8-hour daily maxima in DFW in 2007 vs. 1996, and around 9 ppb lower 8-hour daily maxima in HGB in 2007 vs. 1996. Other areas do not show significant trends over the same period.**

Figure 6.30 Austin-Round Rock actual annual summer-mean and meteorologically-adjusted time series

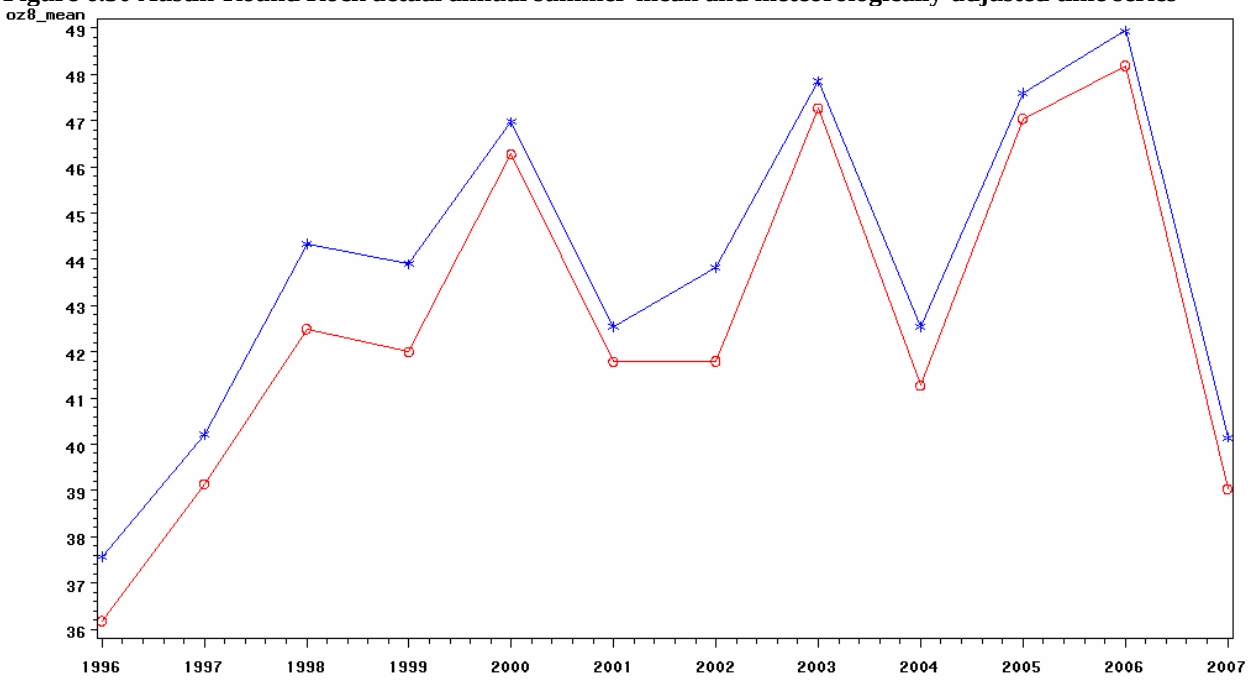

Figure 6.31 Austin-Round Rock residual meteorologically-adjusted trend model

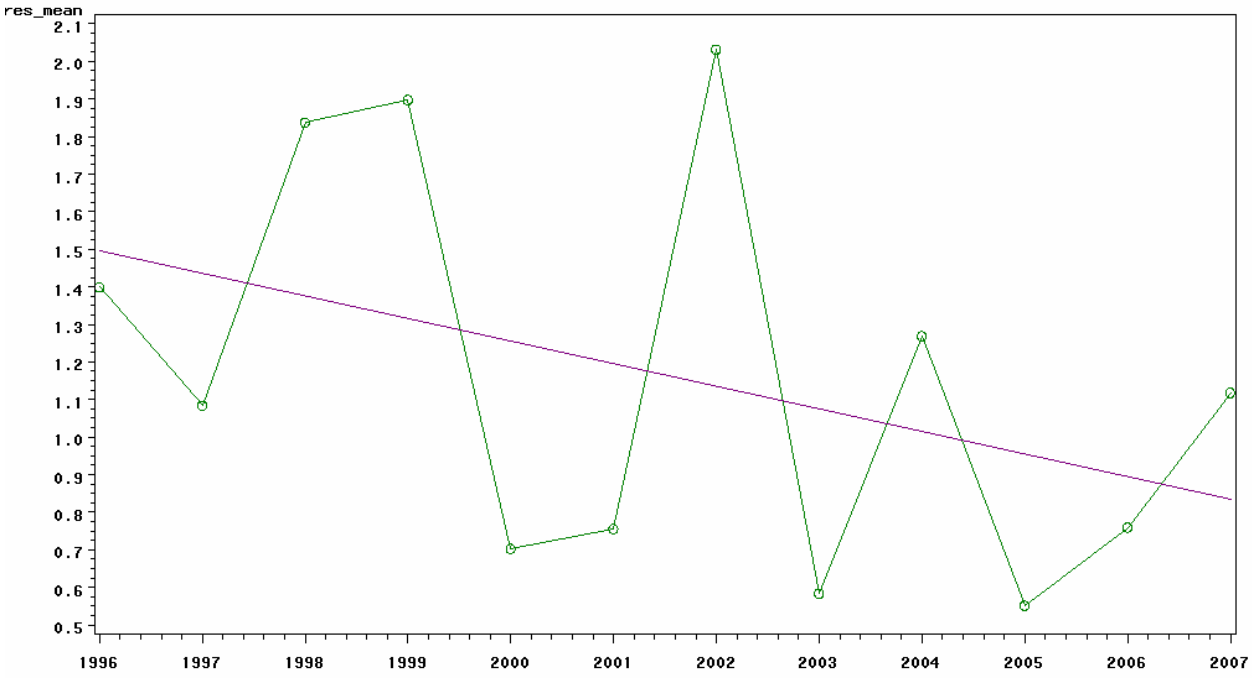

Figure 6.32 Beaumont-Port Arthur actual annual summer-mean and meteorologically-adjusted time series

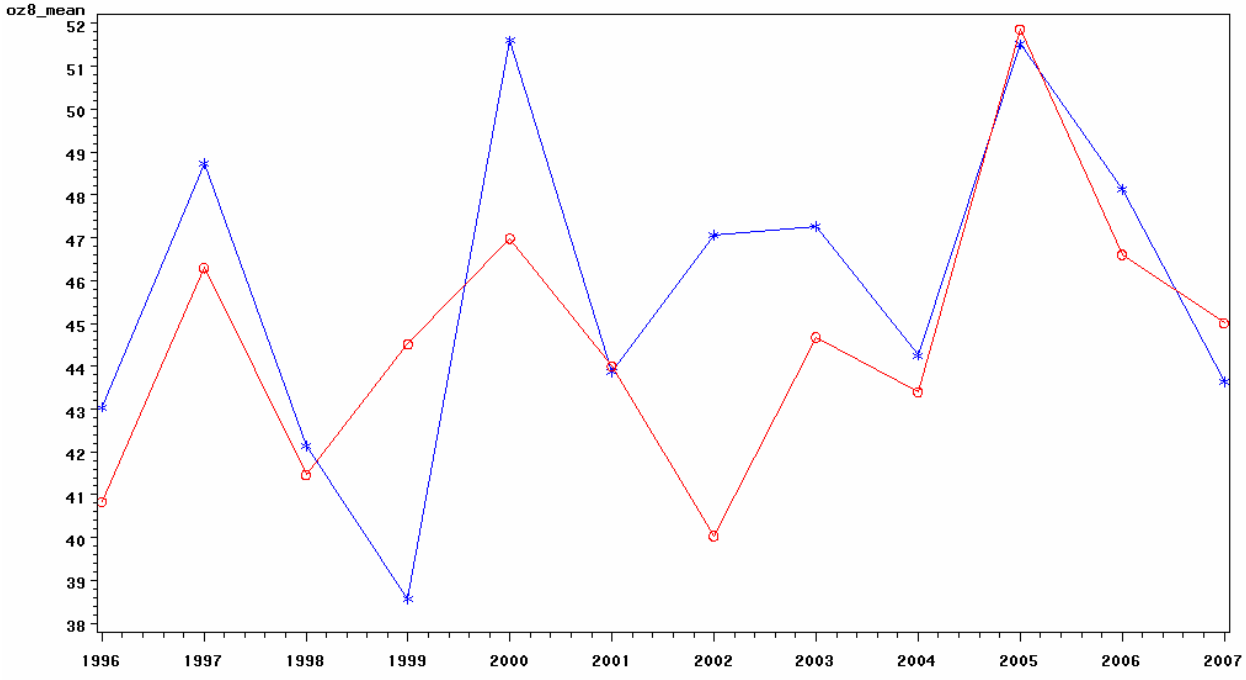

Figure 6.33 Beaumont-Port Arthur residual meteorologically-adjusted trend model

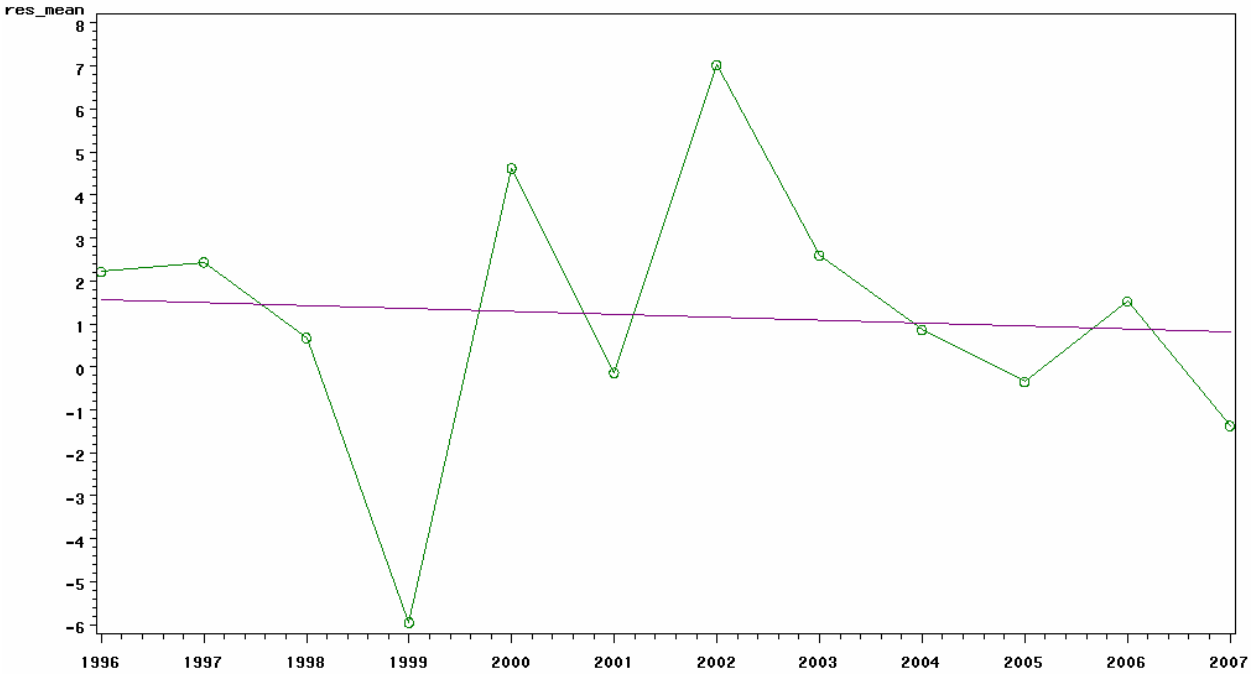

Figure 6.34 Corpus Christi actual annual summer-mean and meteorologically-adjusted time series

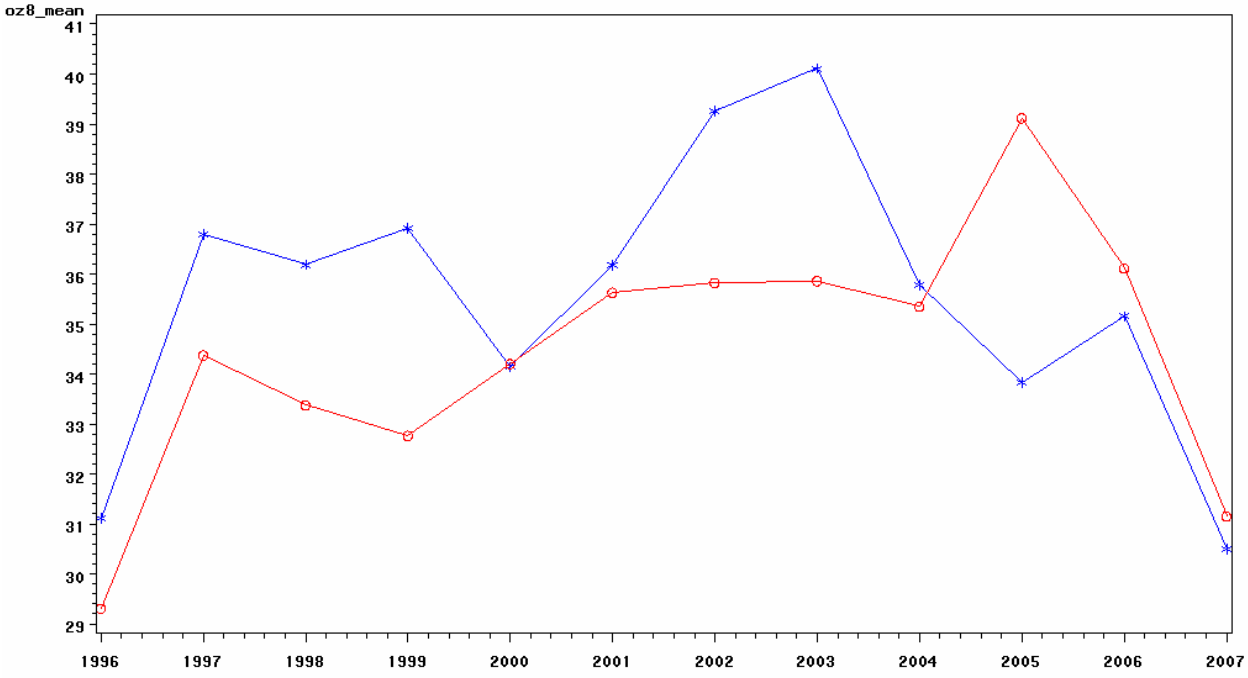

Figure 6.35 Corpus Christi residual meteorologically-adjusted trend model

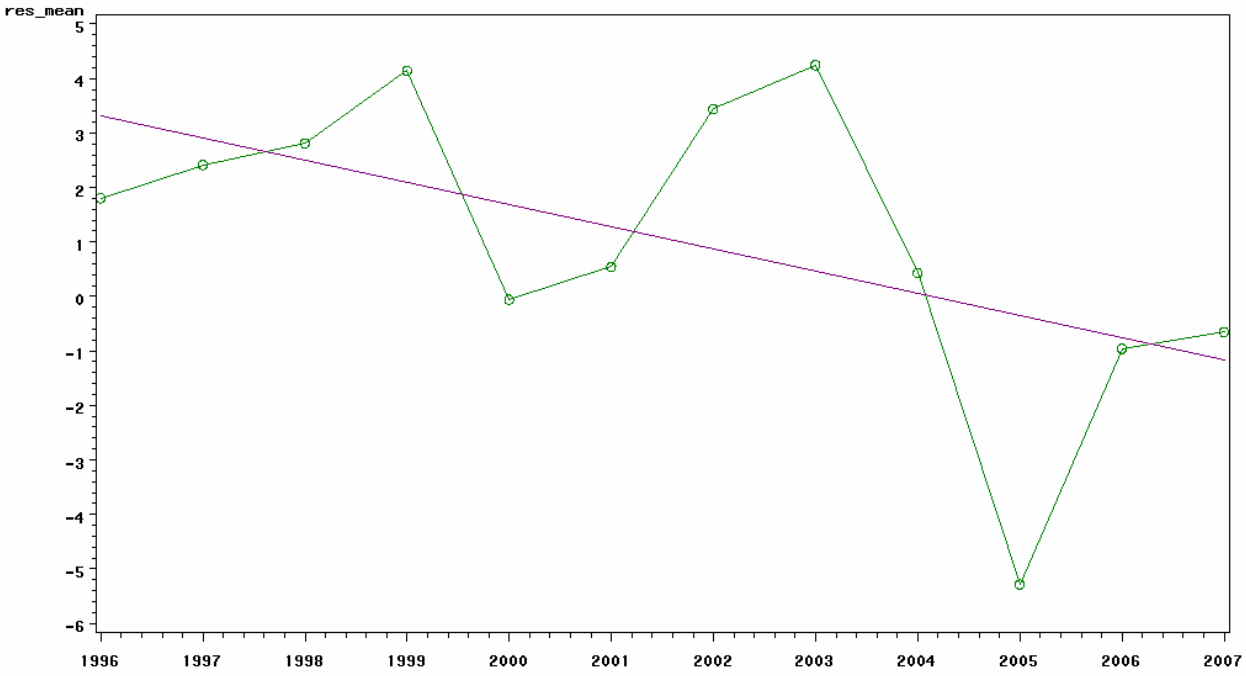

Figure 6.36 Dallas-Fort Worth actual annual summer-mean and meteorologically-adjusted time series

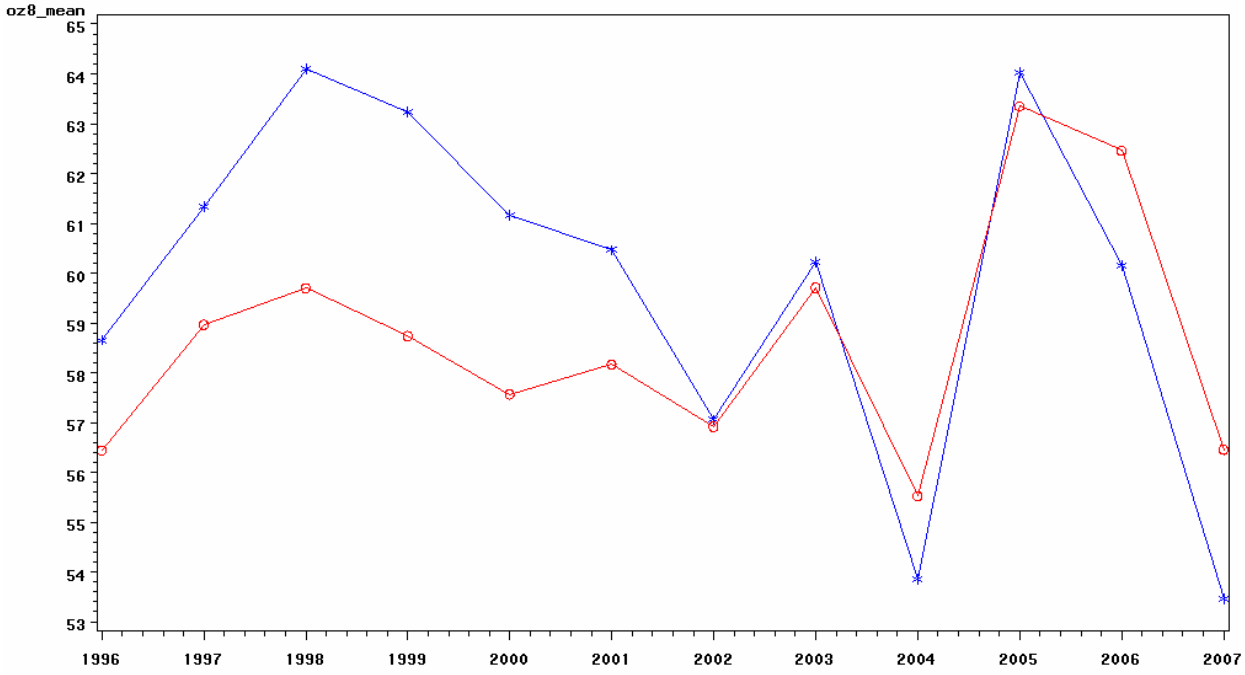

Figure 6.37 Dallas-Fort Worth residual meteorologically-adjusted trend model

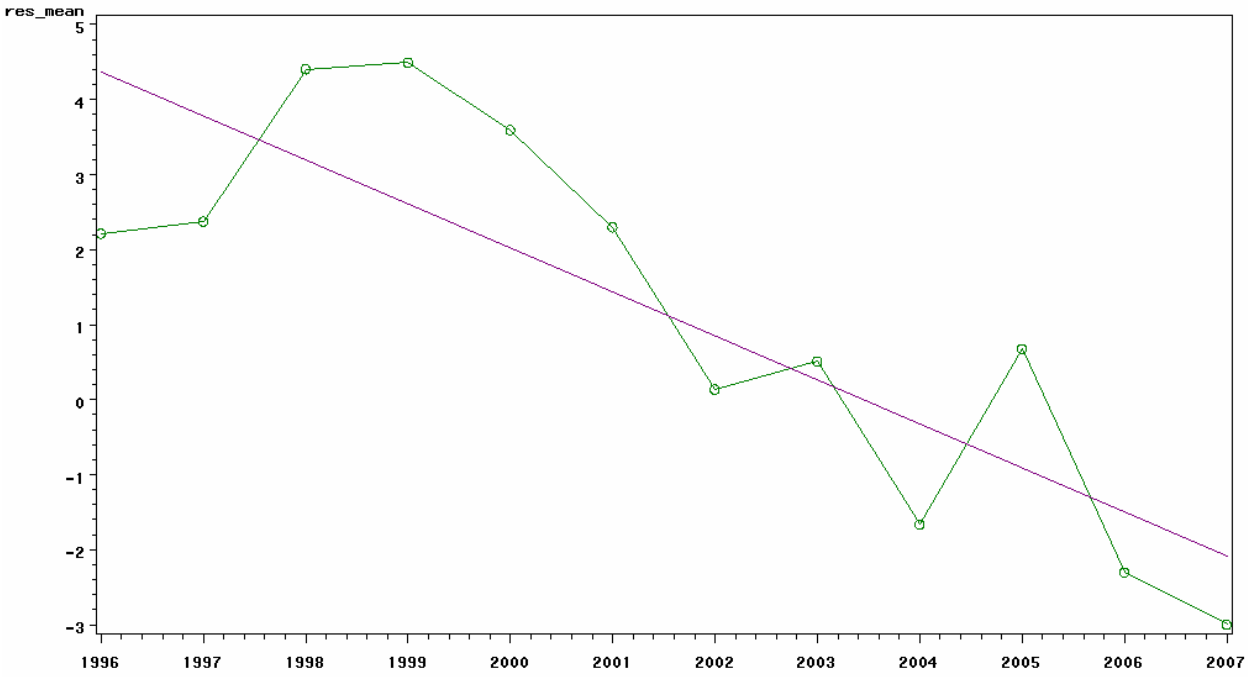

Figure 6.38 El Paso actual annual summer-mean and meteorologically-adjusted time series

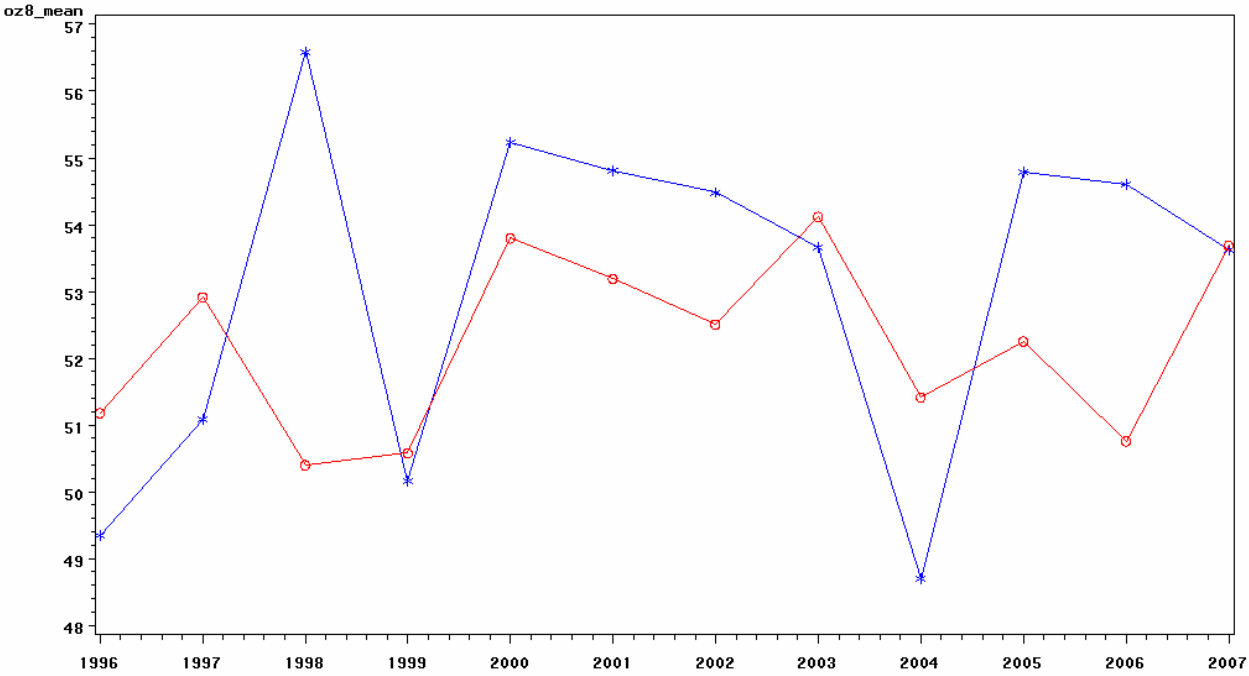

Figure 6.39 El Paso residual meteorologically-adjusted trend model

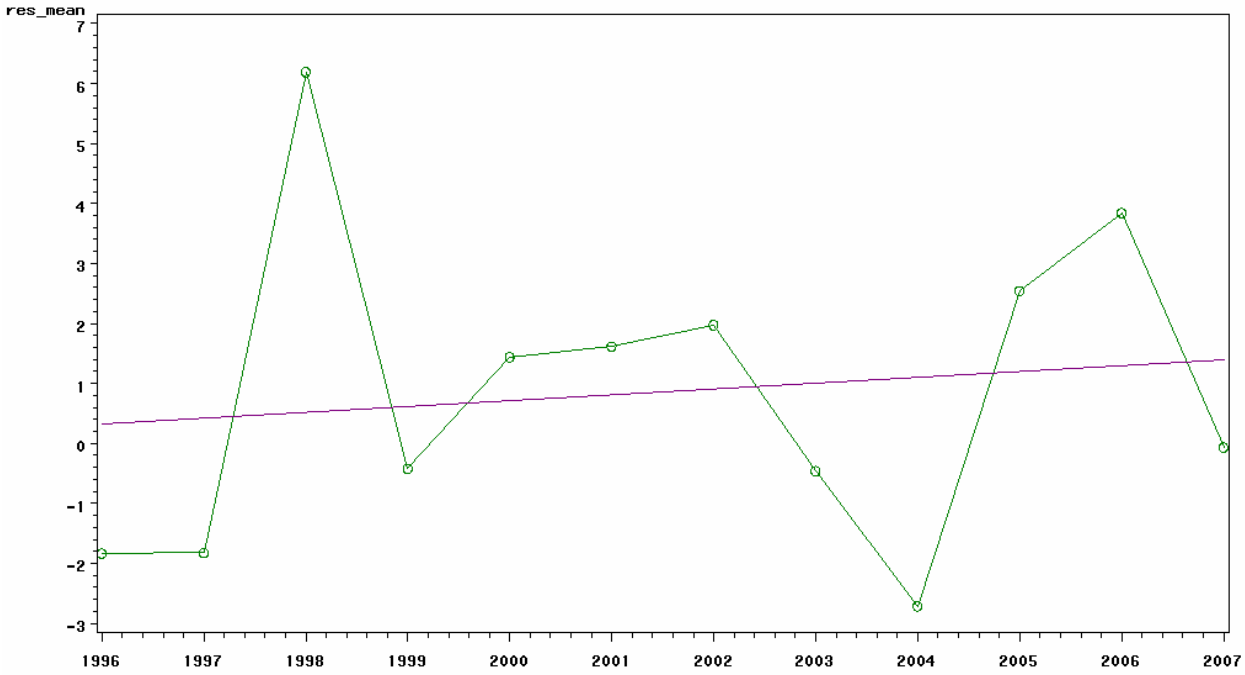

Figure 6.40 Houston-area actual annual summer-mean and meteorologically-adjusted time series

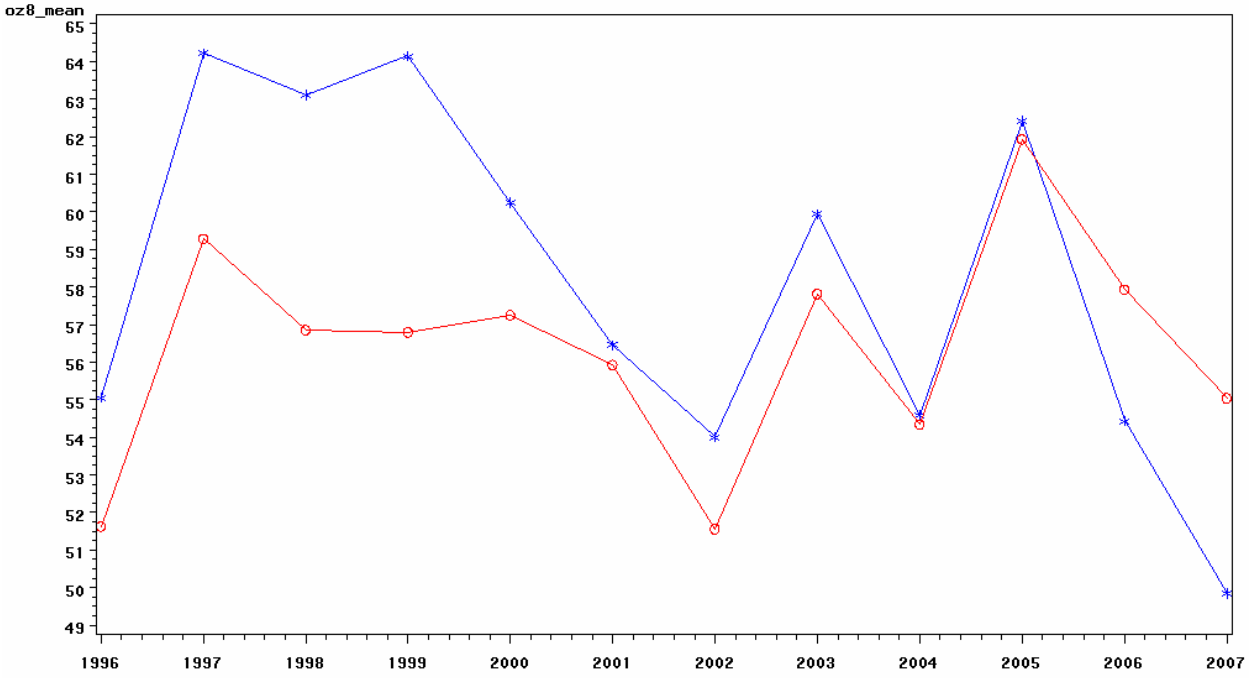

Figure 6.41 Houston-area residual meteorologically-adjusted trend model

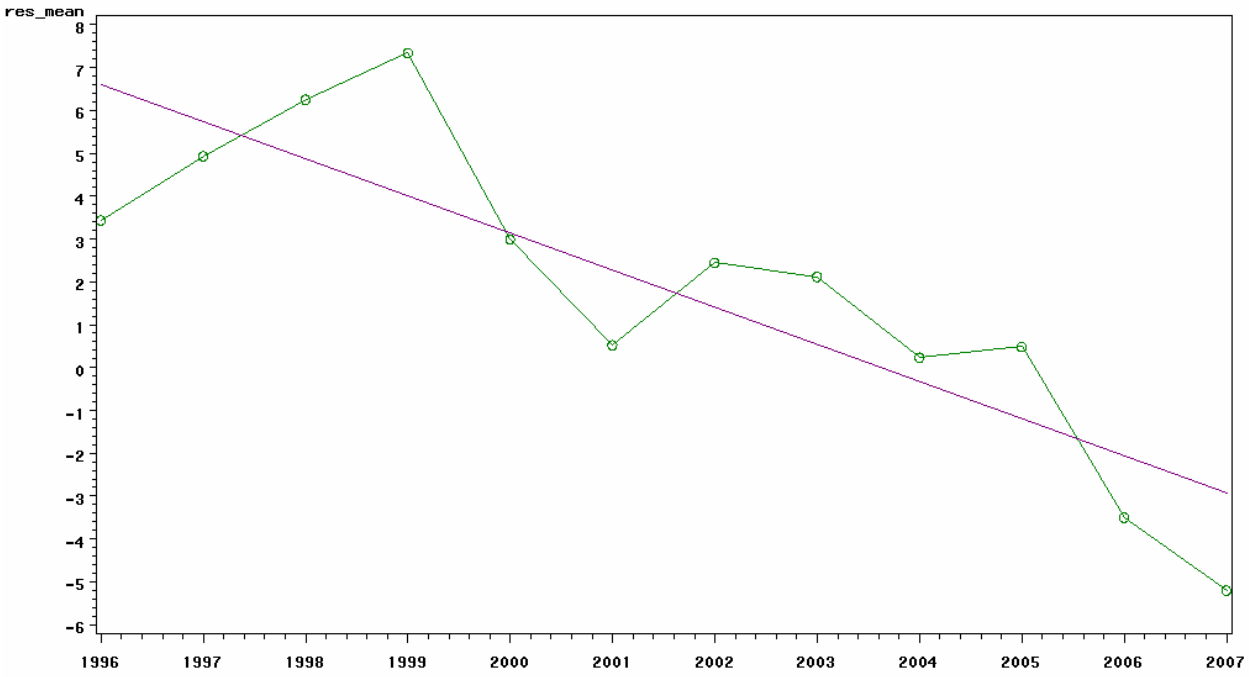

Figure 6.42 San Antonio actual annual summer-mean and meteorologically-adjusted time series

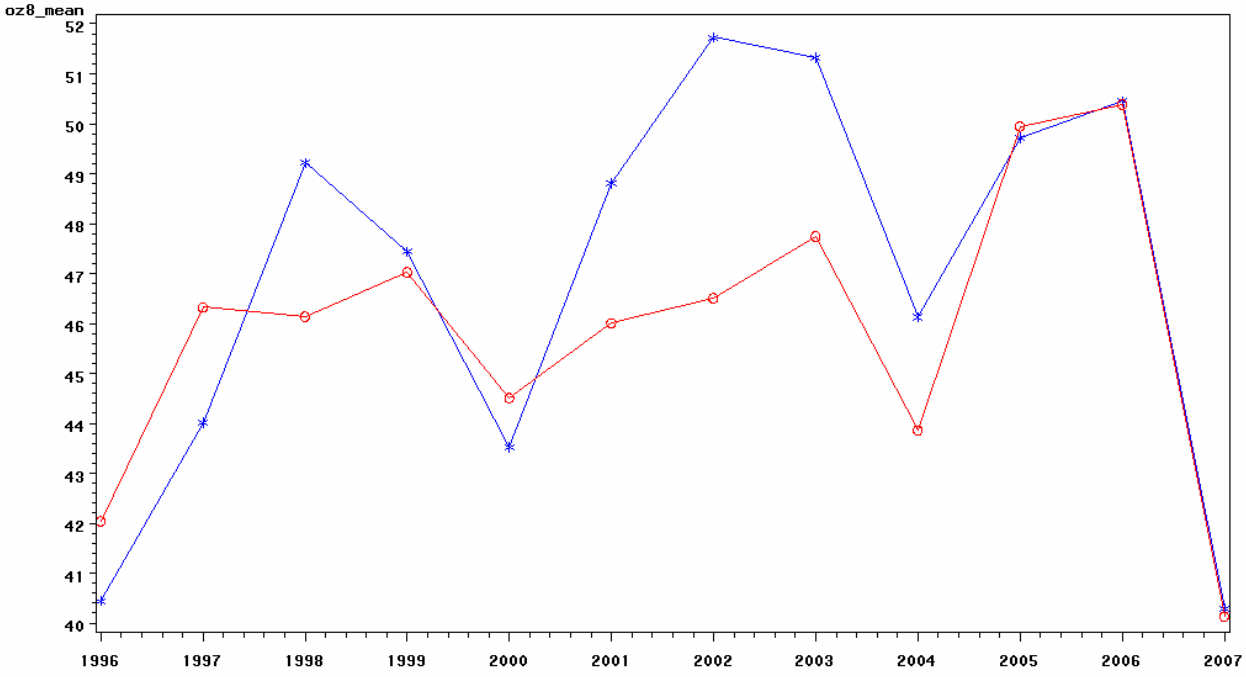

Figure 6.43 San Antonio residual meteorologically-adjusted trend model

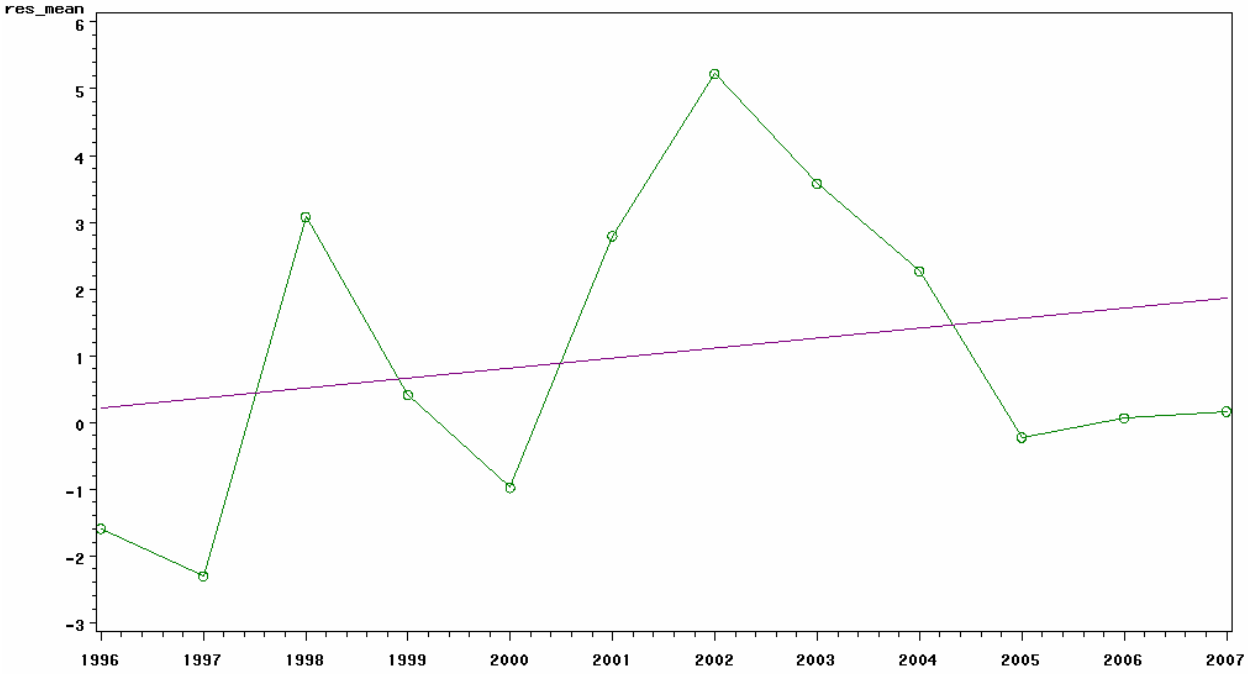

Figure 6.44 Victoria actual annual summer-mean and meteorologically-adjusted time series

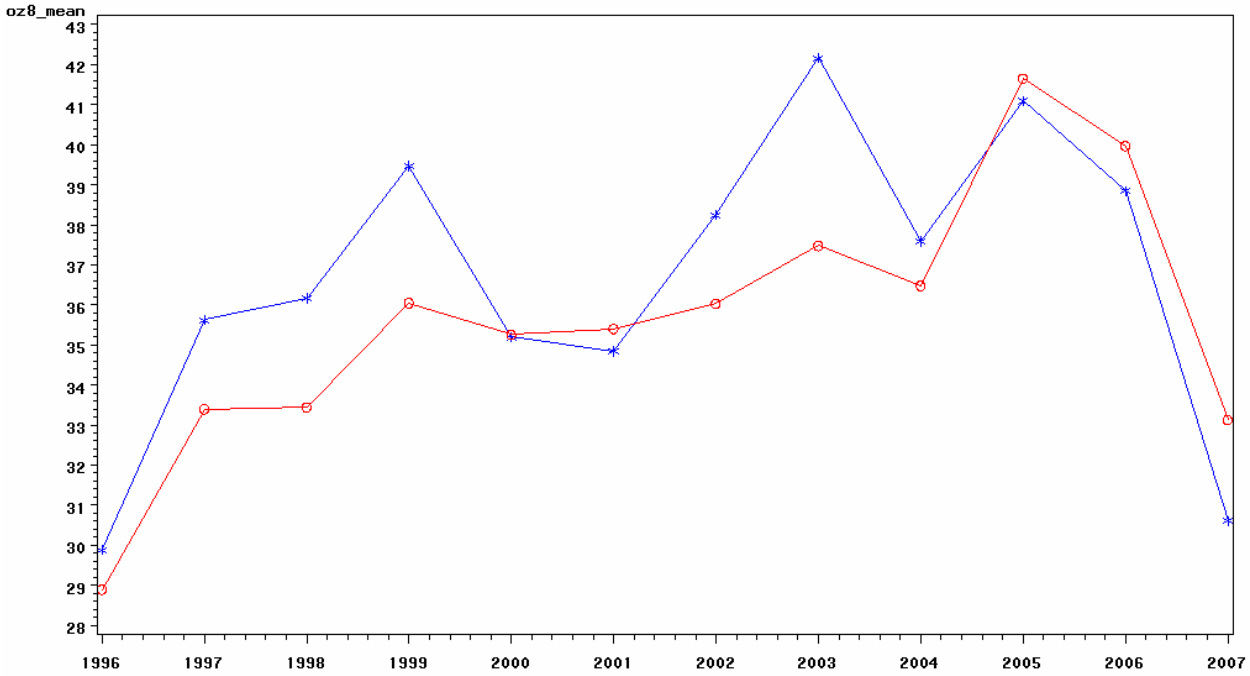

Figure 6.45 Victoria residual meteorologically-adjusted trend model

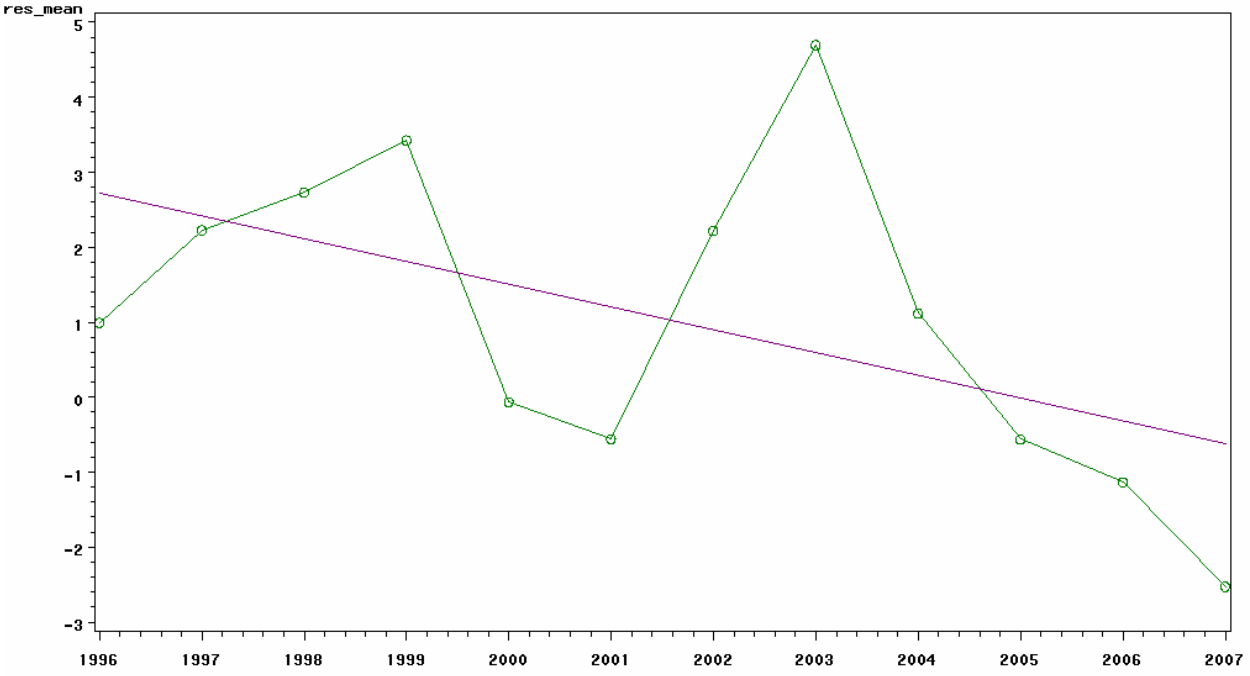

Table 6.7 Summary statistics for met-adjusted ozone trends1996-2007, red values statistically significant

Location	**Intercept**	Slope	t	P-value	Lag 1 Coef.	t
Austin	0.369	0.16	1.43	0.19	0.30	0.95
Beaumont	1.445	-0.04	-0.18	0.86	0.22	0.68
Corpus Christi	3.239	-0.40	-1.73	0.12	-0.13	-0.39
Dallas	**4.244**	**-0.57**	**-3.92**	**0.00**	**-0.20**	**-0.60**
El Paso	0.400	0.09	0.46	0.66	0.20	0.61
Houston	**6.438**	**-0.86**	**-4.20**	**0.00**	**-0.20**	**-0.63**
San Antonio	0.076	0.15	0.59	0.57	-0.32	-1.01
Victoria	2.624	-0.31	-1.54	0.16	-0.27	-0.83

The analyses for Dallas , Houston, and El Paso have been re-run with the addition of morning NOx and hydrocarbons from the PAMS monitoring stations in these cities as predictor variables in the model, along with the same meteorological variables as in the previous analysis. The following figures show the results in a format similar to that above. Note that the strength of the regressions shown in Table 6.8 has been weakened as more of the factors causing ozone have been explained.

Figure 6.46 Dallas actual annual summer-mean and meteorologically and precursor predicted time series

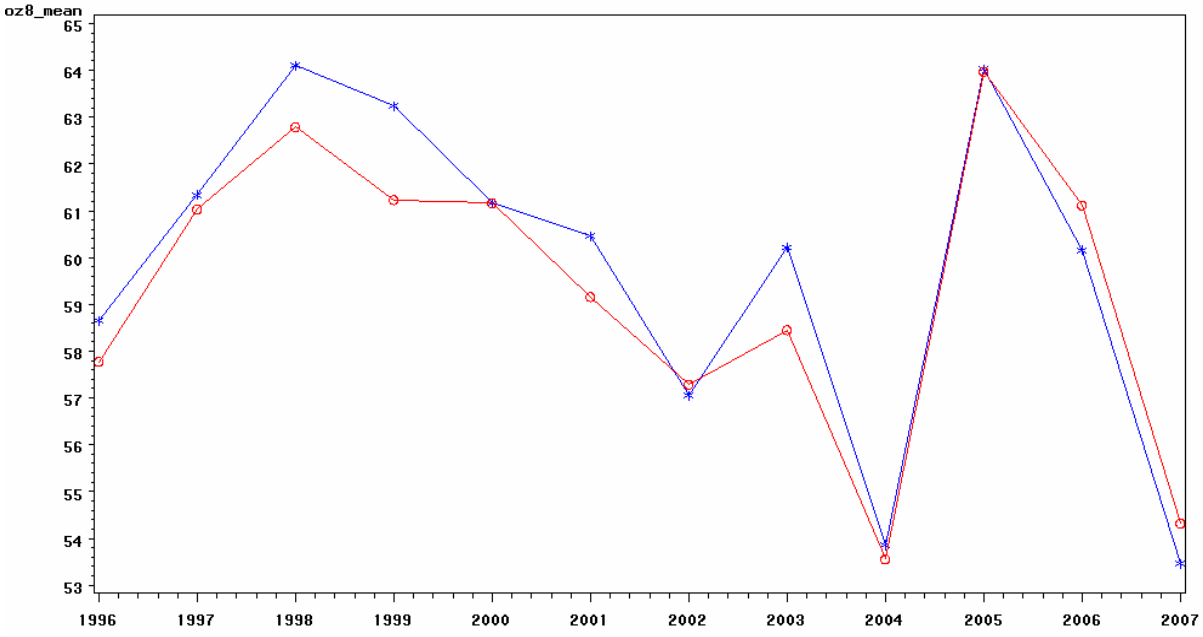

Figure 6.47 Dallas residual meteorologically and precursor adjusted trend model

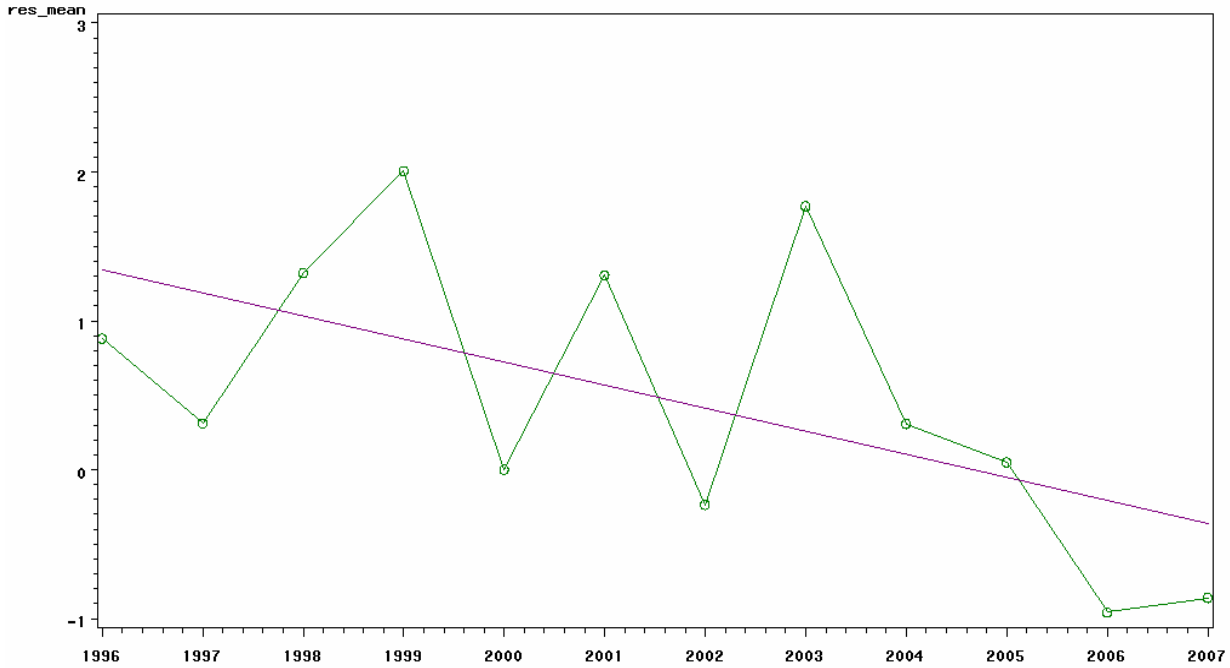

Figure 6.48 El Paso actual annual summer-mean and meteorologically and precursor predicted time series

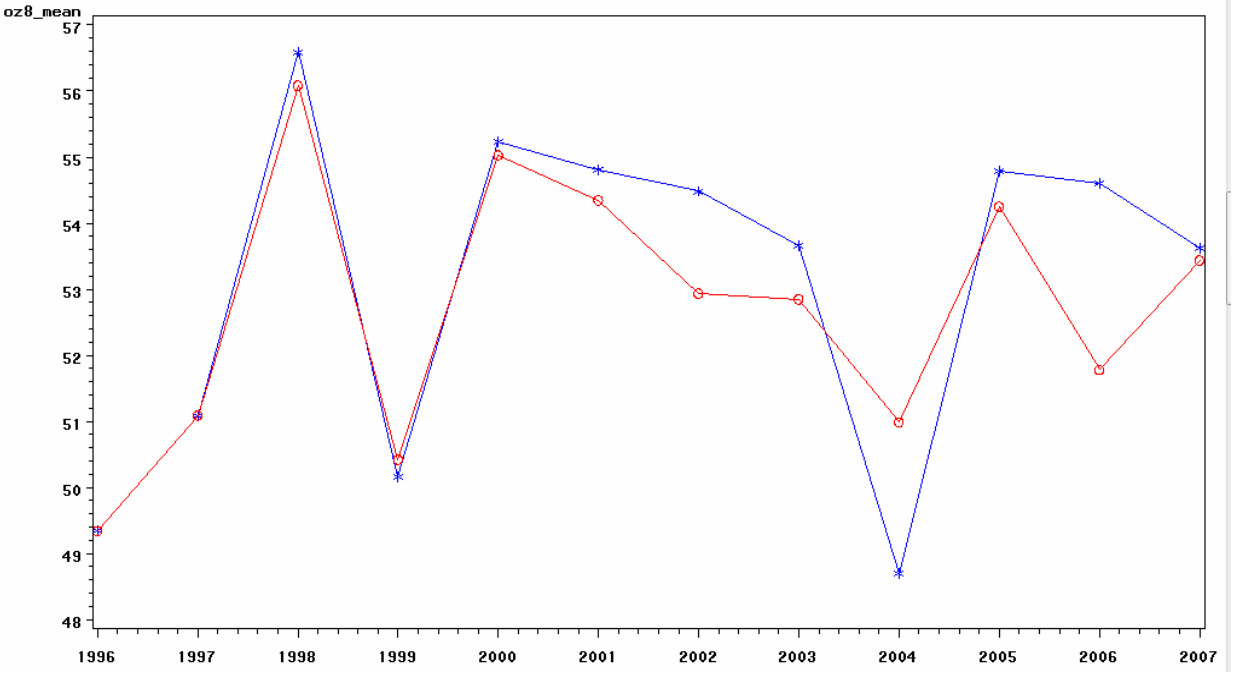

Figure 6.49 El Paso residual meteorologically and precursor adjusted trend model

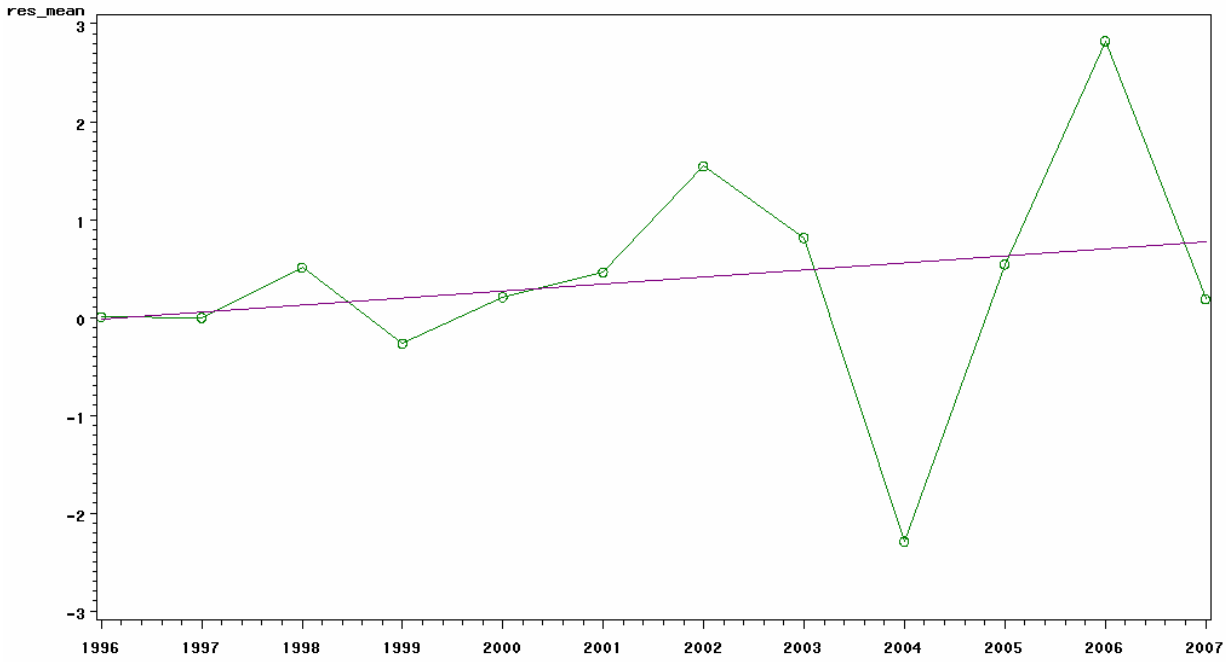

Figure 6.50 Houston actual annual summer-mean and meteorologically and precursor predicted time series

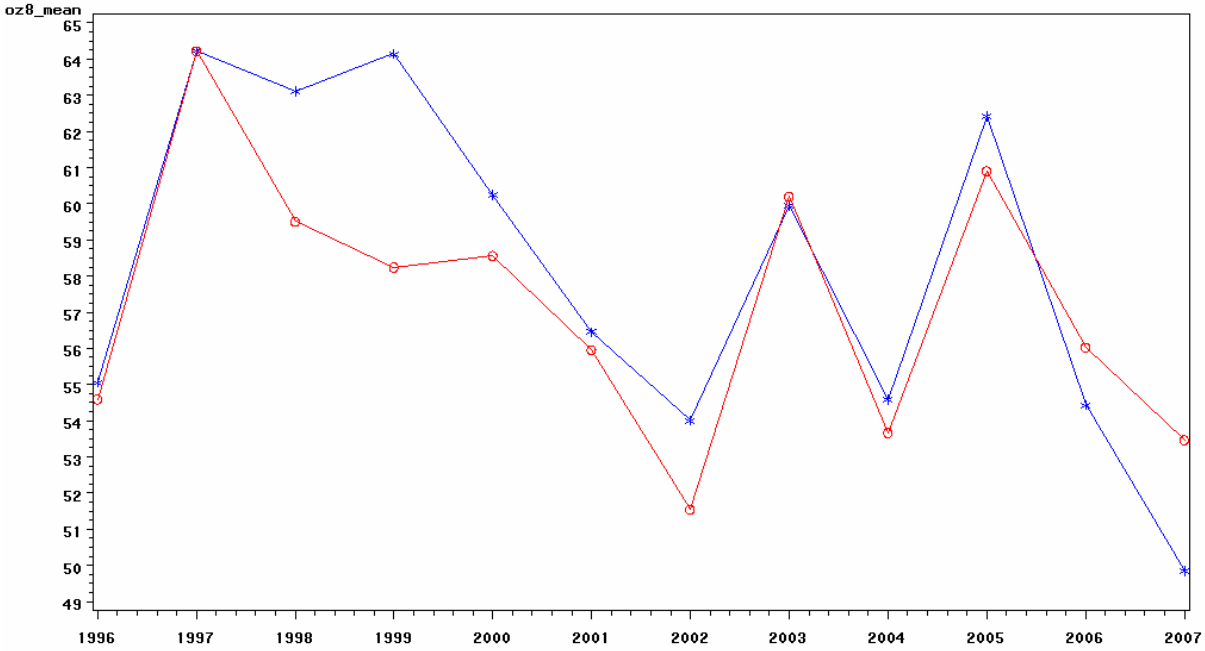

Figure 6.51 Houston residual meteorologically and precursor adjusted trend model

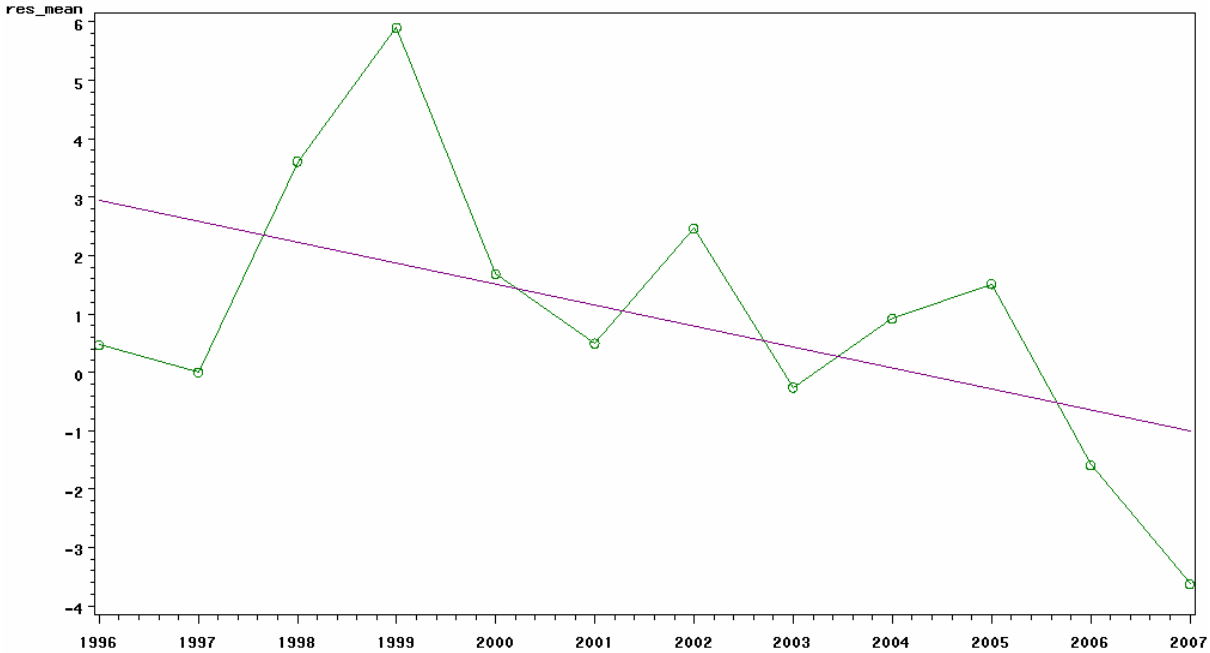

Table 6.8 Second round of regressions with NOx and hydrocarbons included, explaining for of the cause of ozone, leaving less of a trend over time

location	Intercept	Coef.	t	p-value	Lag1 Coef.	t
Dallas	**1.357**	**-0.154**	**-2.56**	**0.031**	**0.244**	**0.75**
El Paso	-0.027	0.075	0.77	0.463	0.121	0.37
Houston	2.859	-0.361	-1.68	0.128	-0.183	-0.56

7. Oxides of Nitrogen Trends

7.1 Oxides of Nitrogen OLS Trends for the Houston Region

The Ordinary least square (OLS) trends were developed after an examination of the diurnal patterns during the ozone season (May – October) in years since 2000. After the examination of individual monitors from urban areas across the state, a representative subset of nine sites (AQS identification numbers 482010024, 481130069, 481410037, 482450009, 484391002, 480290046, 482011039, 484530020, 481670014) were selected to develop a typical diurnal pattern. This is shown in Figure 7.1. From this graph we chose to use the four-hour 5:00 – 8:59 CST period (hours beginning at 5, 6, 7, and 8 CST) for trends. This is the maximum period for NO mean concentration, which is generally modeled as 90 percent of fresh NO_x emissions by mass. NO_2 is clearly bi-modal with nearly equal peaks in morning and nighttime values. The resulting NO_x, ideally the sum of NO and NO_2, is also bi-model with the clear maximum values at the hours beginning at 6 and 7 CST.

Figure 7.1 Composite NOx Diurnal Pattern for Houston

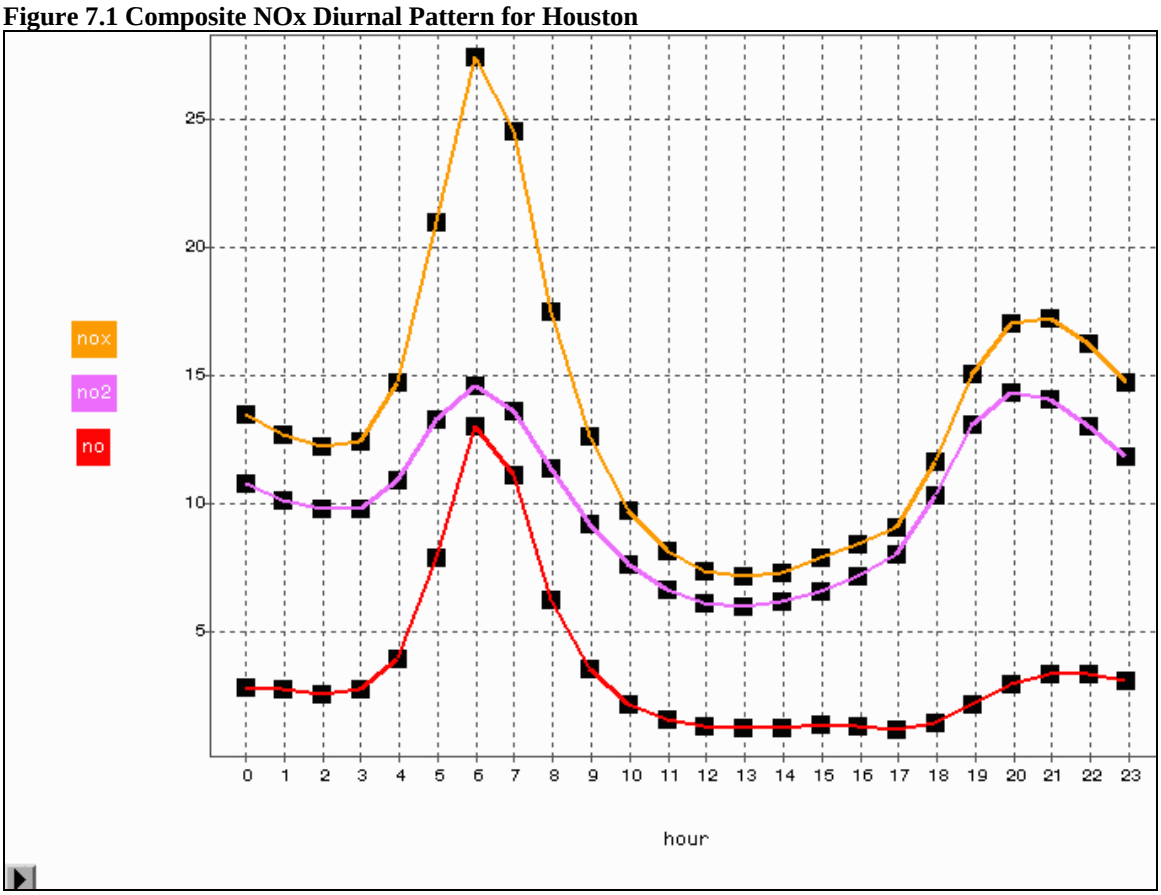

Using the data for each day from the hours and months specified, we calculated the average concentration by year. In order to improve the numerical accuracy of the regressions and to

make the trends more easily interpretable, a "year index" variable was created by subtracting 1990 from each year. We regressed the annual mean morning concentrations on the year index and produced tabular and graphical results. The calculated y-intercept is directly relatable to the expected value for the mean concentration in 1990, which is easily comparable to the most recent year through the regression equation. The calculated slope, of course, is in units of ppb per year. The regression statistics and parameter estimates appear in the tables, while the graphs show the scatterplots of the data, the OLS line fits to the data, and the regression equations for the lines at the bottom of the figures. Unfortunately, SAS GPLOT does not allow one to reposition or reformat the regression equation as does MS Excel.

The OLS trends for NO_x in the Houston Region were developed using data from nine sites listed in Table 7.1, all of which have at least 10 years of data. The Galveston CAMS 34 site with 10 years of data (DoF + 2) shows a weak not-significant positive trend for NO, NO_2, and NO_x, but the concentrations are extremely low, as evidenced by the y-intercepts. The urban Bayland Park CAMS 53 site shows a weak not-significant negative trend for all three variables, also with 10 years of data. Otherwise, the other seven sites, all with a longer time series of data, show statistically significant downward trends for total NO_x, five show statistically significant downward trends for NO, and five show statistically significant downward trends for NO_2.

Table 7.1 Ordinary least squares trends for 5-8 CST mean NOx, NO, and NO2 in the Houston Region

Site Description	Species	Intrcpt	Slope	DoF	Rsq	T	p-val	L95B	U95B
Galveston Aprt C34	nox	1.55	0.36	8	35%	2.0	0.07	-0.04	0.75
Galveston Aprt C34	no	0.34	0.06	8	8%	0.8	0.42	-0.10	0.21
Galveston Aprt C34	no2	2.70	0.20	8	24%	1.6	0.15	-0.09	0.49
Aldine C8	**nox**	**37.82**	**-0.53**	**16**	**25%**	**-2.3**	**0.04**	**-1.01**	**-0.04**
Aldine C8	**no**	**22.93**	**-0.51**	**16**	**41%**	**-3.3**	**0.00**	**-0.83**	**-0.18**
Aldine C8	no2	15.11	-0.02	16	0%	-0.2	0.84	-0.28	0.23
NW Harris Co. C26	**nox**	**16.59**	**-0.37**	**9**	**45%**	**-2.7**	**0.02**	**-0.68**	**-0.06**
NW Harris Co. C26	no	7.27	-0.24	9	35%	-2.2	0.05	-0.48	0.01
NW Harris Co. C26	**no2**	**12.08**	**-0.31**	**9**	**79%**	**-5.9**	**0.00**	**-0.43**	**-0.19**
Lang C408	**nox**	**70.01**	**-1.75**	**16**	**67%**	**-5.6**	**0.00**	**-2.40**	**-1.09**
Lang C408	**no**	**48.54**	**-1.54**	**16**	**73%**	**-6.6**	**0.00**	**-2.03**	**-1.04**
Lang C408	**no2**	**22.33**	**-0.22**	**16**	**28%**	**-2.5**	**0.02**	**-0.41**	**-0.03**
Bayland Park C53	nox	35.51	-0.54	8	9%	-0.8	0.40	-1.93	0.86
Bayland Park C53	no	19.12	-0.47	8	16%	-1.2	0.25	-1.33	0.40
Bayland Park C53	no2	17.27	-0.12	8	3%	-0.4	0.64	-0.68	0.44
East C1	**nox**	**58.56**	**-1.30**	**13**	**69%**	**-5.3**	**0.00**	**-1.82**	**-0.77**
East C1	**no**	**39.60**	**-1.28**	**13**	**77%**	**-6.5**	**0.00**	**-1.70**	**-0.86**
East C1	no2	19.20	-0.02	13	0%	-0.2	0.83	-0.24	0.20
Clinton C403	**nox**	**57.13**	**-1.04**	**16**	**64%**	**-5.3**	**0.00**	**-1.45**	**-0.63**
Clinton C403	**no**	**31.90**	**-0.35**	**16**	**26%**	**-2.3**	**0.03**	**-0.66**	**-0.04**
Clinton C403	**no2**	**25.02**	**-0.62**	**16**	**62%**	**-5.0**	**0.00**	**-0.89**	**-0.36**
Crawford C407	**nox**	**80.00**	**-2.64**	**9**	**69%**	**-4.4**	**0.00**	**-3.96**	**-1.31**
Crawford C407	**no**	**51.46**	**-1.87**	**9**	**59%**	**-3.6**	**0.01**	**-3.03**	**-0.70**
Crawford C407	**no2**	**29.96**	**-0.82**	**9**	**58%**	**-3.5**	**0.01**	**-1.34**	**-0.29**
Deer Park 2 C35	**nox**	**26.00**	**-0.52**	**9**	**40%**	**-2.4**	**0.04**	**-1.00**	**-0.04**
Deer Park 2 C35	no	8.22	-0.14	9	17%	-1.3	0.20	-0.38	0.09
Deer Park 2 C35	**no2**	**16.54**	**-0.27**	**9**	**37%**	**-2.3**	**0.05**	**-0.53**	**-0.01**

The trends for other parts of the state are presented in Table 7.2. Time series graphs for the annual averages of all sites for the three parameter with the OLS lines fit to the data appear in Figures 7.2 – 7.69.

Table 7.2 Ordinary least squares trends for 5-8 CST mean NOx, NO, and NO2 in other Texas Regions

Site Description	Species	Intrcpt	Slope	DoF	Rsq	T	p-val	L95B	U95B
Hinton St. C401	nox	58.38	-1.51	15	65%	-5.26	0.00	-2.12	-0.90
Hinton St. C401	no	38.44	-1.63	15	66%	-5.38	0.00	-2.28	-0.98
Hinton St. C401	no2	21.38	0.00	15	0%	0.00	1.00	-0.24	0.24
Executive Apt C402	nox	28.75	-0.48	11	41%	-2.78	0.02	-0.87	-0.10
Executive Apt C402	no	11.96	-0.37	11	41%	-2.78	0.02	-0.66	-0.08
Executive Apt C402	no2	17.13	-0.14	11	13%	-1.30	0.22	-0.37	0.09
Denton Apt So C56	nox	8.82	0.41	8	19%	1.38	0.20	-0.28	1.10
Denton Apt So C56	no	1.97	0.19	8	19%	1.39	0.20	-0.13	0.51
Denton Apt So C56	no2	6.02	0.28	8	27%	1.70	0.13	-0.10	0.67
Ft. Worth NW C13	nox	26.35	0.08	16	1%	0.43	0.68	-0.32	0.48
Ft. Worth NW C13	no	10.41	0.10	16	5%	0.94	0.36	-0.12	0.31
Ft. Worth NW C13	no2	15.49	0.04	16	1%	0.31	0.76	-0.23	0.31
UTEP C12	nox	47.60	-0.97	16	61%	-5.00	0.00	-1.38	-0.56
UTEP C12	no	22.51	-0.52	16	52%	-4.18	0.00	-0.78	-0.26
UTEP C12	no2	24.68	-0.40	16	44%	-3.58	0.00	-0.64	-0.16
Chamizal C41	nox	55.44	-1.18	8	32%	-1.95	0.09	-2.57	0.22
Chamizal C41	no	29.82	-0.75	8	39%	-2.26	0.05	-1.51	0.02
Chamizal C41	no2	27.84	-0.57	8	22%	-1.50	0.17	-1.44	0.31
Beau-Lamar C2	nox	18.94	-0.22	16	24%	-2.27	0.04	-0.43	-0.01
Beau-Lamar C2	no	8.98	-0.31	16	58%	-4.73	0.00	-0.44	-0.17
Beau-Lamar C2	no2	9.58	0.11	16	8%	1.20	0.25	-0.09	0.31
West Orange C9	nox	20.33	-0.51	16	59%	-4.77	0.00	-0.74	-0.28
West Orange C9	no	7.79	-0.21	16	36%	-2.99	0.01	-0.36	-0.06
West Orange C9	no2	12.41	-0.28	16	57%	-4.65	0.00	-0.41	-0.15
Audubon C38	nox	4.06	0.00	9	0%	0.00	1.00	-0.27	0.27
Audubon C38	no	0.65	-0.01	9	1%	-0.24	0.81	-0.11	0.09
Audubon C38	no2	5.29	-0.12	9	16%	-1.31	0.22	-0.32	0.09
SA Downtown C27	nox	52.86	-1.62	9	62%	-3.85	0.00	-2.57	-0.67
SA Downtown C27	no	26.74	-0.96	9	58%	-3.51	0.01	-1.57	-0.34
SA Downtown C27	no2	27.31	-0.73	9	59%	-3.63	0.01	-1.18	-0.27
Calaveras Lake C59	nox	7.28	0.03	8	0%	0.20	0.85	-0.32	0.38
Calaveras Lake C59	no	2.65	0.01	8	0%	0.07	0.94	-0.16	0.17
Calaveras Lake C59	no2	6.53	-0.10	8	14%	-1.15	0.28	-0.31	0.10

Figure 7.2 NO_2 5-8 CST May-Oct. OLS Trends, years since 1990, Galveston Airport C34

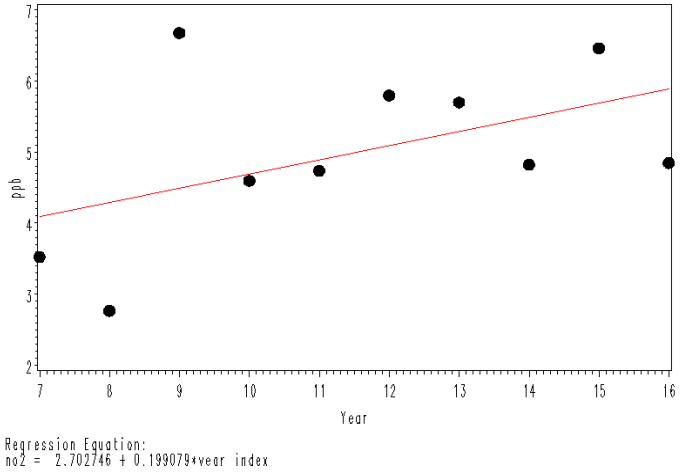

Figure 7.3 NO 5-8 CST May-Oct. OLS Trends, years since 1990, Galveston Airport C34

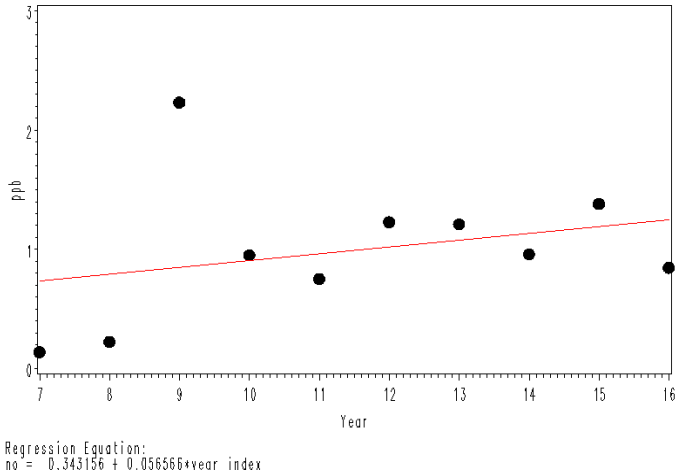

Figure 7.4 NO_x 5-8 CST May-Oct. OLS Trends, years since 1990, Galveston Airport C34

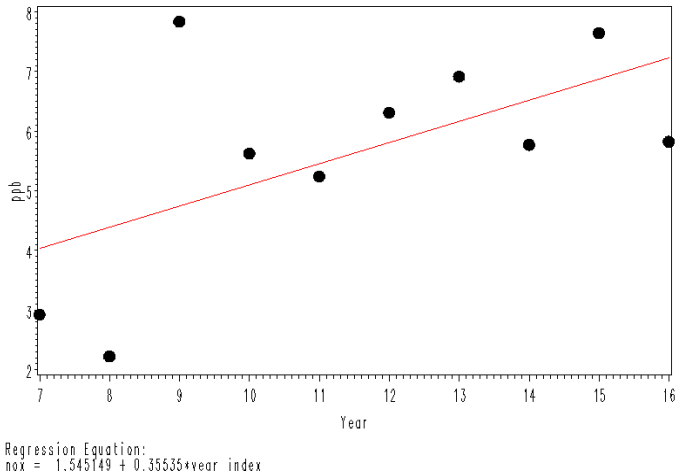

Figure 7.5 NO_2 5-8 CST May-Oct. OLS Trends, years since 1990, Aldine C8

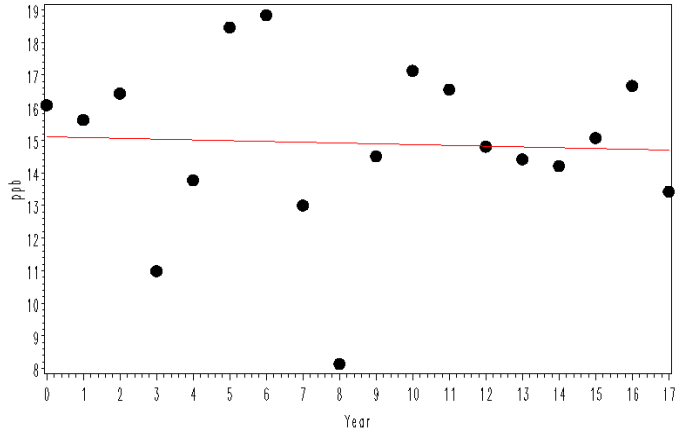

Regression Equation:
no2 = 15.10951 - 0.024952*year index

Figure 7.6 NO 5-8 CST May-Oct. OLS Trends, years since 1990, Aldine C8

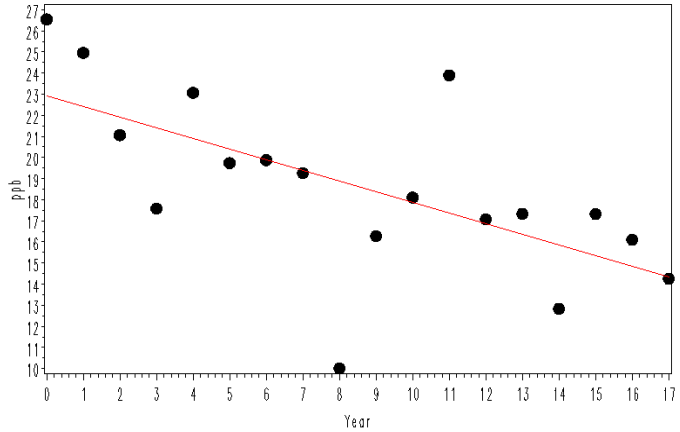

Regression Equation:
no = 22.93217 - 0.505662*year index

Figure 7.7 NO_x 5-8 CST May-Oct. OLS Trends, years since 1990, Aldine C8

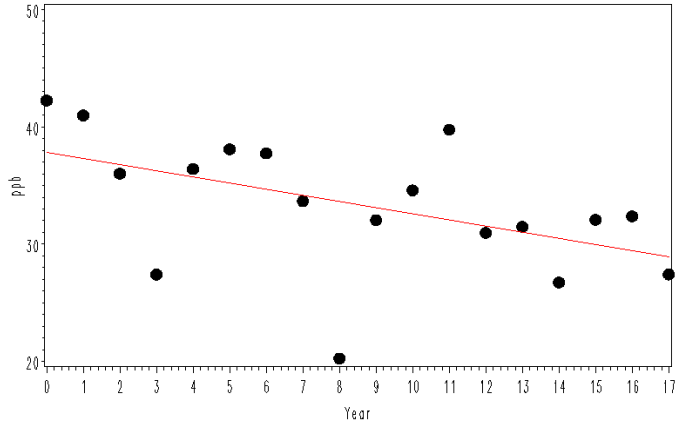

Regression Equation:
nox = 37.82152 - 0.525243*year index

Figure 7.8 NO_2 5-8 CST May-Oct. OLS Trends, years since 1990, NW Harris C26

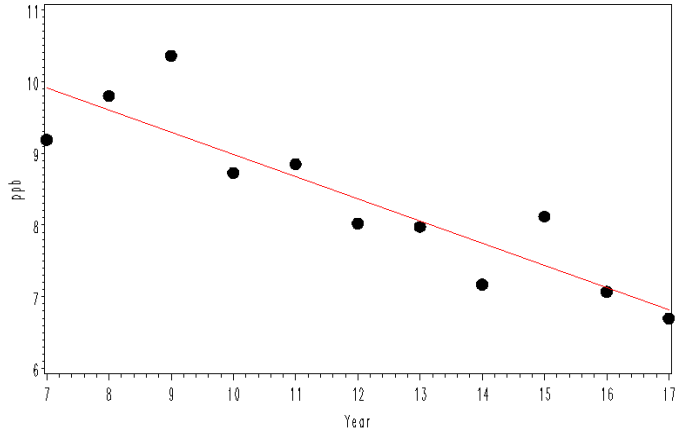

Regression Equation:
no2 = 12.08085 - 0.309751*year index

Figure 7.9 NO 5-8 CST May-Oct. OLS Trends, years since 1990, NW Harris C26

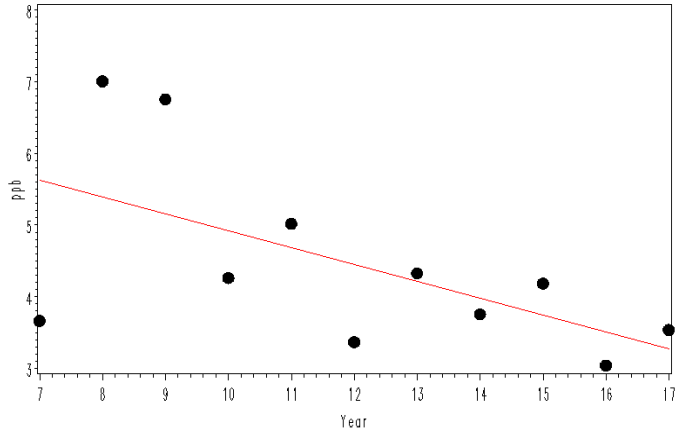

Regression Equation:
no = 7.270153 - 0.235118*year index

Figure 7.10 NO_x 5-8 CST May-Oct. OLS Trends, years since 1990, NW Harris C26

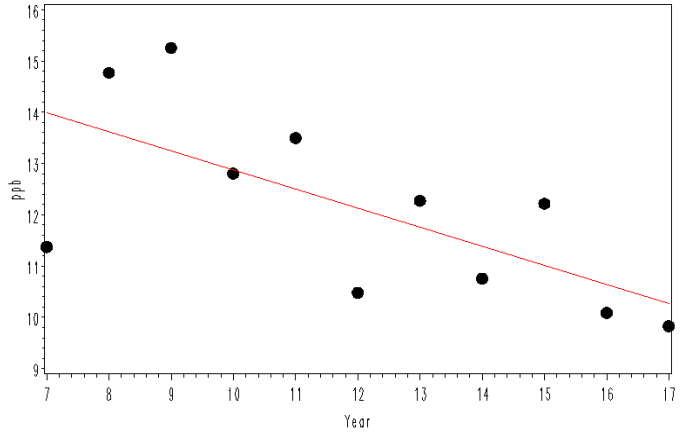

Regression Equation:
nox = 16.58646 - 0.371862*year index

Figure 7.11 NO_2 5-8 CST May-Oct. OLS Trends, years since 1990, Lang C408

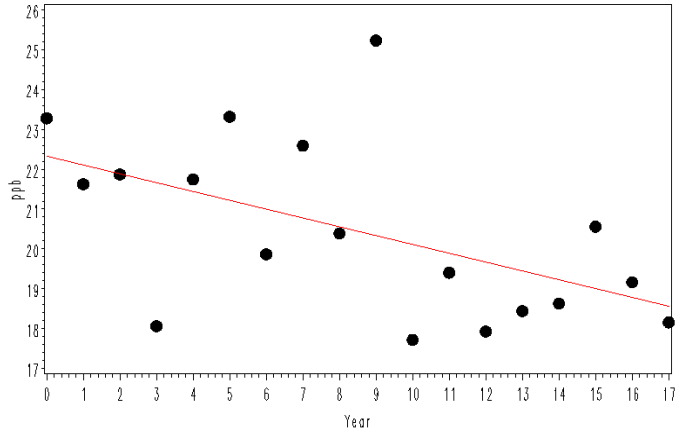

Regression Equation:
no2 = 22.32658 - 0.221122*year index

Figure 7.12 NO 5-8 CST May-Oct. OLS Trends, years since 1990, Lang C408

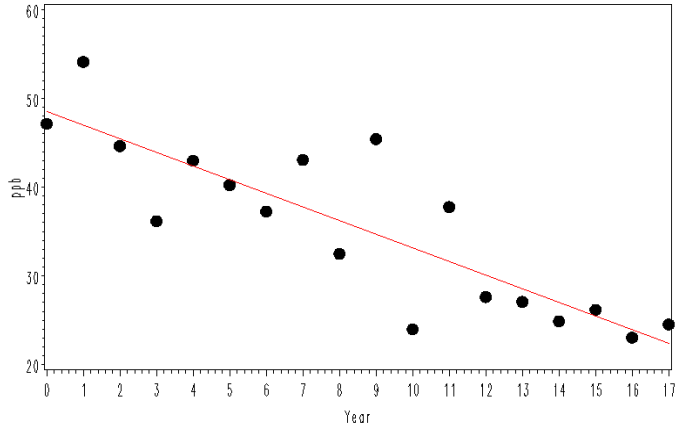

Regression Equation:
no = 48.53771 - 1.53506*year index

Figure 7.13 NO_x 5-8 CST May-Oct. OLS Trends, years since 1990, Lang C408

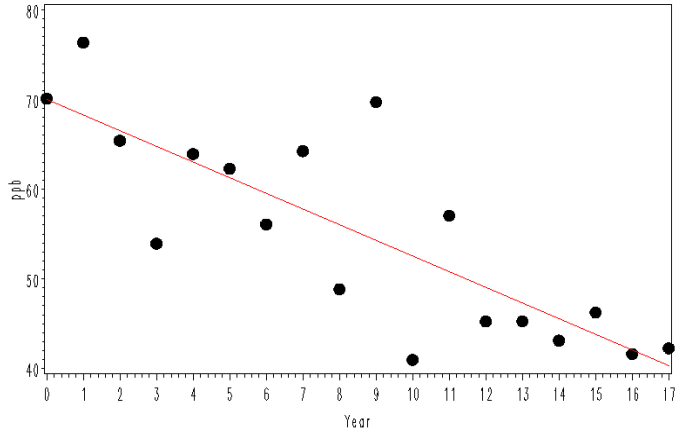

Regression Equation:
nox = 70.01021 - 1.746836*year index

Figure 7.14 NO_2 5-8 CST May-Oct. OLS Trends, years since 1990, Lang C408

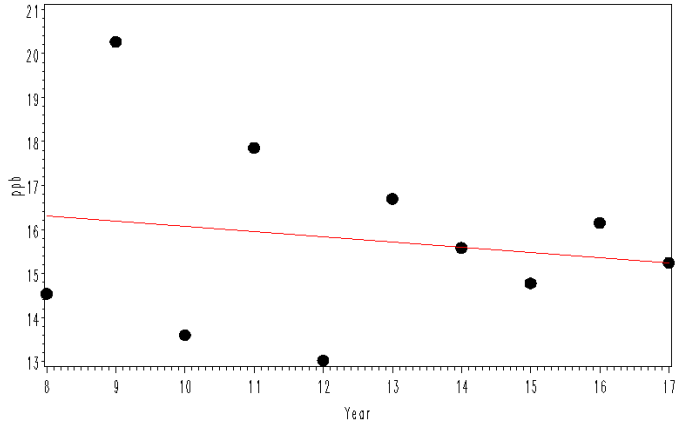

Regression Equation:
no2 = 17.26765 - 0.119351*year index

Figure 7.15 NO 5-8 CST May-Oct. OLS Trends, years since 1990, Lang C408

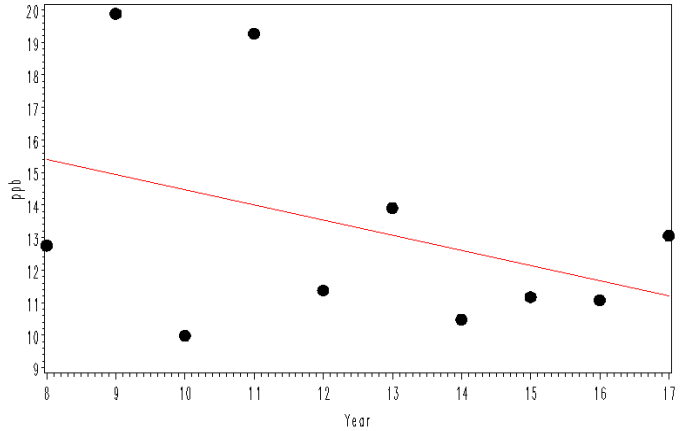

Regression Equation:
no = 19.11616 - 0.465374*year index

Figure 7.16 NO_x 5-8 CST May-Oct. OLS Trends, years since 1990, Lang C408

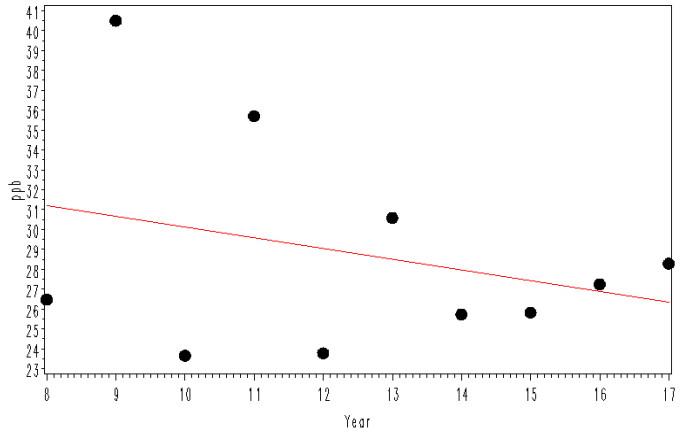

Regression Equation:
nox = 35.50747 - 0.537793*year index

Figure 7.17 NO_2 5-8 CST May-Oct. OLS Trends, years since 1990, East C1

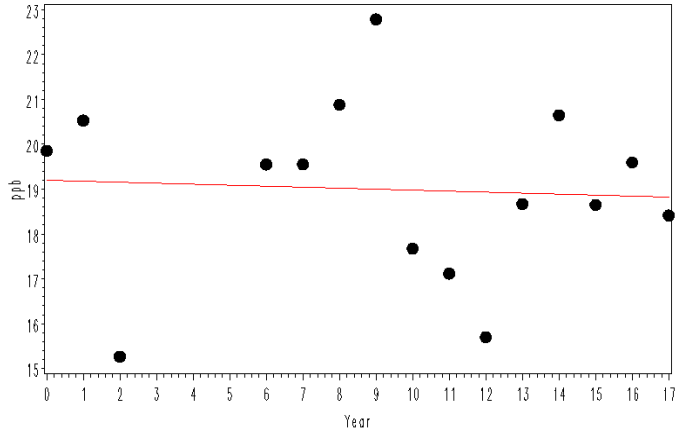

Regression Equation:
no2 = 19.20475 - 0.022158*year index

Figure 7.18 NO 5-8 CST May-Oct. OLS Trends, years since 1990, East C1

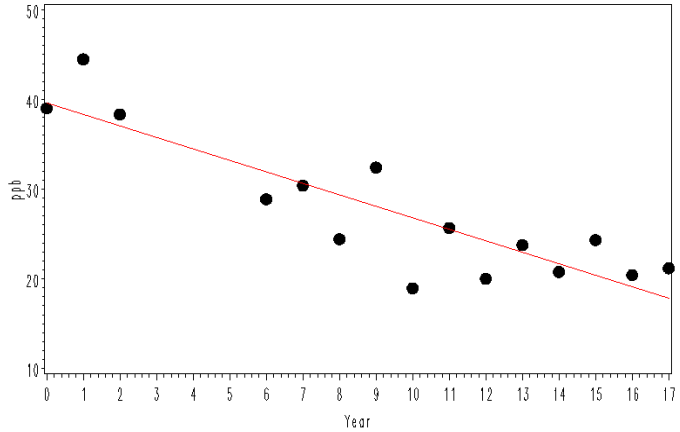

Regression Equation:
no = 39.59579 - 1.281441*year index

Figure 7.19 NO_x 5-8 CST May-Oct. OLS Trends, years since 1990, East C1

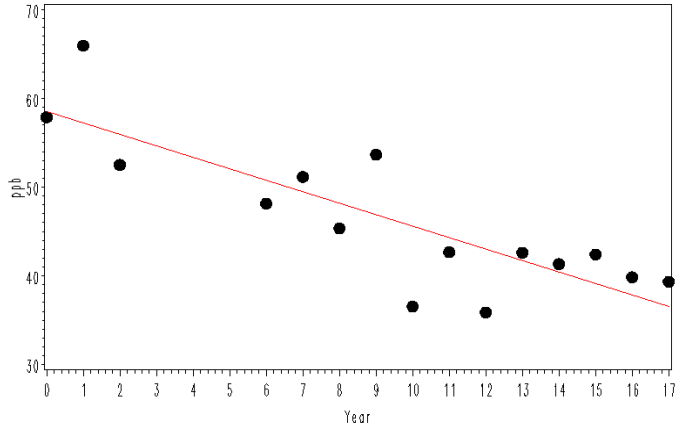

Regression Equation:
nox = 58.55931 - 1.29682*year index

Figure 7.20 NO_2 5-8 CST May-Oct. OLS Trends, years since 1990, Clinton C403

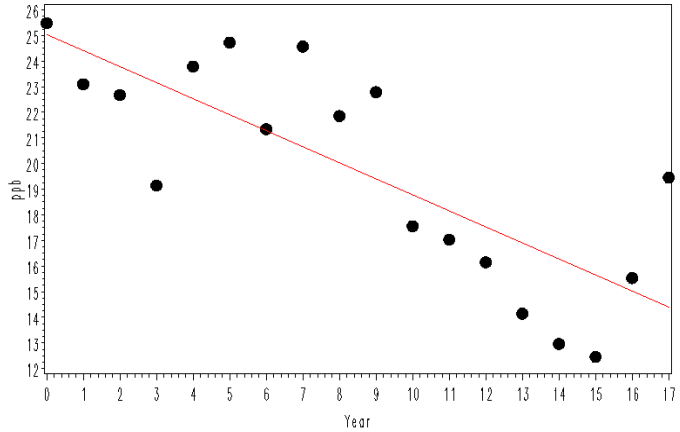

Regression Equation:
no2 = 25.02248 - 0.624669*year index

Figure 7.21 NO 5-8 CST May-Oct. OLS Trends, years since 1990, Clinton C403

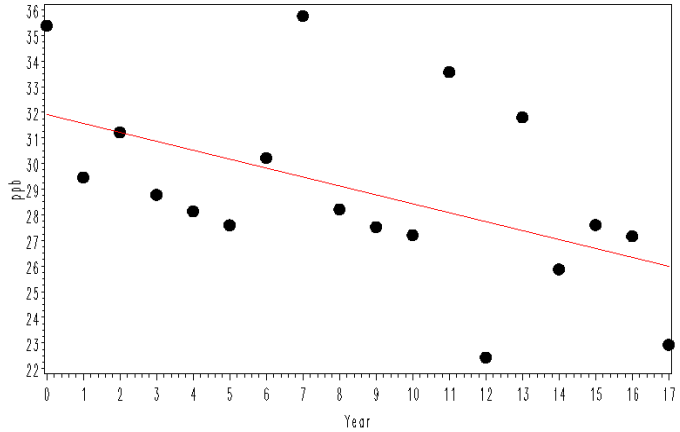

Regression Equation:
no = 31.90406 - 0.348573*year index

Figure 7.22 NO_x 5-8 CST May-Oct. OLS Trends, years since 1990, Clinton C403

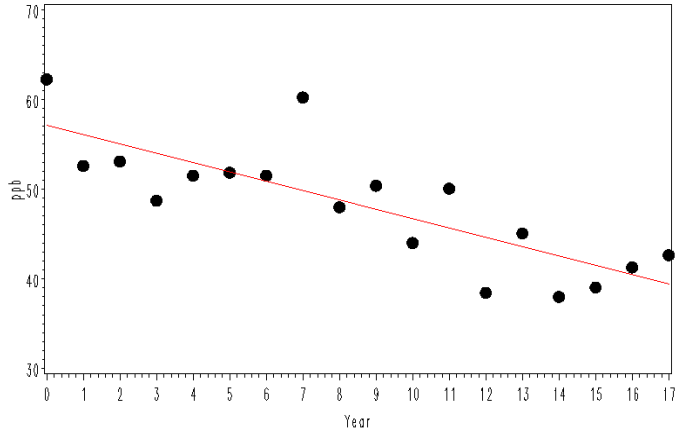

Regression Equation:
nox = 57.12661 - 1.041555*year index

Figure 7.23 NO_2 5-8 CST May-Oct. OLS Trends, years since 1990, Crawford C407

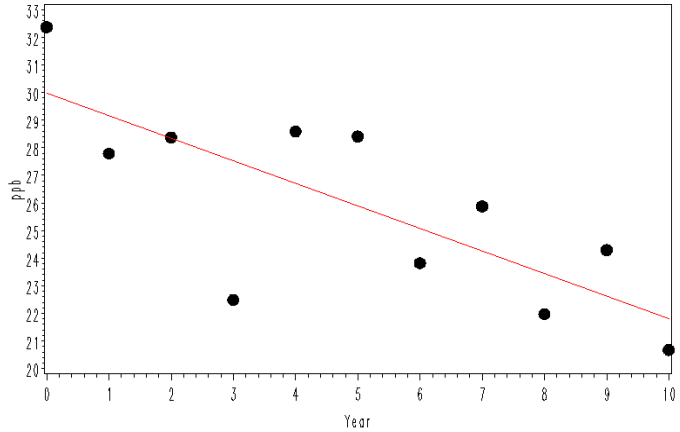

Regression Equation:
no2 = 29.9591 - 0.815121*year index

Figure 7.24 NO 5-8 CST May-Oct. OLS Trends, years since 1990, Crawford C407

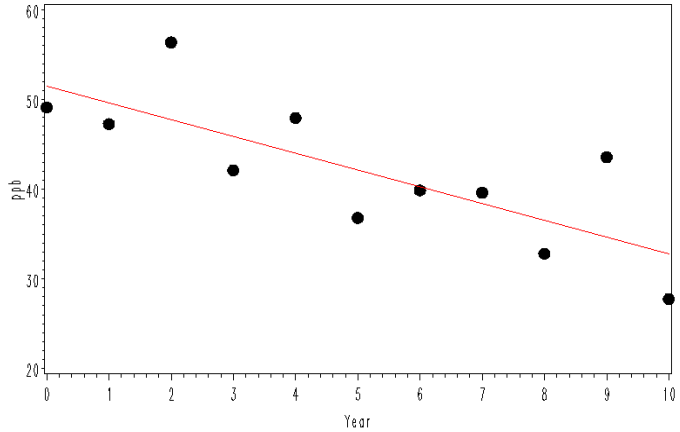

Regression Equation:
no = 51.45578 - 1.866615*year index

Figure 7.25 NO_x 5-8 CST May-Oct. OLS Trends, years since 1990, Crawford C407

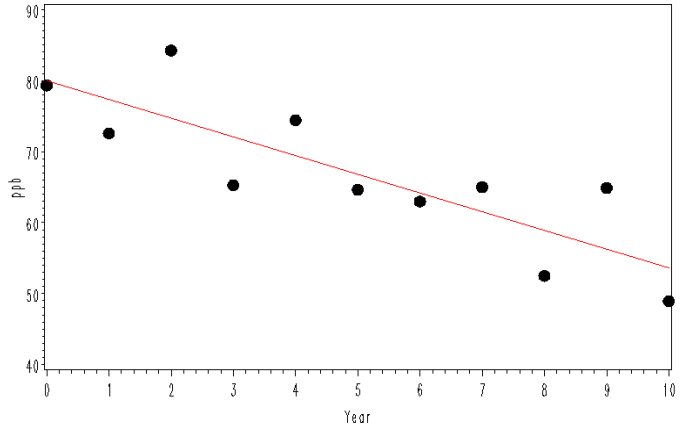

Regression Equation:
nox = 79.99503 - 2.636257*year index

Figure 7.26 NO_2 5-8 CST May-Oct. OLS Trends, years since 1990, Deer Park C35

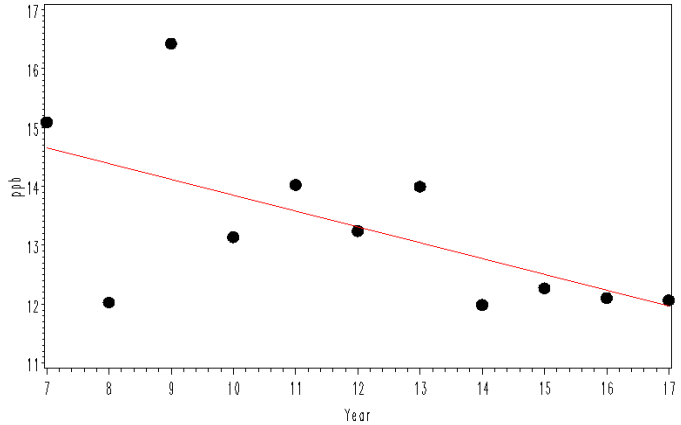

Regression Equation:
no2 = 16.53591 - 0.268993*year index

Figure 7.27 NO 5-8 CST May-Oct. OLS Trends, years since 1990, Deer Park C35

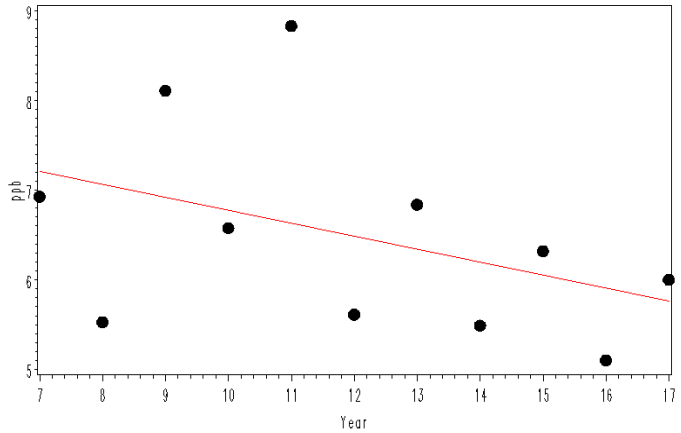

Regression Equation:
no = 8.217731 - 0.144268*year index

Figure 7.28 NO_x 5-8 CST May-Oct. OLS Trends, years since 1990, Deer Park C35

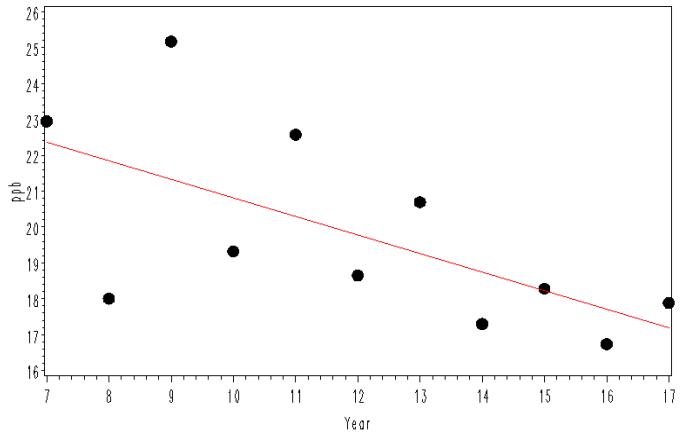

Regression Equation:
nox = 25.99684 - 0.517812*year index

Figure 7.29

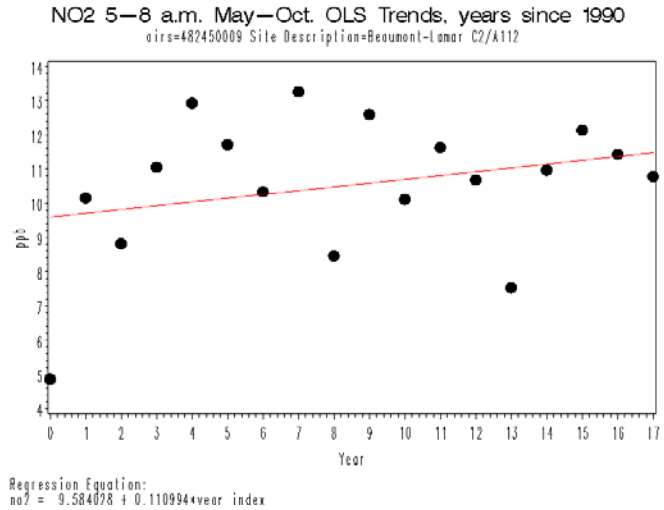

Figure 7.30

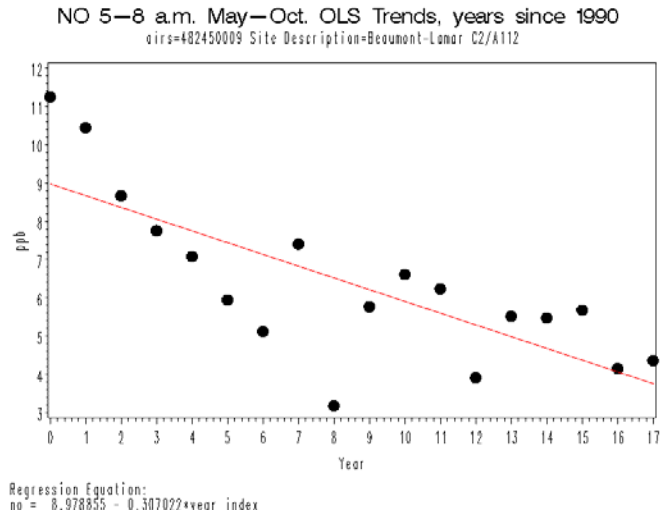

Figure 7.31

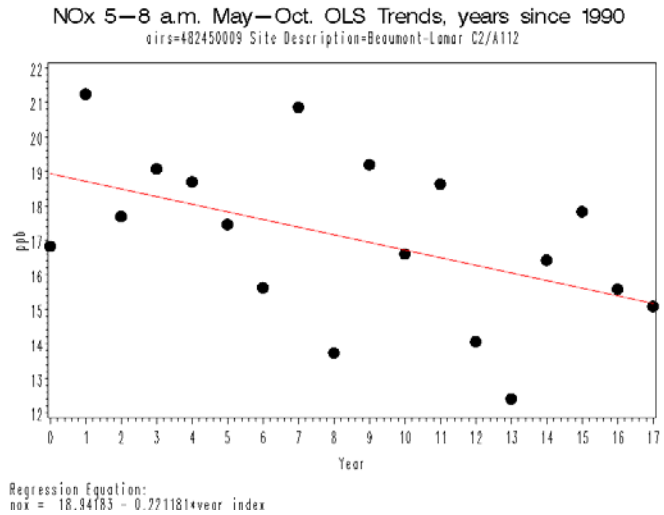

Figure 7.32

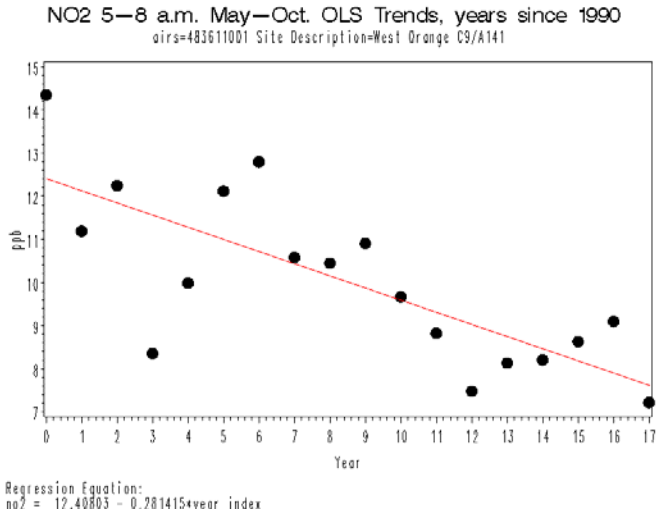

Figure 7.33

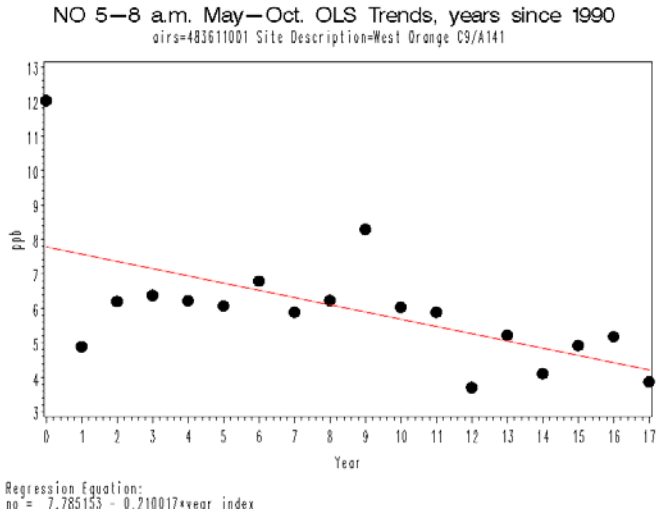

Figure 7.34

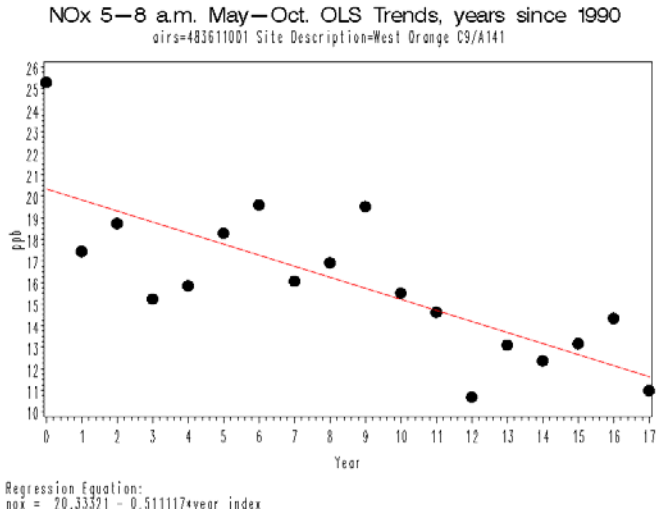

Figure 7.35

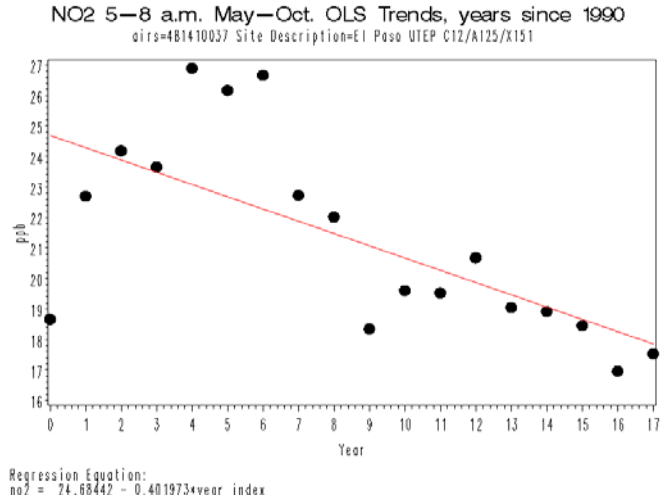

Figure 7.36

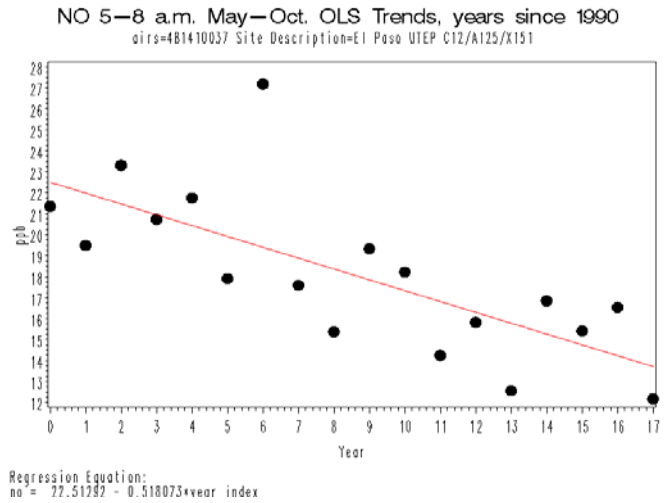

Figure 7.37

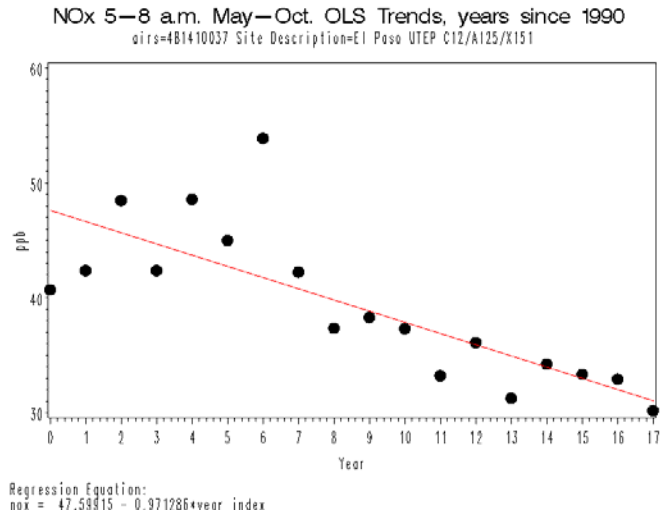

Figure 7.38

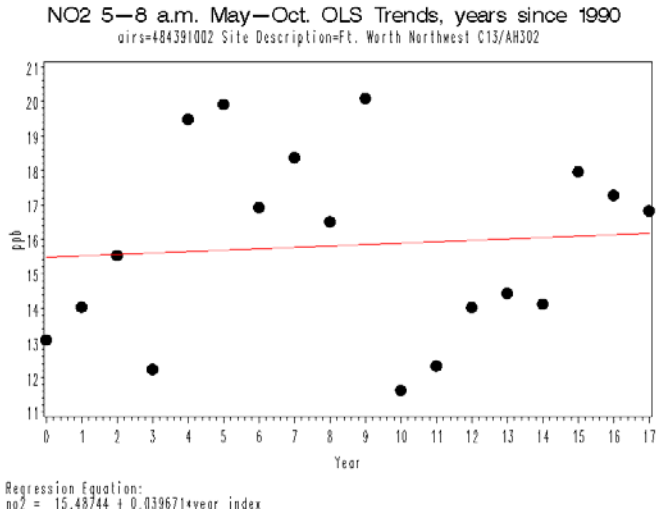

Figure 7.39

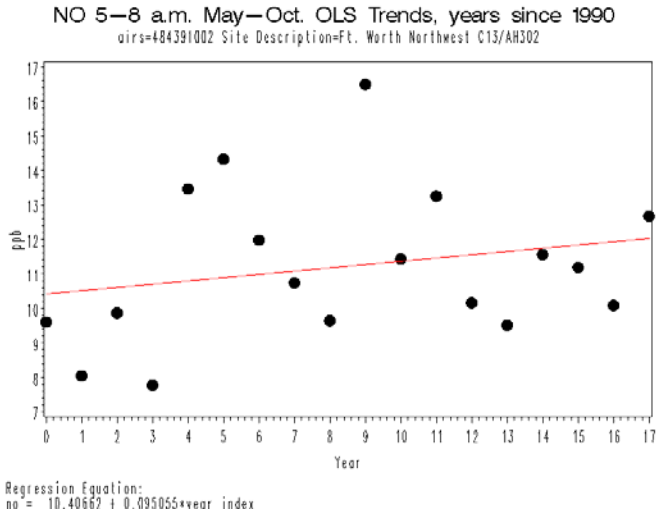

Figure 7.40

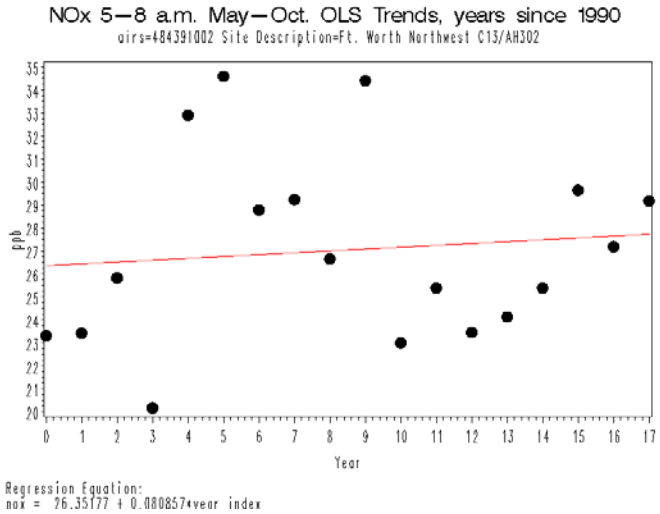

Figure 7.41

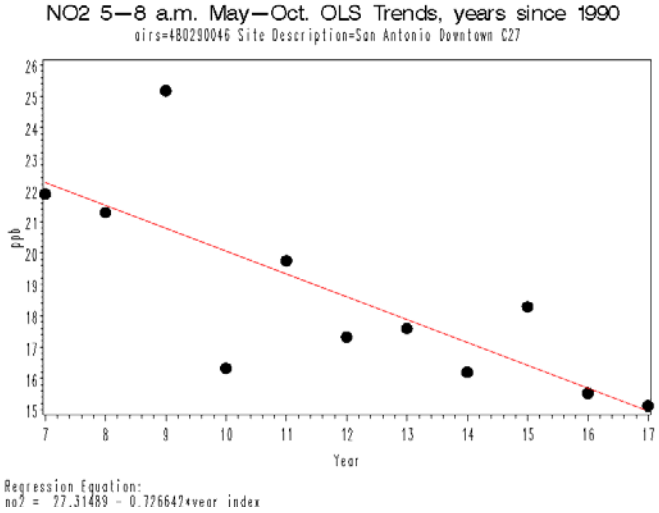

Figure 7.42

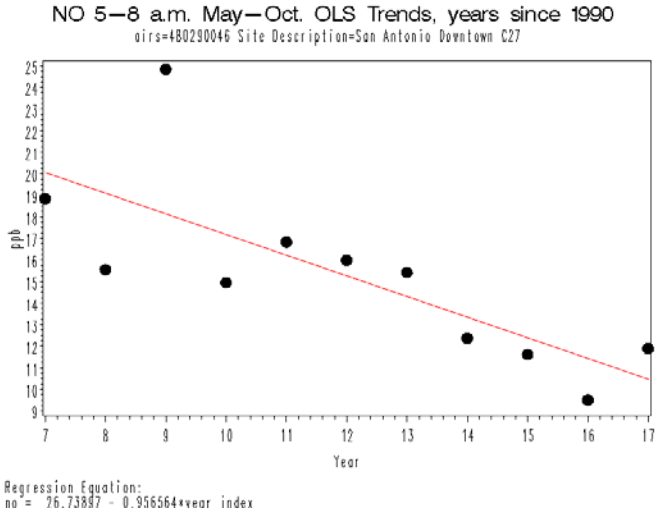

Figure 7.43

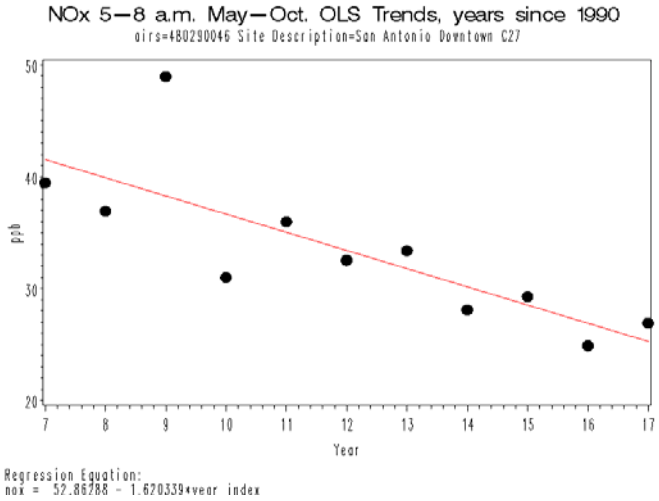

Figure 7.44

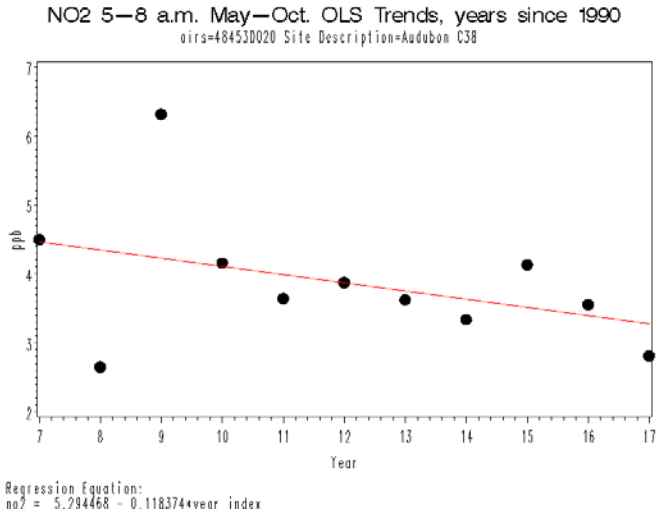

Figure 7.45

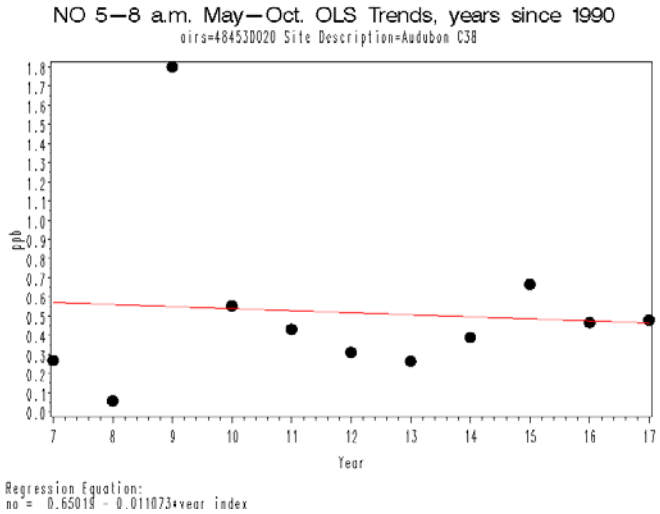

Figure 7.46

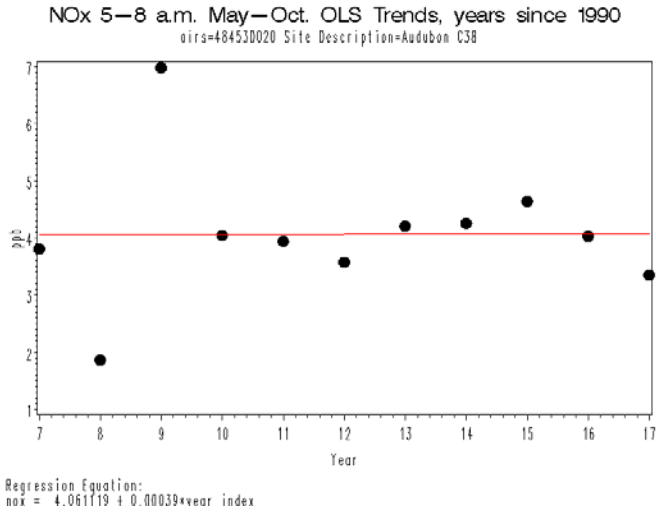

Figure 7.47

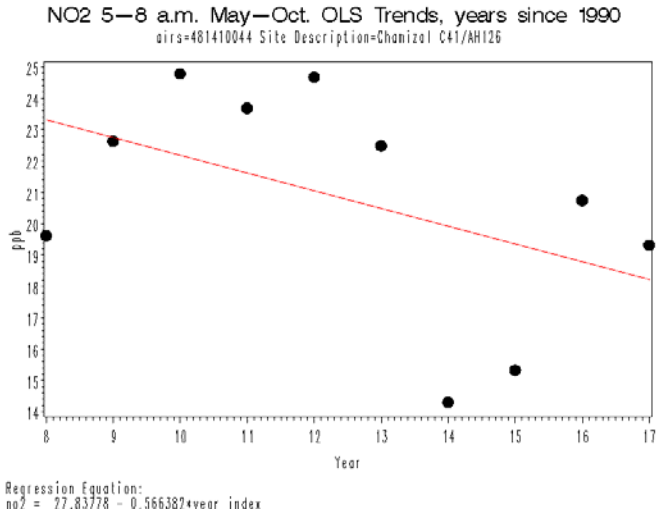

Figure 7.48

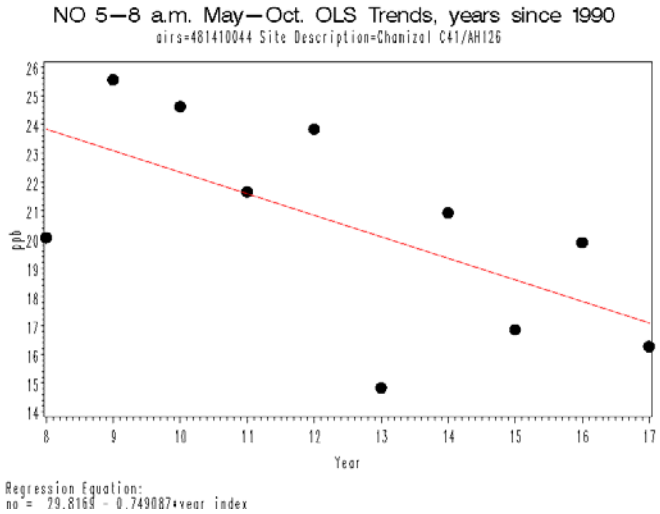

Figure 7.49

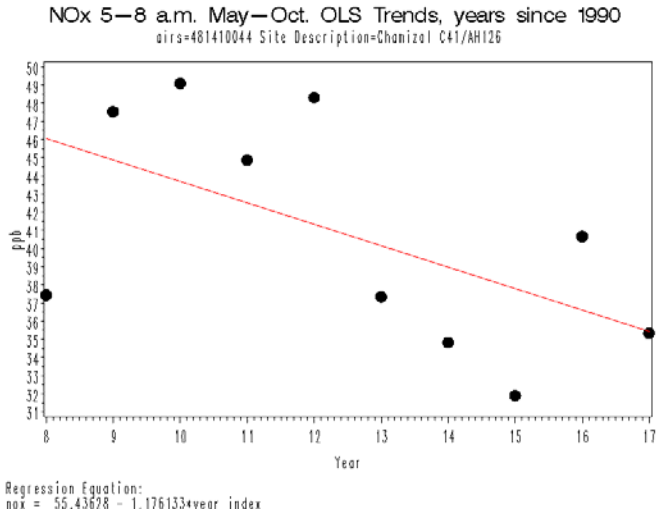

Figure 7.50

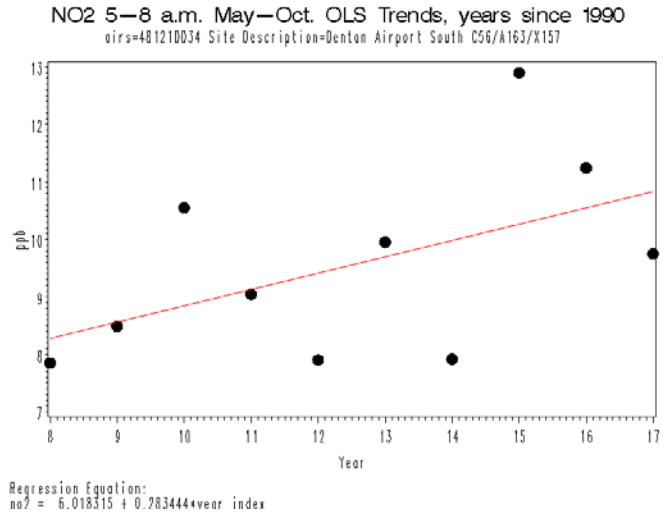

Figure 7.51

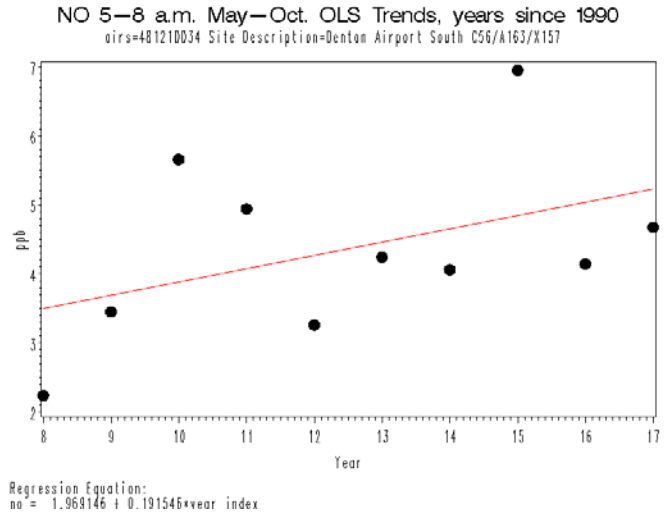

Figure 7.52

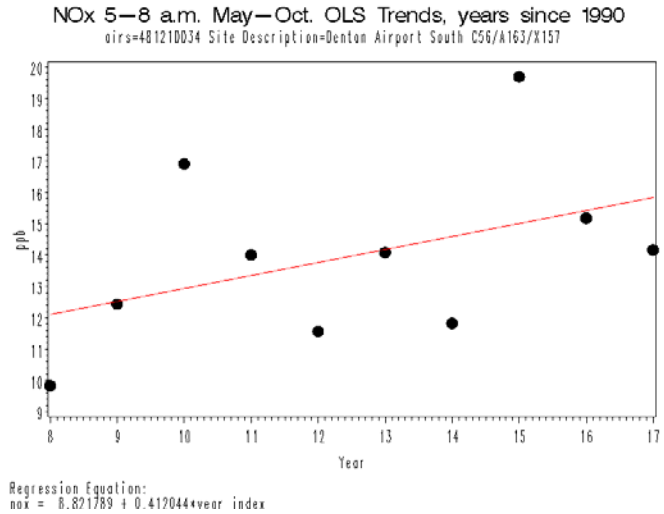

Figure 7.53

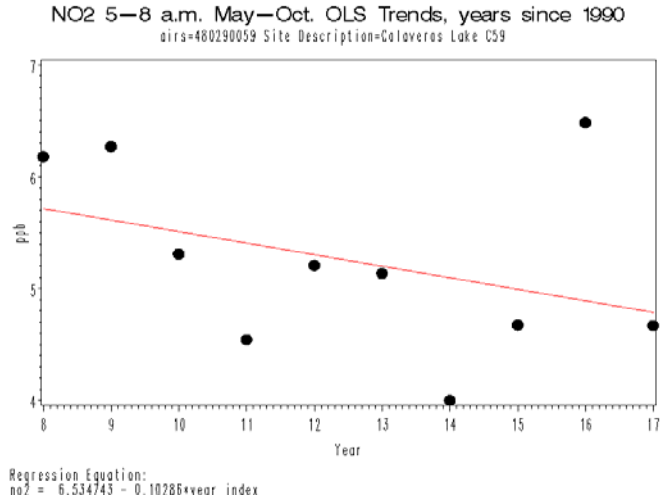

Figure 7.54

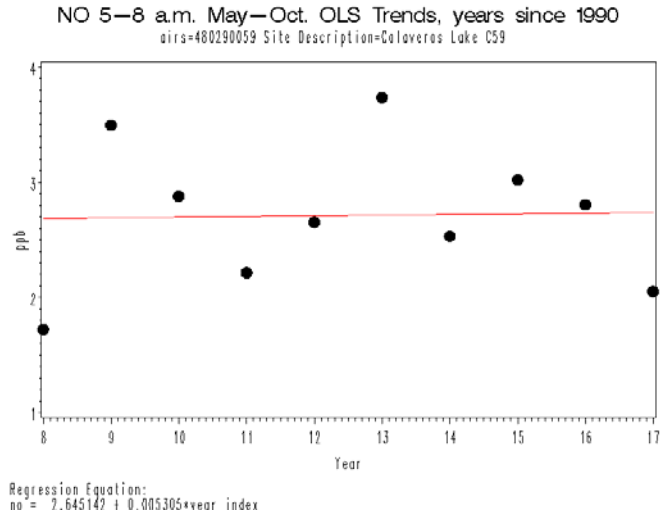

Figure 7.55

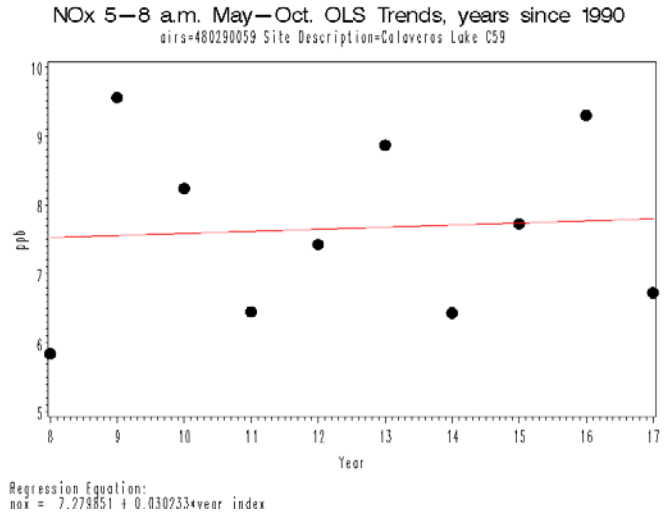

Figure 7.56

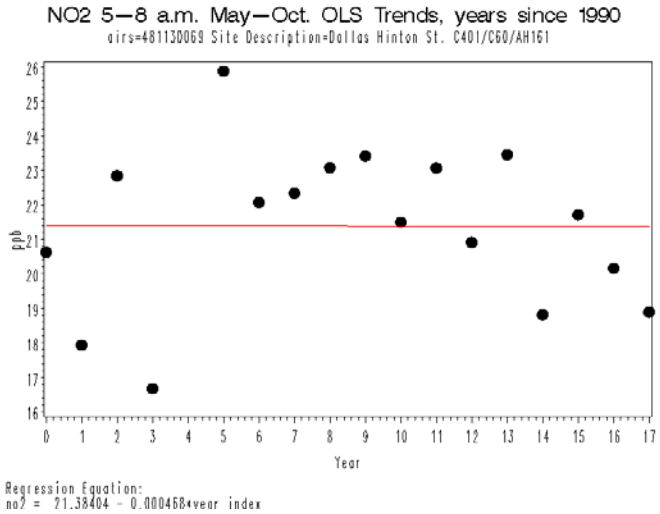

Figure 7.57

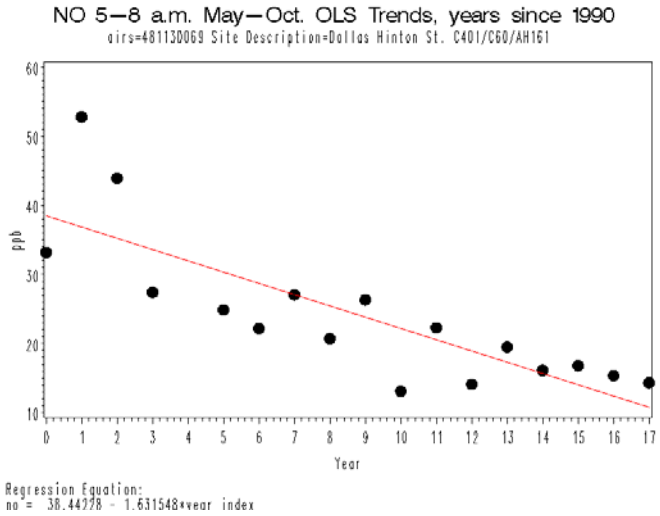

Figure 7.58

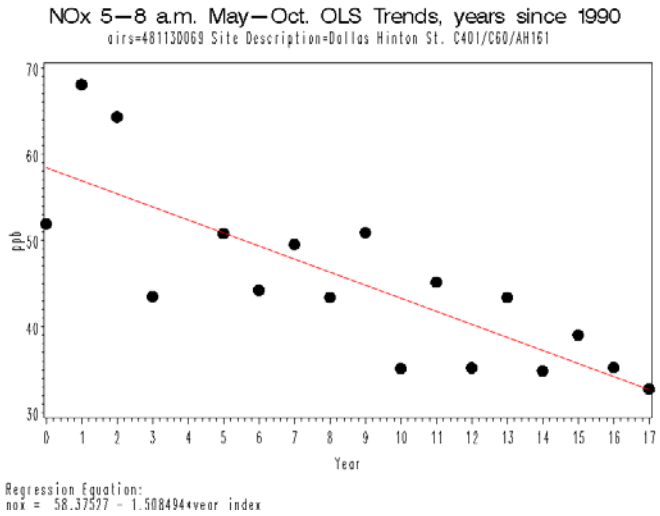

Figure 7.59

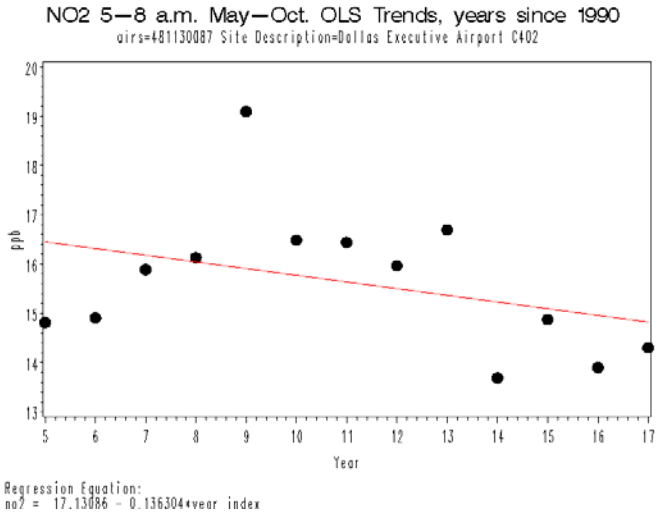

Figure 7.60

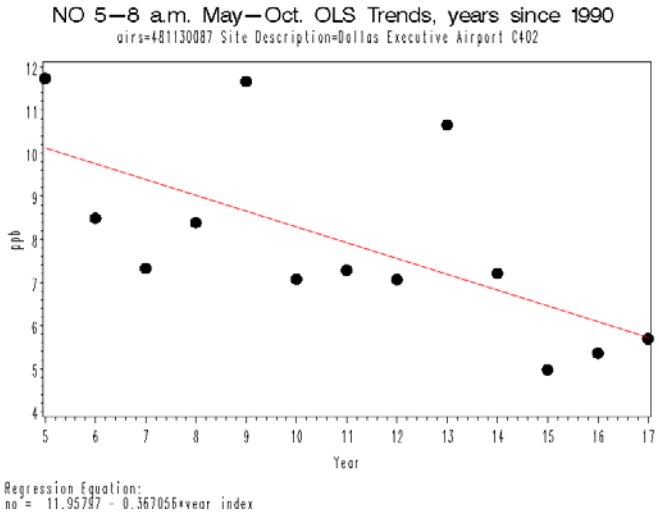

Figure 7.61

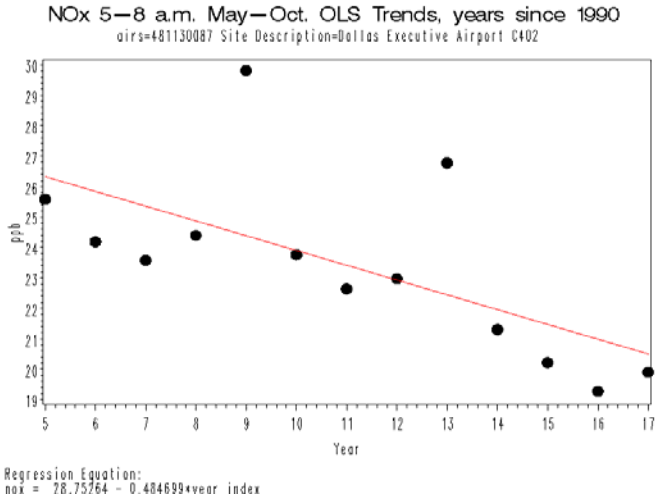

8. Carbon Monoxide (CO) Trends

8.1 Ordinary Least Squares Trends for CO

As was discussed above for NOx, several representative monitors were selected to assess the diurnal patterns for CO trends. Figure 8.1 below shows the result. Interestingly, the relative magnitude of the morning and evening peaks varies by monitor.

Figure 8.1 Pooled diurnal pattern from several representative monitors

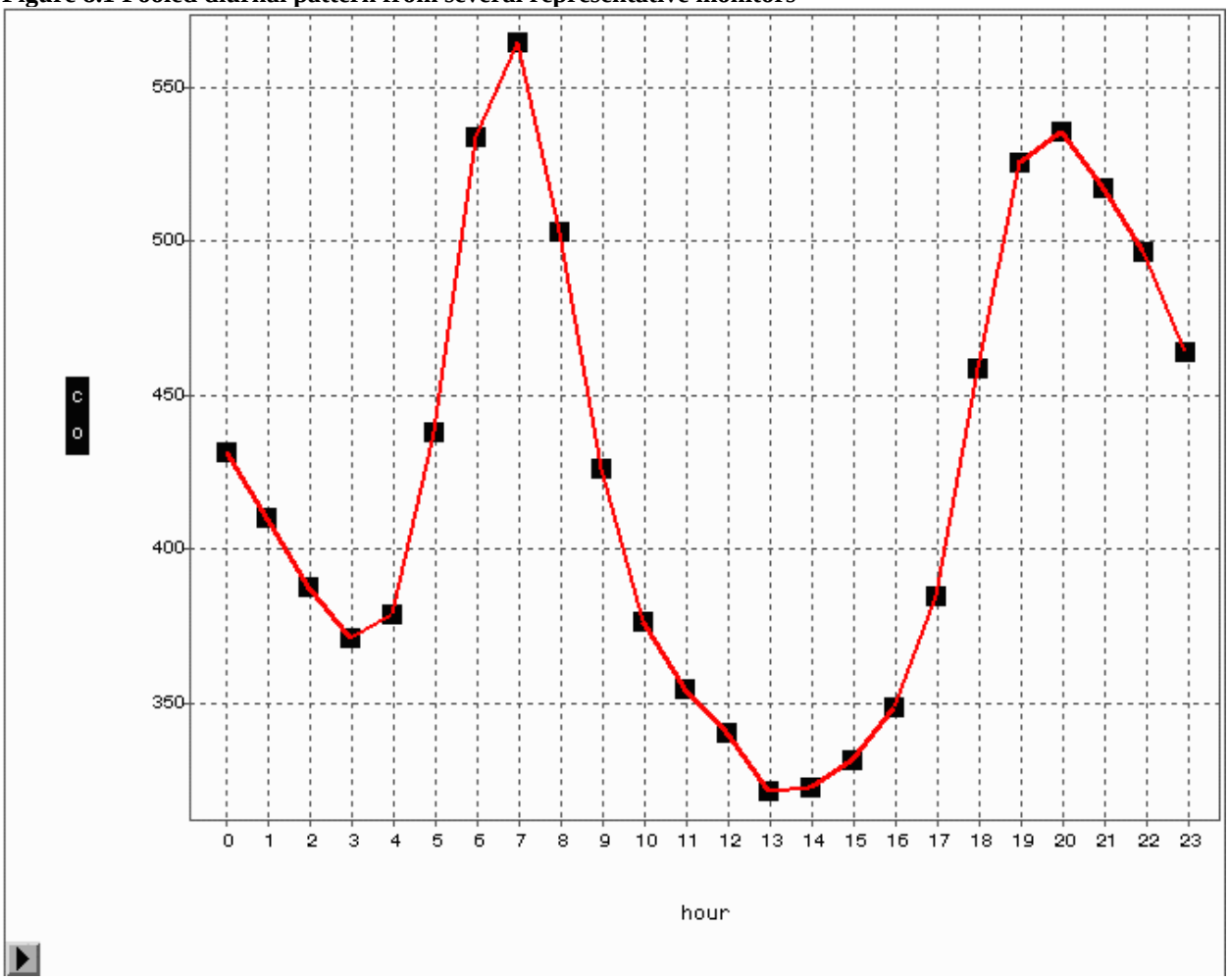

As was the case with NOx, the four morning hours beginning at 5 – 8 CST have been used to calculate an average to represent each day, then averaged over the year. Unlike NOx, the entire calendar year has been used to assess CO trends.

Although the OLS trend graphs following are not arranged by region and are not labeled the same way the NOx graphs are, these will be cleaned up in the next revision of this report. The clear pattern of concentration decreases in all areas at all monitors shows the clear success of emission controls. Historical analysis of comparisons of CO and hydrocarbons measured at auto-GCs has shown high correlations. If CO has come down to the extent it has and the linear relationship still exists, then it is likely that hydrocarbon concentrations have declined as well.

The summary of regression results appears in Table 8.1. Only the Deer Park site is not statistically significant at a 0.05 level, but it is close (p=0.06).

Table 8.1 OLS regrssion results for CO, arranged by TCEQ region

Site Description	Incpt	Slope	DoF	Rsq	T	P-val	L95B	U95B
Hinton St. C401	604.75	-8.35	14	55%	-4.13	0.00	-12.69	-4.01
Ft. Worth NW C13	1109.39	-48.60	16	91%	-12.38	0.00	-56.92	-40.28
Tillman C413	1286.63	-52.63	13	76%	-6.46	0.00	-70.24	-35.02
Downtown C6	2457.08	-138.29	11	91%	-10.88	0.00	-166.27	-110.31
Ivanhoe C414	1253.55	-55.45	12	95%	-14.43	0.00	-63.83	-47.08
UTEP C12	1255.26	-60.01	16	85%	-9.57	0.00	-73.31	-46.71
Chamizal C41	1601.47	-63.76	15	91%	-12.28	0.00	-74.83	-52.69
Sun Metro C40	2100.32	-92.52	9	93%	-11.34	0.00	-110.98	-74.06
Austin NW C3	544.39	-23.61	9	68%	-4.36	0.00	-35.85	-11.37
Aldine C8	1310.13	-57.06	16	71%	-6.22	0.00	-76.51	-37.62
Lang C408	1702.72	-77.54	16	92%	-13.40	0.00	-89.81	-65.27
Clinton C403	1058.96	-45.48	16	71%	-6.25	0.00	-60.91	-30.05
Crawford C407	1701.09	-96.04	9	85%	-7.08	0.00	-126.73	-65.36
DeerPrk 2 C35	700.15	-17.59	9	34%	-2.18	0.06	-35.88	0.70
SA Downtown C27	1308.87	-49.81	14	75%	-6.40	0.00	-66.50	-33.12
Brownsville C80	792.29	-21.59	12	48%	-3.31	0.01	-35.78	-7.39
Laredo C44	909.12	-29.15	9	63%	-3.90	0.00	-46.04	-12.25

Figure 8.2 CO 5-8 CST May-Oct. OLS Trends, years since 1990, Austin NW C3

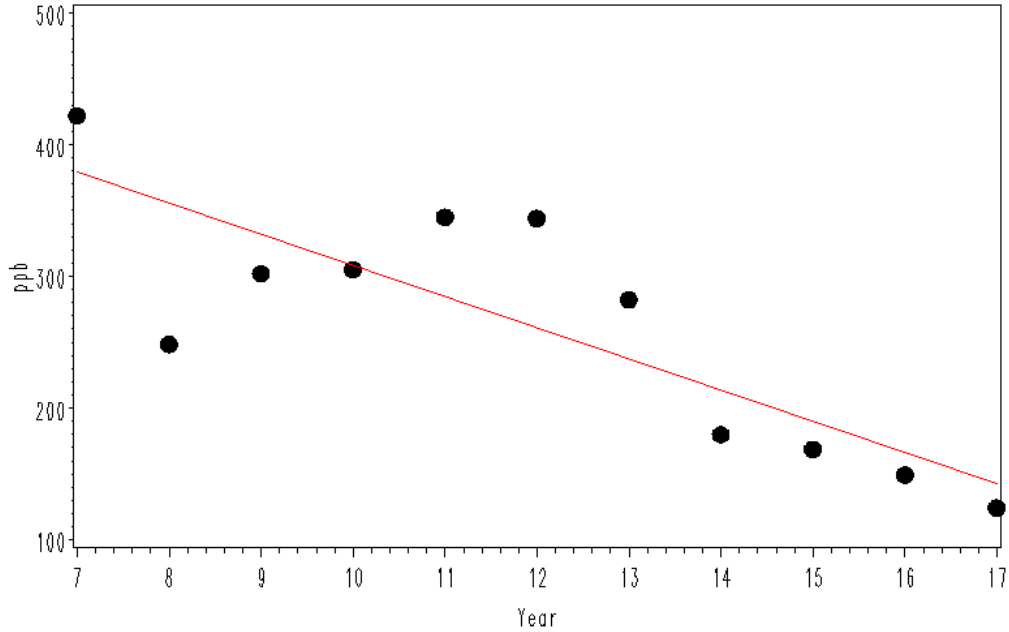

Regression Equation:
co = 544.3891 - 23.60754*year index

Figure 8.3 CO 5-8 CST May-Oct. OLS Trends, years since 1990, El Paso Ivanhoe NW C414

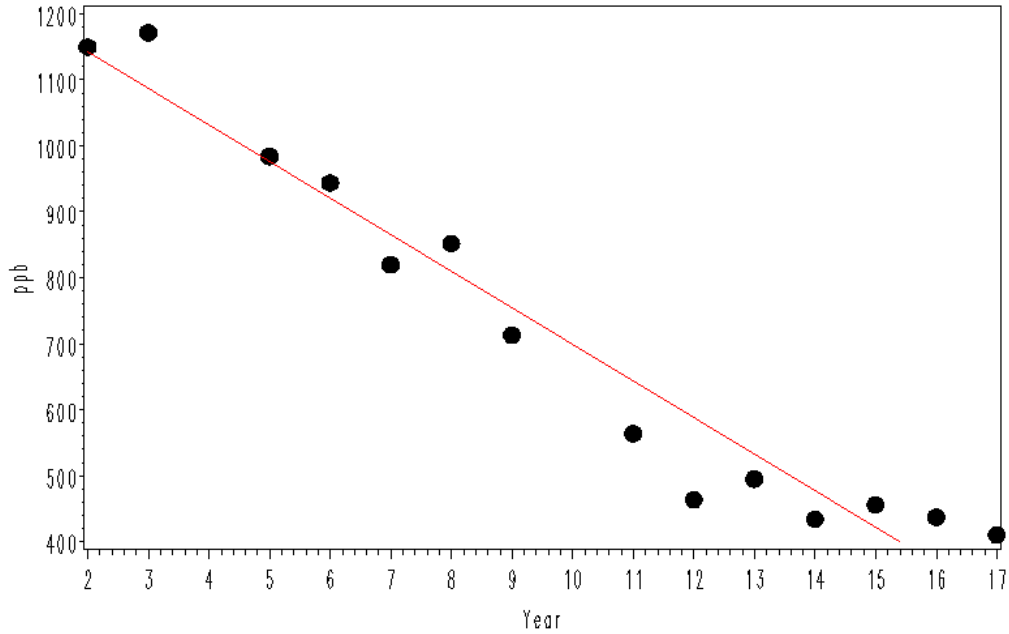

Regression Equation:
co = 1253.554 - 55.45305*year index

Figure 8.4 CO 5-8 CST May-Oct. OLS Trends, years since 1990, El Paso Tillman C413

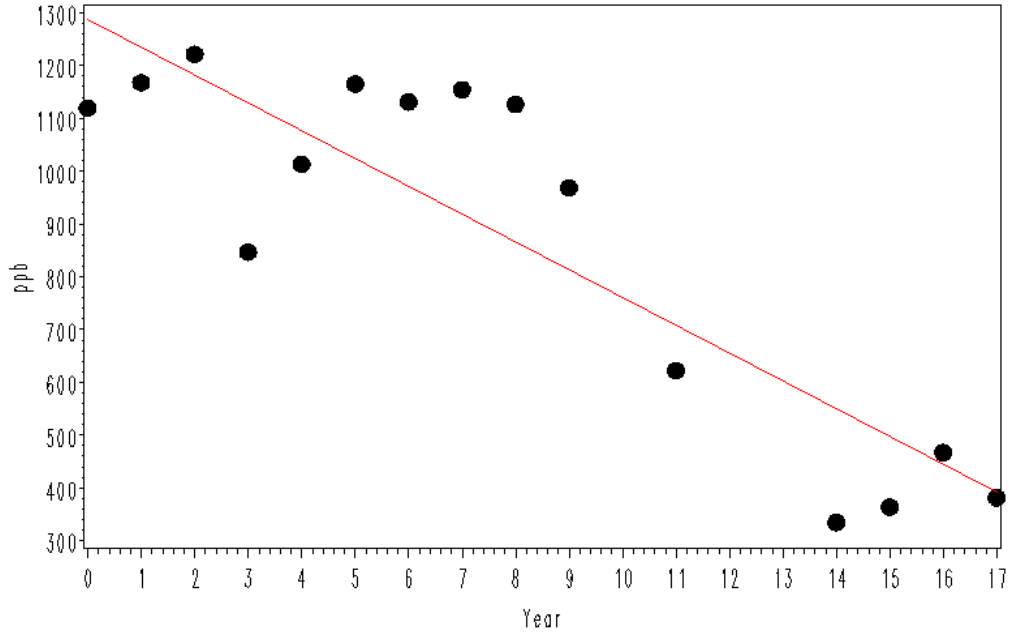

Regression Equation:
co = 1286.63 - 52.62762*year index

Figure 8.4 CO 5-8 CST May-Oct. OLS Trends, years since 1990, Houston Lang C408

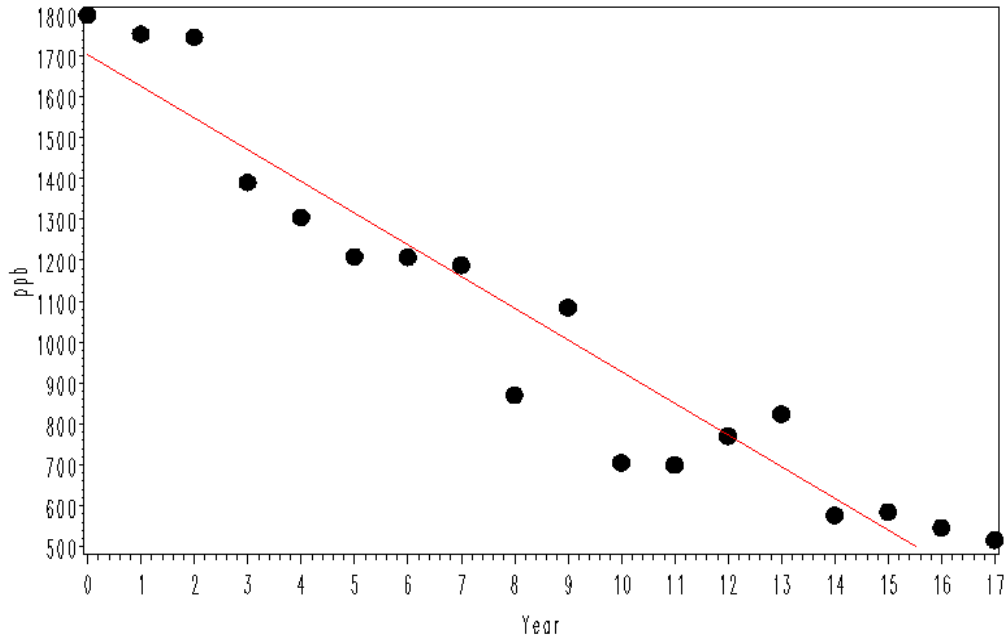

Regression Equation:
co = 1702.718 - 77.54314*year index

Figure 8.5 CO 5-8 CST May-Oct. OLS Trends, years since 1990, Houston Crawford C407

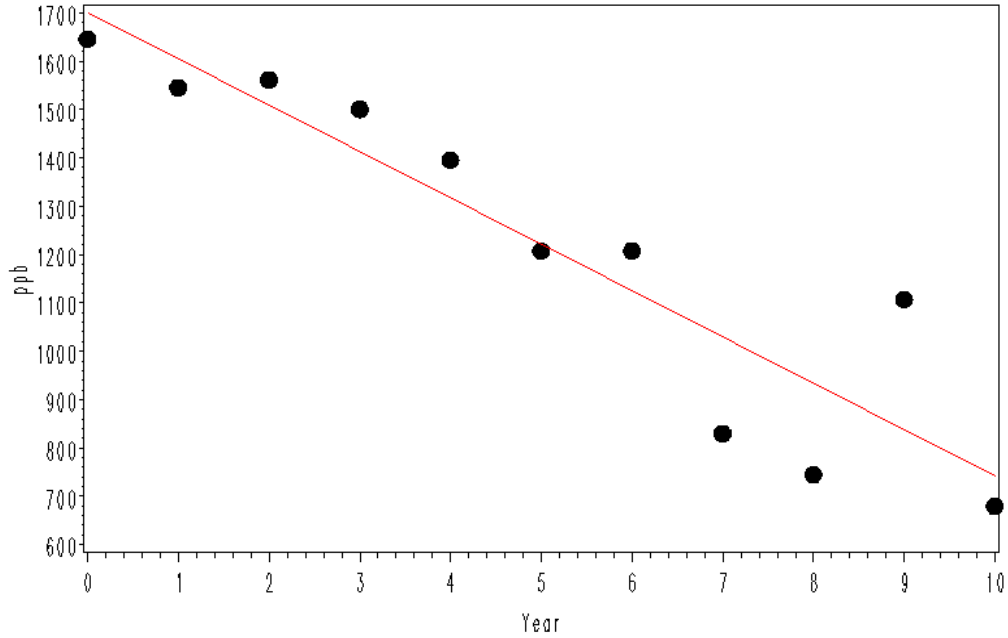

Regression Equation:
co = 1701.095 - 96.04289*year index

Figure 8.6 CO 5-8 CST May-Oct. OLS Trends, years since 1990, Houston Clinton C403

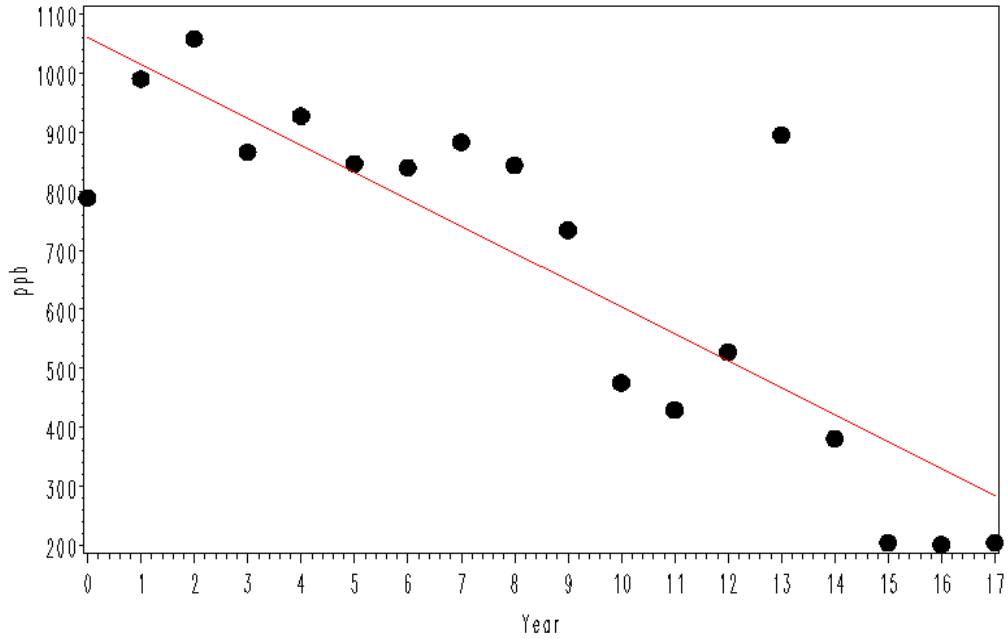

Regression Equation:
co = 1058.959 - 45.48042*year index

Figure 8.7 CO 5-8 CST May-Oct. OLS Trends, years since 1990, Dallas Hinton C401

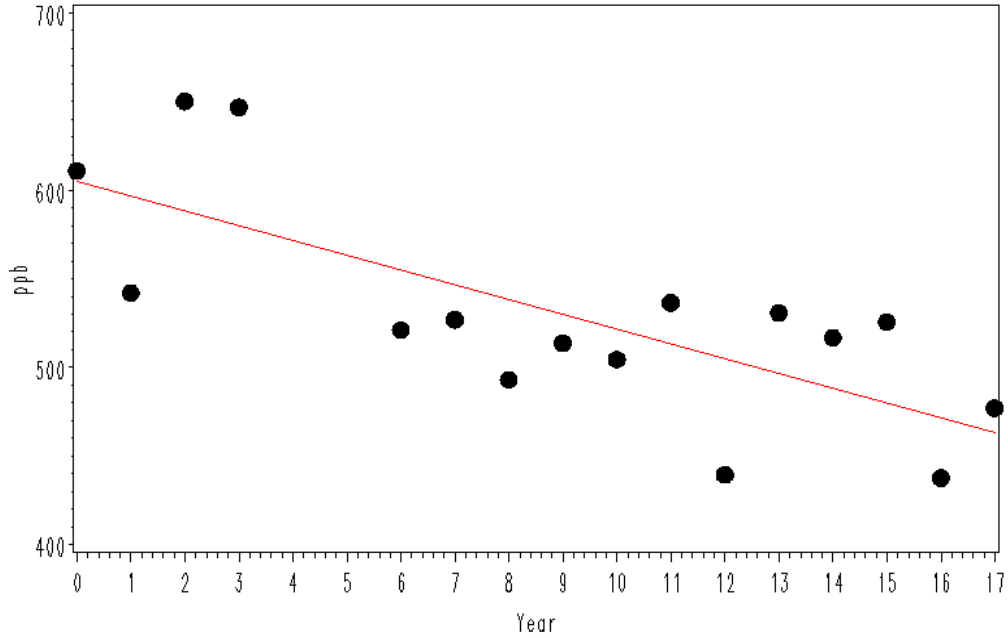

Regression Equation:
co = 604.7454 - 8.346754*year index

Figure 8.8 CO 5-8 CST May-Oct. OLS Trends, years since 1990, Brownsville C80

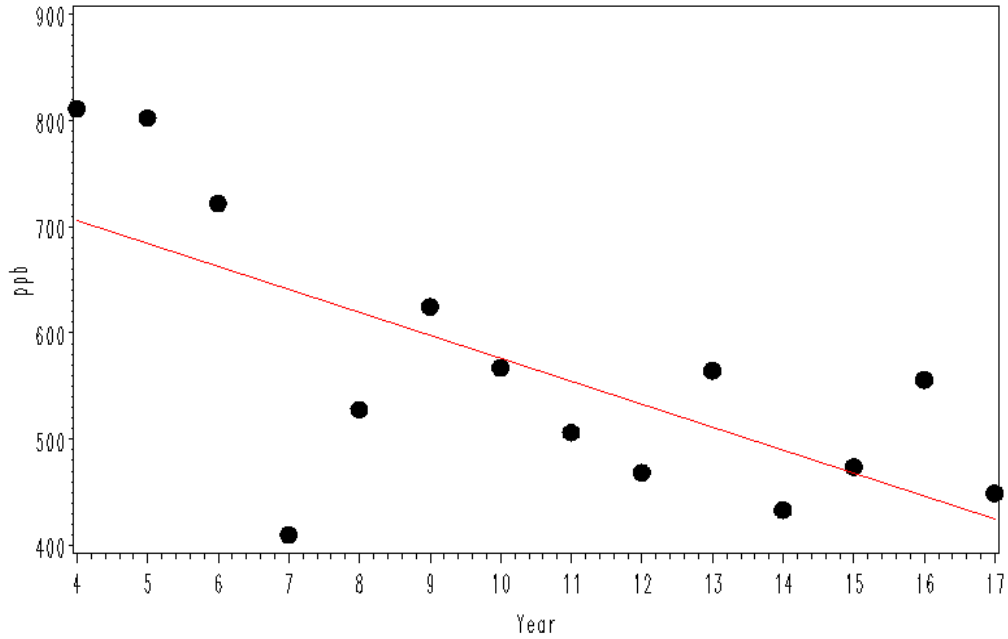

Regression Equation:
co = 792.2857 - 21.5862*year index

Figure 8.9 CO 5-8 CST May-Oct. OLS Trends, years since 1990, Laredo C44

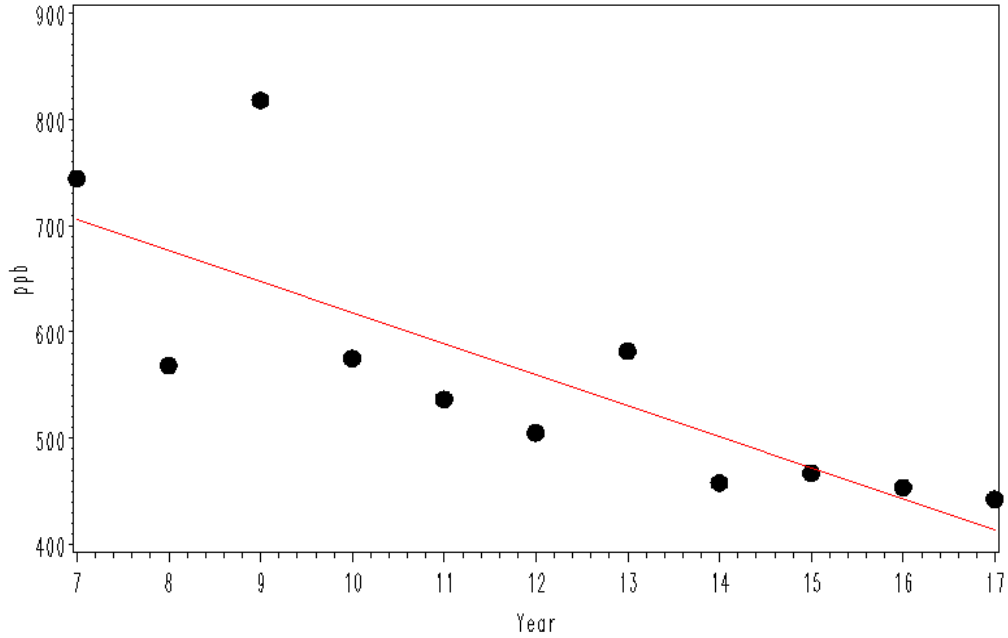

Regression Equation:
co = 909.1171 - 29.14628*year index

Figure 8.10 CO 5-8 CST May-Oct. OLS Trends, years since 1990, El Paso Chamizal C41

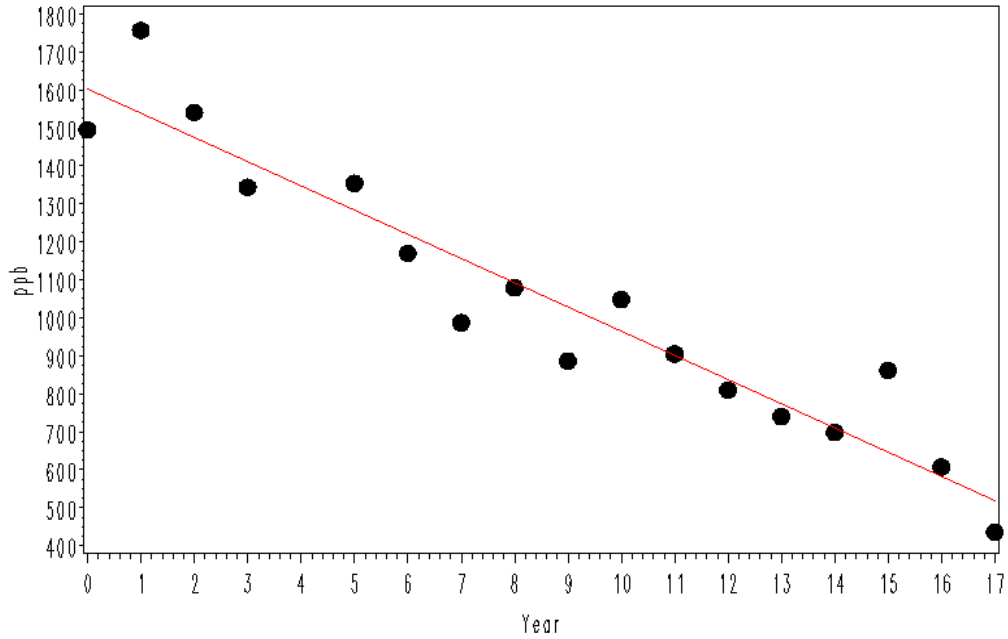

Regression Equation:
co = 1601.471 - 63.76064*year index

Figure 8.11 CO 5-8 CST May-Oct. OLS Trends, years since 1990, El Paso Sun Metro C40

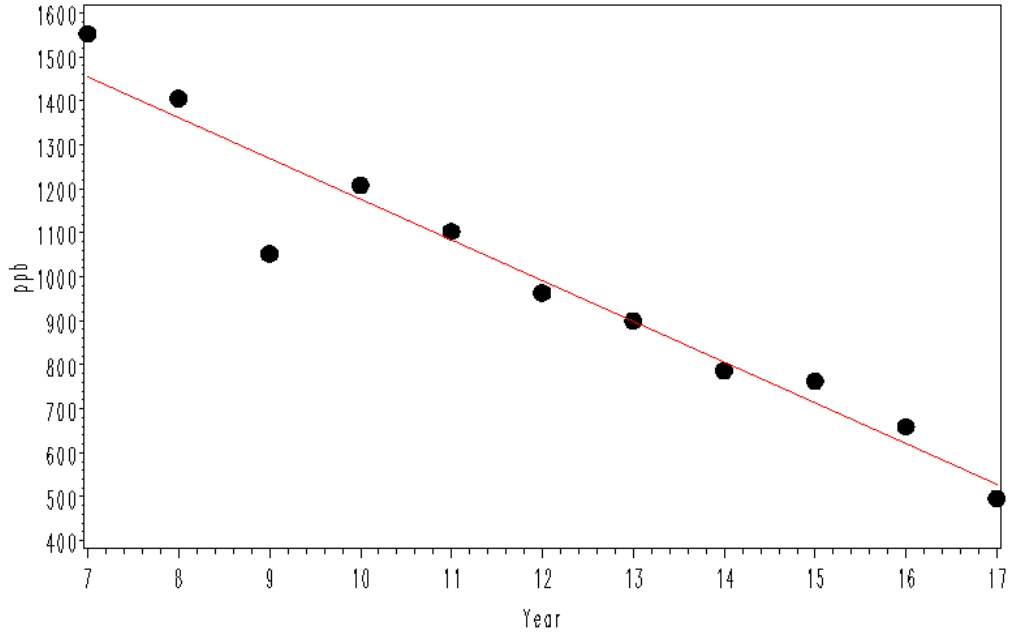

Regression Equation:
co = 2100.319 - 92.5165*year index

Figure 8.12 CO 5-8 CST May-Oct. OLS Trends, years since 1990, Houston Deer Park C35

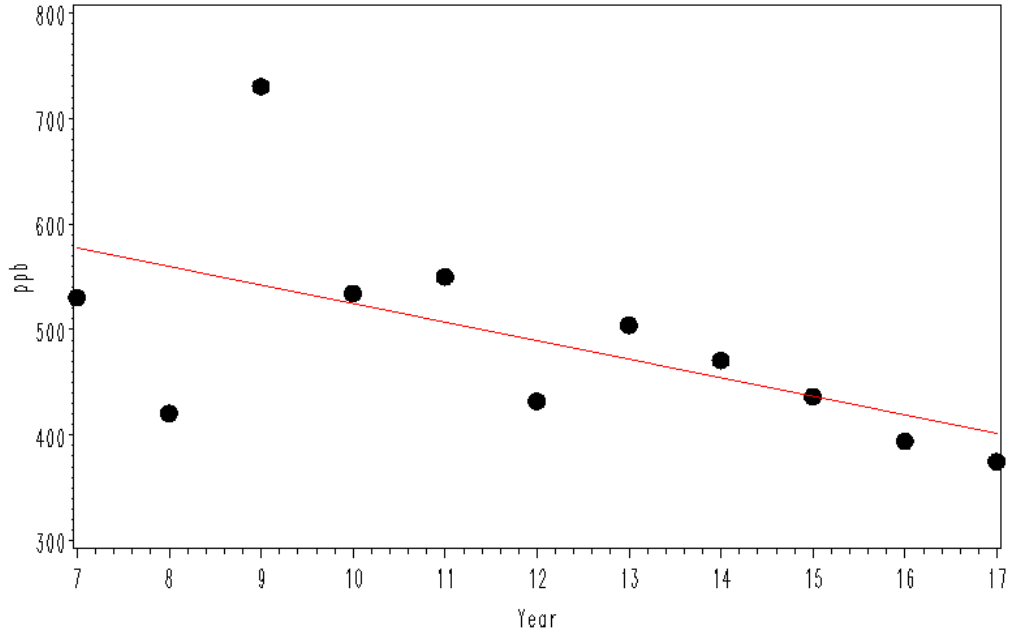

Regression Equation:
co = 700.1525 - 17.59159*year index

Figure 8.13 CO 5-8 CST May-Oct. OLS Trends, years since 1990, San Antonio Downtown C27

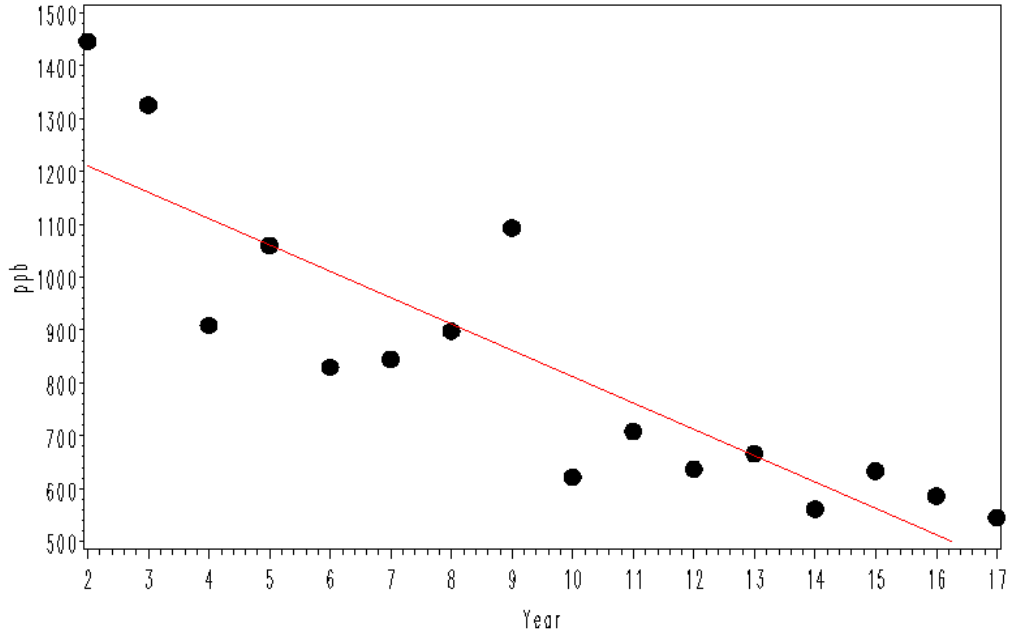

Regression Equation:
co = 1308.871 - 49.80826*year index

Figure 8.14 CO 5-8 CST May-Oct. OLS Trends, years since 1990, Fort Worth NW C13

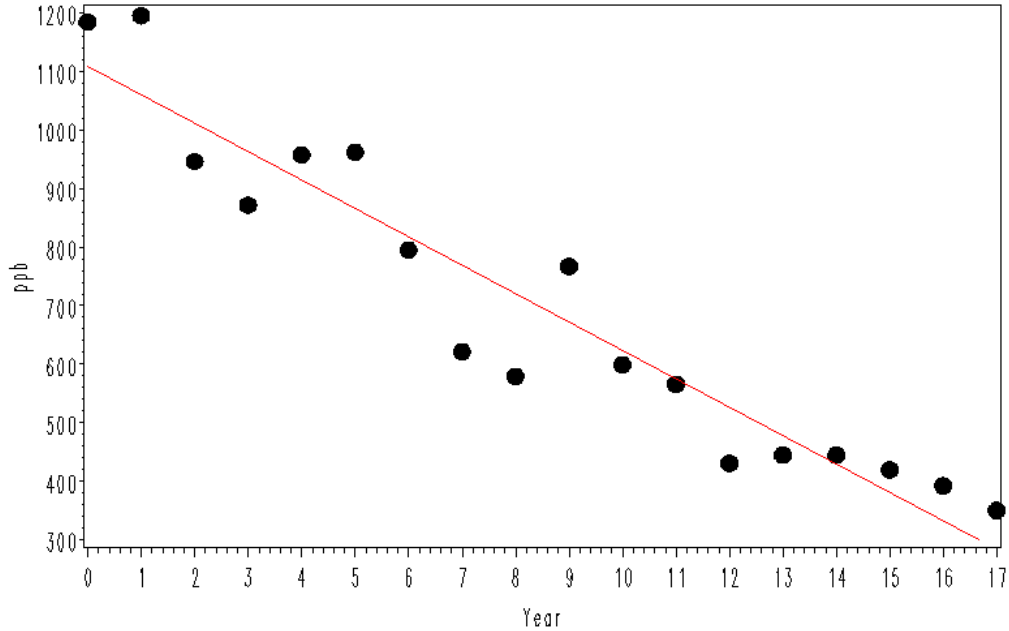

Regression Equation:
co = 1109.387 - 48.60076*year index

Figure 8.15 CO 5-8 CST May-Oct. OLS Trends, years since 1990, El Paso UTEP C12

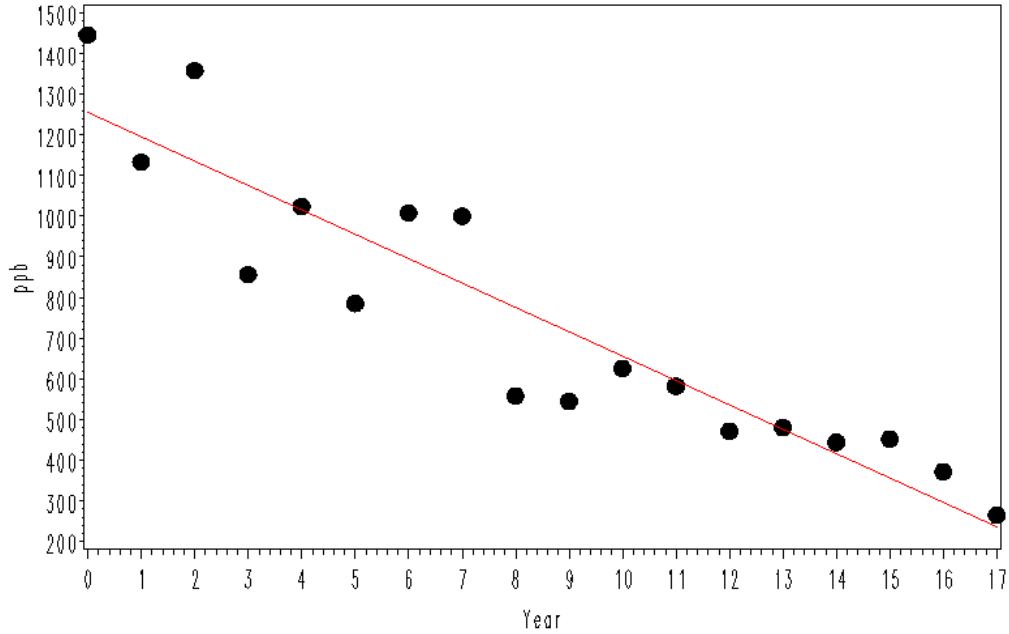

Regression Equation:
co = 1255.256 - 60.01133*year index

Figure 8.16 CO 5-8 CST May-Oct. OLS Trends, years since 1990, Houston Aldine C8

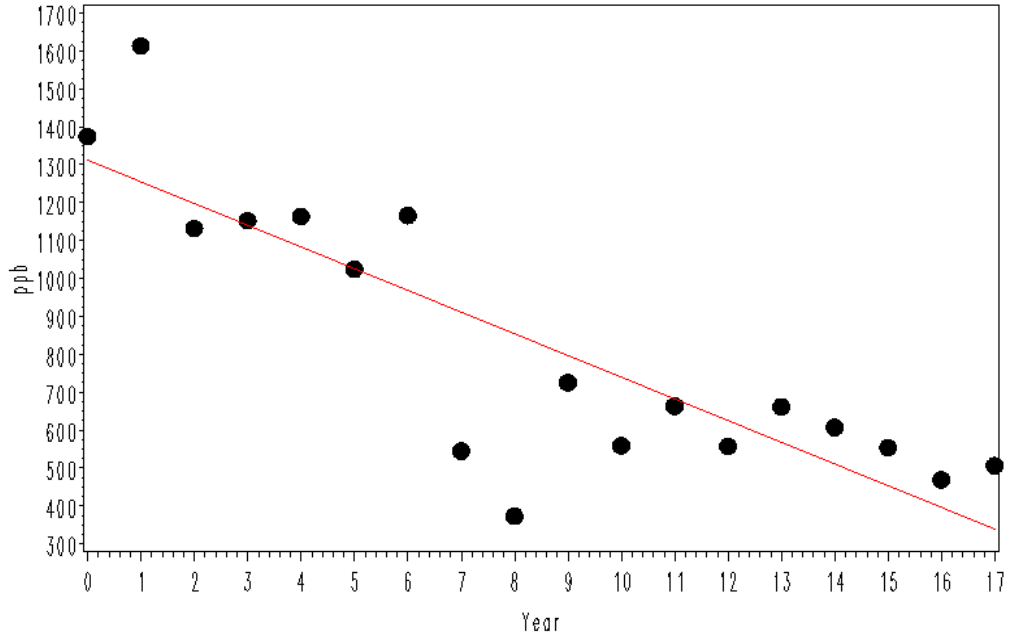

Regression Equation:
co = 1310.134 - 57.06325*year index

Figure 8.17 El Paso Downtown C6

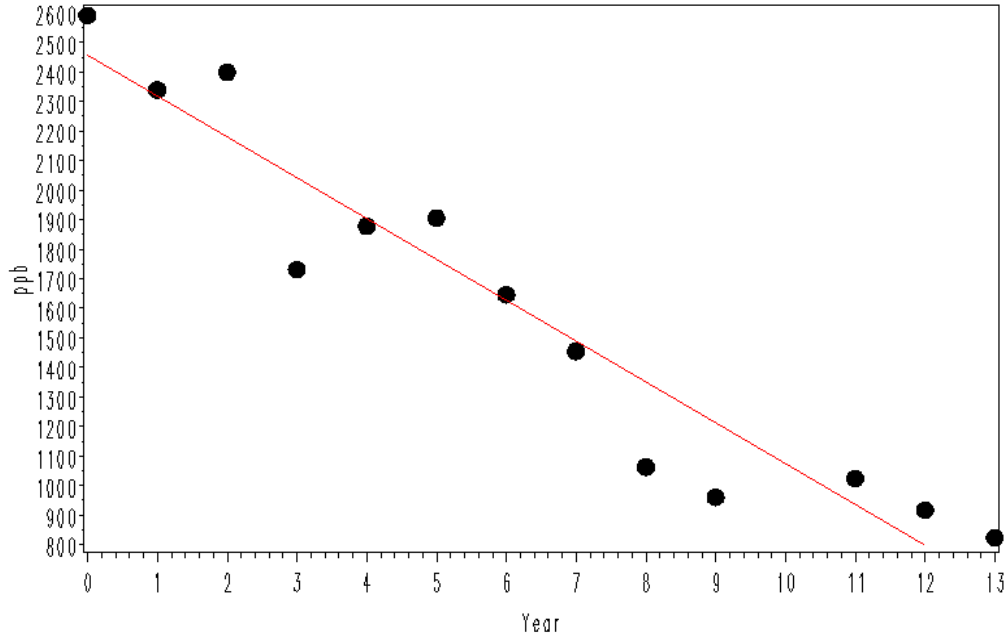

Regression Equation:
co = 2457.08 - 138.2908*year index

9. Sulfur dioxide (SO_2) trends

There are both national and state standards for sulfur dioxide (SO_2). The NAAQS are 140 ppb for 24-hours and 30 ppb for an annual mean. Texas has a 30 minute standard of 400 ppb for residential areas but is constructed based on differencing upwind and downwind concentrations near a facility; in other words, no individual facility can be responsible for having contributed 400 ppb to whatever downwind measurement is made. Thus, the state standard is almost always handled by mobile monitoring and not with CAMS. SO2 is a highly episodic pollutant, and although like other primary pollutants concentrations may be high at night, the mean diurnal patterns vary from site to site and provide little systematic clues as to a best time period to select for trend analysis. Thus, the simple 24-hour average has been chosen.

9.1 SO_2 ordinary least squares trends

Table 9.1 SO2 OLS trend for daily 1hr max and daily mean

Site Description	Variable	Incpt	Slope	DoF	Rsq	T	p-value	L95B	U95B
Hinton StC401	max	8.71	-0.46	14	65%	-5.14	0.00	-0.65	-0.27
Hinton S C401	avg	3.06	-0.17	14	57%	-4.34	0.00	-0.26	-0.09
Mid Towr C94	max	7.54	-0.09	9	10%	-0.99	0.35	-0.31	0.12
Mid Towr C94	avg	1.62	-0.03	9	25%	-1.72	0.12	-0.08	0.01
Mid OFW C52	max	27.77	-1.01	10	23%	-1.72	0.12	-2.32	0.30
Mid OFW C52	avg	4.96	-0.20	10	30%	-2.09	0.06	-0.42	0.01
UTEP C12	max	66.62	-4.72	16	85%	-9.70	0.00	-5.75	-3.69
UTEP C12	avg	11.37	-0.76	16	85%	-9.66	0.00	-0.93	-0.60
Sun Metro C40	max	28.32	-1.66	9	53%	-3.16	0.01	-2.85	-0.47
Sun Metro C40	avg	7.08	-0.38	9	52%	-3.11	0.01	-0.66	-0.11
TX Cty C10	max	26.29	-0.90	12	29%	-2.23	0.05	-1.79	-0.02
TX Cty C10	avg	6.61	-0.18	12	8%	-1.02	0.33	-0.56	0.20
Wayside C405	max	16.62	-0.67	16	86%	-9.87	0.00	-0.82	-0.53
Wayside C405	avg	5.08	-0.21	16	73%	-6.57	0.00	-0.27	-0.14
Croquet C409	max	9.90	-0.31	15	74%	-6.45	0.00	-0.41	-0.21
Croquet C409	avg	2.83	-0.11	15	65%	-5.28	0.00	-0.16	-0.07
Monroe C406	max	13.11	-0.35	16	65%	-5.41	0.00	-0.48	-0.21
Monroe C406	avg	4.18	-0.11	16	37%	-3.08	0.01	-0.18	-0.03
Clinton C403	max	27.16	-0.96	16	68%	-5.88	0.00	-1.30	-0.61
Clinton C403	avg	5.64	-0.06	16	5%	-0.92	0.37	-0.20	0.08
Bea-Lamar C2	max	30.36	-1.02	16	62%	-5.09	0.00	-1.45	-0.60
Bea-Lamar C2	avg	7.62	-0.32	16	74%	-6.67	0.00	-0.43	-0.22
PA West C28	max	25.84	-0.97	16	60%	-4.85	0.00	-1.39	-0.55
PA West C28	avg	5.68	-0.25	16	55%	-4.43	0.00	-0.37	-0.13
CarrollSt C54	max	42.12	-1.71	8	65%	-3.88	0.00	-2.72	-0.69
CarrollSt C54	avg	10.77	-0.53	8	69%	-4.21	0.00	-0.83	-0.24
West C4	max	10.86	-0.52	16	58%	-4.67	0.00	-0.76	-0.28
West C4	avg	1.97	-0.06	16	18%	-1.88	0.08	-0.13	0.01
Tuloso C21	max	8.39	-0.47	15	87%	-9.90	0.00	-0.57	-0.37
Tuloso C21	avg	1.92	-0.10	15	48%	-3.75	0.00	-0.16	-0.05
Huisache C98	max	16.13	-0.69	8	49%	-2.76	0.02	-1.27	-0.11
Huisache C98	avg	2.87	-0.11	8	23%	-1.55	0.16	-0.26	0.05

Figure 9.1 SO2 Daily One-Hour Peak Mean OLS Trends, years since 1990, Houston Croquet C409

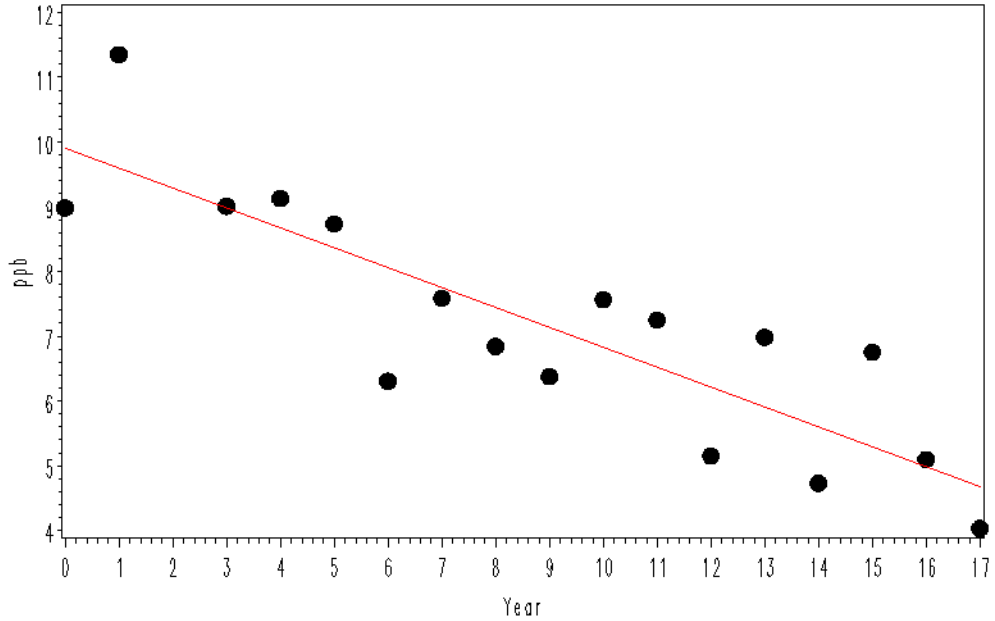

Regression Equation:
so21hrpk = 9.903757 - 0.30755*year index

Figure 9.2 SO2 Annual Mean OLS Trends, years since 1990, Houston Croquet C409

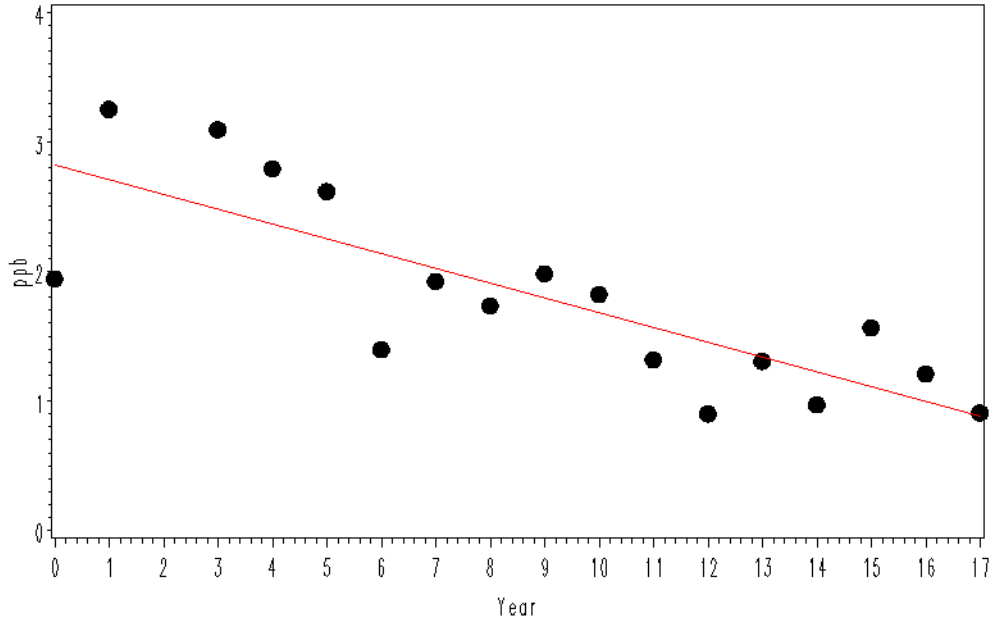

Regression Equation:
so21hrav = 2.825697 - 0.114416*year index

Figure 9.3 SO2 Daily One-Hour Peak Mean OLS Trends, years since 1990, Beaumont-Lamar C2

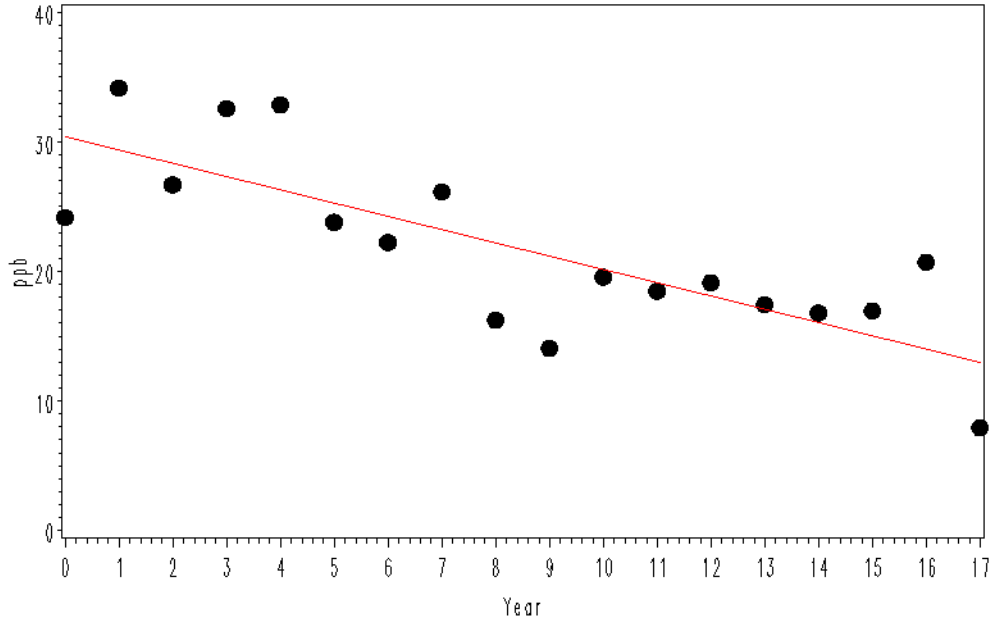

Regression Equation:
so21hrpk = 30.36444 - 1.021662*year index

Figure 9.4 SO2 Annual Mean OLS Trends, years since 1990, Beaumont-Lamar C2

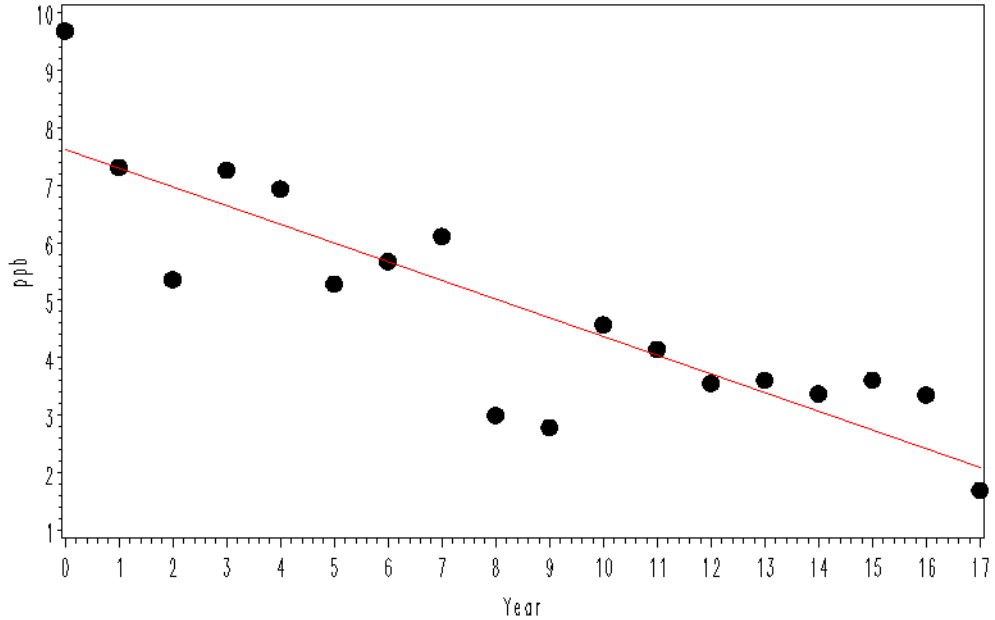

Regression Equation:
so21hrav = 7.615384 - 0.324781*year index

Figure 9.5 SO2 Daily One-Hour Peak Mean OLS Trends, years since 1990, Corpus Christi West C4

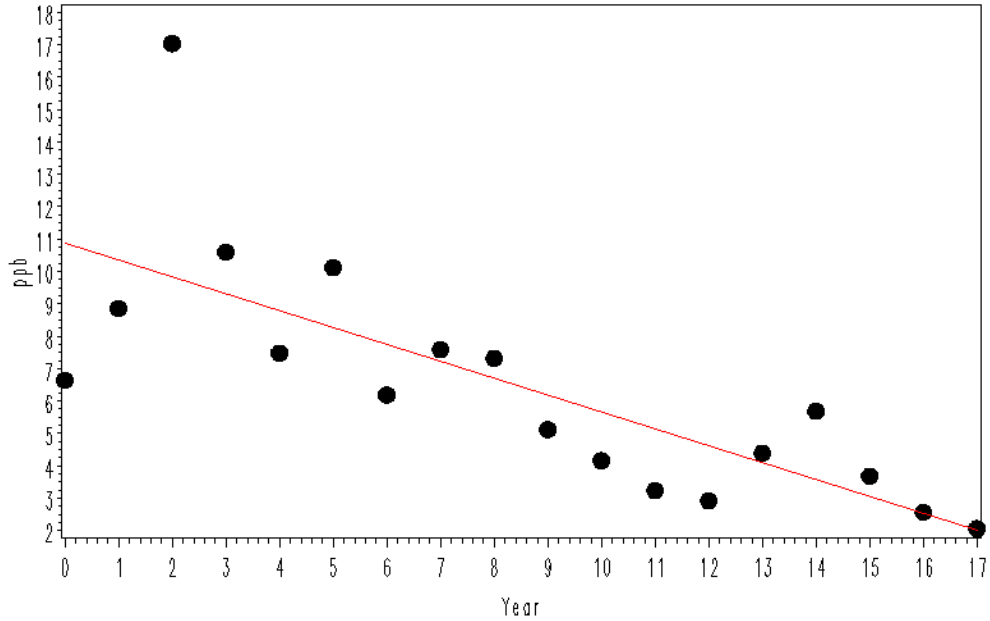

Regression Equation:
so21hrpk = 10.86376 - 0.521623*year index

Figure 9.6 SO2 Annual Mean OLS Trends, years since 1990, Corpus Christi West C4

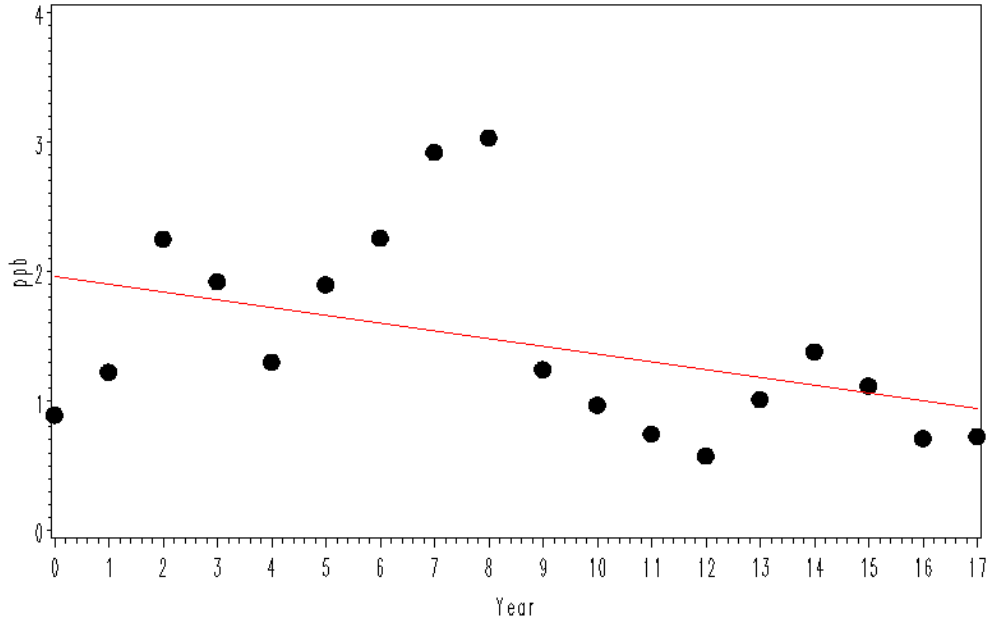

Regression Equation:
so21hrav = 1.965411 - 0.060082*year index

Figure 9.7 SO2 Daily One-Hour Peak Mean OLS Trends, years since 1990, Texas City C10

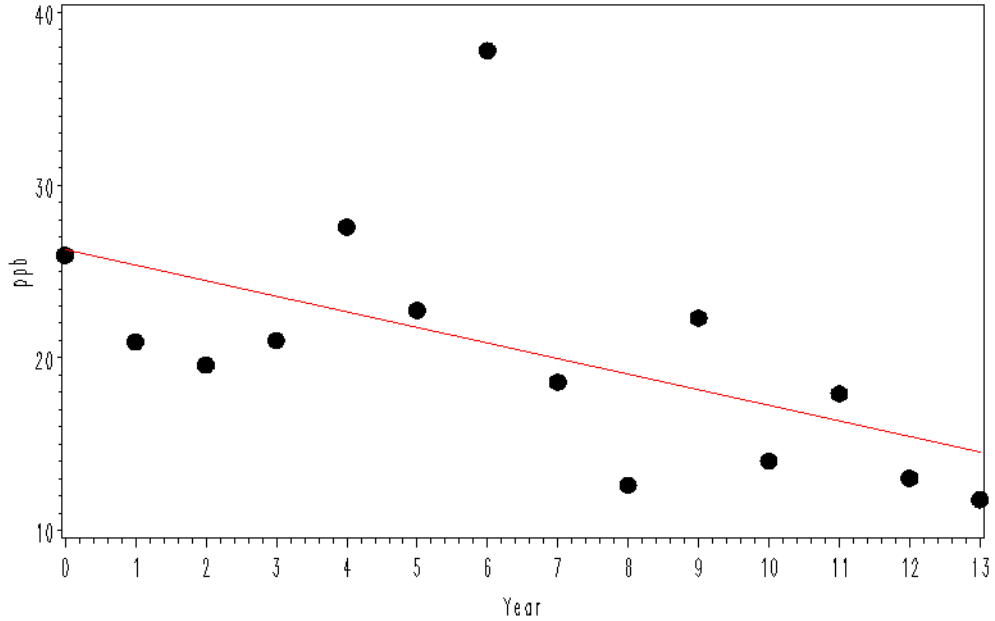

Regression Equation:
so21hrpk = 26.29297 - 0.902474*year index

Figure 9.8 SO2 Annual Mean OLS Trends, years since 1990, Texas City C10

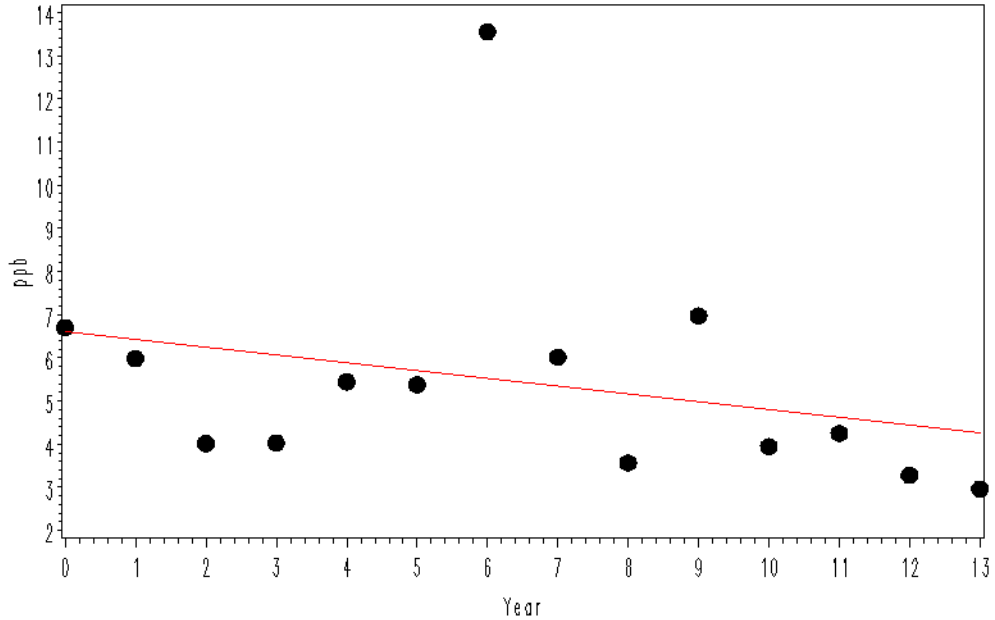

Regression Equation:
so21hrav = 6.613475 - 0.18055*year index

Figure 9.9 SO2 Daily One-Hour Peak Mean OLS Trends, years since 1990, El Paso UTEP C12

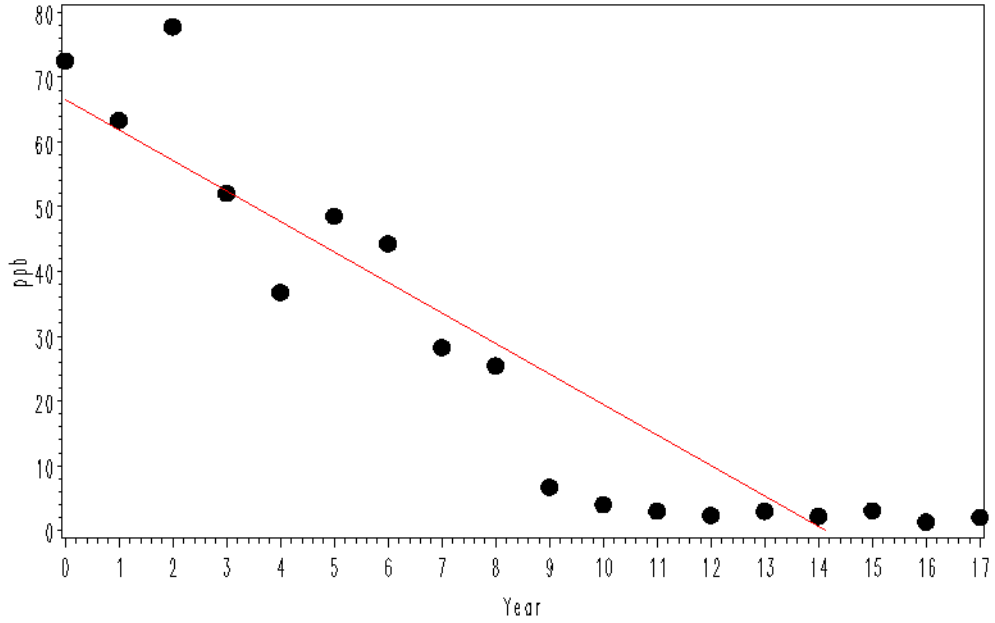

Regression Equation:
so21hrpk = 66.61507 - 4.719285*year index

Figure 9.10 SO2 Annual Mean OLS Trends, years since 1990, El Paso UTEP C12

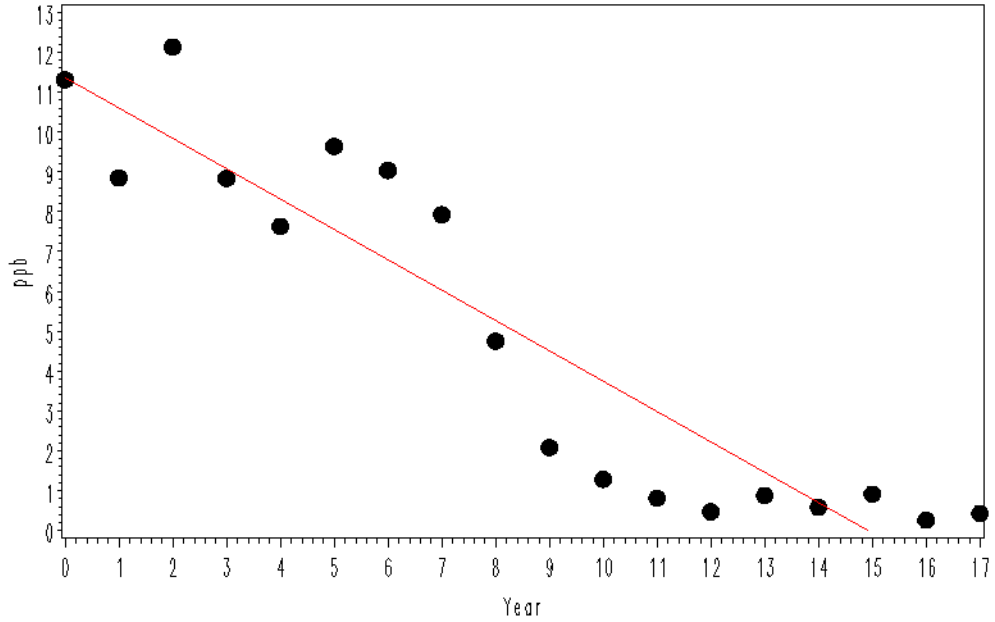

Regression Equation:
so21hrav = 11.36833 - 0.762738*year index

Figure 9.11 SO2 Daily One-Hour Peak Mean OLS Trends, years since 1990, Corpus Christi Tuloso C21

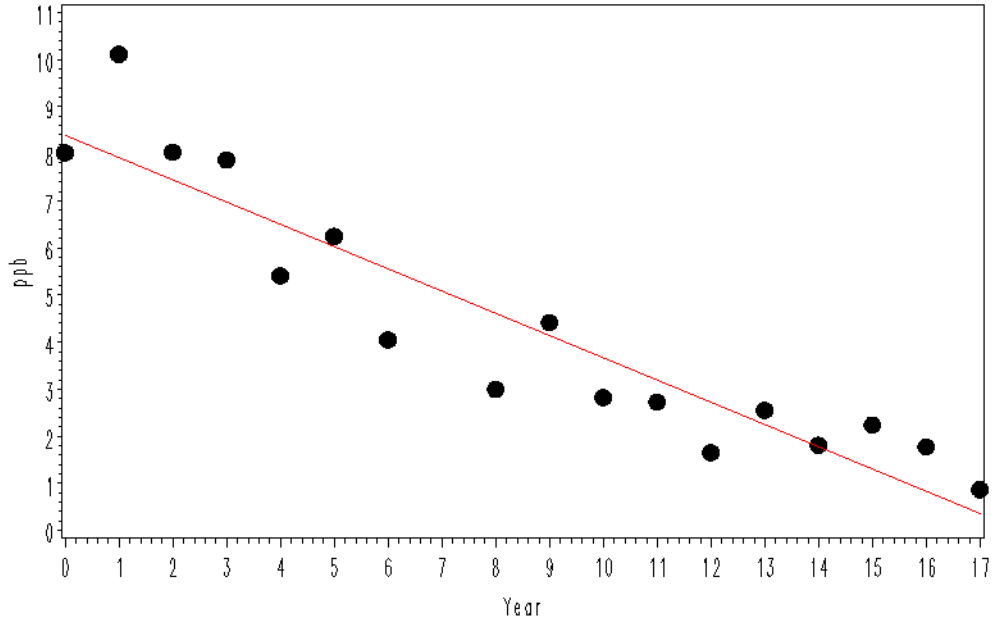

Regression Equation:
so21hrpk = 8.394483 - 0.472875*year index

Figure 9.12 SO2 Annual Mean OLS Trends, years since 1990, Corpus Christi Tuloso C21

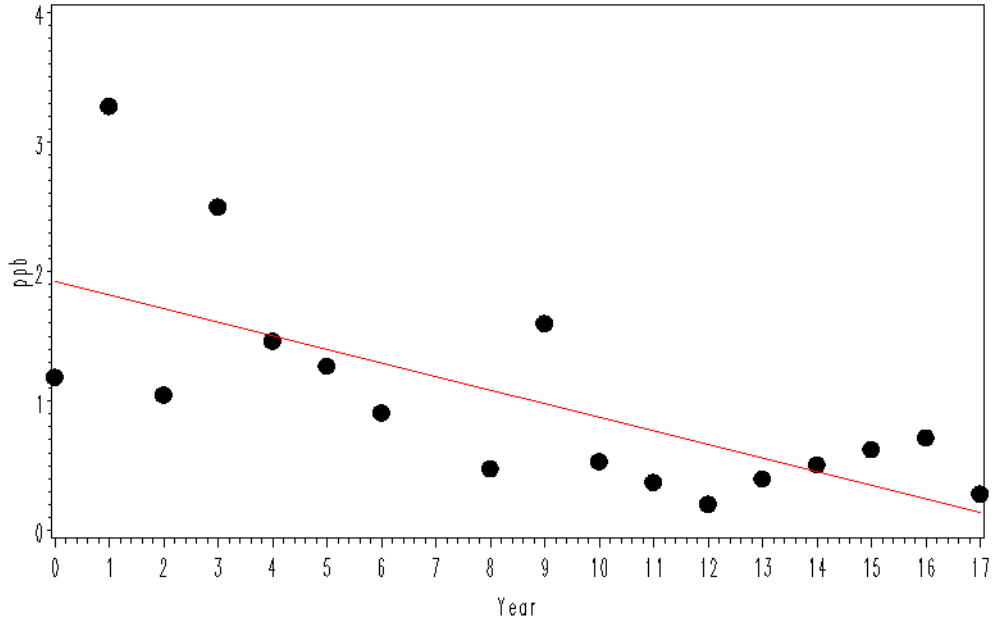

Regression Equation:
so21hrav = 1.923499 - 0.104898*year index

Figure 9.13 SO2 Daily One-Hour Peak Mean OLS Trends, years since 1990, Port Arthur West C28

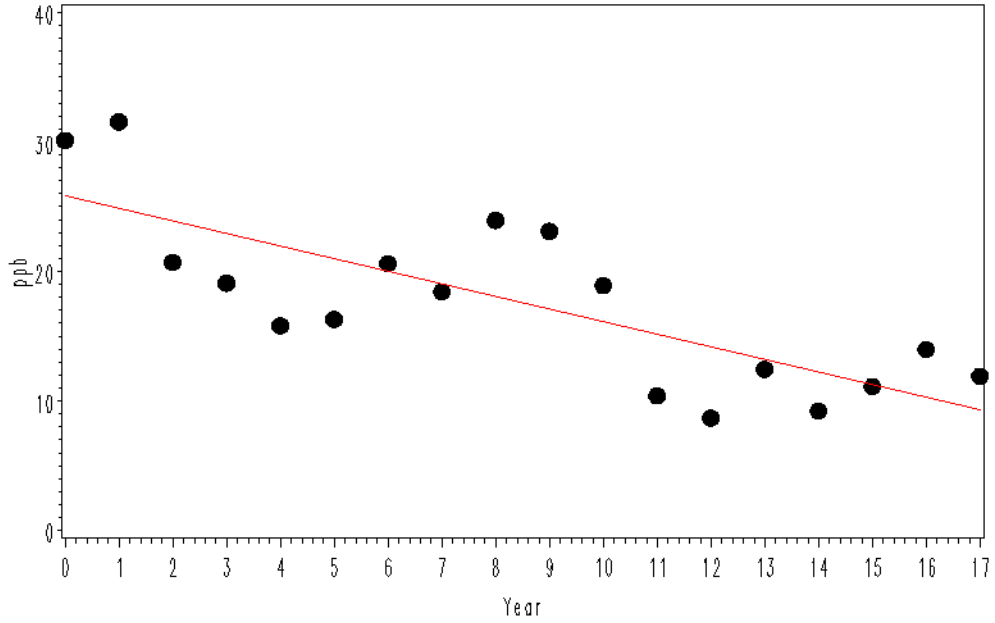

Regression Equation:
so21hrpk = 25.83536 - 0.969993*year index

Figure 9.14 SO2 Annual Mean OLS Trends, years since 1990, Port Arthur West C28

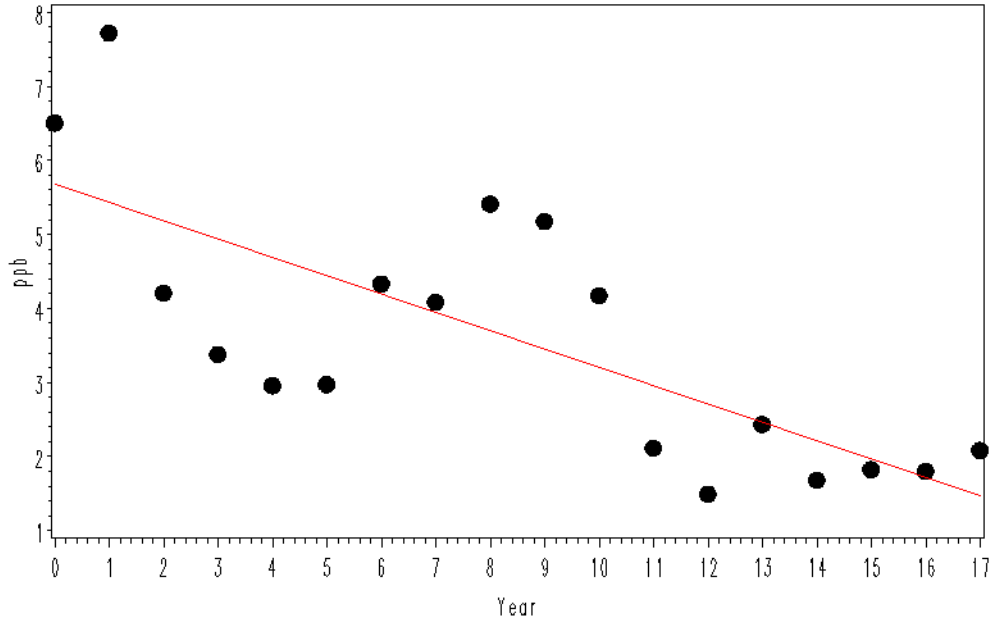

Regression Equation:
so21hrav = 5.680915 - 0.247471*year index

Figure 9.15 SO2 Daily One-Hour Peak Mean OLS Trends, years since 1990, El Paso Sun Metro C40

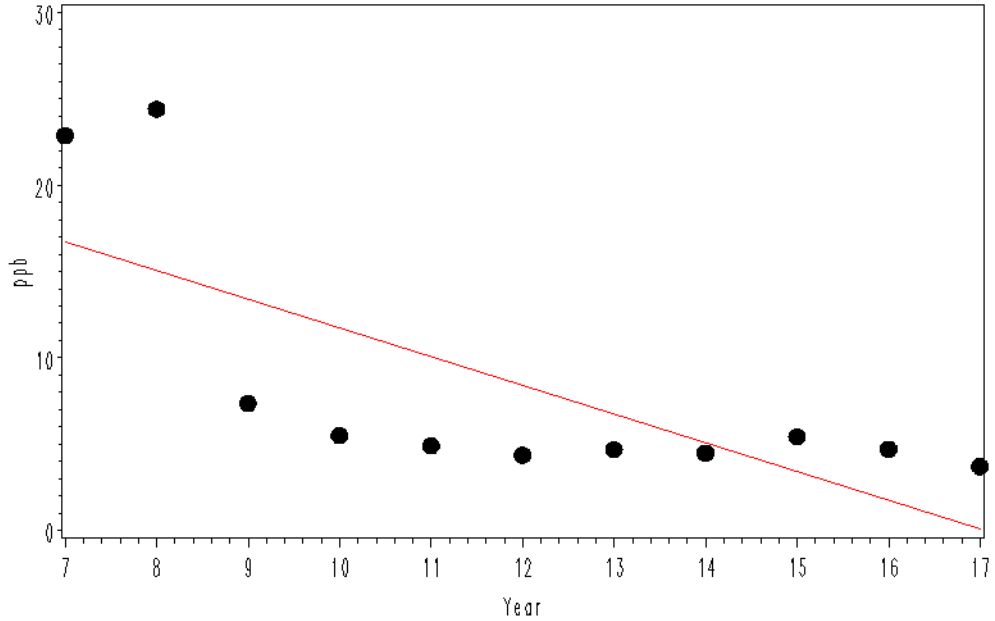

Regression Equation:
so21hrpk = 28.3208 - 1.659216*year index

Figure 9.16 SO2 Annual Mean OLS Trends, years since 1990, El Paso Sun Metro C40

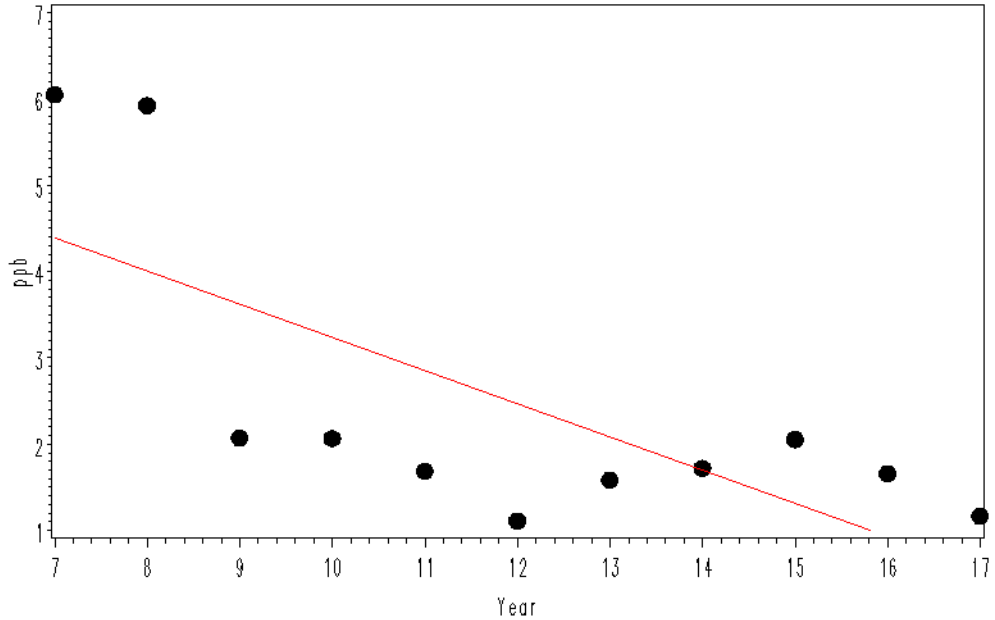

Regression Equation:
so21hrav = 7.078428 - 0.384488*year index

Figure 9.17 SO2 Daily One-Hour Peak Mean OLS Trends, years since 1990, Midlothian OFW C52

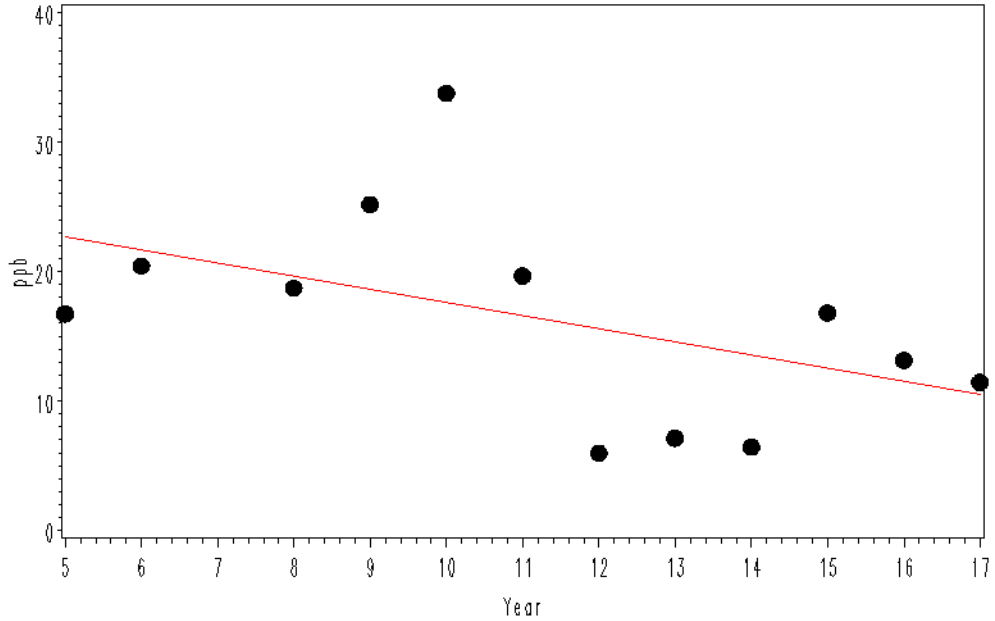

Regression Equation:
so21hrpk = 27.77319 - 1.012957*year index

Figure 9.18 SO2 Annual Mean OLS Trends, years since 1990, Midlothian OFW C52

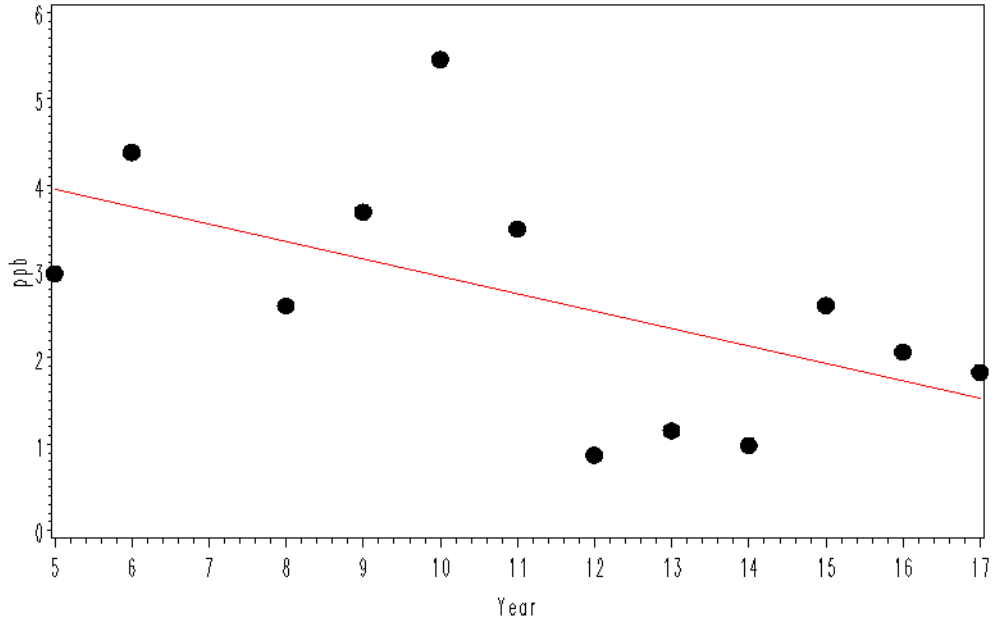

Regression Equation:
so21hrav = 4.961224 - 0.201465*year index

Figure 9.19 SO2 Daily One-Hour Peak Mean OLS Trends, years since 1990, Carroll St Park C54

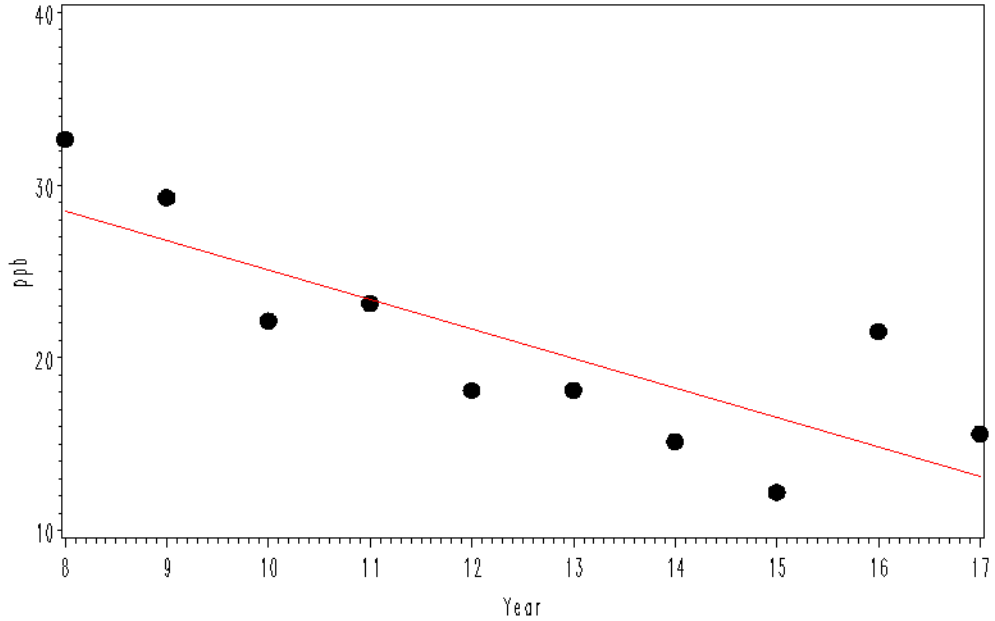

Regression Equation:
so21hrpk = 42.11623 - 1.705014*year index

Figure 9.20 SO2 Annual Mean OLS Trends, years since 1990, Carroll St Park C54

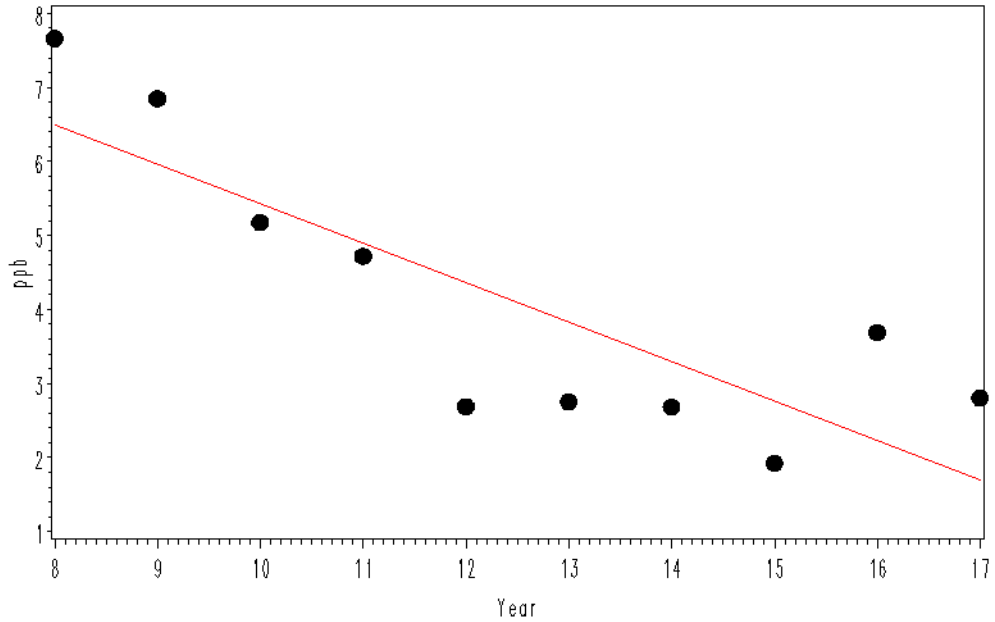

Regression Equation:
so21hrav = 10.77153 - 0.534024*year index

Figure 9.21 SO2 Daily One-Hour Peak Mean OLS Trends, years since 1990, Midlothian Tower C94

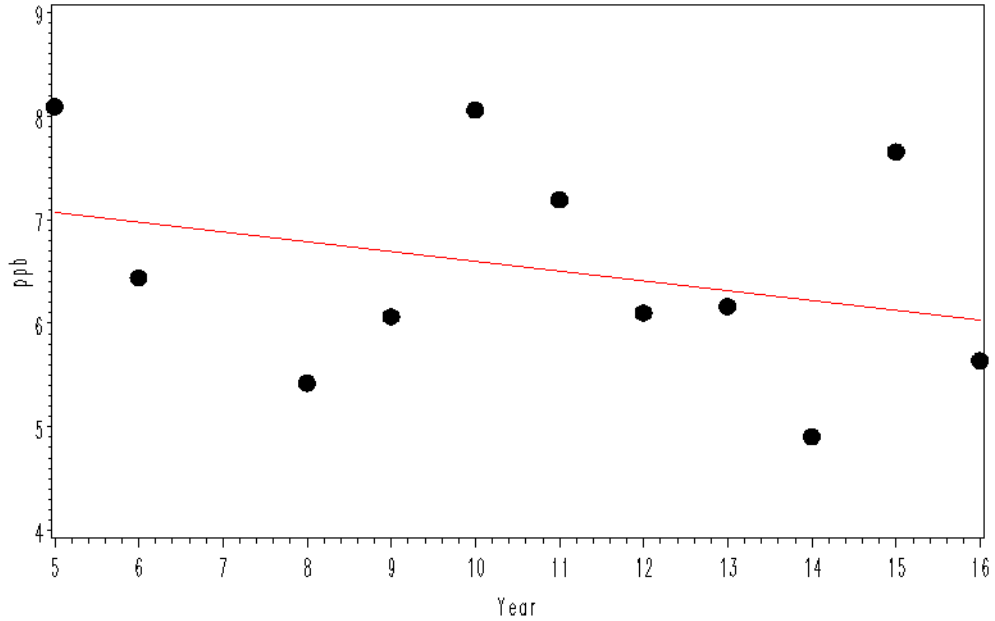

Regression Equation:
so21hrpk = 7.538315 - 0.093947*year index

Figure 9.22 SO2 Annual Mean OLS Trends, years since 1990, Midlothian Tower C94

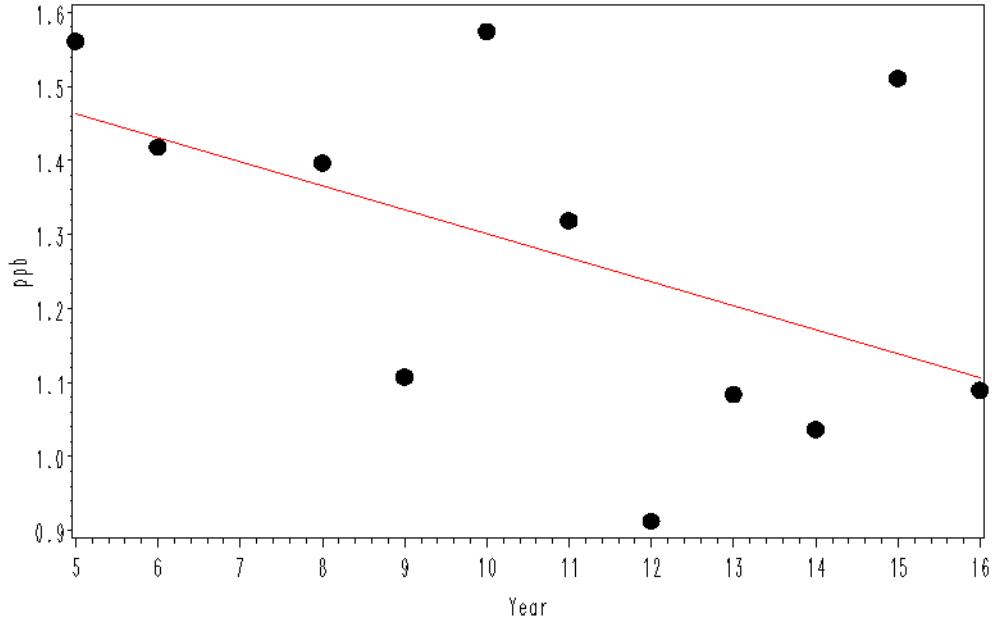

Regression Equation:
so21hrav = 1.624914 - 0.032452*year index

Figure 9.23 SO2 Daily One-Hour Peak Mean OLS Trends, years since 1990, Corpus Christi Huisache C98

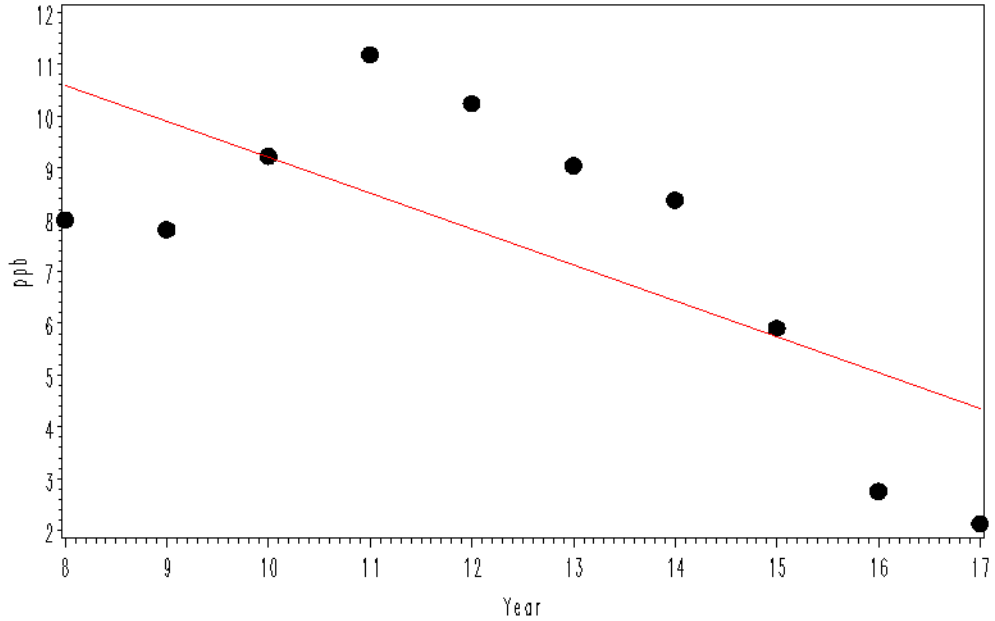

Regression Equation:
so21hrpk = 16.13364 - 0.693136*year index

Figure 9.24 SO2 Annual Mean OLS Trends, years since 1990, Corpus Christi Huisache C98

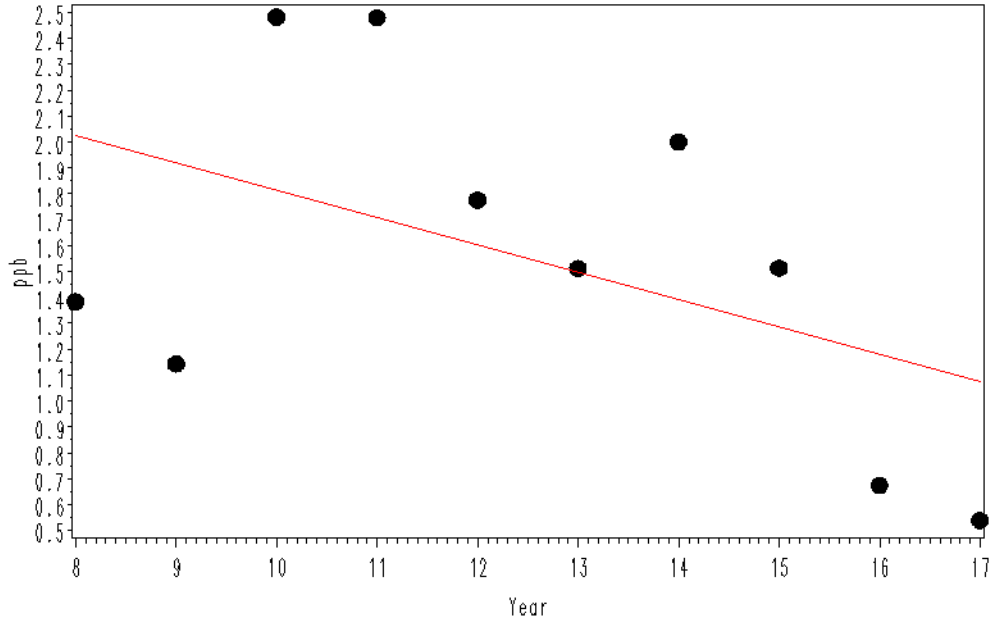

Regression Equation:
so21hrav = 2.871263 - 0.105639*year index

Figure 9.25 SO2 Daily One-Hour Peak Mean OLS Trends, years since 1990, Dallas Hinton C401

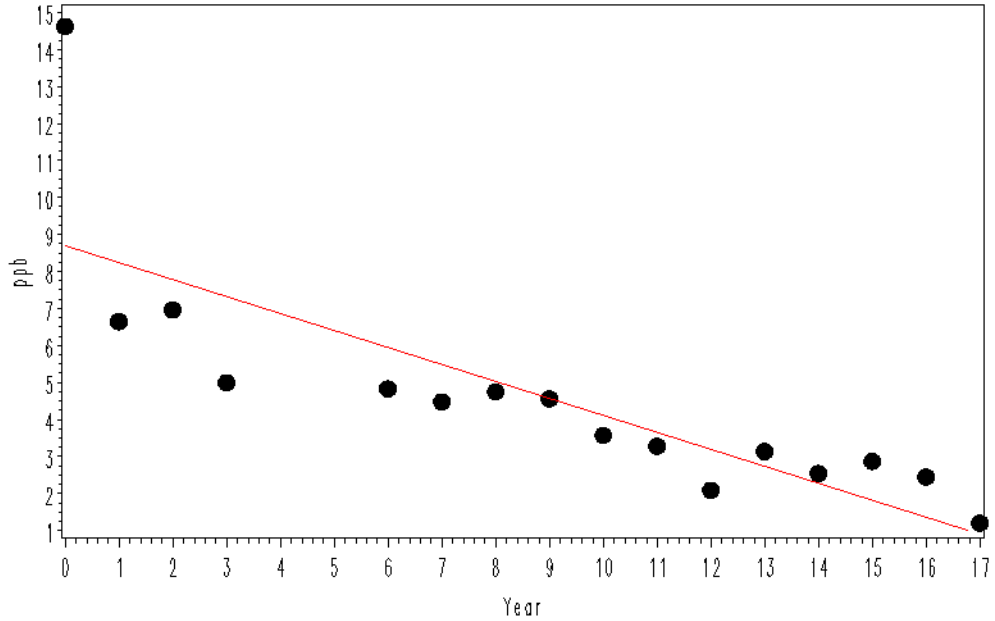

Regression Equation:
so21hrpk = 8.705982 - 0.459927*year index

Figure 9.26 SO2 Annual Mean OLS Trends, years since 1990, Dallas Hinton C401

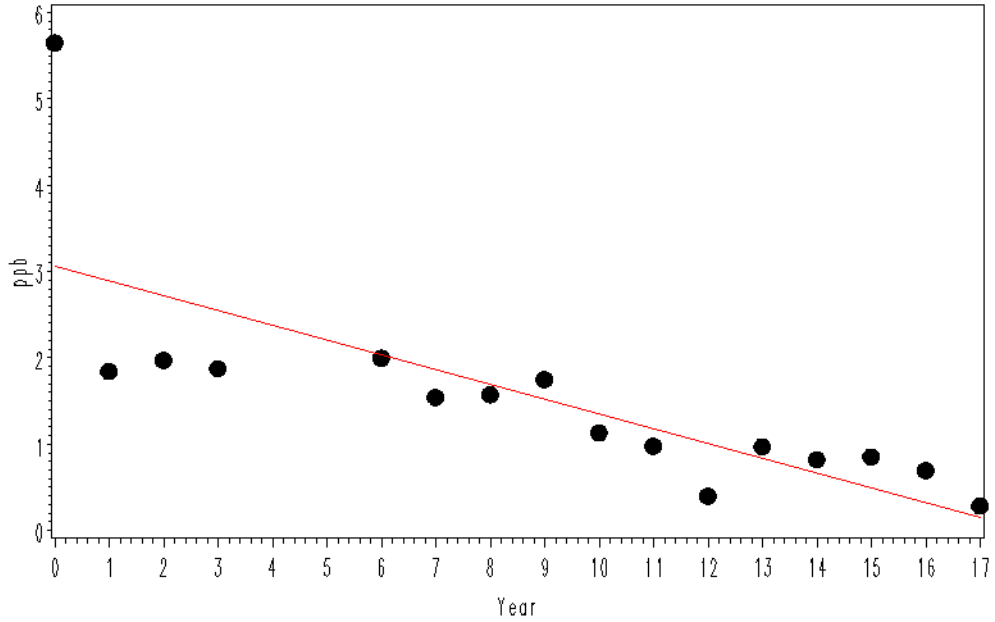

Regression Equation:
so21hrav = 3.064308 - 0.171338*year index

Figure 9.27 SO2 Daily One-Hour Peak Mean OLS Trends, years since 1990, Houston Clinton C403

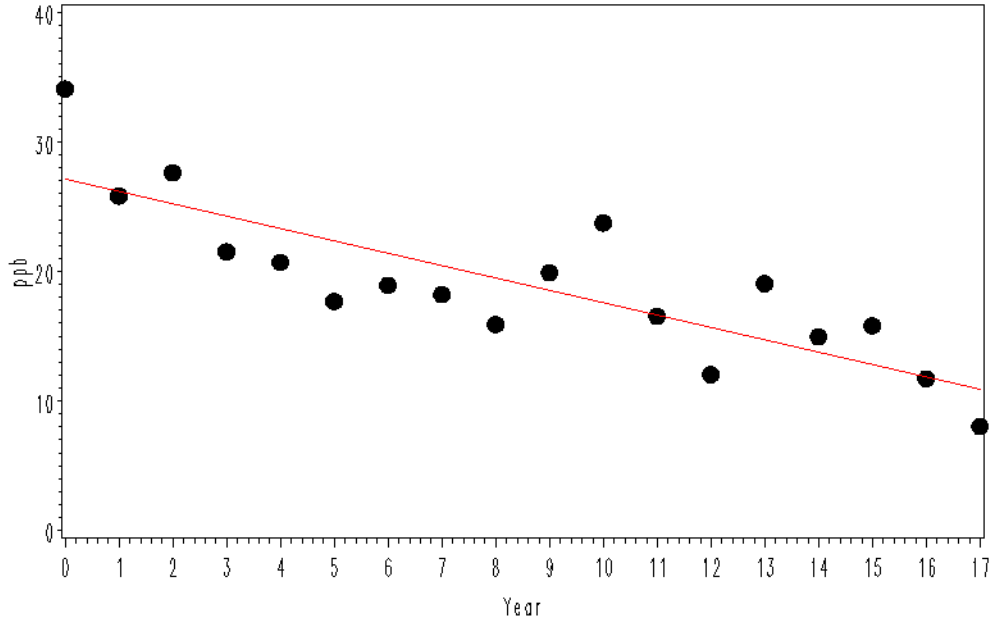

Regression Equation:
so21hrpk = 27.1566 - 0.955849*year index

Figure 9.28 SO2 Annual Mean OLS Trends, years since 1990, Houston Clinton C403

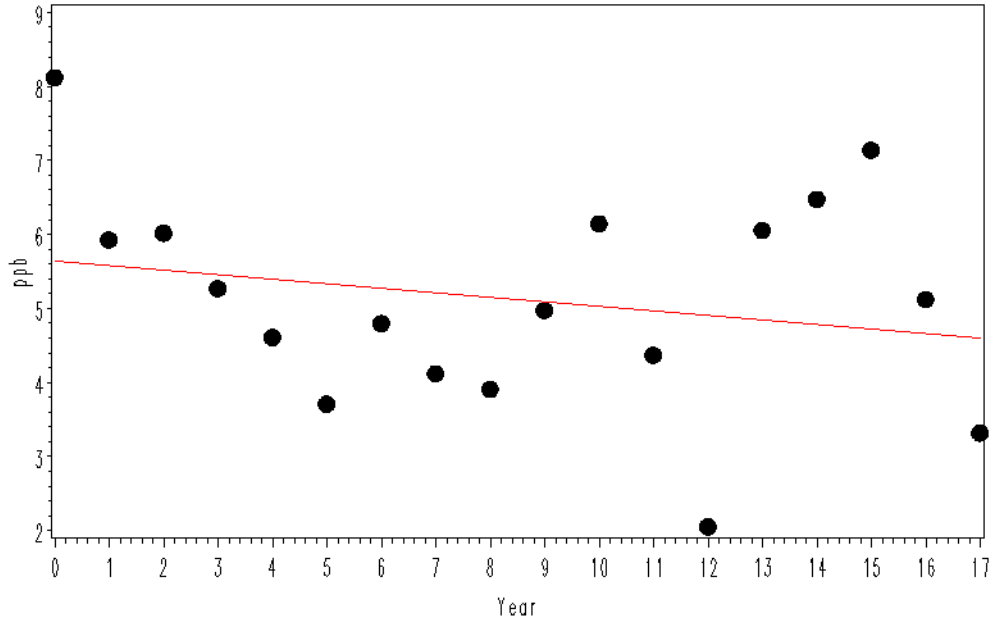

Regression Equation:
so21hrav = 5.642412 - 0.061413*year index

Figure 9.29 SO2 Daily One-Hour Peak Mean OLS Trends, years since 1990, Houston North Wayside C405

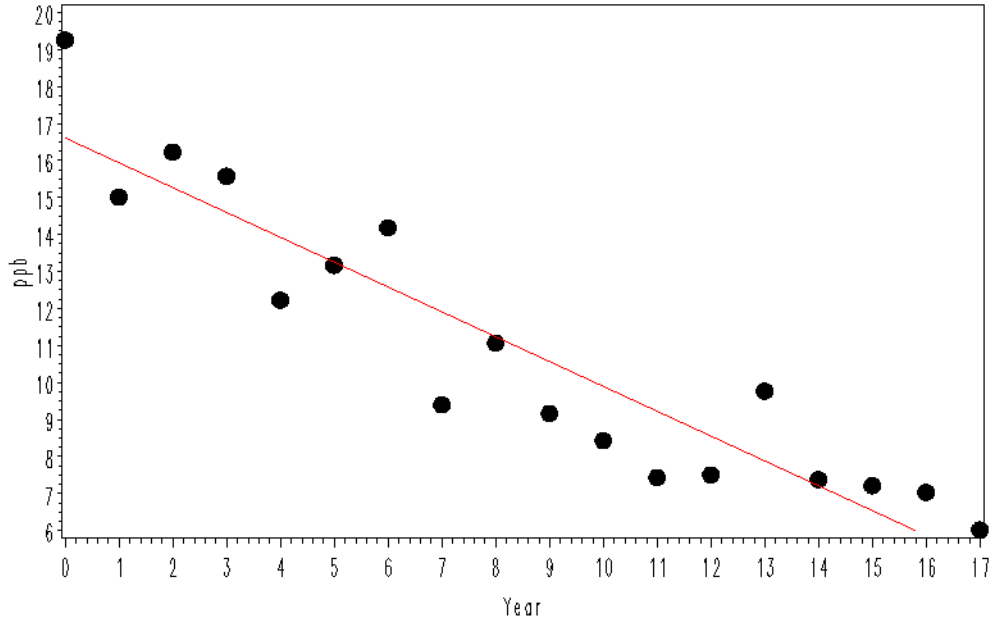

Regression Equation:
so21hrpk = 16.61899 - 0.673196*year index

Figure 9.30 SO2 Annual Mean OLS Trends, years since 1990, Houston North Wayside C405

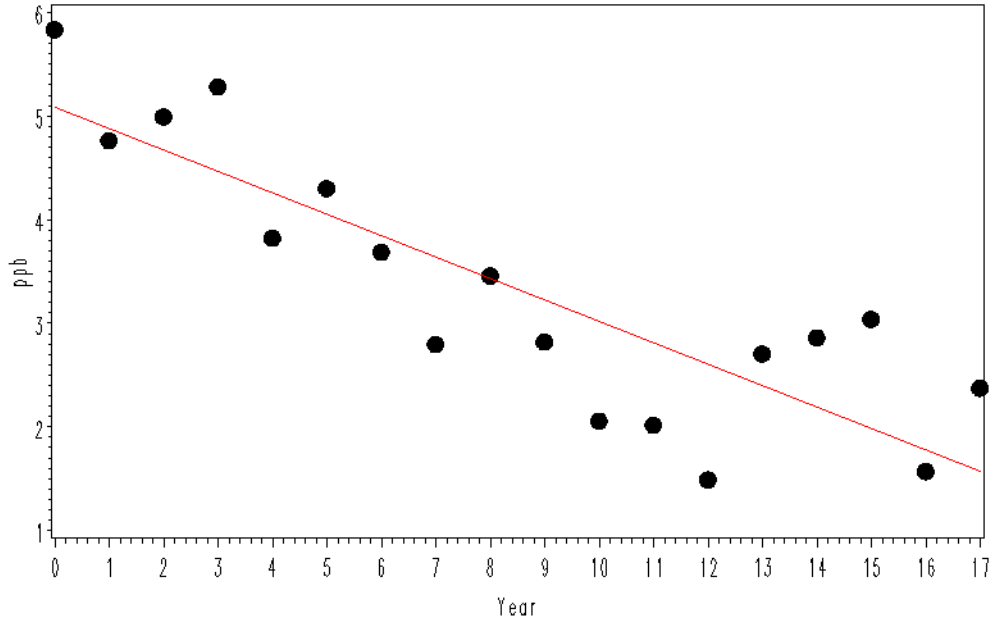

Regression Equation:
so21hrav = 5.078191 - 0.206067*year index

Figure 9.31 SO2 Daily One-Hour Peak Mean OLS Trends, years since 1990, Houston Monroe C406

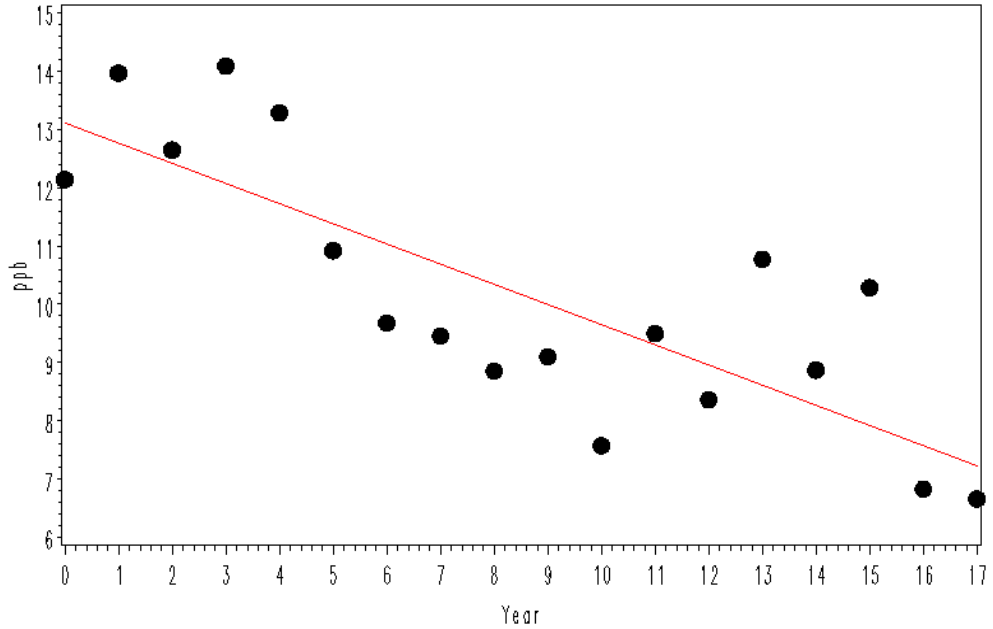

Regression Equation:
so21hrpk = 13.10645 - 0.345517*year index

Figure 9.32 SO2 Annual Mean OLS Trends, years since 1990, Houston Monroe C406

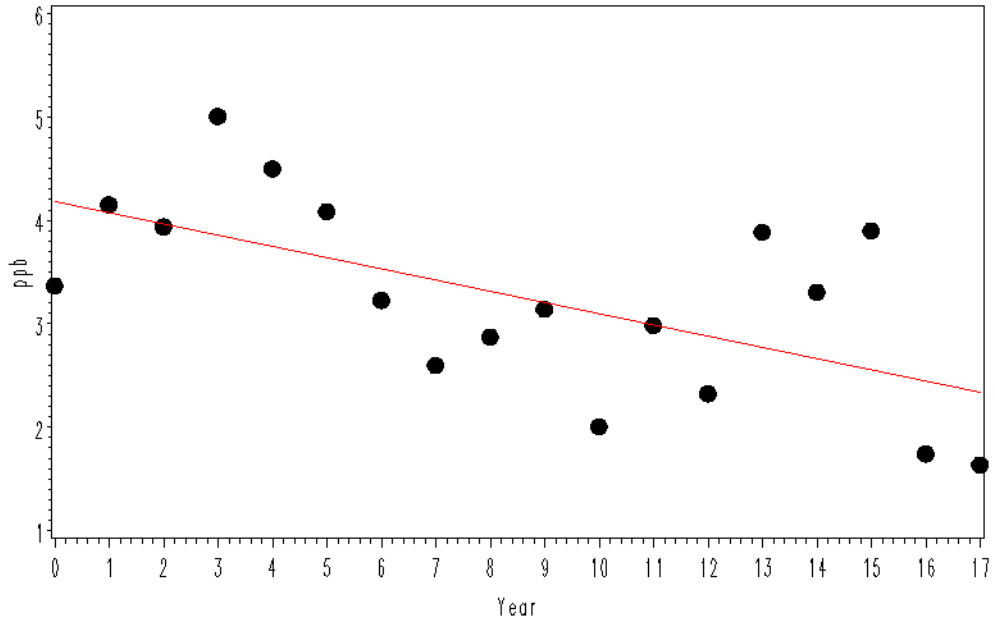

Regression Equation:
so21hrav = 4.184936 - 0.108725*year index

10. Hydrocarbon Species Trends (HRVOC, BTEX, Significant Alkane Compounds)

Only four auto-GCs operating in Texas have data for more than 10 years. These are:

481130069 Dallas Hinton Street CAMS 401
481410044 El Paso Chamizal CAMS 41
482011035 Houston Clinton Drive CAMS 403
482011039 Deer Park CAMS 35

Data were examined from May – October for all years since 1995. Deer Park began in 1997 and lacks "complete" data for three years since then. In an initial analysis, a 75 percent completeness by year was required, and this was lowered to 50 percent to try to increase data inclusion for Deer Park. This lowering of completeness had negligible affect on the trends and did have a slight increase in including missing years for other sites, but did not help Deer Park.

10.1 Ordinary Least Squares Trends for HC

Several species from the four long-running auto-GCs in Dallas, Houston, and El Paso have been selected for analysis. These species represent three classes of hydrocarbons:

- Highly reactive species: ethylene, propylene, 1-butene
- "BTEX" substituted aromatics: benzene, toluene, ethyl benzene, m/p-xylene, and o-xylene
- Significant alkanes: n-butane, isobutane, n-pentane, isopentane

The OLS trends for these 12 species are summarized in Table 10.1 and graphed in Figures 10.1 – 10.48.

Table 10.1

Site Description	species	Intercept	slope	DoF	R2	T	p-value	L95B	U95B
Hinton St. C401	Ethylene	8.55	-0.39	10	0.797	-6.27	0.00	-0.53	-0.25
Hinton St. C401	Propylene	3.67	-0.11	10	0.463	-2.94	0.01	-0.19	-0.03
Hinton St. C401	1-Butene	0.58	-0.01	10	0.279	-1.97	0.08	-0.03	0.00
Hinton St. C401	Benzene	4.30	-0.19	10	0.634	-4.17	0.00	-0.29	-0.09
Hinton St. C401	Toluene	14.20	-0.44	10	0.366	-2.40	0.04	-0.85	-0.03
Hinton St. C401	m/p-Xylene	10.67	-0.54	10	0.765	-5.71	0.00	-0.75	-0.33
Hinton St. C401	o-Xylene	3.59	-0.18	10	0.730	-5.20	0.00	-0.25	-0.10
Hinton St. C401	Ethyl Benzene	3.05	-0.15	10	0.744	-5.39	0.00	-0.21	-0.09
Hinton St. C401	n-Butane	10.30	-0.32	10	0.504	-3.18	0.01	-0.54	-0.09
Hinton St. C401	Isobutane	3.85	-0.05	10	0.167	-1.41	0.19	-0.12	0.03
Hinton St. C401	n-Pentane	8.21	-0.31	10	0.422	-2.70	0.02	-0.57	-0.05
Hinton St. C401	Isopentane	16.60	-0.68	10	0.634	-4.16	0.00	-1.05	-0.32
Chamizal C41	Ethylene	16.79	-0.78	11	0.743	-5.64	0.00	-1.08	-0.47
Chamizal C41	Propylene	7.65	-0.31	11	0.680	-4.84	0.00	-0.45	-0.17
Chamizal C41	1-Butene	1.28	-0.04	11	0.402	-2.72	0.02	-0.08	-0.01
Chamizal C41	Benzene	13.59	-0.64	11	0.797	-6.56	0.00	-0.85	-0.42
Chamizal C41	Toluene	34.48	-1.54	11	0.841	-7.62	0.00	-1.98	-1.09
Chamizal C41	m/p-Xylene	21.27	-1.05	11	0.910	-10.55	0.00	-1.27	-0.83
Chamizal C41	o-Xylene	8.13	-0.41	11	0.889	-9.41	0.00	-0.50	-0.31
Chamizal C41	Ethyl Benzene	6.42	-0.30	11	0.790	-6.44	0.00	-0.40	-0.20
Chamizal C41	n-Butane	16.91	-0.66	11	0.493	-3.27	0.01	-1.10	-0.21
Chamizal C41	Isobutane	5.40	-0.12	11	0.208	-1.70	0.12	-0.28	0.04
Chamizal C41	n-Pentane	16.42	-0.60	11	0.549	-3.66	0.00	-0.95	-0.24
Chamizal C41	Isopentane	23.80	-0.80	11	0.528	-3.51	0.00	-1.30	-0.30
Clinton C403	Ethylene	21.51	-0.87	10	0.710	-4.95	0.00	-1.27	-0.48
Clinton C403	Propylene	17.71	-0.69	10	0.852	-7.59	0.00	-0.89	-0.49
Clinton C403	1-Butene	3.45	-0.10	10	0.237	-1.76	0.11	-0.22	0.03
Clinton C403	Benzene	9.73	-0.41	10	0.719	-5.06	0.00	-0.58	-0.23
Clinton C403	Toluene	20.89	-0.85	10	0.693	-4.75	0.00	-1.25	-0.45
Clinton C403	m/p-Xylene	14.45	-0.66	10	0.756	-5.57	0.00	-0.93	-0.40
Clinton C403	o-Xylene	5.02	-0.23	10	0.789	-6.12	0.00	-0.31	-0.14
Clinton C403	Ethyl Benzene	4.19	-0.18	10	0.614	-3.98	0.00	-0.27	-0.08
Clinton C403	n-Butane	32.84	-0.70	10	0.212	-1.64	0.13	-1.65	0.25
Clinton C403	Isobutane	34.18	-0.83	10	0.037	-0.62	0.55	-3.82	2.16
Clinton C403	n-Pentane	16.51	-0.34	10	0.500	-3.16	0.01	-0.58	-0.10
Clinton C403	Isopentane	32.59	-0.63	10	0.490	-3.10	0.01	-1.09	-0.18
DeerPark C35	Ethylene	29.72	-1.13	7	0.531	-2.82	0.03	-2.07	-0.18
DeerPark C35	Propylene	39.68	-1.36	8	0.334	-2.00	0.08	-2.93	0.20
DeerPark C35	1-Butene	2.69	-0.05	8	0.046	-0.62	0.55	-0.26	0.15
DeerPark C35	Benzene	6.01	-0.03	8	0.006	-0.21	0.84	-0.37	0.31
DeerPark C35	Toluene	10.47	-0.17	8	0.110	-0.99	0.35	-0.55	0.22
DeerPark C35	m/p-Xylene	4.78	-0.10	8	0.199	-1.41	0.20	-0.26	0.06
DeerPark C35	o-Xylene	1.88	-0.05	8	0.315	-1.92	0.09	-0.10	0.01
DeerPark C35	Ethyl Benzene	1.87	-0.05	8	0.328	-1.98	0.08	-0.10	0.01
DeerPark C35	n-Butane	15.85	0.07	8	0.006	0.22	0.83	-0.66	0.80
DeerPark C35	Isobutane	23.78	-0.45	8	0.215	-1.48	0.18	-1.15	0.25
DeerPark C35	n-Pentane	8.26	0.09	8	0.026	0.47	0.65	-0.34	0.52
DeerPark C35	Isopentane	17.18	0.00	8	0.000	-0.01	0.99	-0.70	0.70

Figure 10.1 1-Butene 6-9 CST May-Oct. OLS Trend, years since 1990, Deer Park C35

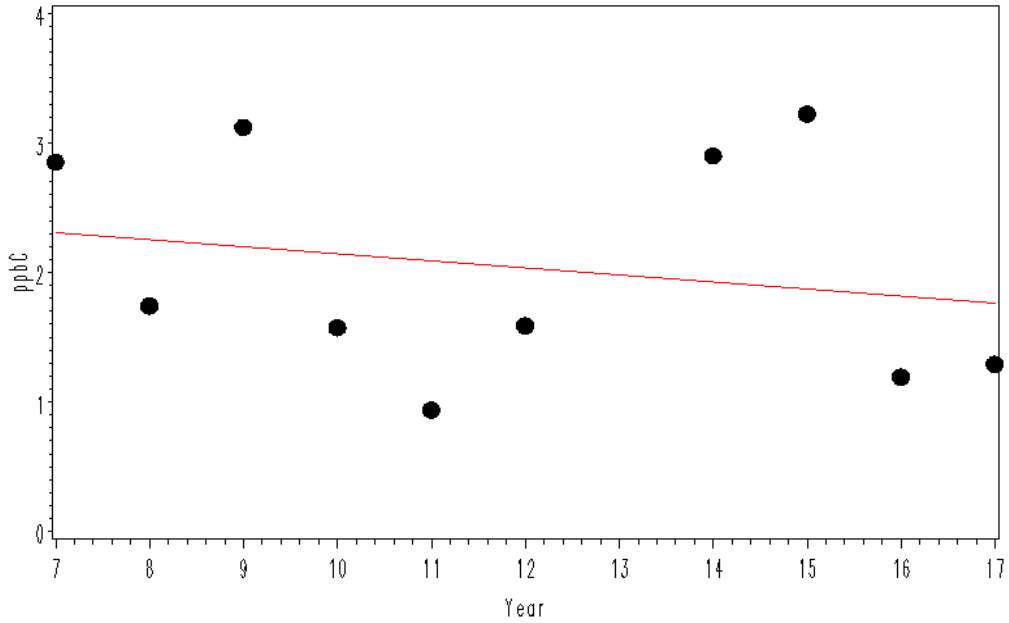

Regression Equation:
1 Butene = 2.691392 - 0.054425*year index

Figure 10.2 Benzene 6-9 CST May-Oct. OLS Trend, years since 1990, Deer Park C35

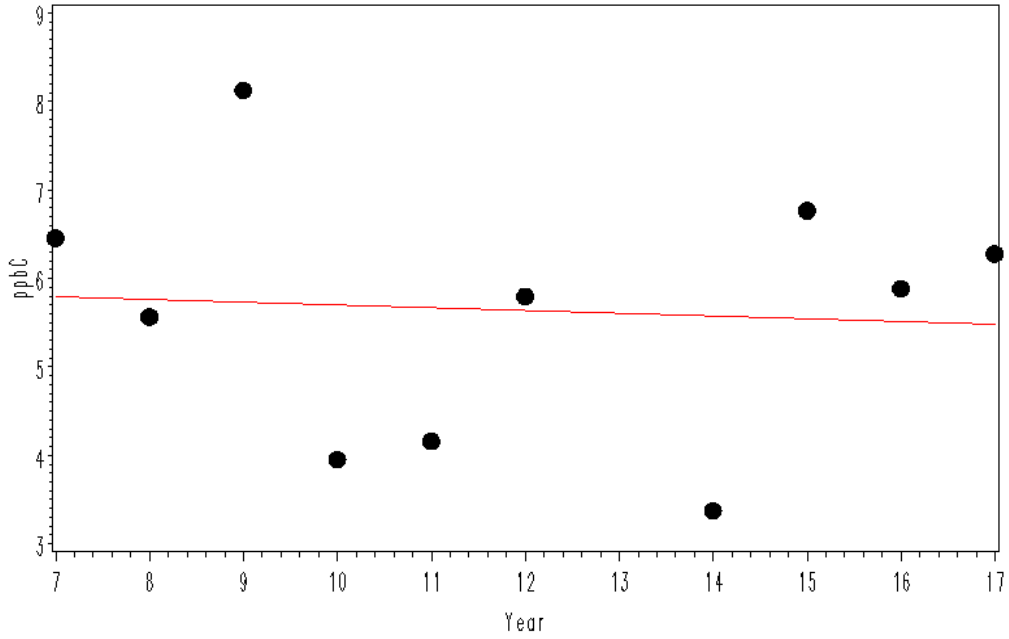

Regression Equation:
Benzene = 6.005662 - 0.030994*year index

Figure 10.3 Ethyl Benzene 6-9 CST May-Oct. OLS Trend, years since 1990, Deer Park C35

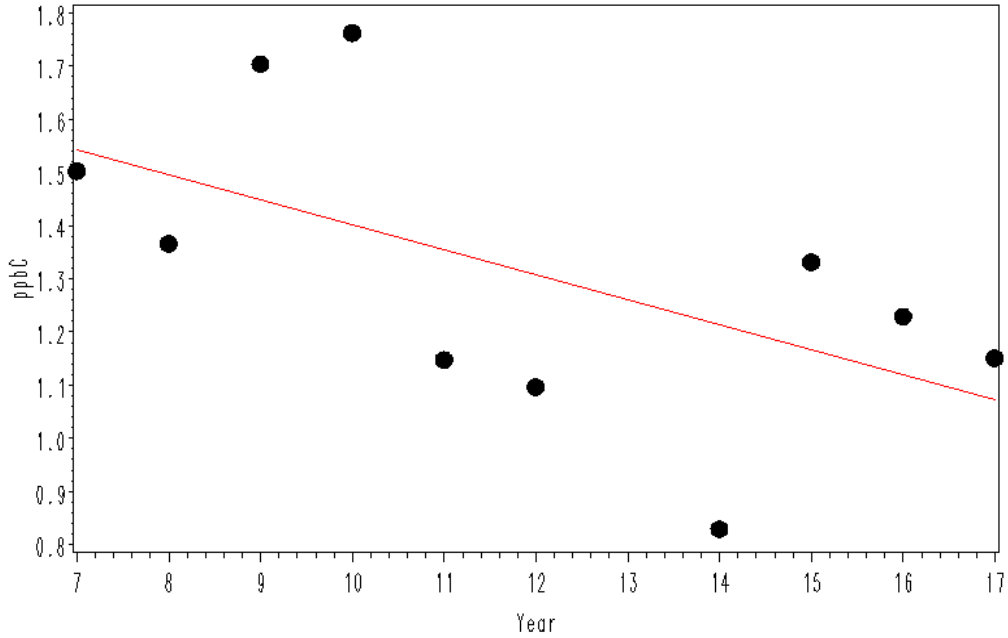

Regression Equation:
Ethyl Benzene = 1.87242 - 0.047078*year index

Figure 10.4 Ethylene 6-9 CST May-Oct. OLS Trend, years since 1990, Deer Park C35

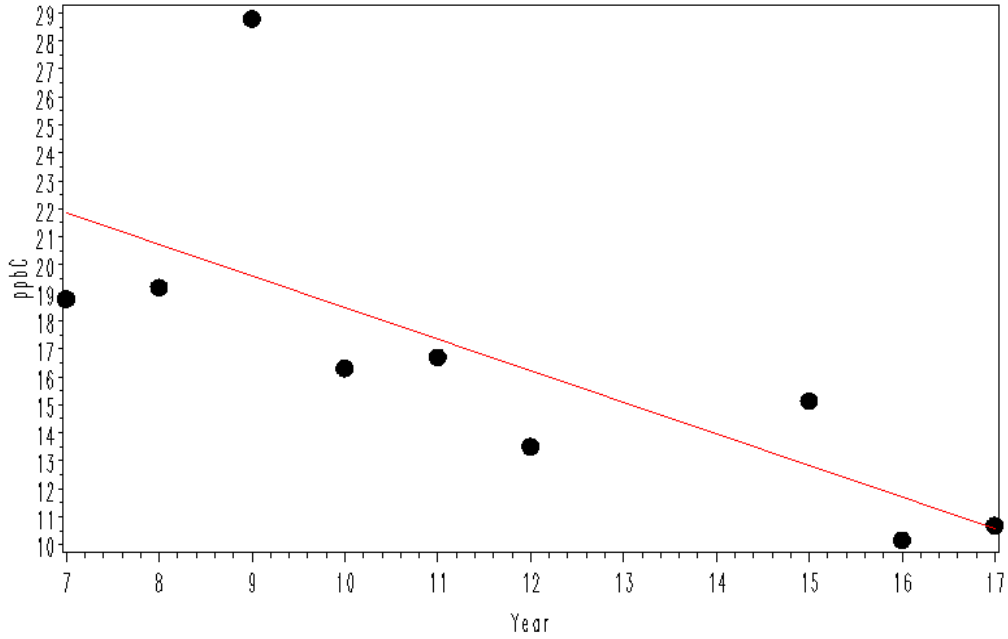

Regression Equation:
Ethylene = 29.71925 - 1.125538*year index

Figure 10.5 Isobutane 6-9 CST May-Oct. OLS Trend, years since 1990, Deer Park C35

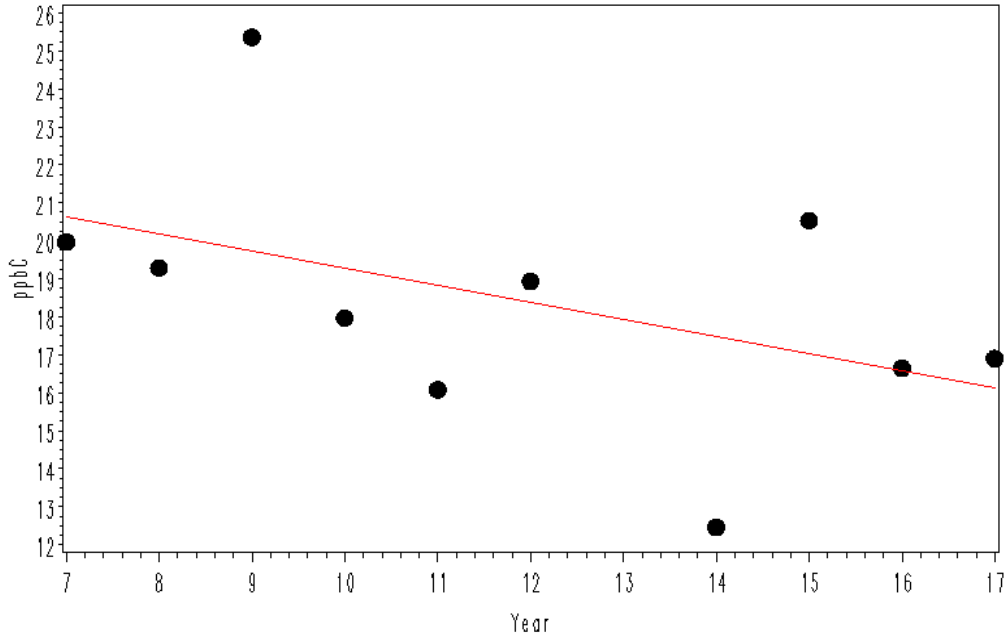

Regression Equation:
Isobutane = 23.77701 - 0.450377*year index

Figure 10.6 Isopentane 6-9 CST May-Oct. OLS Trend, years since 1990, Deer Park C35

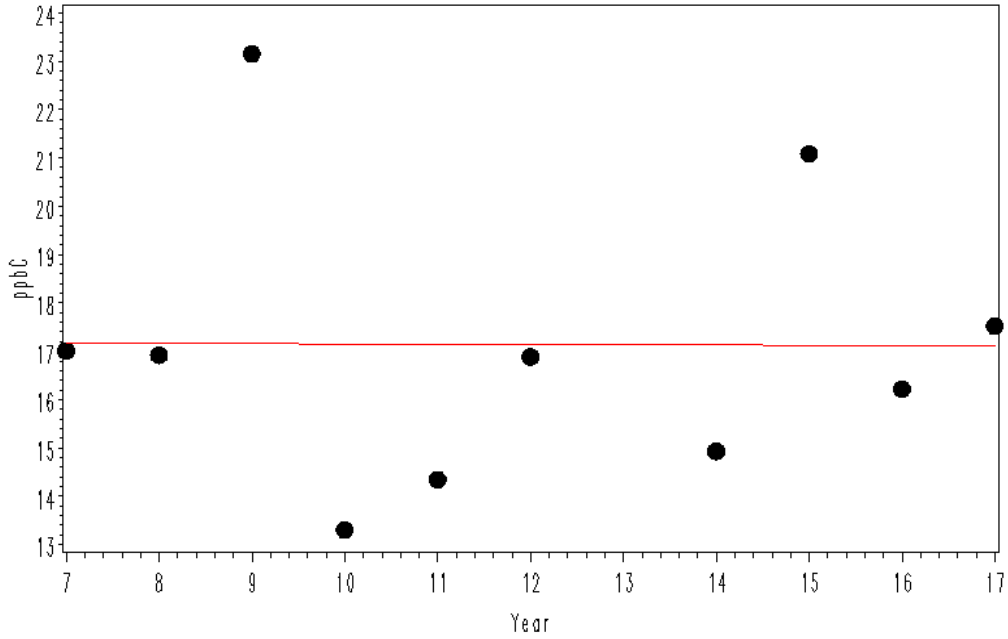

Regression Equation:
Isopentane = 17.18489 - 0.003732*year index

Figure 10.7 m/p-Xylene 6-9 CST May-Oct. OLS Trend, years since 1990, Deer Park C35

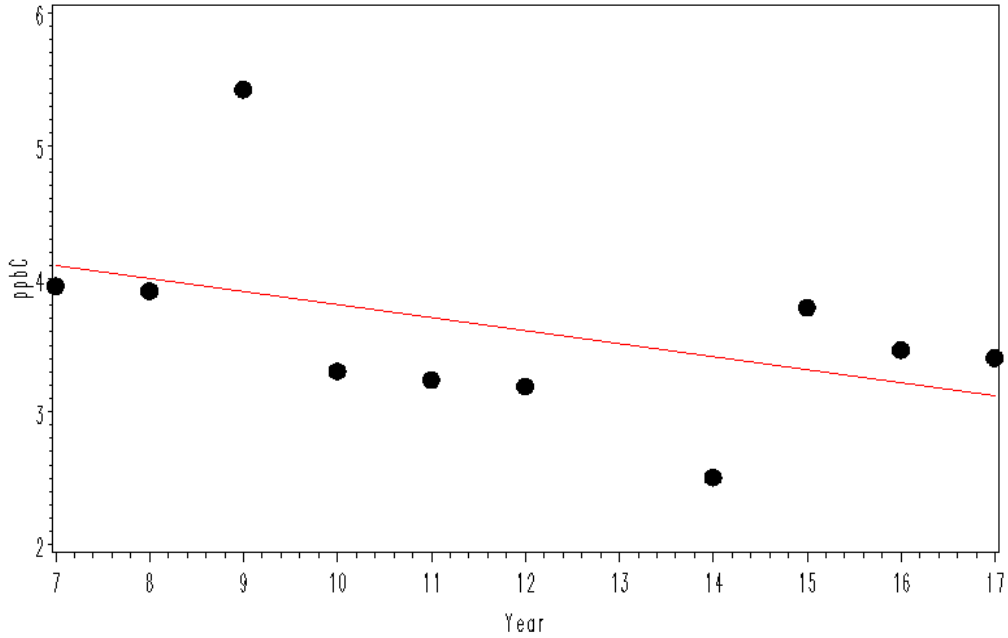

Figure 10.8 n-Pentane 6-9 CST May-Oct. OLS Trend, years since 1990, Deer Park C35

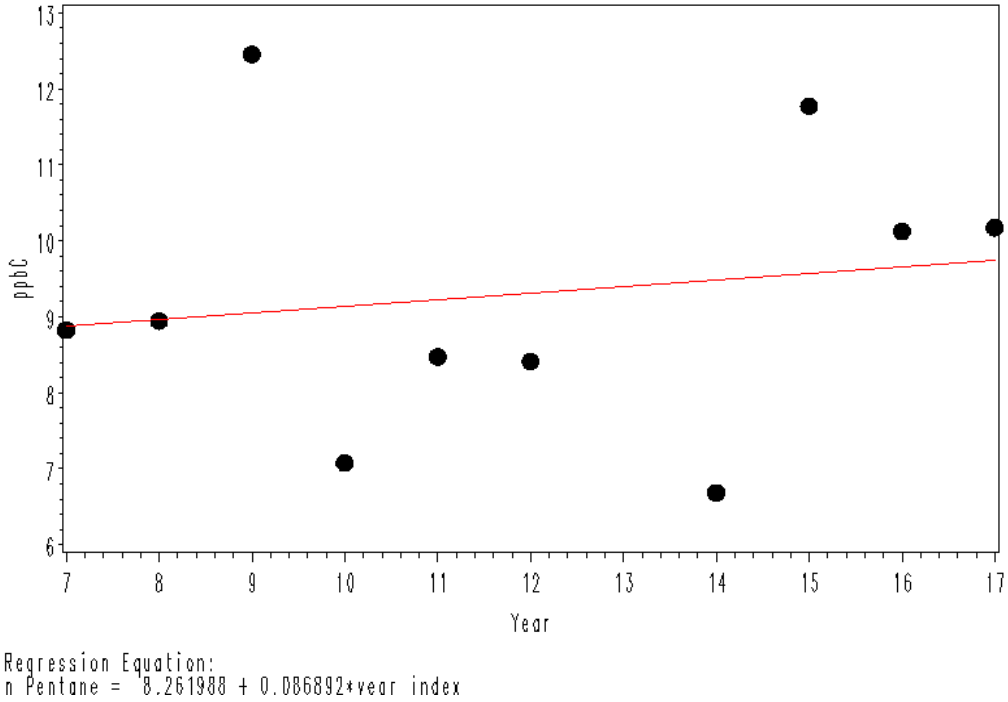

Figure 10.9 n-Butane 6-9 CST May-Oct. OLS Trend, years since 1990, Deer Park C35

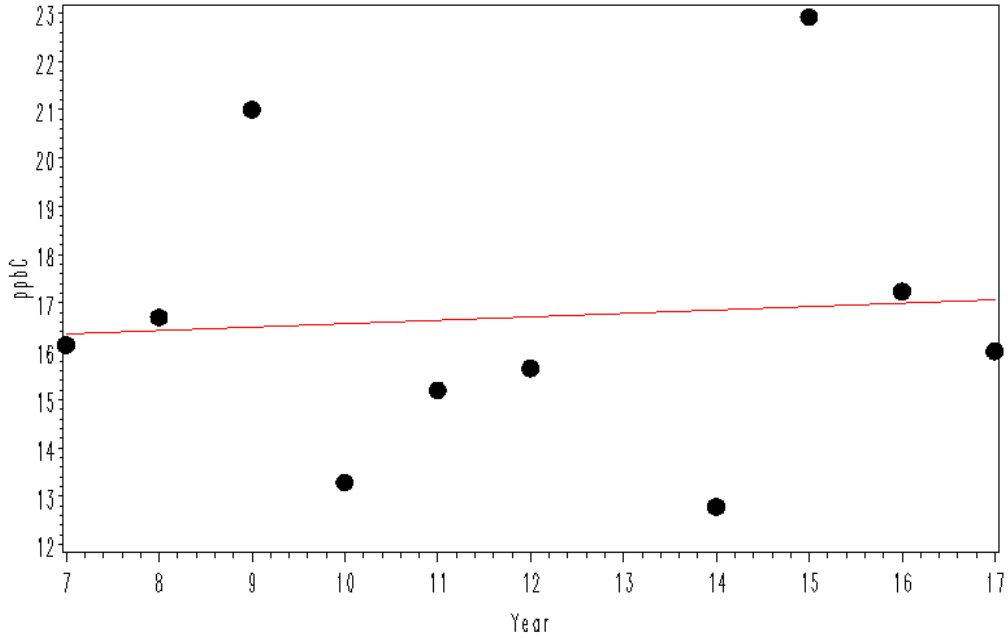

Regression Equation:
n Butane = 15.84907 + 0.070926*year index

Figure 10.10 o-Xylene 6-9 CST May-Oct. OLS Trend, years since 1990, Deer Park C35

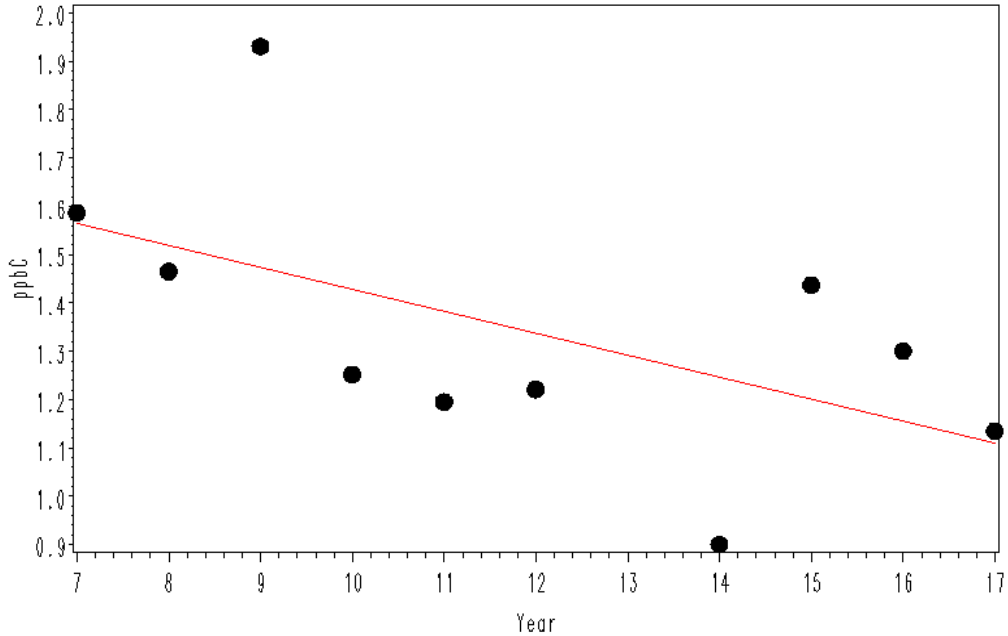

Regression Equation:
o Xylene = 1.883838 - 0.045471*year index

Figure 10.11 Propylene 6-9 CST May-Oct. OLS Trend, years since 1990, Deer Park C35

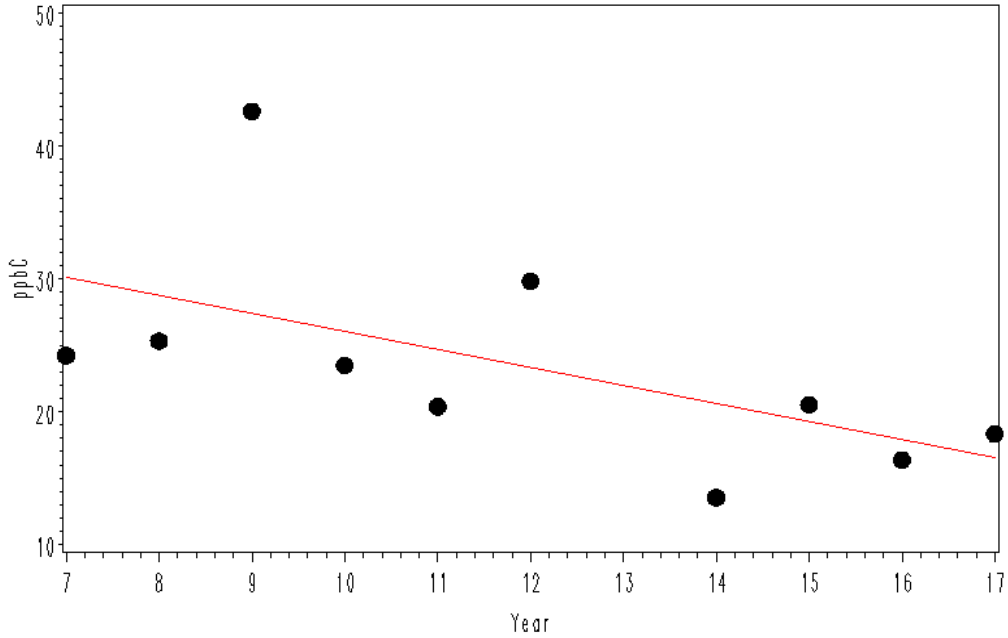

Regression Equation:
Propylene = 39.67799 - 1.361614*year index

Figure 10.12 Toluene 6-9 CST May-Oct. OLS Trend, years since 1990, Deer Park C35

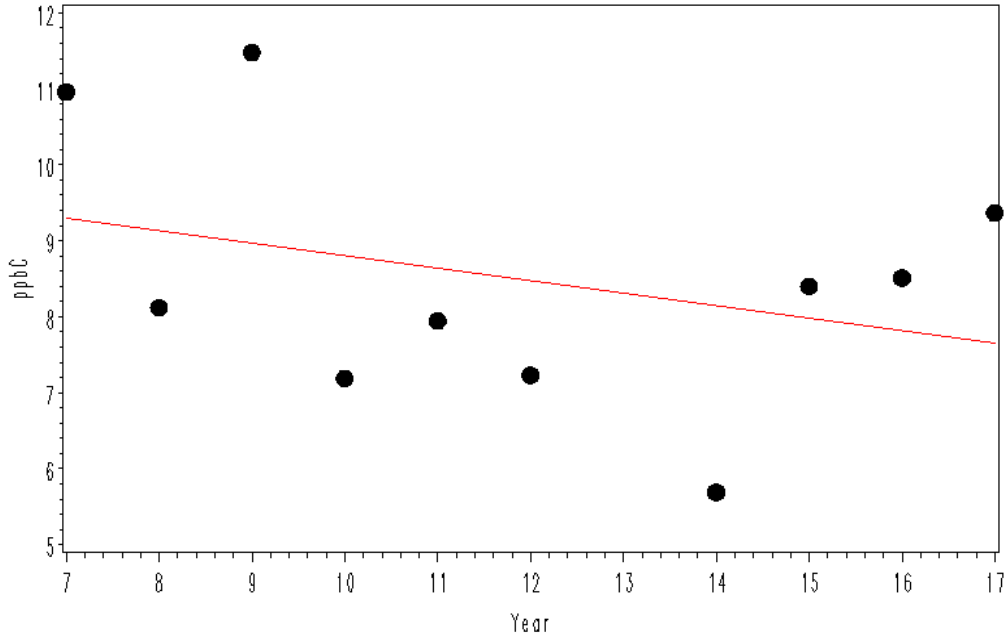

Regression Equation:
Toluene = 10.46712 - 0.166048*year index

Figure 10.13 1-Butene 6-9 CST May-Oct. OLS Trend, years since 1990, Chamizal C41

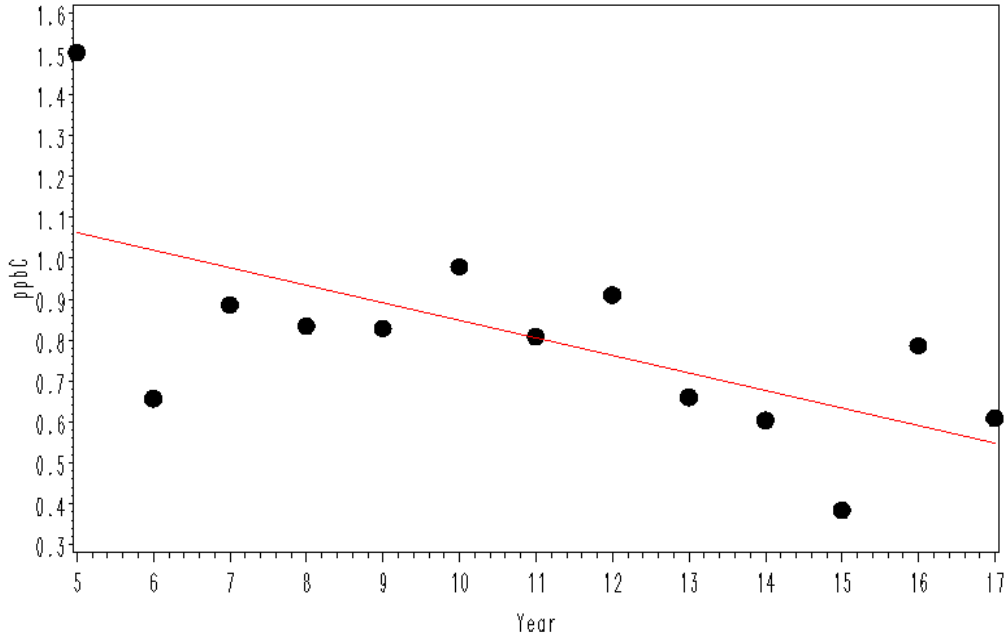

Regression Equation:
1 Butene = 1.277087 - 0.042971*year index

Figure 10.14 Benzene 6-9 CST May-Oct. OLS Trend, years since 1990, Chamizal C41

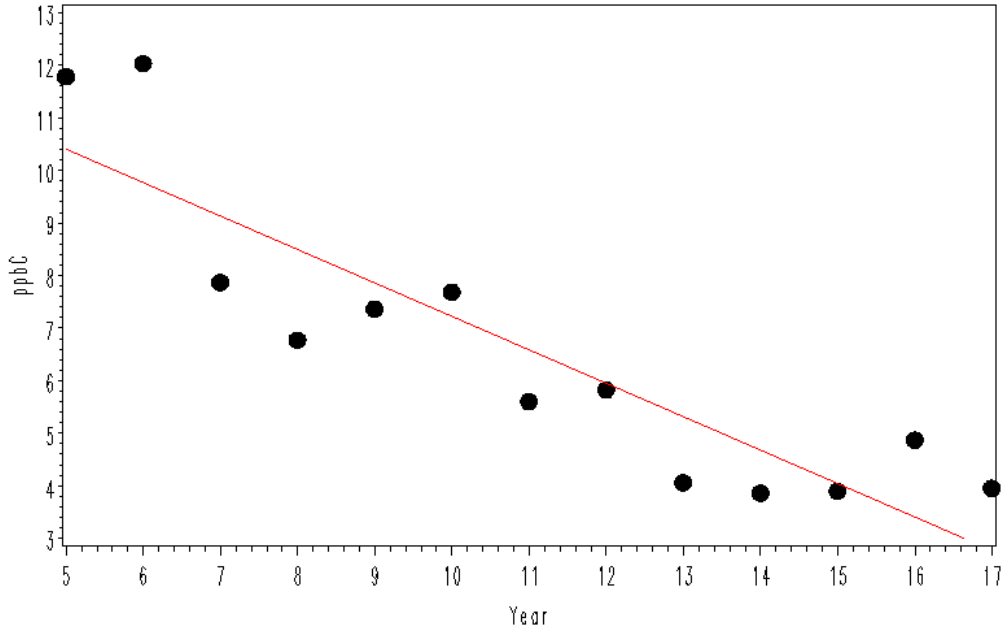

Regression Equation:
Benzene = 13.58886 - 0.636631*year index

Figure 10.15 Ethyl Benzene 6-9 CST May-Oct. OLS Trend, years since 1990, Chamizal C41

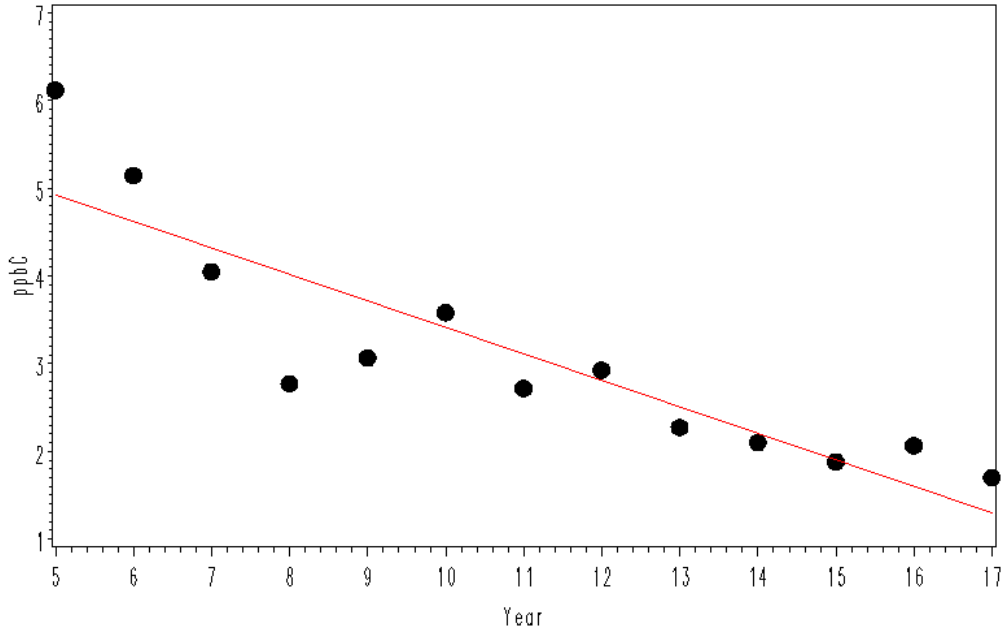

Regression Equation:
Ethyl Benzene = 6.420966 - 0.301056*year index

Figure 10.16 Ethylene 6-9 CST May-Oct. OLS Trend, years since 1990, Chamizal C41

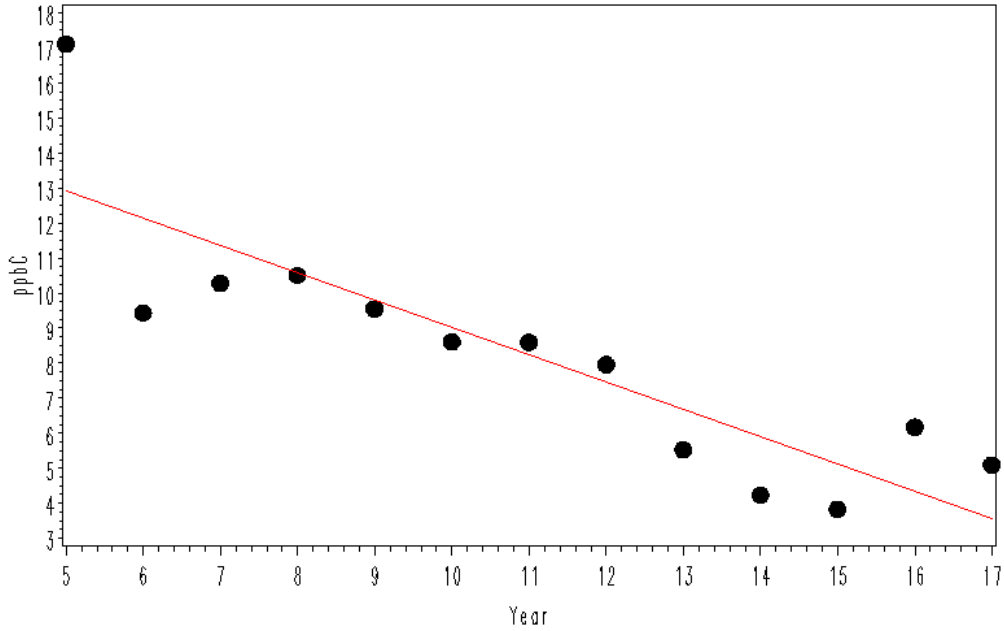

Regression Equation:
Ethylene = 16.79001 - 0.778311*year index

Figure 10.17 Isobutane 6-9 CST May-Oct. OLS Trend, years since 1990, Chamizal C41

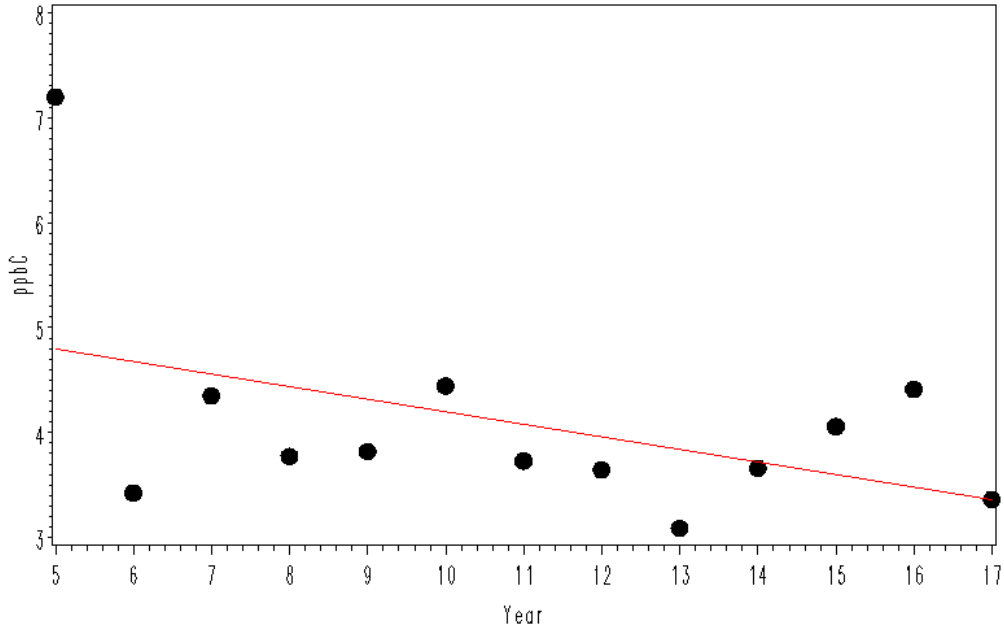

Figure 10.18 Isopentane 6-9 CST May-Oct. OLS Trend, years since 1990, Chamizal C41

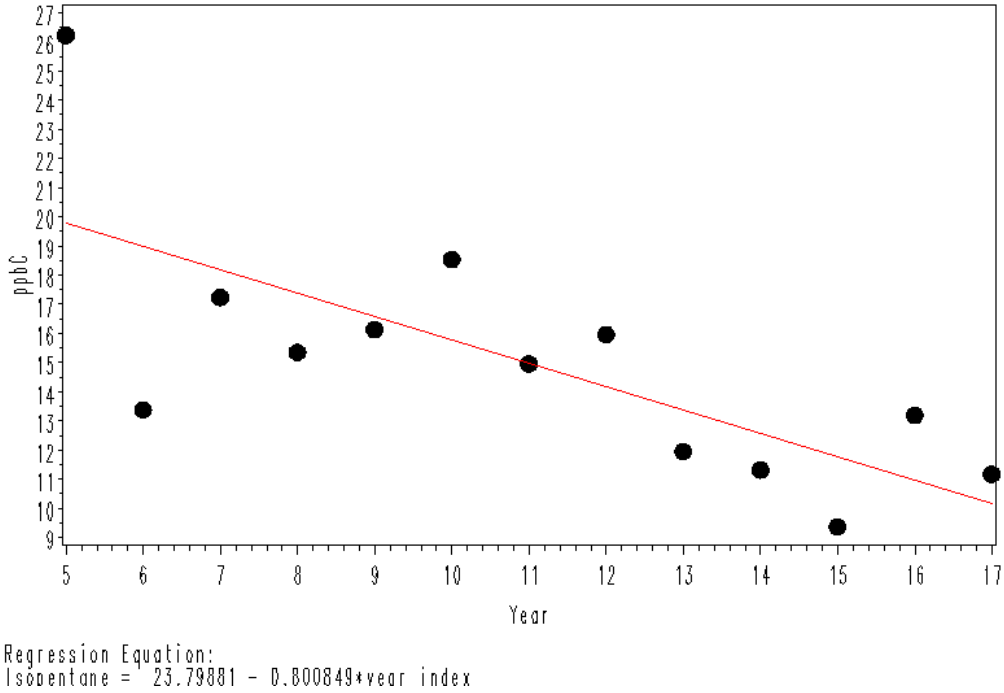

Figure 10.19 m/p-Xylene 6-9 CST May-Oct. OLS Trend, years since 1990, Chamizal C41

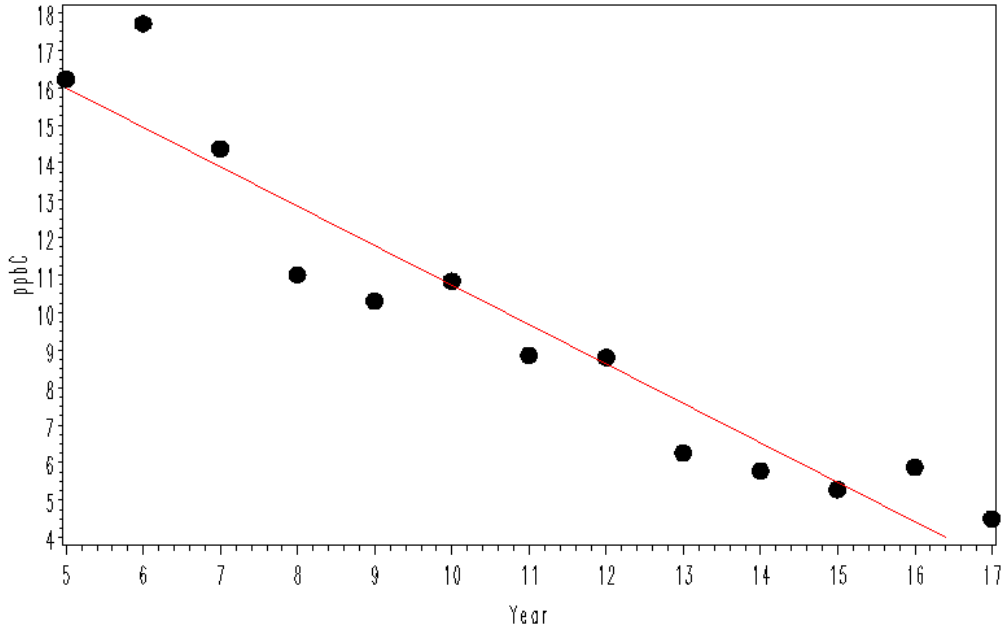

Figure 10.20 n-Butane 6-9 CST May-Oct. OLS Trend, years since 1990, Chamizal C41

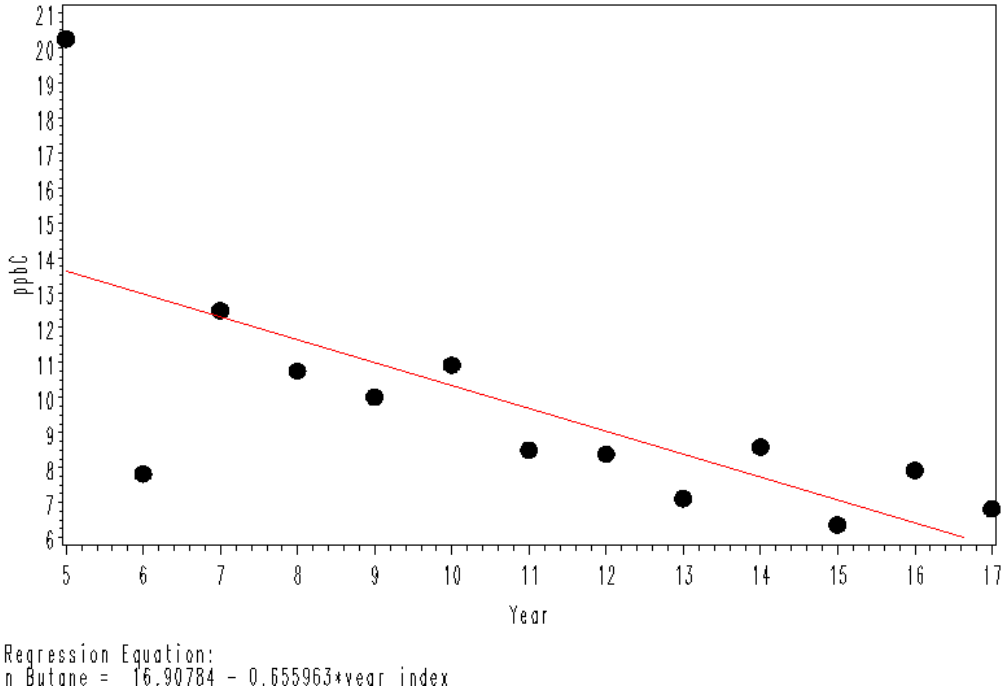

Figure 10.21n-Pentane 6-9 CST May-Oct. OLS Trend, years since 1990, Chamizal C41

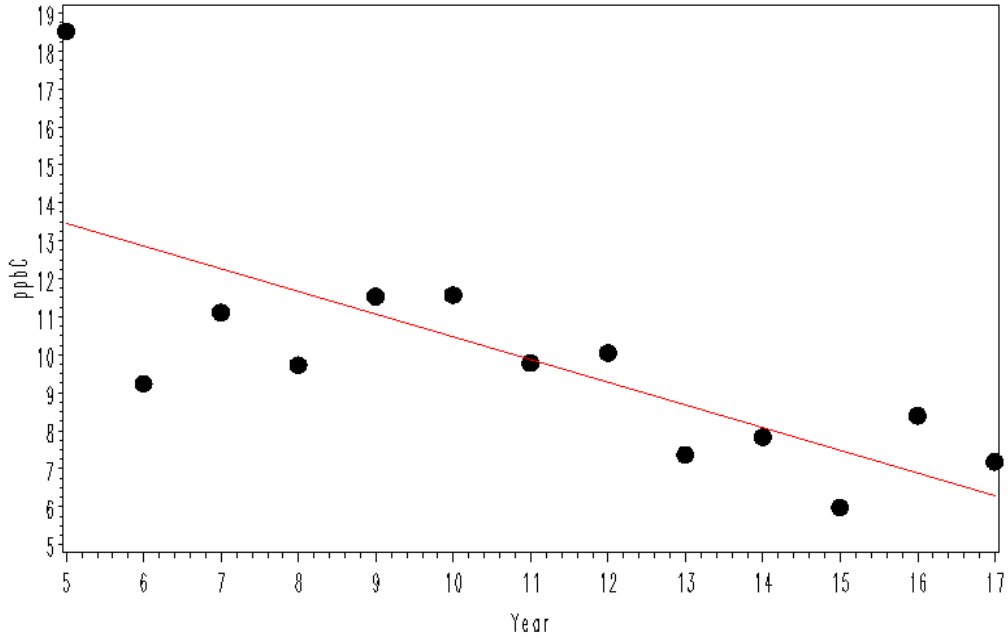

Regression Equation:
n Pentane = 16.41976 - 0.595191*year index

Figure 10.22 o-Xylene 6-9 CST May-Oct. OLS Trend, years since 1990, Chamizal C41

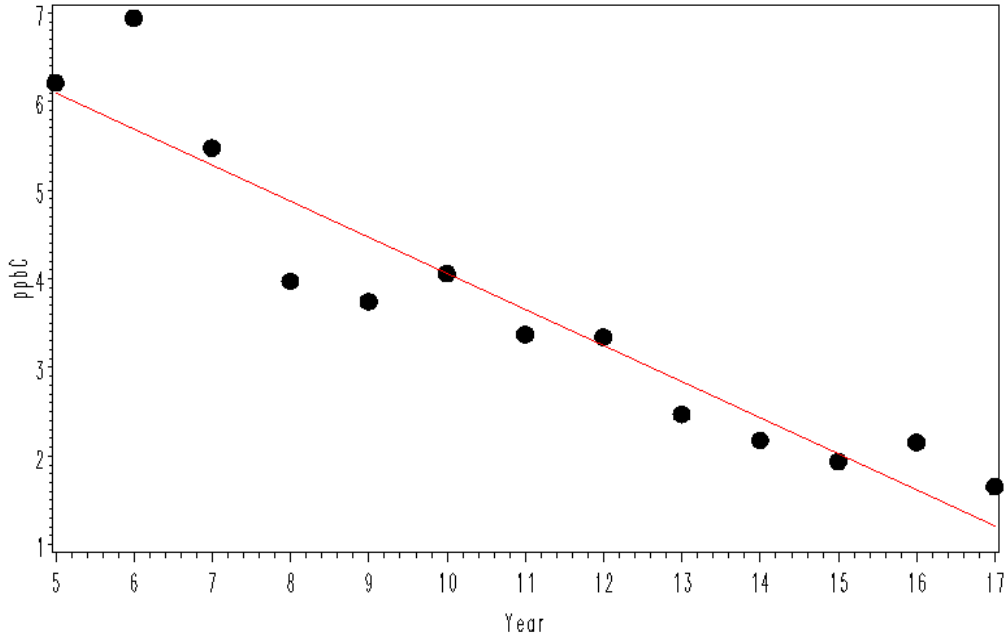

Regression Equation:
o Xylene = 8.133353 - 0.407043*year index

Figure 10.23 Propylene 6-9 CST May-Oct. OLS Trend, years since 1990, Chamizal C41

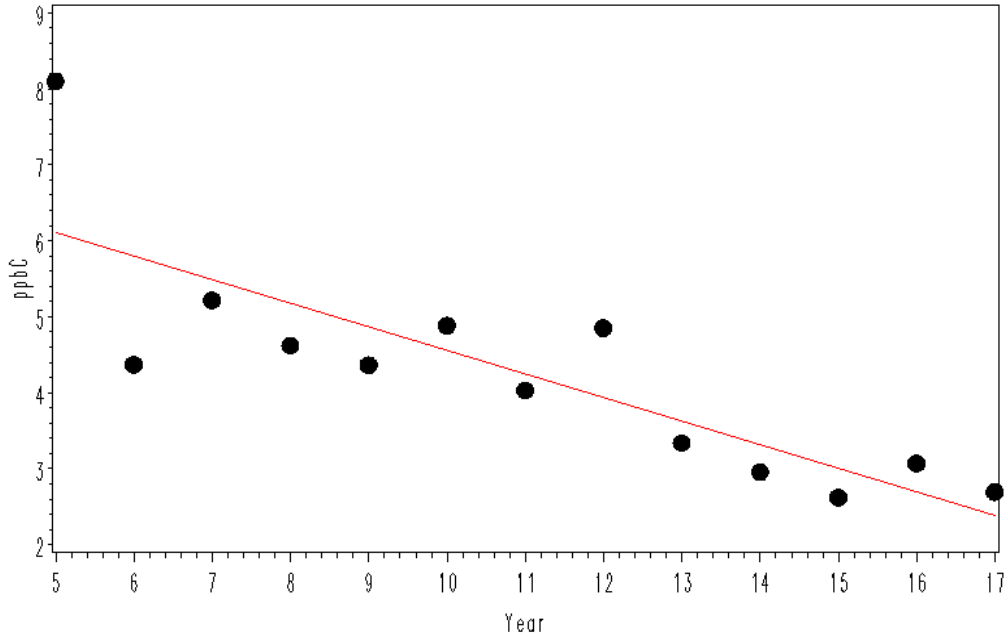

Figure 10.24 Toluene 6-9 CST May-Oct. OLS Trend, years since 1990, Chamizal C41

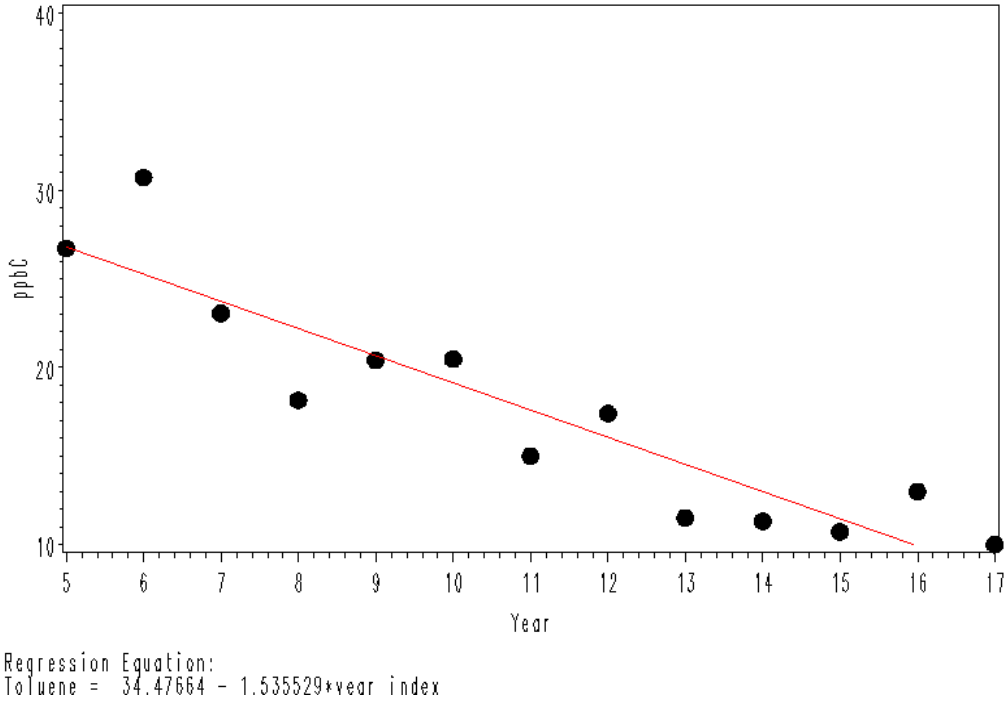

Figure 10.25 1-Butene 6-9 CST May-Oct. OLS Trend, years since 1990, Dallas Hinton C401

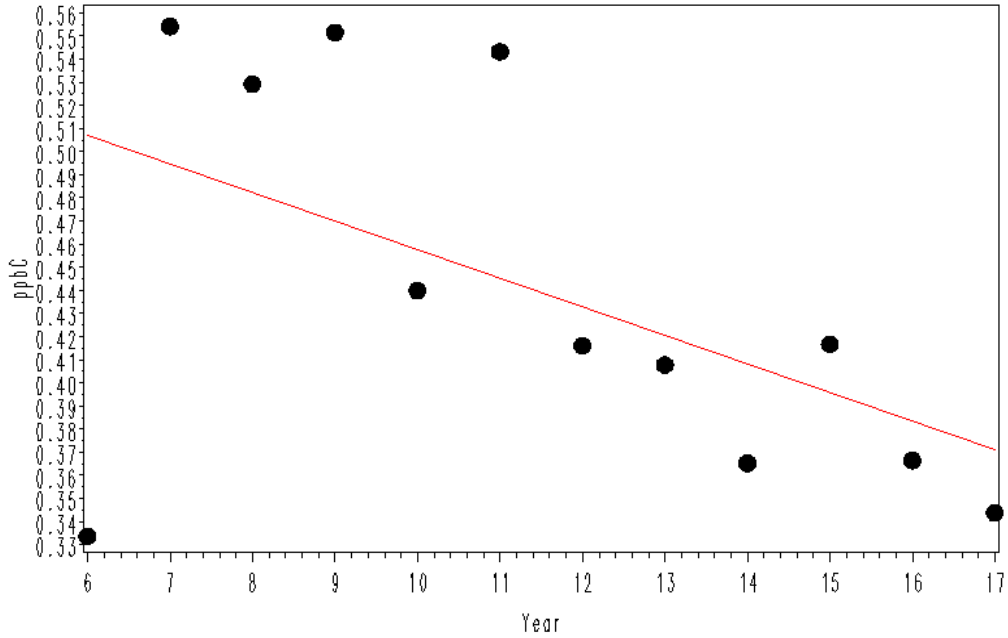

Regression Equation:
1 Butene = 0.580651 - 0.012314*year index

Figure 10.26 Benzene 6-9 CST May-Oct. OLS Trend, years since 1990, Dallas Hinton C401

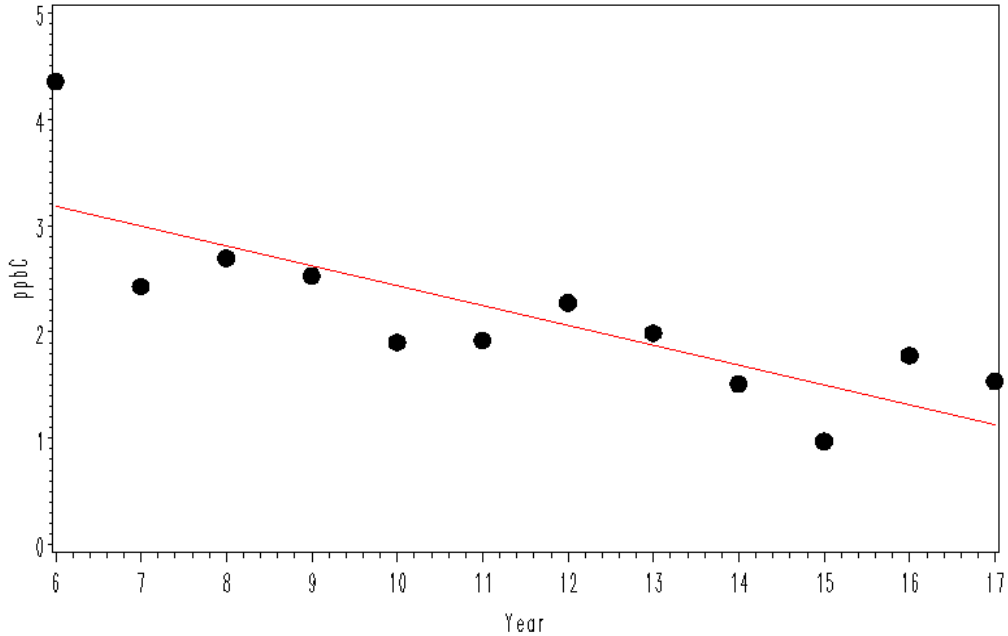

Regression Equation:
Benzene = 4.30416 - 0.186552*year index

Figure 10.27 Ethyl Benzene 6-9 CST May-Oct. OLS Trend, years since 1990, Dallas Hinton C401

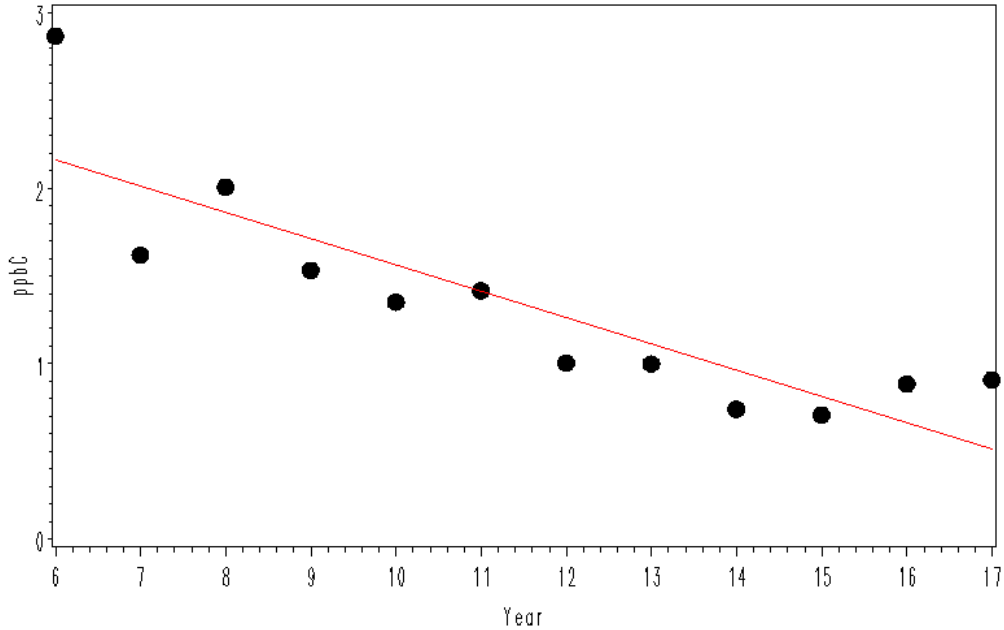

Regression Equation:
Ethyl Benzene = 3.052968 - 0.149181*year index

Figure 10.28 Ethylene 6-9 CST May-Oct. OLS Trend, years since 1990, Dallas Hinton C401

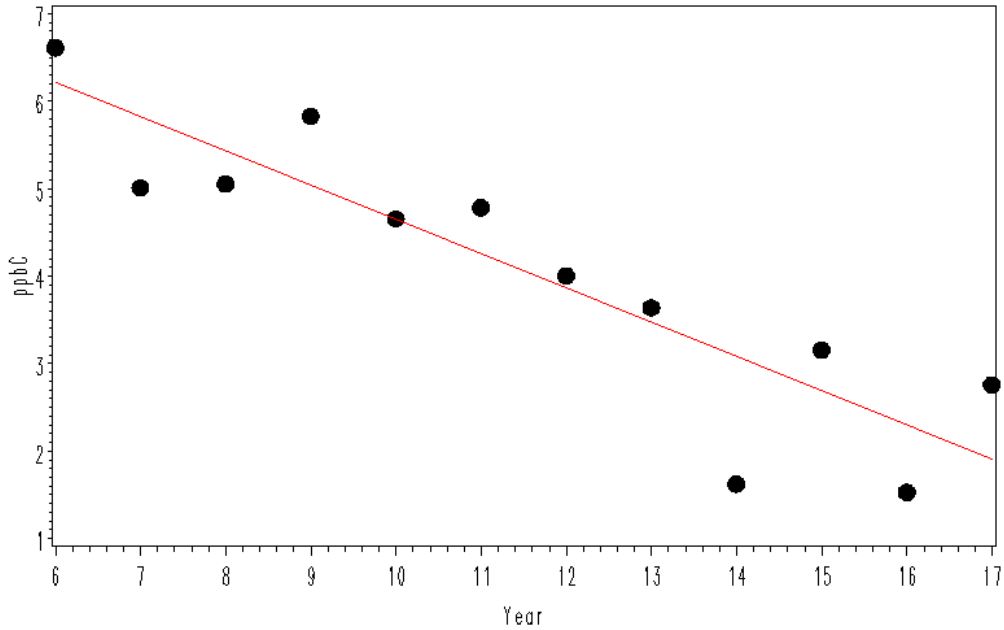

Regression Equation:
Ethylene = 8.551496 - 0.39095*year index

Figure 10.29 isobutane 6-9 CST May-Oct. OLS Trend, years since 1990, Dallas Hinton C401

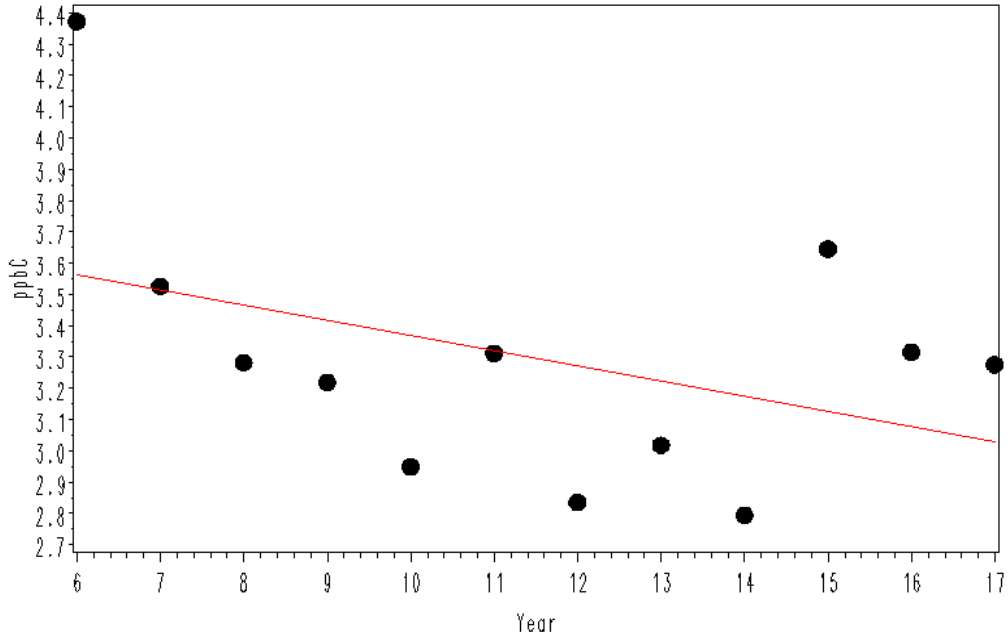

Regression Equation:
Isobutane = 3.851348 - 0.0483*year index

Figure 10.30 Isopentane 6-9 CST May-Oct. OLS Trend, years since 1990, Dallas Hinton C401

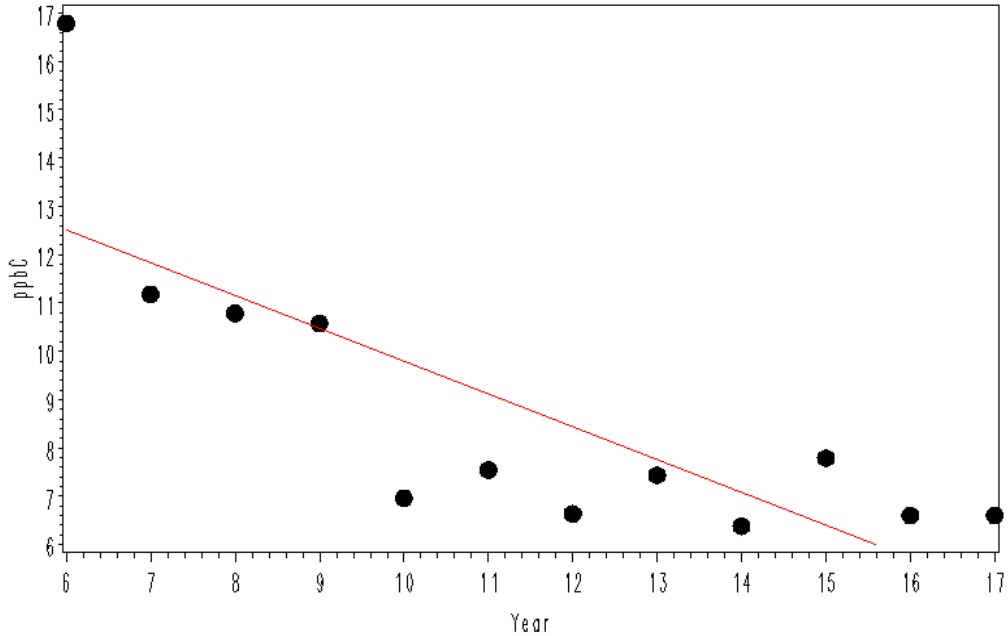

Regression Equation:
Isopentane = 16.60294 - 0.680406*year index

Figure 10.31 m/p-Xylene 6-9 CST May-Oct. OLS Trend, years since 1990, Dallas Hinton C401

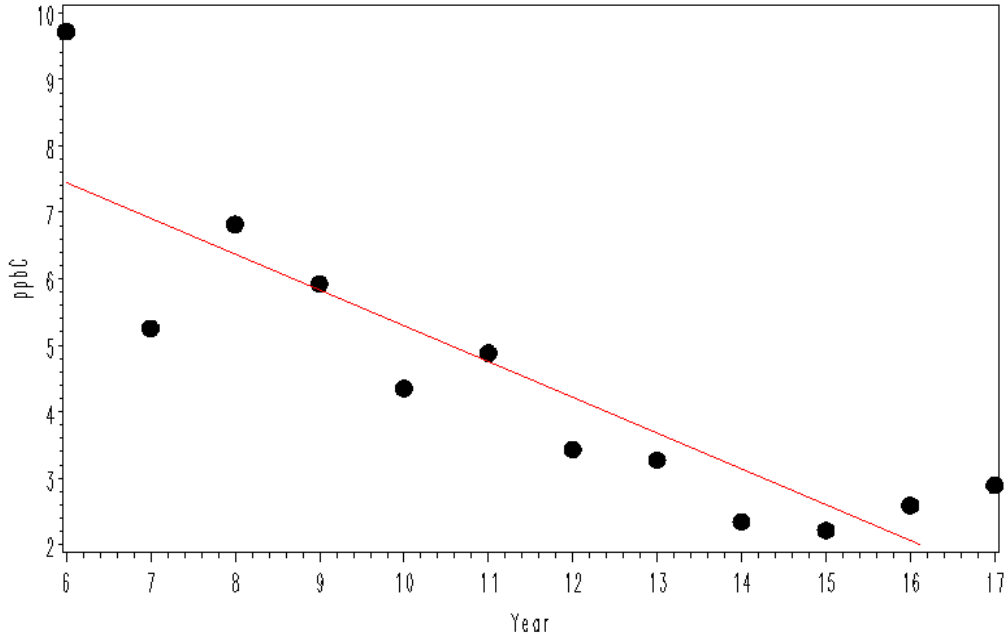

Regression Equation:
p Xylene m Xylene = 10.66563 - 0.538148*year index

Figure 10.32 n-Butane 6-9 CST May-Oct. OLS Trend, years since 1990, Dallas Hinton C401

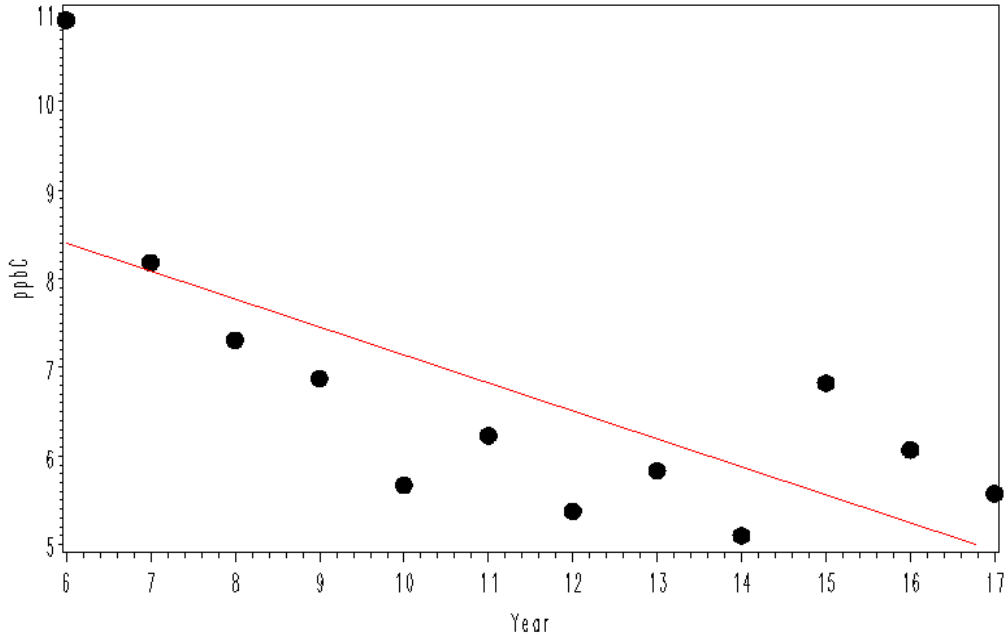

Regression Equation:
n Butane = 10.3013 - 0.316135*year index

Figure 10.33 n-Pentane 6-9 CST May-Oct. OLS Trend, years since 1990, Dallas Hinton C401

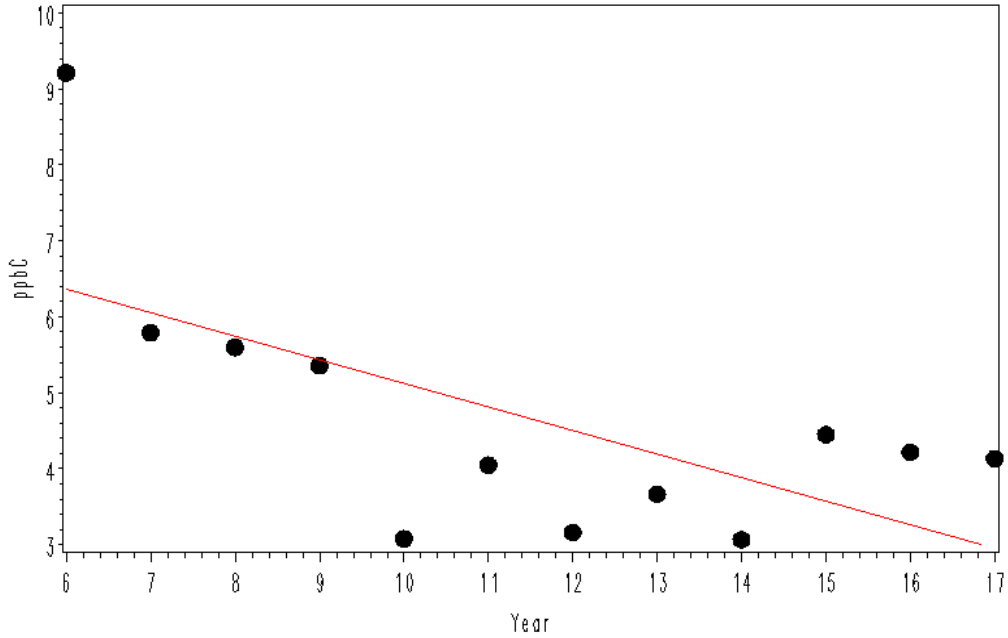

Regression Equation:
n Pentane = 8.213938 - 0.309863*year index

Figure 10.34 o-Xylene 6-9 CST May-Oct. OLS Trend, years since 1990, Dallas Hinton C401

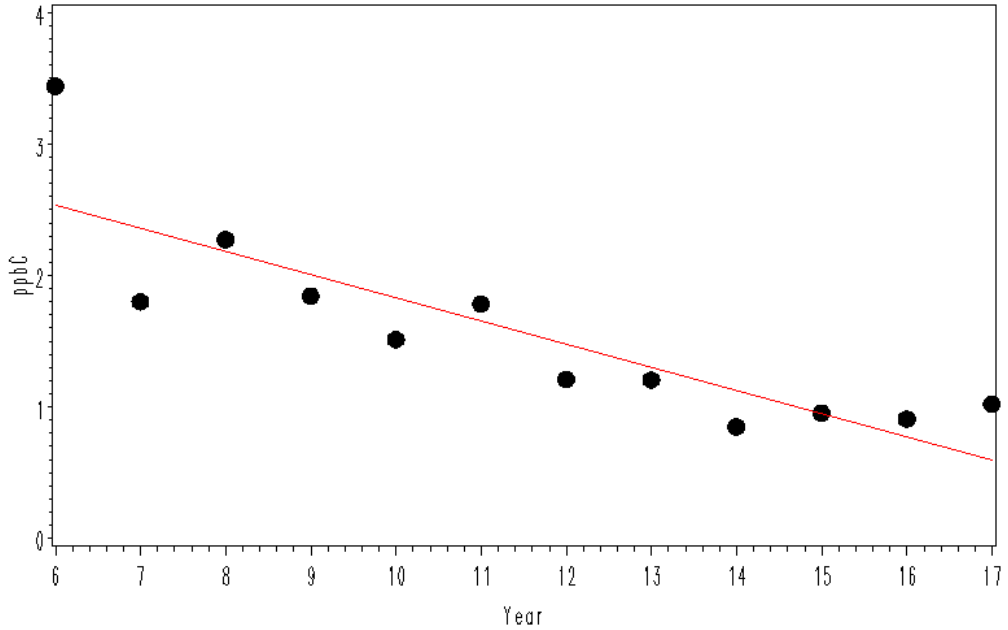

Regression Equation:
o Xylene = 3.592844 - 0.176035*year index

Figure 10.35 Propylene 6-9 CST May-Oct. OLS Trend, years since 1990, Dallas Hinton C401

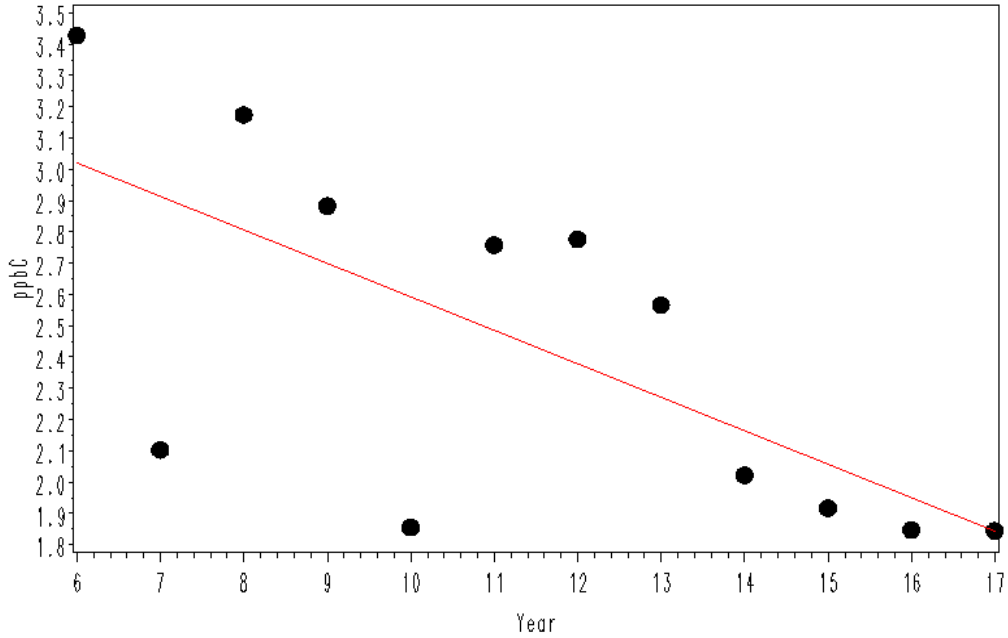

Regression Equation:
Propylene = 3.665057 - 0.107252*year index

Figure 10.36 Toluene 6-9 CST May-Oct. OLS Trend, years since 1990, Dallas Hinton C401

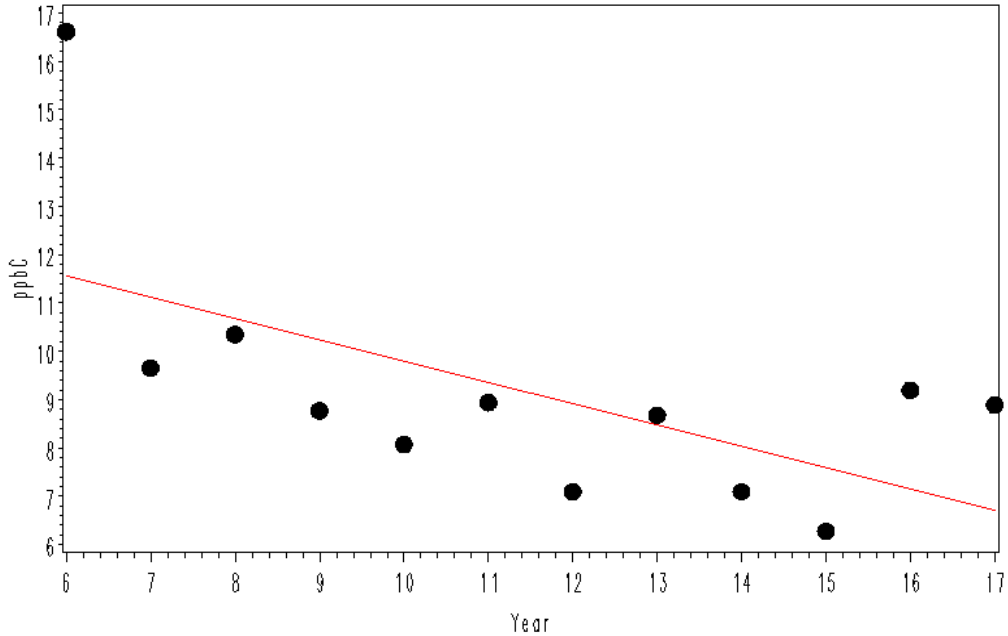

Regression Equation:
Toluene = 14.2034 - 0.440373*year index

Figure 10.37 1-Butene 6-9 CST May-Oct. OLS Trend, years since 1990, Clinton Dr. C403

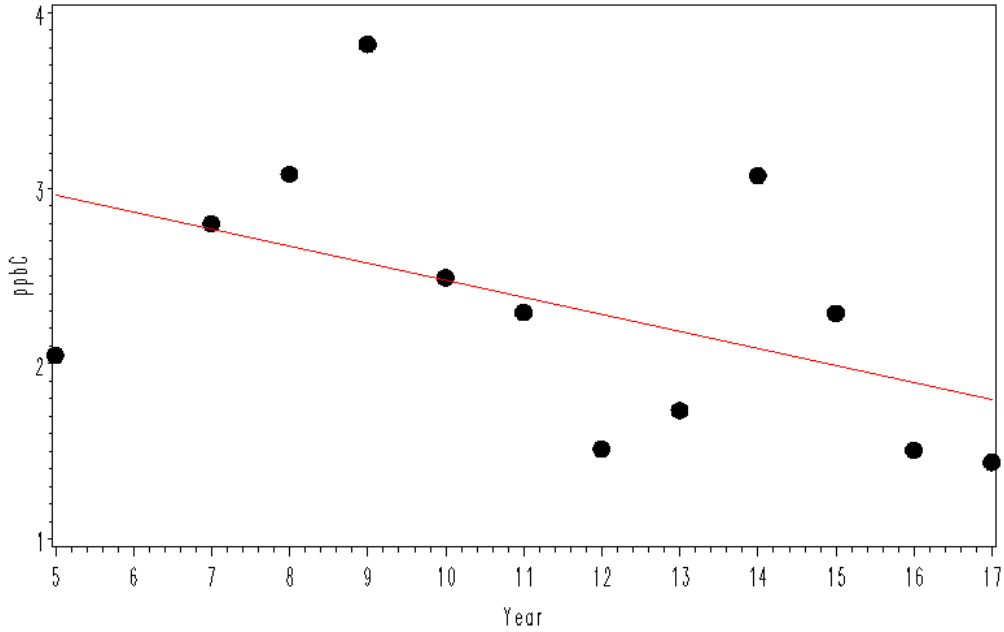

Figure 10.38 Benzene 6-9 CST May-Oct. OLS Trend, years since 1990, Clinton Dr. C403

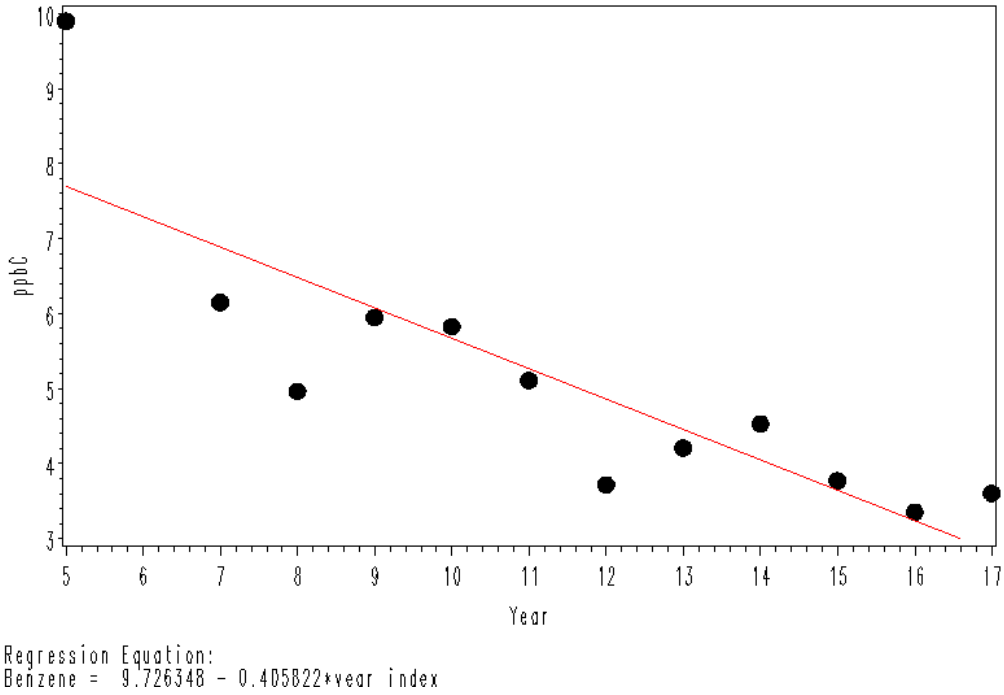

Figure 10.39 Ethyl Benzene 6-9 CST May-Oct. OLS Trend, years since 1990, Clinton Dr. C403

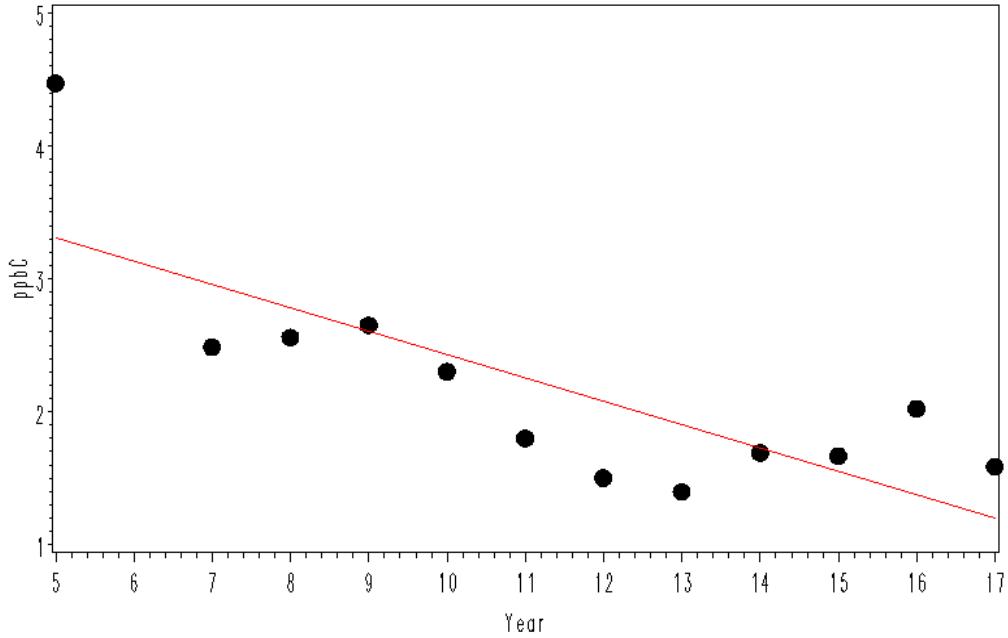

Figure 10.40 Ethylene 6-9 CST May-Oct. OLS Trend, years since 1990, Clinton Dr. C403

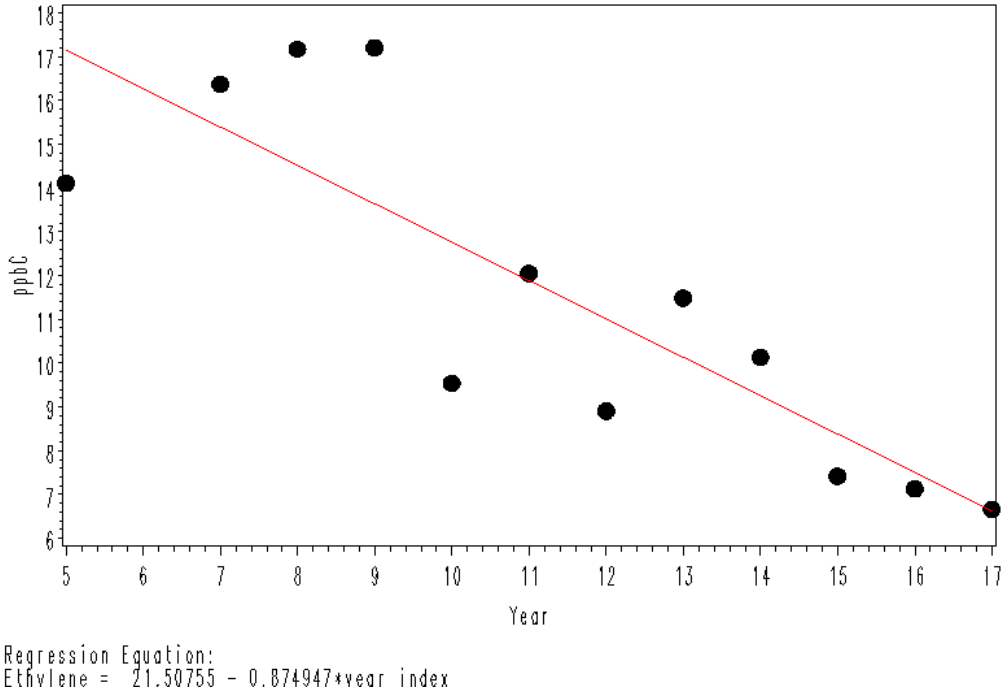

Figure 10.41 Isobutane 6-9 CST May-Oct. OLS Trend, years since 1990, Clinton Dr. C403

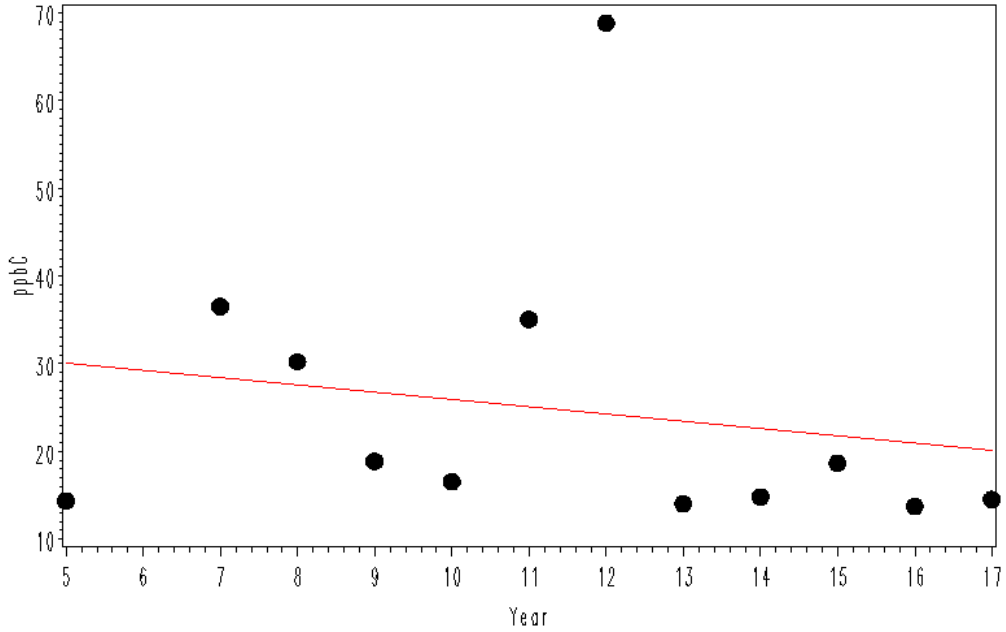

Figure 10.42 Isopentane 6-9 CST May-Oct. OLS Trend, years since 1990, Clinton Dr. C403

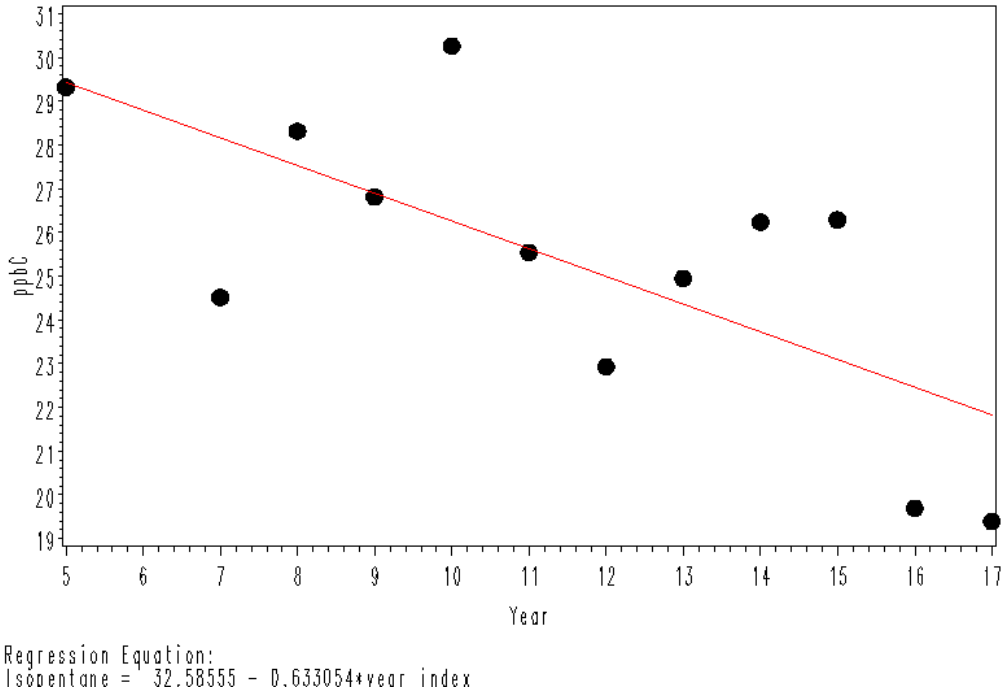

Figure 10.43 m/p-Xylene 6-9 CST May-Oct. OLS Trend, years since 1990, Clinton Dr. C403

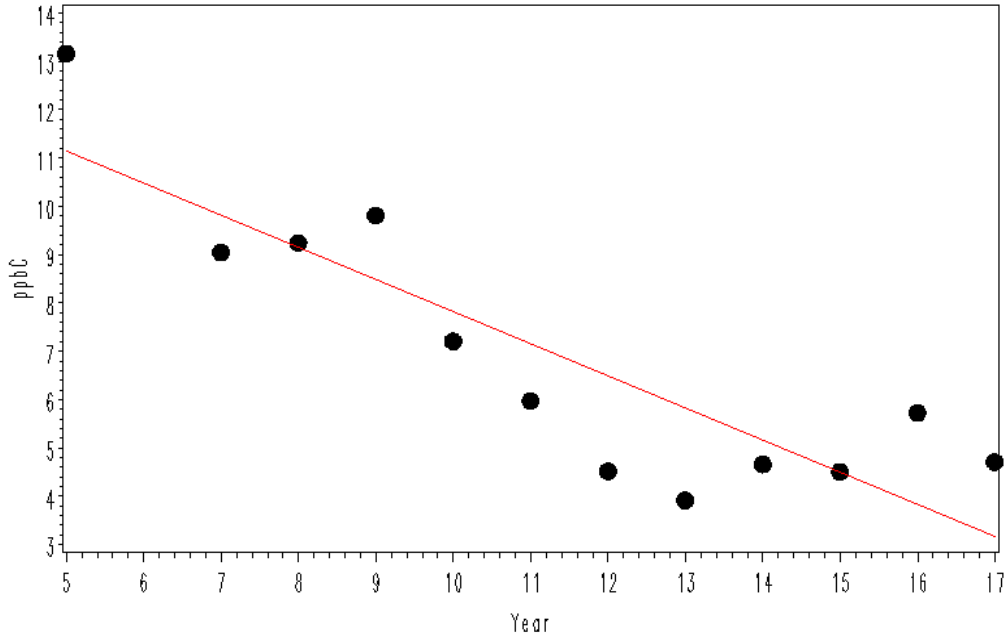

Regression Equation:
p Xylene m Xylene = 14.45328 - 0.663604*year index

Figure 10.44 n-Butane 6-9 CST May-Oct. OLS Trend, years since 1990, Clinton Dr. C403

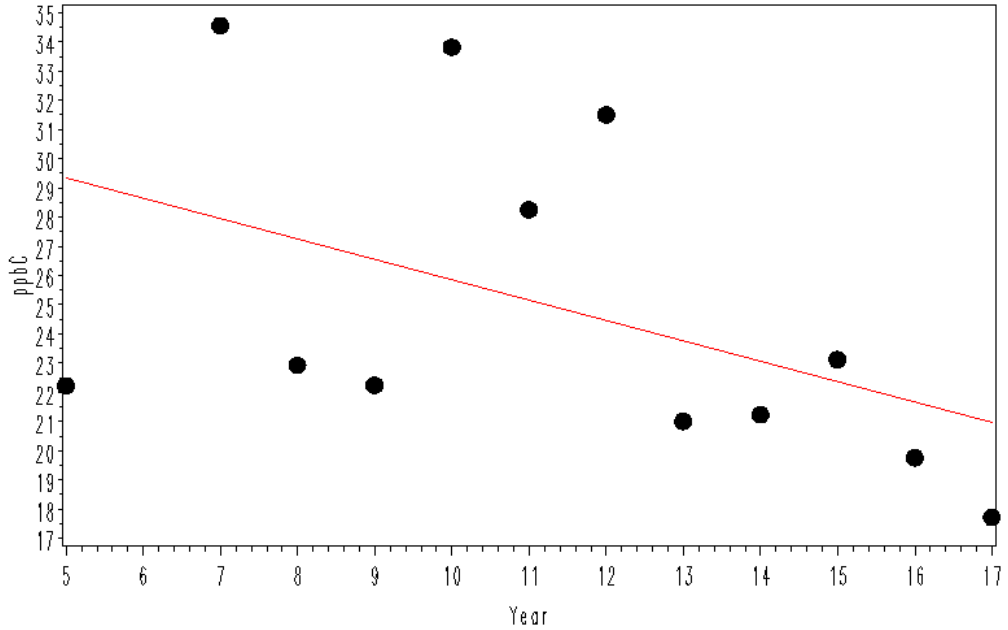

Regression Equation:
n Butane = 32.84475 - 0.698337*year index

Figure 10.45 n-Pentane 6-9 CST May-Oct. OLS Trend, years since 1990, Clinton Dr. C403

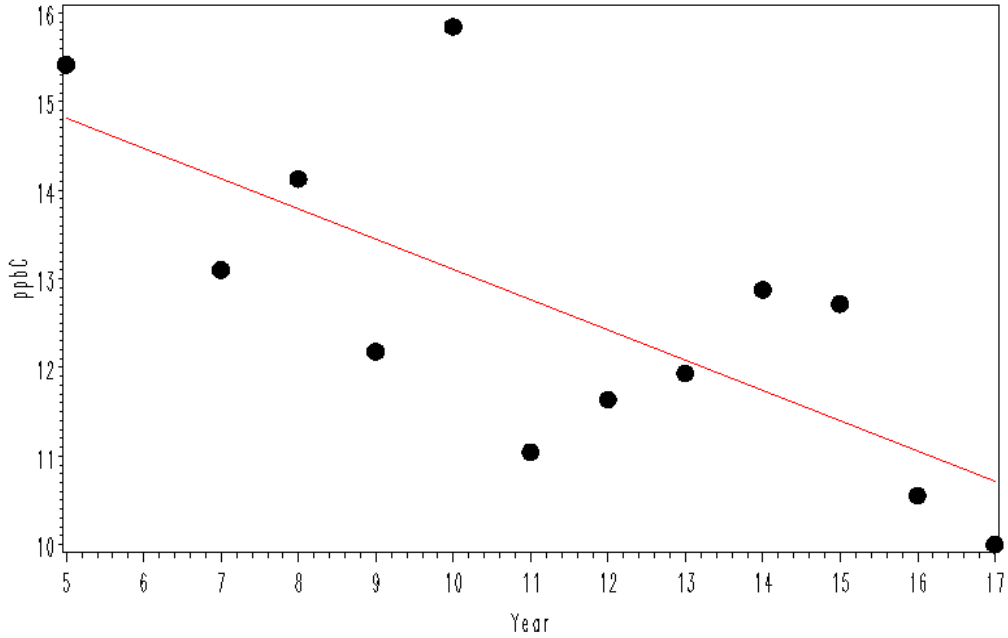

Figure 10.46 o-Xylene 6-9 CST May-Oct. OLS Trend, years since 1990, Clinton Dr. C403

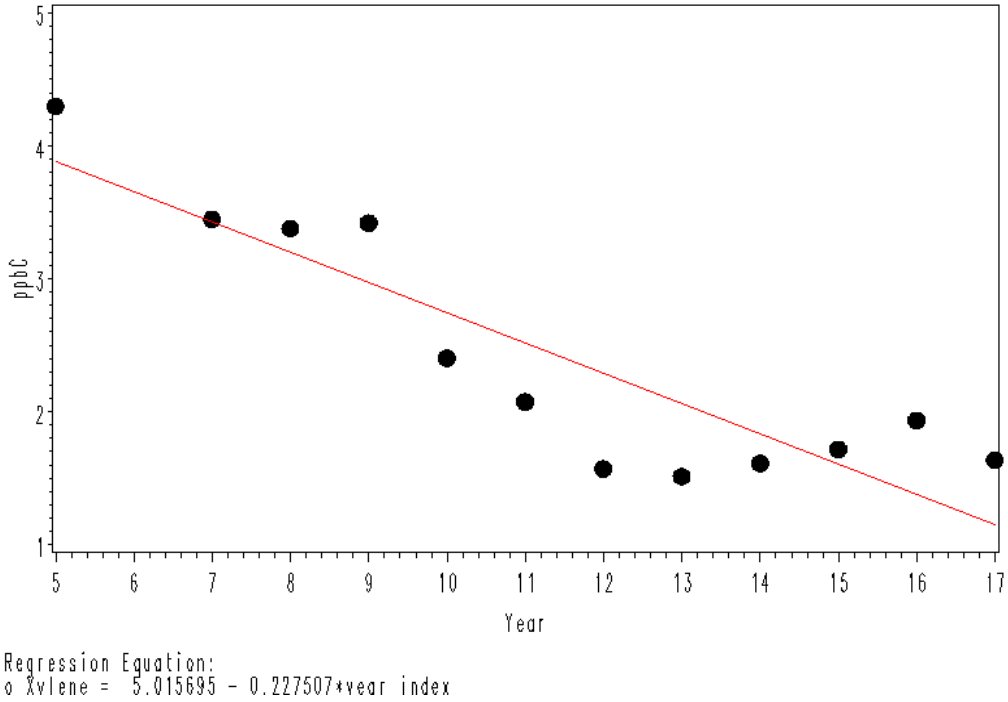

Figure 10.47 Propylene 6-9 CST May-Oct. OLS Trend, years since 1990, Clinton Dr. C403

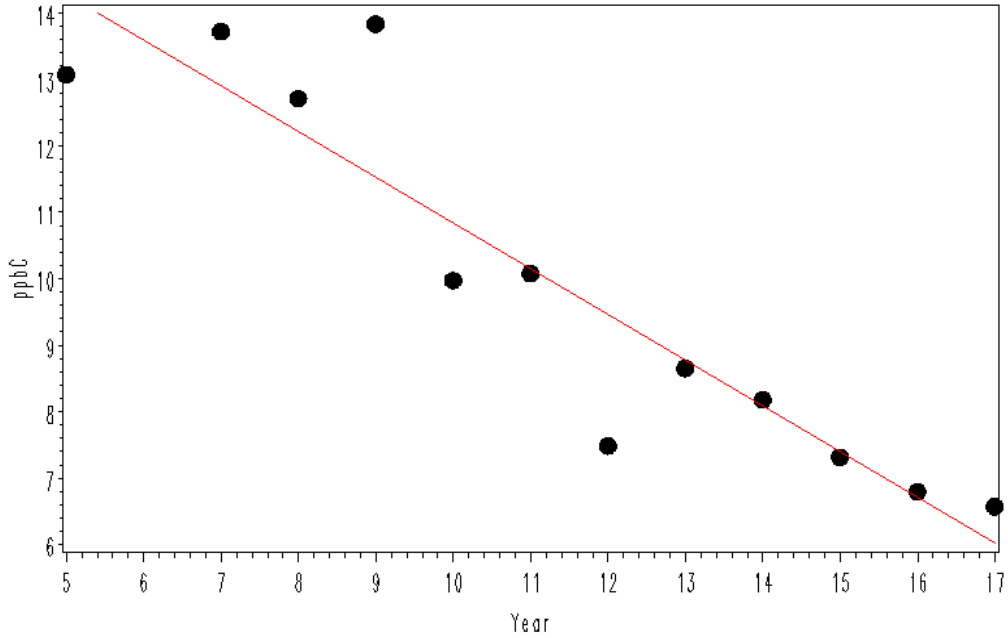

Regression Equation:
Propylene = 17.71088 - 0.686954*year index

Figure 10.48 Toluene 6-9 CST May-Oct. OLS Trend, years since 1990, Clinton Dr. C403

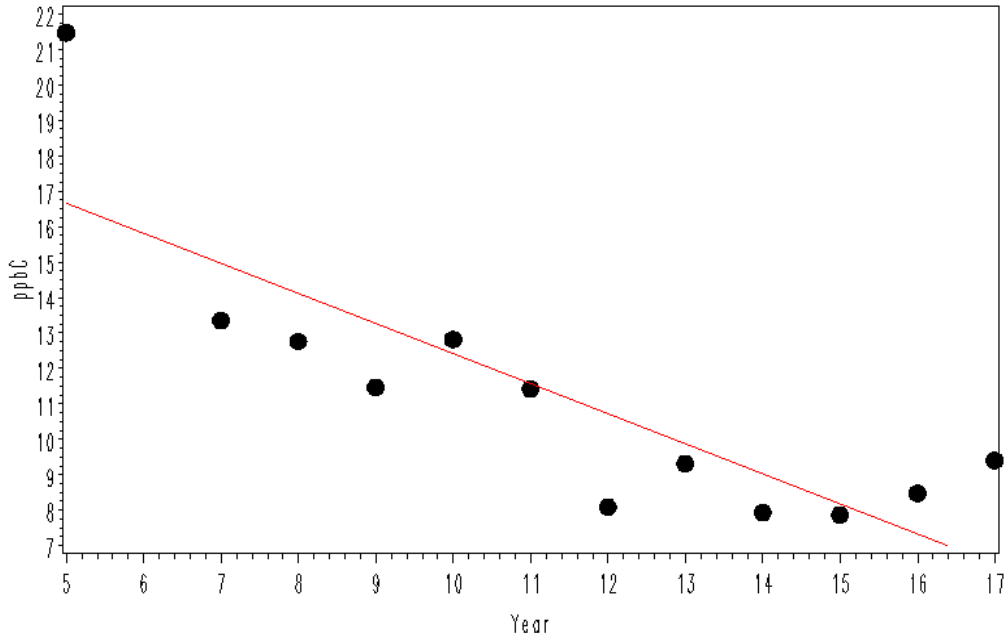

Regression Equation:
Toluene = 20.89038 - 0.848492*year index

10.2 Meteorologically-adjusted Trends for HCs

Tables 10.2 – 10.5 show the Pearson correlations for the regional meteorological data with the natural logarithm of the morning average for the four PAMS monitoring sites with long term data. Correlations are color-coded such that correlations greater than or equal to 0.3 are orange, correlations greater than or equal to 0.6 are red, and less than or equal to -0.4 are blue. The results appear in the table for each of the regional meteorological parameters.

A similar analysis was conducted using Spearman rank-based correlations were also assessed and found to have nearly identical results, suggesting the skewness in the data are not a major issue.

The last row in Tables 10.2 – 10.5 is the variable "yr". This is a variable for the year, and the correlation reflects whether a species mean morning concentration tended to increase or decrease by year. In most cases in the four tables, the value is negative, indicating a tendency for lower concentrations.

The specific set of parameters having the highest absolute values in correlations have been selected for use as independent variables in the meteorological adjusted trends.

Table 10.2 Correlations for morning hydrocarbons species with METDAT variables at Hinton Street DFW

481130069	1_Butene	Benzene	Ethyl benzene	Ethylene	Isobutane	Isopentan	Propylene	Toluene	Butane	Pentane	o-Xylene	mp_xylen
CCAVGPM	-0.15	-0.12	-0.13	-0.14	-0.13	-0.21	-0.15	-0.14	-0.14	-0.21	-0.13	-0.13
CCAVTAM	-0.27	-0.23	-0.25	-0.25	-0.19	-0.31	-0.25	-0.27	-0.18	-0.29	-0.25	-0.25
MRMAX	-0.20	-0.21	0.00	-0.18	-0.43	-0.17	-0.19	0.00	-0.55	-0.26	0.01	0.03
RAINHRS	-0.09	-0.06	-0.10	-0.08	-0.04	-0.11	-0.09	-0.10	-0.03	-0.11	-0.10	-0.10
RHAVGMID	-0.14	-0.08	-0.15	-0.09	-0.06	-0.17	-0.12	-0.17	-0.05	-0.16	-0.14	-0.14
D24T850	0.16	0.18	0.19	0.20	0.12	0.17	0.19	0.19	0.09	0.12	0.19	0.19
DEVH700	0.18	0.16	0.18	0.17	0.08	0.12	0.20	0.19	0.07	0.08	0.19	0.19
DEVH850	0.21	0.21	0.23	0.23	0.14	0.18	0.22	0.23	0.12	0.15	0.24	0.22
DEVT700	-0.01	-0.05	-0.03	-0.04	-0.08	-0.07	0.02	-0.03	-0.08	-0.10	-0.02	-0.01
DEVT850	0.02	-0.03	0.00	-0.03	-0.04	-0.01	0.02	0.01	-0.03	-0.04	0.01	0.02
DPAVG	-0.15	-0.18	0.03	-0.14	-0.39	-0.14	-0.14	0.04	-0.52	-0.24	0.05	0.07
DPMAX	-0.17	-0.19	0.01	-0.16	-0.39	-0.15	-0.16	0.02	-0.51	-0.24	0.03	0.05
DT700	0.20	0.29	0.08	0.27	0.40	0.19	0.27	0.06	0.50	0.25	0.08	0.06
DT850	0.23	0.30	0.13	0.29	0.38	0.24	0.28	0.12	0.47	0.27	0.13	0.12
DT925	0.42	0.49	0.41	0.51	0.50	0.50	0.49	0.43	0.52	0.48	0.42	0.40
H500	-0.06	-0.08	0.14	-0.03	-0.32	-0.03	-0.03	0.16	-0.44	-0.14	0.15	0.16
H700	0.00	-0.02	0.18	0.03	-0.25	0.02	0.03	0.20	-0.36	-0.09	0.20	0.20
H850	0.13	0.14	0.25	0.17	-0.01	0.16	0.15	0.26	-0.07	0.09	0.26	0.25
SLPAVG	0.19	0.21	0.10	0.20	0.27	0.16	0.18	0.08	0.34	0.21	0.10	0.07
STPAVG	0.12	0.20	0.11	0.18	0.23	0.16	0.15	0.10	0.29	0.19	0.11	0.09
T500	-0.12	-0.13	0.09	-0.08	-0.33	-0.05	-0.09	0.11	-0.45	-0.15	0.10	0.11
T700	-0.14	-0.18	0.02	-0.14	-0.40	-0.14	-0.11	0.03	-0.51	-0.24	0.03	0.05
T850	-0.13	-0.18	0.04	-0.15	-0.39	-0.12	-0.13	0.05	-0.50	-0.22	0.05	0.07
T925	-0.04	-0.09	0.14	-0.05	-0.30	0.00	-0.03	0.17	-0.42	-0.11	0.16	0.17
TAAVG	-0.14	-0.19	0.06	-0.14	-0.42	-0.12	-0.14	0.08	-0.56	-0.23	0.07	0.09
TAMAX	-0.09	-0.14	0.11	-0.09	-0.36	-0.05	-0.08	0.13	-0.50	-0.16	0.12	0.14
TAMIN	-0.20	-0.25	0.00	-0.20	-0.47	-0.18	-0.21	0.01	-0.60	-0.29	0.00	0.03
TAVGAM	-0.12	-0.18	0.07	-0.13	-0.41	-0.10	-0.12	0.09	-0.54	-0.21	0.09	0.10
TAVGPM	-0.04	-0.10	0.14	-0.05	-0.32	-0.01	-0.04	0.16	-0.45	-0.12	0.15	0.17
TD850	-0.23	-0.23	-0.06	-0.21	-0.37	-0.20	-0.21	-0.05	-0.48	-0.28	-0.05	-0.04
TDELTA	0.35	0.34	0.34	0.34	0.31	0.40	0.36	0.36	0.32	0.39	0.34	0.34
TMAX	-0.06	-0.12	0.13	-0.07	-0.34	-0.03	-0.06	0.15	-0.47	-0.14	0.13	0.15
TRANDIS	-0.36	-0.47	-0.47	-0.46	-0.40	-0.54	-0.41	-0.50	-0.36	-0.48	-0.48	-0.46
TRANU	0.07	0.09	0.06	0.06	0.16	0.17	0.06	0.08	0.26	0.24	0.04	0.05
TRANV	-0.09	-0.13	-0.04	-0.10	-0.26	-0.17	-0.07	-0.05	-0.31	-0.23	-0.04	-0.01
TRANW	0.17	0.18	0.09	0.15	0.34	0.25	0.16	0.11	0.43	0.32	0.07	0.06
WNDRUN	-0.34	-0.45	-0.47	-0.45	-0.38	-0.53	-0.40	-0.50	-0.34	-0.48	-0.47	-0.46
UAVG	-0.08	-0.14	-0.19	-0.15	0.00	-0.07	-0.14	-0.16	0.11	0.01	-0.21	-0.20
UAVGAM	-0.09	-0.16	-0.16	-0.16	-0.06	-0.07	-0.15	-0.13	0.00	-0.01	-0.18	-0.17
UAVGPM	-0.06	-0.11	-0.18	-0.12	0.03	-0.07	-0.11	-0.16	0.12	0.01	-0.19	-0.18
VAVG	0.00	-0.05	0.03	-0.01	-0.14	-0.08	0.03	0.03	-0.21	-0.12	0.04	0.05
VAVGAM	-0.01	-0.03	0.02	0.00	-0.15	-0.08	0.03	0.02	-0.21	-0.13	0.03	0.05
VAVGPM	0.04	0.00	0.06	0.04	-0.09	-0.03	0.06	0.06	-0.14	-0.07	0.07	0.08
WSAVG	-0.38	-0.40	-0.42	-0.43	-0.37	-0.50	-0.38	-0.47	-0.33	-0.43	-0.43	-0.41
WSAVGAM	-0.41	-0.40	-0.44	-0.44	-0.35	-0.49	-0.40	-0.50	-0.29	-0.41	-0.45	-0.43
WSAVGPM	-0.19	-0.22	-0.24	-0.23	-0.18	-0.28	-0.19	-0.28	-0.14	-0.22	-0.25	-0.23
yr	0.04	-0.32	-0.26	-0.30	-0.08	-0.31	-0.19	-0.19	-0.18	-0.25	-0.28	-0.29

Table 10.3 Correlations for morning hydrocarbons species with METDAT variables at Chamizal El Paso

481410044	1_Butene	Benzene	Ethyl benzene	Ethylene	Isobutane	Isopentan	Propylene	Toluene	Butane	Pentane	o-Xylen	mp_xylen
CCAVGPM	-0.01	-0.05	-0.02	-0.05	0.02	-0.02	-0.04	-0.05	-0.01	-0.01	-0.04	-0.04
CCAVTAM	-0.06	-0.11	-0.09	-0.09	-0.02	-0.08	-0.08	-0.11	-0.02	-0.07	-0.10	-0.10
MRMAX	-0.09	-0.07	0.02	-0.15	-0.19	-0.03	-0.10	0.03	-0.30	-0.07	0.03	0.02
RAINHRS	-0.08	-0.10	-0.09	-0.09	-0.09	-0.10	-0.09	-0.09	-0.08	-0.09	-0.07	-0.08
RHAVGMID	-0.03	-0.08	-0.07	-0.02	0.00	-0.07	-0.05	-0.10	0.04	-0.05	-0.05	-0.05
D24T850	0.27	0.29	0.30	0.26	0.24	0.30	0.27	0.31	0.23	0.29	0.30	0.30
DEVH500	0.29	0.31	0.32	0.31	0.35	0.36	0.31	0.32	0.31	0.34	0.32	0.32
DEVH700	0.29	0.31	0.31	0.32	0.37	0.36	0.30	0.31	0.33	0.35	0.32	0.32
DEVH850	0.18	0.20	0.18	0.22	0.27	0.21	0.19	0.17	0.23	0.21	0.19	0.19
DEVT500	0.15	0.16	0.16	0.15	0.13	0.18	0.16	0.18	0.12	0.16	0.17	0.17
DEVT700	0.26	0.28	0.30	0.26	0.29	0.33	0.28	0.31	0.26	0.31	0.30	0.30
DEVT850	0.24	0.25	0.26	0.22	0.22	0.30	0.24	0.28	0.21	0.28	0.27	0.27
DPAVG	-0.07	-0.06	0.04	-0.14	-0.16	-0.01	-0.08	0.04	-0.27	-0.05	0.05	0.04
DPMAX	-0.08	-0.07	0.03	-0.16	-0.18	-0.02	-0.10	0.03	-0.29	-0.06	0.03	0.02
DT700	0.36	0.35	0.30	0.44	0.48	0.35	0.38	0.27	0.57	0.38	0.31	0.32
DT850	0.46	0.46	0.42	0.51	0.52	0.48	0.47	0.42	0.59	0.49	0.44	0.44
H700	0.12	0.16	0.23	0.09	0.11	0.23	0.13	0.24	-0.02	0.19	0.23	0.23
H850	0.19	0.19	0.19	0.22	0.27	0.23	0.19	0.18	0.23	0.23	0.20	0.20
MHMAX	-0.36	-0.35	-0.31	-0.40	-0.47	-0.39	-0.35	-0.30	-0.51	-0.41	-0.33	-0.33
SLPAVG	0.16	0.12	0.07	0.23	0.30	0.13	0.15	0.03	0.36	0.17	0.08	0.08
STPAVG	0.10	0.09	0.10	0.12	0.19	0.13	0.09	0.07	0.14	0.14	0.10	0.09
T700	0.02	0.08	0.17	-0.04	-0.06	0.14	0.03	0.19	-0.19	0.08	0.16	0.15
T850	-0.01	0.04	0.13	-0.10	-0.12	0.10	-0.01	0.16	-0.26	0.04	0.12	0.12
TAAVG	-0.12	-0.07	0.03	-0.21	-0.25	-0.03	-0.12	0.06	-0.40	-0.09	0.02	0.01
TAMAX	-0.05	0.01	0.11	-0.13	-0.17	0.06	-0.04	0.14	-0.32	-0.01	0.09	0.09
TAMIN	-0.19	-0.16	-0.06	-0.29	-0.33	-0.12	-0.21	-0.04	-0.47	-0.18	-0.07	-0.08
TAVGAM	-0.13	-0.07	0.02	-0.22	-0.25	-0.03	-0.13	0.05	-0.40	-0.09	0.01	0.01
TAVGPM	-0.04	0.02	0.11	-0.12	-0.16	0.07	-0.03	0.14	-0.31	0.00	0.10	0.09
TD850	-0.14	-0.14	-0.05	-0.22	-0.21	-0.10	-0.16	-0.06	-0.32	-0.13	-0.06	-0.06
TDELTA	0.37	0.44	0.42	0.41	0.41	0.44	0.41	0.44	0.40	0.43	0.41	0.42
TMAX	-0.04	0.02	0.11	-0.13	-0.16	0.06	-0.04	0.14	-0.31	0.00	0.09	0.09
TRANDIS	-0.32	-0.35	-0.36	-0.35	-0.33	-0.36	-0.33	-0.35	-0.32	-0.35	-0.36	-0.36
TRANU	-0.13	-0.15	-0.16	-0.12	-0.26	-0.20	-0.12	-0.13	-0.16	-0.20	-0.16	-0.16
TRANV	0.14	0.15	0.17	0.13	0.06	0.15	0.16	0.19	0.05	0.13	0.18	0.18
TRANW	0.22	0.24	0.24	0.25	0.24	0.25	0.22	0.23	0.24	0.25	0.23	0.24
WNDRUN	-0.32	-0.35	-0.36	-0.36	-0.32	-0.36	-0.34	-0.36	-0.31	-0.35	-0.36	-0.36
UAVG	-0.19	-0.21	-0.23	-0.20	-0.30	-0.27	-0.20	-0.21	-0.22	-0.27	-0.22	-0.22
UAVGAM	-0.26	-0.28	-0.29	-0.26	-0.36	-0.33	-0.27	-0.27	-0.29	-0.33	-0.29	-0.29
UAVGPM	-0.08	-0.09	-0.11	-0.08	-0.15	-0.13	-0.07	-0.09	-0.08	-0.13	-0.11	-0.10
VAVG	0.14	0.14	0.18	0.10	0.03	0.14	0.14	0.19	0.02	0.12	0.17	0.17
VAVGAM	0.16	0.14	0.18	0.11	0.04	0.15	0.16	0.19	0.05	0.13	0.17	0.17
VAVGPM	0.13	0.15	0.17	0.11	0.08	0.14	0.15	0.18	0.06	0.12	0.17	0.16
WSAVG	-0.34	-0.38	-0.38	-0.38	-0.42	-0.42	-0.36	-0.36	-0.38	-0.41	-0.37	-0.37
WSAVGAM	-0.36	-0.39	-0.41	-0.38	-0.42	-0.44	-0.36	-0.39	-0.37	-0.43	-0.39	-0.40
WSAVGPM	-0.16	-0.18	-0.19	-0.19	-0.23	-0.21	-0.18	-0.18	-0.20	-0.21	-0.19	-0.19
yr	-0.23	-0.25	-0.23	-0.30	-0.07	-0.20	-0.27	-0.26	-0.16	-0.20	-0.32	-0.32

Table 10.4 Correlations for morning hydrocarbons species with METDAT variables at Clinton Dr. Houston

482011035	1_Butene	Benzene	Ethyl benzene	Ethylene	Isobutane	Isopentan	Propylene	Toluene	Butane	Pentane	o-Xylene	mp_xylen
CCAVGPM	0.14	-0.02	-0.09	-0.02	0.11	0.03	0.09	-0.08	0.03	0.04	-0.08	-0.06
CCAVTAM	0.03	-0.14	-0.20	-0.14	0.00	-0.10	-0.03	-0.21	-0.07	-0.08	-0.19	-0.17
MRMAX	0.17	0.00	0.17	0.02	0.02	0.08	0.12	0.13	-0.17	0.03	0.18	0.18
RAINHRS	0.01	-0.06	-0.14	-0.03	0.00	-0.04	0.01	-0.13	-0.02	-0.02	-0.12	-0.11
RHAVGMID	0.20	0.06	-0.04	0.07	0.16	0.10	0.18	-0.04	0.11	0.12	-0.02	0.01
D24T850	0.26	0.20	0.23	0.20	0.19	0.22	0.24	0.21	0.18	0.19	0.23	0.24
D24TD850	0.09	0.05	0.04	0.05	0.07	0.07	0.09	0.04	0.05	0.07	0.05	0.06
DEVH700	0.21	0.14	0.12	0.12	0.18	0.17	0.18	0.10	0.14	0.15	0.11	0.12
DEVH850	0.18	0.17	0.11	0.15	0.18	0.18	0.18	0.12	0.16	0.17	0.10	0.11
DEVT500	0.06	-0.03	0.00	-0.04	0.04	0.01	0.02	-0.02	0.01	0.00	0.00	0.00
DEVT700	0.15	0.01	0.06	-0.02	0.10	0.07	0.07	0.02	0.05	0.04	0.07	0.09
DEVT850	0.08	-0.03	0.04	-0.05	0.01	0.00	0.02	-0.01	-0.02	-0.01	0.05	0.06
DPAVG	0.23	0.05	0.21	0.07	0.07	0.13	0.17	0.17	-0.11	0.08	0.21	0.22
DPMAX	0.22	0.04	0.21	0.06	0.06	0.13	0.16	0.16	-0.11	0.07	0.21	0.21
DT700	0.07	0.18	0.04	0.16	0.18	0.12	0.11	0.06	0.31	0.15	0.03	0.04
DT850	0.02	0.16	0.05	0.14	0.10	0.08	0.09	0.06	0.21	0.10	0.04	0.05
DT925	0.13	0.27	0.22	0.25	0.18	0.21	0.21	0.23	0.25	0.21	0.21	0.21
H700	0.16	0.05	0.16	0.06	0.06	0.12	0.13	0.13	-0.09	0.06	0.14	0.14
H850	0.16	0.13	0.15	0.13	0.11	0.16	0.17	0.14	0.04	0.13	0.13	0.13
SLPAVG	-0.11	0.03	-0.11	0.01	0.00	-0.02	-0.05	-0.07	0.11	0.01	-0.13	-0.14
STPAVG	-0.11	0.03	-0.11	0.01	0.00	-0.02	-0.05	-0.07	0.11	0.01	-0.12	-0.13
T850	0.05	-0.09	0.09	-0.07	-0.07	-0.02	0.00	0.04	-0.25	-0.08	0.08	0.08
T925	0.09	-0.04	0.15	-0.03	-0.04	0.03	0.05	0.11	-0.21	-0.02	0.14	0.13
TAAVG	0.15	-0.01	0.20	0.01	0.00	0.07	0.10	0.15	-0.20	0.01	0.19	0.19
TAMAX	0.17	0.04	0.26	0.06	0.02	0.11	0.13	0.21	-0.16	0.04	0.25	0.25
TAMIN	0.11	-0.07	0.12	-0.05	-0.04	0.02	0.05	0.07	-0.24	-0.04	0.11	0.11
TAVGAM	0.17	0.01	0.22	0.03	0.02	0.10	0.11	0.18	-0.17	0.04	0.21	0.22
TAVGPM	0.15	0.05	0.27	0.06	0.00	0.10	0.11	0.23	-0.16	0.03	0.26	0.25
TD850	-0.07	-0.17	-0.08	-0.17	-0.13	-0.12	-0.10	-0.09	-0.26	-0.14	-0.08	-0.09
TDELTA	0.11	0.27	0.35	0.25	0.11	0.21	0.16	0.35	0.20	0.17	0.34	0.32
TMAX	0.16	0.04	0.27	0.06	0.00	0.11	0.11	0.23	-0.17	0.03	0.26	0.25
TRANDIS	-0.09	-0.30	-0.37	-0.32	-0.09	-0.25	-0.22	-0.40	-0.12	-0.21	-0.34	-0.31
TRANU	-0.30	-0.06	0.04	-0.08	-0.27	-0.18	-0.21	0.05	-0.17	-0.19	0.06	0.02
TRANV	0.35	0.12	0.26	0.11	0.18	0.19	0.23	0.18	0.07	0.14	0.28	0.31
TRANW	-0.32	-0.19	-0.24	-0.19	-0.21	-0.22	-0.28	-0.20	-0.07	-0.18	-0.22	-0.23
WNDRUN	-0.09	-0.30	-0.36	-0.32	-0.09	-0.24	-0.22	-0.40	-0.11	-0.21	-0.34	-0.30
UAVG	-0.28	-0.18	-0.01	-0.21	-0.30	-0.23	-0.27	-0.04	-0.24	-0.25	0.02	-0.01
UAVGAM	-0.26	-0.19	0.01	-0.22	-0.33	-0.24	-0.26	-0.03	-0.30	-0.29	0.04	0.02
UAVGPM	-0.24	-0.19	-0.08	-0.22	-0.25	-0.23	-0.26	-0.11	-0.18	-0.23	-0.05	-0.07
VAVG	0.46	0.25	0.38	0.23	0.29	0.33	0.34	0.32	0.21	0.28	0.39	0.43
VAVGAM	0.48	0.23	0.34	0.20	0.30	0.32	0.34	0.27	0.22	0.28	0.35	0.39
VAVGPM	0.44	0.25	0.35	0.23	0.29	0.31	0.33	0.29	0.21	0.27	0.35	0.38
WSAVG	-0.26	-0.33	-0.45	-0.37	-0.22	-0.35	-0.33	-0.46	-0.19	-0.29	-0.42	-0.39
WSAVGAM	-0.30	-0.38	-0.48	-0.40	-0.25	-0.38	-0.37	-0.49	-0.24	-0.32	-0.46	-0.43
WSAVGPM	-0.02	-0.11	-0.17	-0.17	-0.03	-0.11	-0.11	-0.18	-0.01	-0.07	-0.14	-0.11
yr	-0.04	-0.27	-0.28	-0.27	-0.02	-0.10	-0.14	-0.27	-0.04	-0.10	-0.35	-0.35

Table 10.5 Correlations for morning hydrocarbons species with METDAT variables at Deer Park (Houston area)

482011039	1_Butene	Benzene	Ethyl benzene	Ethylene	Isobutane	Isopentan	Propylene	Toluene	Butane	Pentane	o-Xylene	mp_xylen
CCAVGPM	-0.22	-0.21	-0.24	-0.18	-0.19	-0.29	-0.13	-0.24	-0.29	-0.28	-0.23	-0.24
CCAVTAM	-0.29	-0.31	-0.36	-0.30	-0.30	-0.40	-0.20	-0.36	-0.37	-0.38	-0.36	-0.37
MRMAX	-0.21	-0.25	-0.10	-0.16	-0.28	-0.20	-0.19	-0.11	-0.42	-0.26	-0.09	-0.08
RAINHRS	-0.07	-0.09	-0.16	-0.05	-0.07	-0.16	0.00	-0.13	-0.12	-0.15	-0.15	-0.15
RHAVGMID	-0.25	-0.24	-0.28	-0.17	-0.21	-0.33	-0.15	-0.27	-0.29	-0.32	-0.25	-0.27
D24T850	-0.09	-0.01	0.04	-0.01	-0.05	-0.03	-0.07	0.03	-0.04	-0.06	0.06	0.04
D24TD850	-0.08	-0.06	-0.06	-0.07	-0.06	-0.08	-0.06	-0.05	-0.08	-0.09	-0.05	-0.06
DEVH500	-0.16	-0.09	-0.07	-0.10	-0.10	-0.13	-0.08	-0.09	-0.15	-0.13	-0.08	-0.09
DEVH700	-0.11	-0.02	-0.01	-0.03	-0.03	-0.06	-0.01	-0.01	-0.09	-0.06	-0.01	-0.02
DEVT700	-0.21	-0.20	-0.16	-0.20	-0.22	-0.20	-0.21	-0.19	-0.21	-0.21	-0.17	-0.18
DEVT850	-0.18	-0.19	-0.15	-0.20	-0.21	-0.19	-0.19	-0.17	-0.20	-0.20	-0.15	-0.16
DPAVG	-0.20	-0.23	-0.08	-0.14	-0.25	-0.20	-0.16	-0.09	-0.40	-0.25	-0.07	-0.07
DPMAX	-0.20	-0.22	-0.08	-0.14	-0.25	-0.19	-0.17	-0.09	-0.38	-0.24	-0.07	-0.07
DT700	0.09	0.19	0.11	0.12	0.18	0.15	0.07	0.10	0.31	0.16	0.11	0.09
DT850	0.09	0.19	0.14	0.12	0.16	0.15	0.07	0.13	0.27	0.17	0.14	0.13
DT925	0.16	0.27	0.28	0.21	0.24	0.27	0.14	0.27	0.32	0.26	0.29	0.28
H700	-0.10	-0.06	0.04	-0.03	-0.09	-0.05	-0.02	0.04	-0.25	-0.08	0.04	0.05
MHMAX	-0.02	0.02	0.11	0.06	0.01	0.06	0.00	0.10	-0.06	0.02	0.10	0.11
SLPAVG	0.16	0.22	0.14	0.16	0.24	0.20	0.19	0.15	0.29	0.23	0.12	0.13
STPAVG	0.16	0.22	0.13	0.16	0.24	0.20	0.19	0.15	0.28	0.23	0.12	0.13
T700	-0.18	-0.20	-0.09	-0.15	-0.23	-0.17	-0.16	-0.10	-0.35	-0.20	-0.10	-0.09
T850	-0.16	-0.20	-0.07	-0.15	-0.24	-0.16	-0.15	-0.08	-0.37	-0.19	-0.07	-0.06
T925	-0.12	-0.15	-0.01	-0.10	-0.18	-0.10	-0.10	-0.02	-0.31	-0.14	-0.01	0.00
TAAVG	-0.16	-0.20	-0.04	-0.12	-0.23	-0.15	-0.14	-0.05	-0.38	-0.19	-0.04	-0.02
TAMAX	-0.12	-0.15	0.03	-0.07	-0.18	-0.08	-0.11	0.02	-0.31	-0.13	0.04	0.05
TAMIN	-0.18	-0.23	-0.10	-0.15	-0.26	-0.20	-0.14	-0.11	-0.43	-0.24	-0.10	-0.09
TAVGAM	-0.14	-0.17	-0.01	-0.10	-0.20	-0.11	-0.12	-0.02	-0.35	-0.16	-0.01	0.01
TAVGPM	-0.06	-0.08	0.10	-0.02	-0.13	-0.01	-0.07	0.08	-0.24	-0.06	0.10	0.11
TD850	-0.14	-0.18	-0.14	-0.17	-0.20	-0.18	-0.11	-0.13	-0.32	-0.20	-0.14	-0.13
TDELTA	0.24	0.31	0.42	0.26	0.27	0.41	0.13	0.40	0.40	0.37	0.42	0.42
TMAX	-0.08	-0.10	0.08	-0.04	-0.14	-0.03	-0.09	0.06	-0.27	-0.08	0.08	0.09
TRANDIS	-0.38	-0.45	-0.57	-0.42	-0.42	-0.53	-0.32	-0.57	-0.42	-0.50	-0.56	-0.57
TRANU	0.25	0.21	0.29	0.15	0.15	0.33	0.07	0.28	0.31	0.31	0.27	0.28
TRANV	-0.39	-0.39	-0.23	-0.31	-0.43	-0.39	-0.36	-0.27	-0.48	-0.45	-0.20	-0.22
TRANW	0.22	0.15	0.07	0.08	0.17	0.21	0.10	0.07	0.32	0.23	0.05	0.06
WNDRUN	-0.38	-0.46	-0.57	-0.43	-0.43	-0.53	-0.34	-0.58	-0.42	-0.51	-0.56	-0.57
UAVG	0.05	-0.04	0.09	-0.11	-0.12	0.10	-0.16	0.05	0.05	0.05	0.08	0.08
UAVGAM	-0.04	-0.14	0.05	-0.19	-0.23	0.01	-0.26	0.00	-0.07	-0.05	0.04	0.04
UAVGPM	0.01	-0.07	-0.01	-0.14	-0.12	0.01	-0.15	-0.04	0.03	-0.01	-0.02	-0.02
VAVG	-0.33	-0.32	-0.13	-0.23	-0.34	-0.27	-0.32	-0.17	-0.36	-0.35	-0.10	-0.13
VAVGAM	-0.40	-0.39	-0.22	-0.30	-0.40	-0.36	-0.38	-0.26	-0.43	-0.43	-0.19	-0.21
VAVGPM	-0.28	-0.25	-0.10	-0.17	-0.27	-0.23	-0.24	-0.13	-0.31	-0.29	-0.07	-0.10
WSAVG	-0.28	-0.33	-0.50	-0.34	-0.30	-0.43	-0.25	-0.50	-0.27	-0.37	-0.51	-0.51
WSAVGAM	-0.27	-0.33	-0.50	-0.34	-0.28	-0.41	-0.24	-0.50	-0.28	-0.36	-0.51	-0.51
WSAVGPM	-0.23	-0.26	-0.32	-0.27	-0.22	-0.29	-0.23	-0.34	-0.19	-0.27	-0.31	-0.33
yr	-0.07	-0.12	-0.15	-0.16	-0.04	-0.05	-0.09	-0.15	-0.04	-0.05	-0.18	-0.15

Regressions have been run on a select set of meteorological variables that tended to have the most significant correlations for all four sites. Tables 10.6 – 10.8 contain the statistical summaries of the runs. The "PVALUE" elements are color codes yellow for p-value less than 0.05, reflecting statistical significance. The "R2" column shows the r-squared values, which tend to be fairly low despite the significance. Only the Clinton Dr. site was used for Houston. Dtxxx is the highest available pressure level – 850 mb for El Paso and 925 mbfor the other cities.

Table 10.6 Alkane model

CBSA	type	Intercept	v am	wsa am	trnsdis	t-delta	dtxxx	cloud am	rh-mid	R2
DFW	PARMS	42.92	-0.34	-1.84	-0.03	1.29	1.70	0.46	0.00	0.30
DFW	T	6.16	-1.56	-3.85	-7.05	6.11	9.79	1.95	-0.05	.
DFW	PVALUE	0.00	0.12	0.00	0.00	0.00	0.00	0.05	0.96	.
DFW	L95B	29.25	-0.78	-2.79	-0.03	0.87	1.36	0.00	-0.14	.
DFW	U95B	56.59	0.09	-0.90	-0.02	1.70	2.04	0.92	0.13	.
ElPaso	PARMS	4.97	4.98	-0.12	-0.05	3.19	3.27	1.54	0.45	0.25
ElPaso	T	0.32	8.19	-0.13	-4.87	7.80	9.73	2.81	3.13	.
ElPaso	PVALUE	0.75	0.00	0.90	0.00	0.00	0.00	0.01	0.00	.
ElPaso	L95B	-25.43	3.78	-1.99	-0.07	2.39	2.61	0.46	0.17	.
ElPaso	U95B	35.37	6.17	1.75	-0.03	3.99	3.93	2.61	0.74	.
HGB	PARMS	99.90	7.82	-3.56	0.02	0.16	5.44	-5.91	1.52	0.06
HGB	T	2.08	5.41	-1.24	1.03	0.12	4.85	-3.58	3.66	.
HGB	PVALUE	0.04	0.00	0.22	0.30	0.90	0.00	0.00	0.00	.
HGB	L95B	5.74	4.98	-9.20	-0.02	-2.32	3.24	-9.15	0.71	.
HGB	U95B	194.07	10.65	2.08	0.06	2.63	7.63	-2.67	2.34	.

Table 10.7 BTEX Model

CBSA	type	Intercept	v am	wsa am	trnsdis	t-delta	dtxxx	cloud am	rh-mid	R2
DFW	PARMS	23.60	0.28	-1.41	-0.02	0.61	0.82	0.20	0.02	0.25
DFW	T	5.39	2.01	-4.68	-7.90	4.63	7.52	1.32	0.38	.
DFW	PVALUE	0.00	0.05	0.00	0.00	0.00	0.00	0.19	0.70	.
DFW	L95B	15.01	0.01	-2.01	-0.02	0.35	0.61	-0.09	-0.07	.
DFW	U95B	32.18	0.55	-0.82	-0.01	0.87	1.03	0.49	0.10	.
ElPaso	PARMS	12.09	2.23	-0.31	-0.02	1.38	1.72	0.41	0.20	0.28
ElPaso	T	1.76	8.28	-0.74	-4.80	7.63	11.58	1.68	3.18	.
ElPaso	PVALUE	0.08	0.00	0.46	0.00	0.00	0.00	0.09	0.00	.
ElPaso	L95B	-1.38	1.70	-1.14	-0.03	1.03	1.43	-0.07	0.08	.
ElPaso	U95B	25.56	2.76	0.52	-0.01	1.74	2.02	0.88	0.33	.
HGB	PARMS	20.20	1.00	-1.90	-0.01	0.75	1.09	-1.26	0.36	0.19
HGB	T	2.76	4.55	-4.21	-3.95	3.91	6.42	-5.02	5.61	.
HGB	PVALUE	0.01	0.00	0.00	0.00	0.00	0.00	0.00	0.00	.
HGB	L95B	5.83	0.57	-2.78	-0.02	0.37	0.76	-1.76	0.23	.
HGB	U95B	34.57	1.43	-1.01	-0.01	1.13	1.43	-0.77	0.48	.

Table 10.8 HRVOC Model

CBSA	type	Intercept	v am	wsa am	trnsdis	t-delta	dtxxx	cloud am	rh-mid	R2
DFW	PARMS	7.71	0.05	-0.47	-0.01	0.33	0.34	0.08	0.02	0.25
DFW	T	3.63	0.81	-3.28	-5.05	5.11	6.45	1.17	1.08	.
DFW	PVALUE	0.00	0.42	0.00	0.00	0.00	0.00	0.24	0.28	.
DFW	L95B	3.54	-0.08	-0.76	-0.01	0.20	0.24	-0.06	-0.02	.
DFW	U95B	11.89	0.18	-0.19	0.00	0.46	0.44	0.22	0.06	.
ElPaso	PARMS	8.12	0.91	-0.17	-0.01	0.45	0.77	0.07	0.11	0.24
ElPaso	T	2.71	7.81	-0.91	-3.36	5.62	11.77	0.70	3.74	.
ElPaso	PVALUE	0.01	0.00	0.36	0.00	0.00	0.00	0.48	0.00	.
ElPaso	L95B	2.24	0.68	-0.53	-0.01	0.29	0.64	-0.13	0.05	.
ElPaso	U95B	14.00	1.14	0.19	0.00	0.60	0.89	0.28	0.16	.
HGB	PARMS	2.66	0.92	-0.49	0.00	0.61	1.42	-1.12	0.56	0.11
HGB	T	0.29	3.26	-0.86	0.04	2.55	6.65	-3.56	7.03	.
HGB	PVALUE	0.77	0.00	0.39	0.97	0.01	0.00	0.00	0.00	.
HGB	L95B	-15.40	0.36	-1.61	-0.01	0.14	1.00	-1.74	0.40	.
HGB	U95B	20.72	1.47	0.63	0.01	1.09	1.84	-0.50	0.71	.

The next step is to regress the annual mean residuals resulting from the meteorological regressions on year. This is similar to the Camalier et al. approach, but omitting the spline fits and using two stages of OLS. The need for log-transforms has been reduced since the dependent hydrocarbon variables were formed from averaging over four hours and then adding across species. The results of the met-adjusted residual regressions appear in Figures 10.49 – 10.57 and are summarized in Table 10.9. Note that one observation is excluded from calculations in Figures 10.49 – 10.51 for Clinton Drive, as there were too few observation in 1996.

Table 10.9 Results of regressing annual mean residuals of the regression of composite species in meteorological variables

Site Description	Model	Intercept	slope	R2	T	p-value
Clinton Dr	Alkanes	18.05	-1.53	0.08	-0.86	0.41
	BTEX	22.44	-1.92	0.70	-4.48	0.00
	HRVOC	16.35	-1.37	0.77	-5.55	0.00
Dallas Hinton	Alkanes	19.26	-1.57	0.41	-2.63	0.03
	BTEX	16.27	-1.34	0.61	-3.96	0.00
	HRVOC	5.68	-0.49	0.45	-2.88	0.02
El Paso Chamizal	Alkanes	25.61	-2.01	0.03	-1.87	0.10
	BTEX	27.18	-2.13	0.76	-5.09	0.00
	HRVOC	10.17	-0.78	0.47	-2.64	0.03

BTEX and HRVOC species appear to be declining significantly. Alkanes are significant only at Dallas Hinton, but do show negative slopes at the other two sites.

Figure 10.49 HGB met-adjusted alkane trend, years since 1990

CBSA_Title = Houston-Sugar Land-Baytown, TX

alkane_resid	=	yr
Response Distribution:	Normal	
Link Function:	Identity	

Model Equation
alkane_resid = 18.0405 - 1.5304 yr

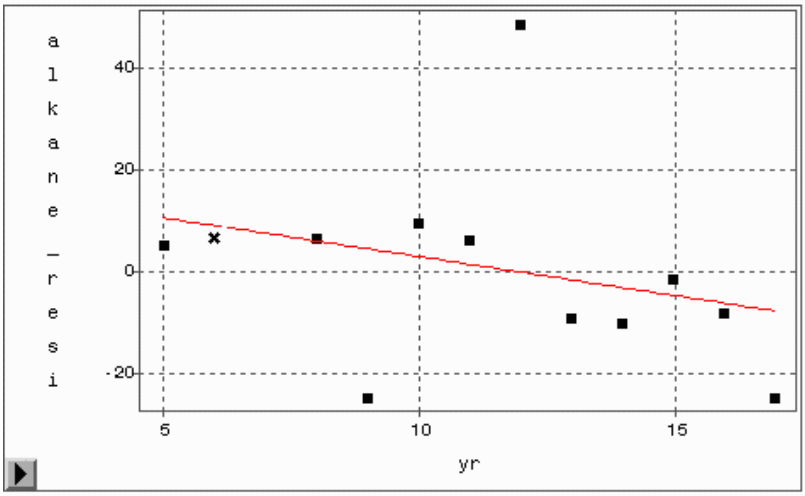

Parametric Regression Fit

		Model		Error				
Curve	Degree(Polynomial)	DF	Mean Square	DF	Mean Square	R-Square	F Stat	Pr > F
	1	1	313.0102	9	418.5659	0.0767	0.75	0.4096

Summary of Fit

Mean of Response	-0.0466	R-Square	0.0767
Root MSE	20.4589	Adj R-Sq	0

Parameter Estimates

Variable	DF	Estimate	Std Error	t Stat	Pr >|t|	Tolerance	Var Inflation
Intercept	1	18.0405	21.8063	0.83	0.4295	.	0
yr	1	-1.5304	1.7698	-0.86	0.4096	1.0000	1.0000

Figure 10.50 HGB met-adjusted BTEX trend, years since 1990

CBSA_Title = Houston-Sugar Land-Baytown, TX

btex_resid	=	yr
Response Distribution:	Normal	
Link Function:	Identity	

Model Equation
btex_resid = 22.4354 - 1.9172 yr

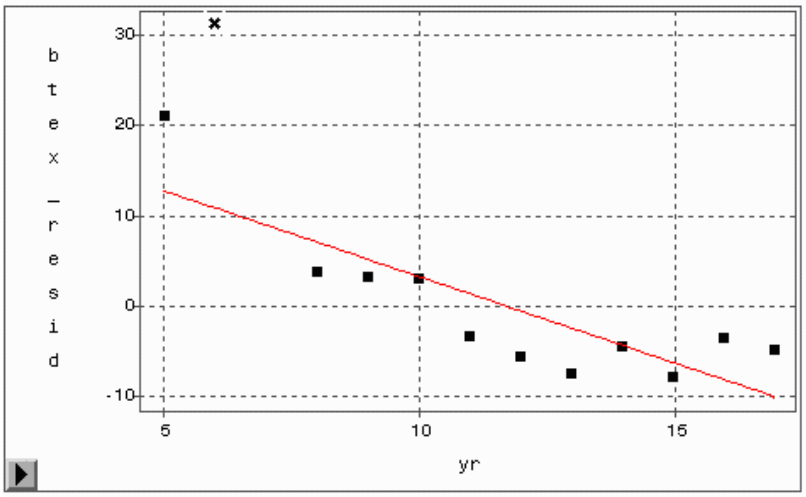

Parametric Regression Fit								
		Model		Error				
Curve	Degree(Polynomial)	DF	Mean Square	DF	Mean Square	R-Square	F Stat	Pr > F
	1	1	491.1905	9	23.3665	0.7002	21.02	0.0013

Summary of Fit			
Mean of Response	-0.2221	R-Square	0.7002
Root MSE	4.8339	Adj R-Sq	0.6669

Parameter Estimates							
Variable	DF	Estimate	Std Error	t Stat	Pr >|t|	Tolerance	Var Inflation
Intercept	1	22.4354	5.1522	4.35	0.0018	.	0
yr	1	-1.9172	0.4182	-4.58	0.0013	1.0000	1.0000

Figure 10.51 HGB met-adjusted HRVOC trend, years since 1990

CBSA_Title = Houston-Sugar Land-Baytown, TX

hrvoc_resid	=	yr
Response Distribution:	Normal	
Link Function:	Identity	

Model Equation
hrvoc_resid = 15.1432 - 1.2793 yr

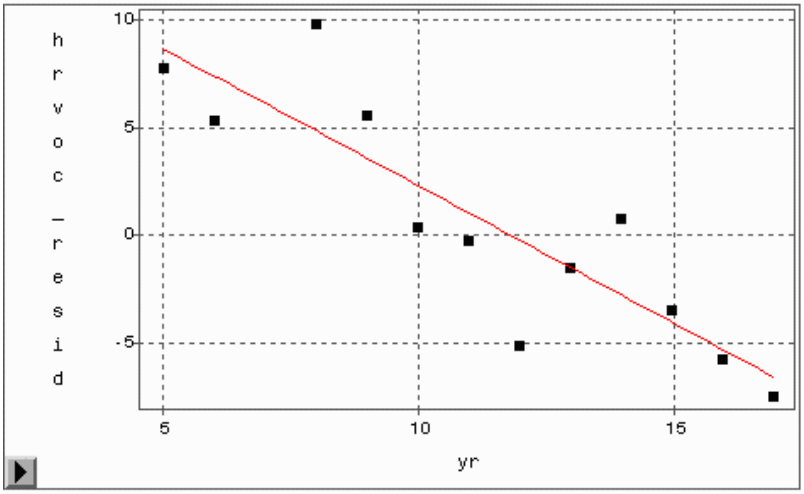

Parametric Regression Fit								
		Model		Error				
Curve	Degree(Polynomial)	DF	Mean Square	DF	Mean Square	R-Square	F Stat	Pr > F
	1	1	269.4988	10	7.8110	0.7753	34.50	0.0002

Summary of Fit			
Mean of Response	0.6443	R-Square	0.7753
Root MSE	2.7948	Adj R-Sq	0.7528

Parameter Estimates							
Variable	DF	Estimate	Std Error	t Stat	Pr >|t|	Tolerance	Var Inflation
Intercept	1	15.1432	2.5969	5.83	0.0002	.	0
yr	1	-1.2793	0.2178	-5.87	0.0002	1.0000	1.0000

Figure 10.52 DFW met-adjusted alkane trend, years since 1990

CBSA_Title = Dallas-Fort Worth-Arlington, TX

alkane_resid	=	yr
Response Distribution:	Normal	
Link Function:	Identity	

Model Equation
alkane_resid = 19.2646 - 1.5715 yr

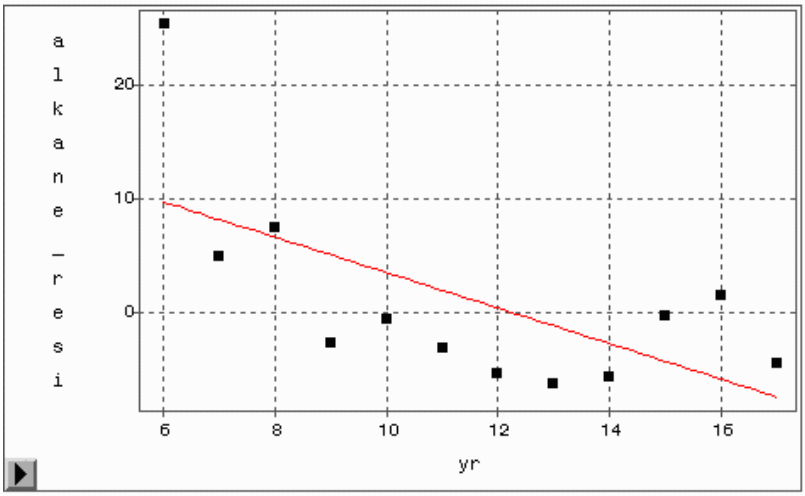

Parametric Regression Fit								
		Model		Error				
Curve	Degree(Polynomial)	DF	Mean Square	DF	Mean Square	R-Square	F Stat	Pr > F
	1	1	353.1723	10	51.0620	0.4089	6.92	0.0252

Summary of Fit			
Mean of Response	1.1919	R-Square	0.4089
Root MSE	7.1458	Adj R-Sq	0.3497

Parameter Estimates							
Variable	DF	Estimate	Std Error	t Stat	Pr >|t|	Tolerance	Var Inflation
Intercept	1	19.2646	7.1749	2.69	0.0229	.	0
yr	1	-1.5715	0.5976	-2.63	0.0252	1.0000	1.0000

Figure 10.53 DFW met-adjusted BTEX trend, years since 1990

CBSA_Title = Dallas-Fort Worth-Arlington, TX

btex_resid	=	yr
Response Distribution:	Normal	
Link Function:	Identity	

Model Equation
btex_resid = 16.2695 - 1.3420 yr

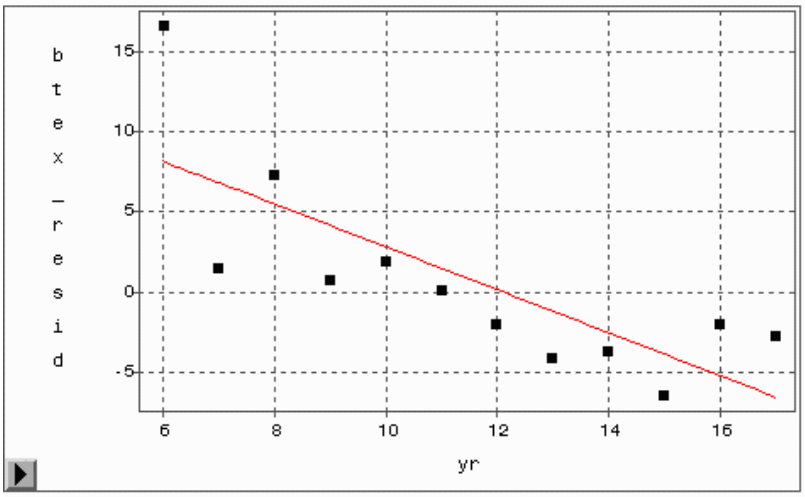

Parametric Regression Fit								
		Model		Error				
Curve	Degree(Polynomial)	DF	Mean Square	DF	Mean Square	R-Square	F Stat	Pr > F
	1	1	257.5387	10	16.4397	0.6104	15.67	0.0027

Summary of Fit			
Mean of Response	0.8365	R-Square	0.6104
Root MSE	4.0546	Adj R-Sq	0.5714

Parameter Estimates							
Variable	DF	Estimate	Std Error	t Stat	Pr >|t|	Tolerance	Var Inflation
Intercept	1	16.2695	4.0711	4.00	0.0025	.	0
yr	1	-1.3420	0.3391	-3.96	0.0027	1.0000	1.0000

Figure 10.54 DFW met-adjusted HRVOC trend, years since 1990

CBSA_Title = Dallas-Fort Worth-Arlington, TX

hrvoc_resid	=	yr
Response Distribution:	Normal	
Link Function:	Identity	

Model Equation
hrvoc_resid = 5.6827 - 0.4948 yr

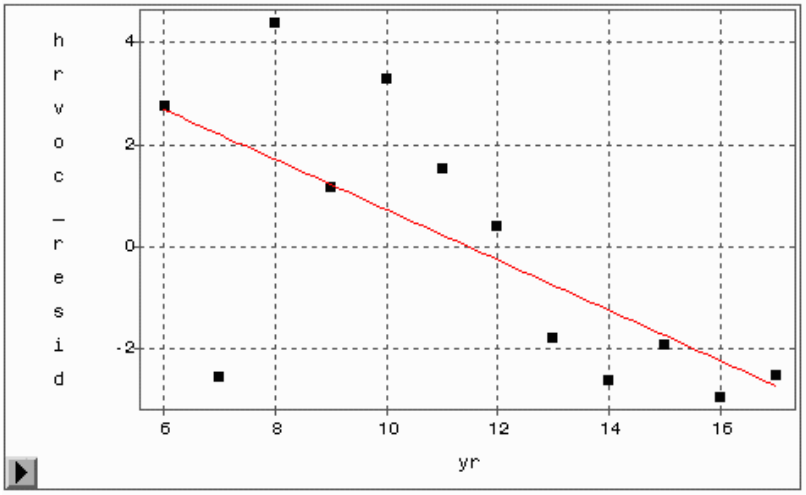

Parametric Regression Fit								
		Model		Error				
Curve	Degree(Polynomial)	DF	Mean Square	DF	Mean Square	R-Square	F Stat	Pr > F
	1	1	35.0100	10	4.2312	0.4528	8.27	0.0165

Summary of Fit			
Mean of Response	-0.0075	R-Square	0.4528
Root MSE	2.0570	Adj R-Sq	0.3981

Parameter Estimates							
Variable	DF	Estimate	Std Error	t Stat	Pr >|t|	Tolerance	Var Inflation
Intercept	1	5.6827	2.0654	2.75	0.0204	.	0
yr	1	-0.4948	0.1720	-2.88	0.0165	1.0000	1.0000

Figure 10.55 El Paso met-adjusted alkane trend, years since 1990

CBSA_Title = El Paso, TX

alkane_resid	=	yr
Response Distribution:	Normal	
Link Function:	Identity	

Model Equation
alkane_resid = 25.6123 - 2.0116 yr

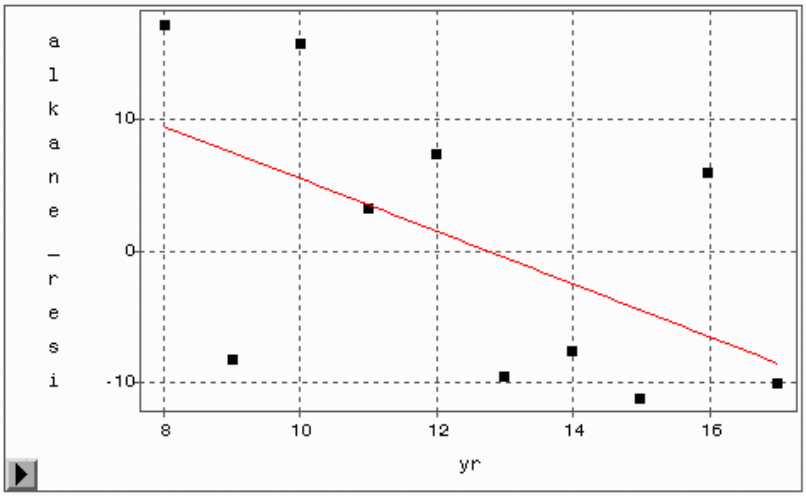

Parametric Regression Fit

		Model		Error				
Curve	Degree(Polynomial)	DF	Mean Square	DF	Mean Square	R-Square	F Stat	Pr > F
	1	1	333.8421	8	95.6009	0.3039	3.49	0.0986

Summary of Fit

Mean of Response	0.4672	R-Square	0.3039
Root MSE	9.7776	Adj R-Sq	0.2168

Parameter Estimates

Variable	DF	Estimate	Std Error	t Stat	Pr >|t|	Tolerance	Var Inflation
Intercept	1	25.6123	13.8066	1.86	0.1007	.	0
yr	1	-2.0116	1.0765	-1.87	0.0986	1.0000	1.0000

Figure 10.56 El Paso met-adjusted BTEX trend, years since 1990

CBSA_Title = El Paso, TX

btex_resid	=	yr
Response Distribution:	Normal	
Link Function:	Identity	

Model Equation
btex_resid = 27.1786 - 2.1280 yr

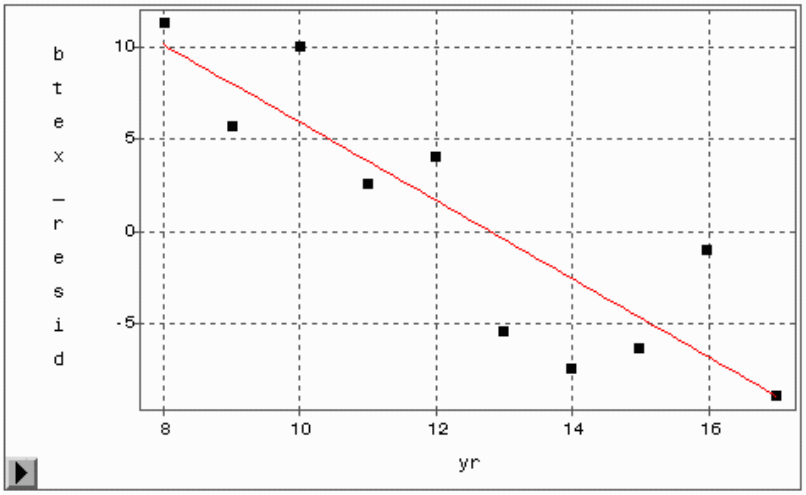

Parametric Regression Fit								
		Model		Error				
Curve	Degree(Polynomial)	DF	Mean Square	DF	Mean Square	R-Square	F Stat	Pr > F
	1	1	373.5852	8	14.4448	0.7638	25.86	0.0009

Summary of Fit			
Mean of Response	0.5788	R-Square	0.7638
Root MSE	3.8006	Adj R-Sq	0.7342

Parameter Estimates							
Variable	DF	Estimate	Std Error	t Stat	Pr >|t|	Tolerance	Var Inflation
Intercept	1	27.1786	5.3668	5.06	0.0010	.	0
yr	1	-2.1280	0.4184	-5.09	0.0009	1.0000	1.0000

Figure 10.57 El Paso met-adjusted HRVOC trend, years since 1990

CBSA_Title = El Paso, TX

hrvoc_resid	=	yr
Response Distribution:	Normal	
Link Function:	Identity	

Model Equation
hrvoc_resid = 10.1691 - 0.7837 yr

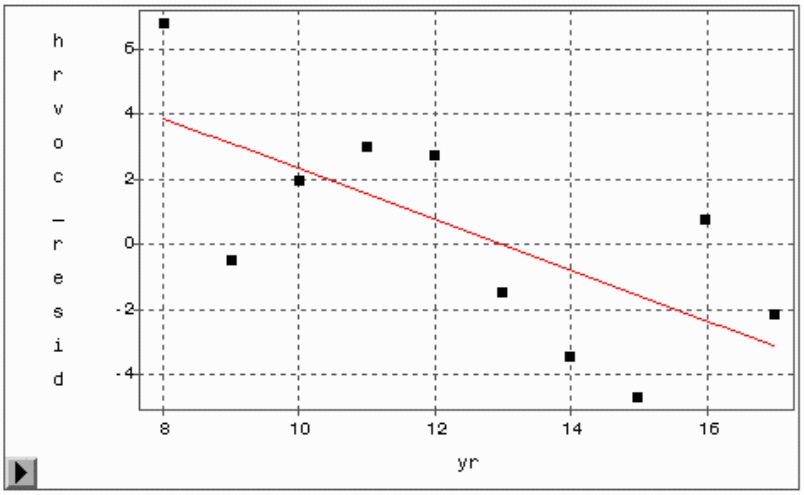

Parametric Regression Fit								
		Model		Error				
Curve	Degree(Polynomial)	DF	Mean Square	DF	Mean Square	R-Square	F Stat	Pr > F
	1	1	50.6686	8	7.2493	0.4663	6.99	0.0295

Summary of Fit			
Mean of Response	0.3730	R-Square	0.4663
Root MSE	2.6924	Adj R-Sq	0.3996

Parameter Estimates							
Variable	DF	Estimate	Std Error	t Stat	Pr >|t|	Tolerance	Var Inflation
Intercept	1	10.1691	3.8019	2.67	0.0282	.	0
yr	1	-0.7837	0.2964	-2.64	0.0295	1.0000	1.0000

11. $PM_{2.5}$ Trends

Particulate matter sized 2.5 microns and less ($PM_{2.5}$) is a complicated pollutant. First, it is not a single chemical, and the instruments that measure it are varied. In general, data collected by the federal reference method samplers (FRMs) are used to determine NAAQS compliance, based on a variable that is reported under parameter code 88101. However, speciation monitors generate very similar results, and in Texas the speciation sampler is generally identical to the FRM sampler. Speciation $PM_{2.5}$ mass is reported as parameter number 88502. Recently there has been some confusion as to which parameter is reported, and more detail can be provided on this matter upon request. The point is that based on the similar behavior of the data, both 88101 and 88502 have been used herein without distinction.

The approach taken has been to use the annual mean for individual sampling sites that have at least 50 percent data return every quarter for at least six years ending in 2007. In Texas, 22 sites meet these criteria giving good coverage for the state:

- Dallas / Fort Worth (5 sites)
- Northeast Texas (2 sites)
- Houston area (4 sites)
- Beaumont / Port Arthur area (2 sites)
- Austin (1 site)
- Corpus Christi (2 sites)
- Lower Rio Grande Valley (1 site)
- El Paso (3 sites),
- Odessa (1 site)
- Big Bend (1 site)

The OLS regression results show that the five Dallas / Fort Worth sites and one Northeast Texas Texarkana site show statistically significant downward trends. All other sites but one show no significant trend.

Only one site in the state shows a statistically significant upward trend, and that is the Houston Clinton Drive site 482011035. This site is a known hotspot affected by dust from local activities in the prevailing upwind direction to the south. More recent data from 2008 shows a possible reversal in the trend for the past couple of years.

Results are summarized in Table 11.1 and graphs of the annual time series and OLS regression lines appear in Figures 11.1 – 11.22. Note that units on the y-axes are missing and should be micrograms per cubic meter.

Table 11.1 Summary of OLS regressions of annual mean $PM_{2.5}$ on year, years since 2000

airs	Site Description	Intercept	slope	R2	T	p-value	L95B	U95B
480370004	Texarkana	14.49	-0.31	0.54	-2.64	0.04	-0.60	-0.02
480430101	BRAVO Big Bend C67	6.78	-0.16	0.39	-2.13	0.07	-0.34	0.02
481130050	Convention Ctr C312	14.62	-0.35	0.48	-2.53	0.04	-0.68	-0.02
481130069	Dallas Hinton St. C401	13.53	-0.37	0.72	-4.24	0.00	-0.58	-0.17
481130087	Dallas Exec Air C402	12.05	-0.20	0.53	-2.60	0.04	-0.38	-0.01
481350003	Odessa Hays C47	7.15	0.15	0.46	2.07	0.09	-0.04	0.34
481410037	El Paso UTEP C12	9.68	-0.08	0.17	-1.00	0.36	-0.29	0.13
481410044	Chamizal C41	9.30	0.05	0.04	0.55	0.60	-0.17	0.28
481410053	El Paso Sun Metro C40	15.82	0.31	0.18	1.03	0.35	-0.46	1.09
482010024	Houston Aldine C8	12.63	0.11	0.13	0.85	0.43	-0.22	0.43
482010058	Baytown A148	12.81	-0.26	0.38	-1.93	0.10	-0.58	0.07
482011035	***Clinton C403***	***13.79***	***0.31***	***0.75***	***4.24***	***0.01***	***0.13***	***0.48***
482011039	Deer Park C35	11.40	0.04	0.01	0.24	0.82	-0.33	0.40
482030002	Karnack C85	11.67	-0.01	0.00	-0.09	0.93	-0.42	0.39
482150043	Mission C43	10.70	0.05	0.04	0.50	0.64	-0.19	0.28
482450021	PA Mem School C303	11.42	0.02	0.01	0.20	0.85	-0.18	0.21
483550032	CC Huisache C98	10.13	0.07	0.06	0.62	0.56	-0.20	0.34
483550034	Dona Park C635	8.50	0.26	0.47	2.11	0.09	-0.06	0.59
483611001	West Orange C9	11.55	-0.06	0.05	-0.51	0.63	-0.34	0.23
484391002	Ft. Worth NW C13	12.48	-0.21	0.66	-3.38	0.01	-0.37	-0.06
484391006	Haws Athletic Ctr C310	13.73	-0.32	0.49	-1.96	0.12	-0.77	0.13
484530020	Audubon C38	9.20	0.03	0.03	0.32	0.77	-0.27	0.33

Figure 11.1 PM2.5 Annual mean OLS trend, Austin Audubon C38, years since 2000

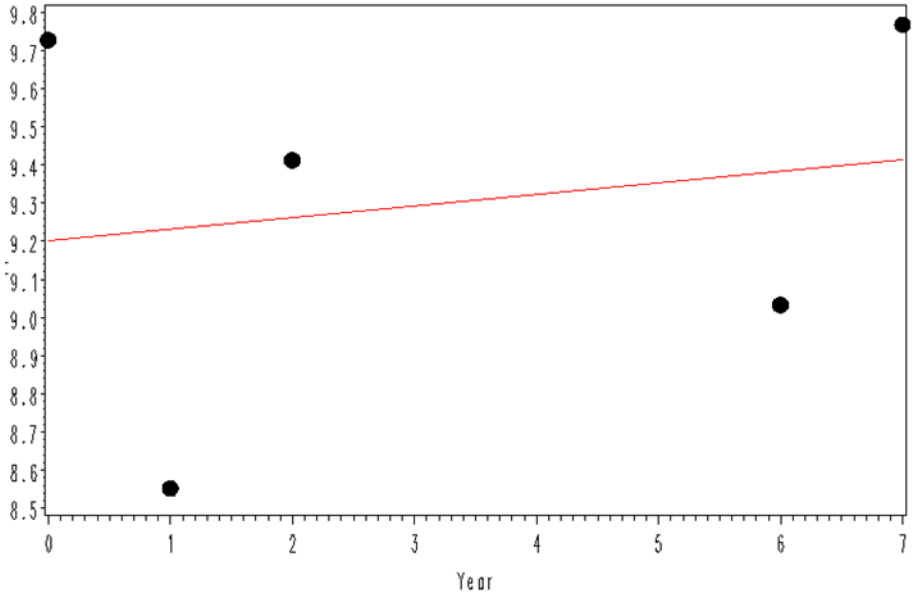

ression Equation:
25 yr = 9.202532 + 0.030243*year index

Figure 11.2 PM2.5 Annual mean OLS trend, Fort Worth Haws Athletic Center C310, years since 2000

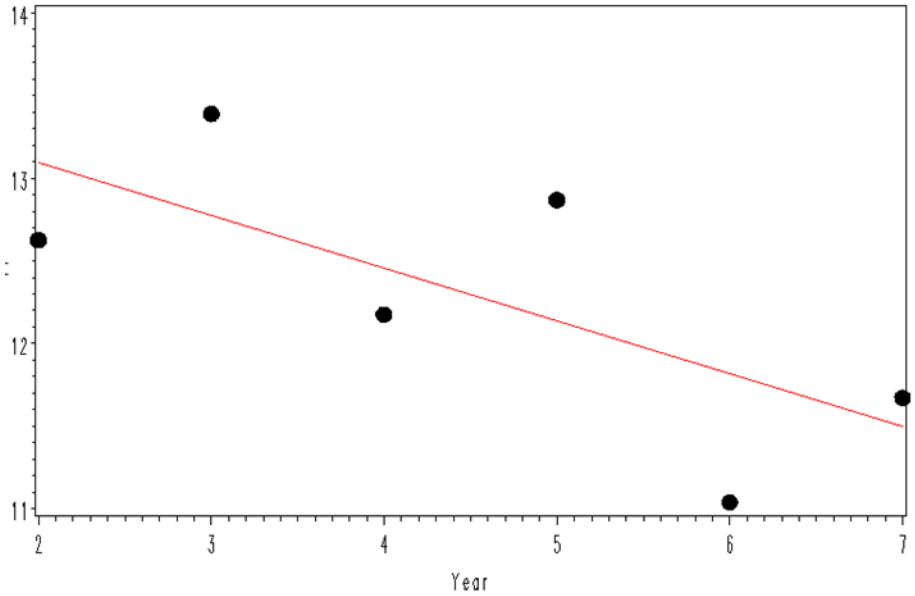

ression Equation:
25 yr = 13.72623 - 0.317808*year index

Figure 11.3 PM2.5 Annual mean OLS trend, Dallas Hinton St. C401, years since 2000

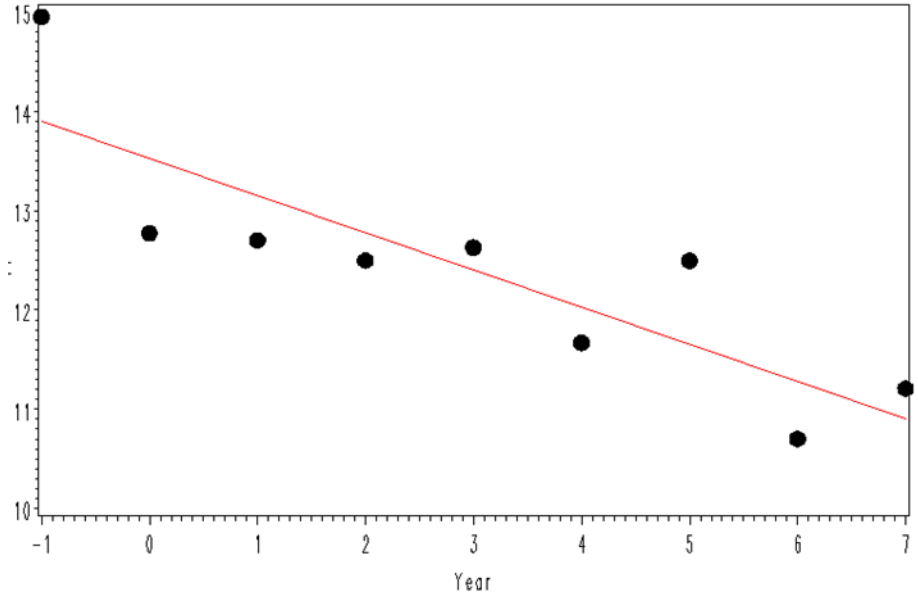

ression Equation:
5 vr = 13.52616 - 0.373752*year index

Figure 11.4 PM2.5 Annual mean OLS trend, Dallas Convention Center C312, years since 2000

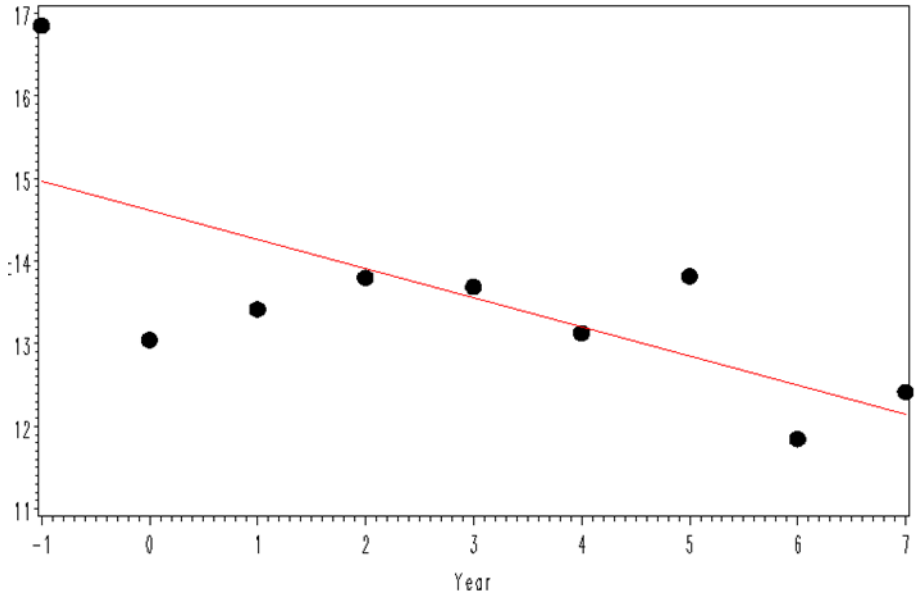

ression Equation:
5 vr = 14.61727 - 0.353162*year index

Figure 11.5 PM2.5 Annual mean OLS trend, Dallas Executive Airport C402, years since 2000

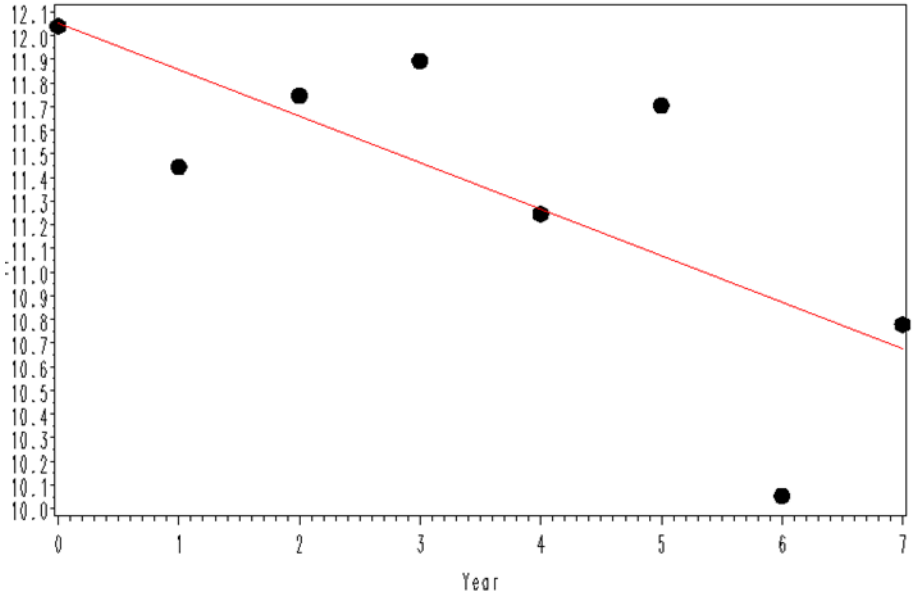

ression Equation:
?5 vr = 12.05367 - 0.197104*year index

Figure 11.6 PM2.5 Annual mean OLS trend, Fort Worth NW C13, years since 2000

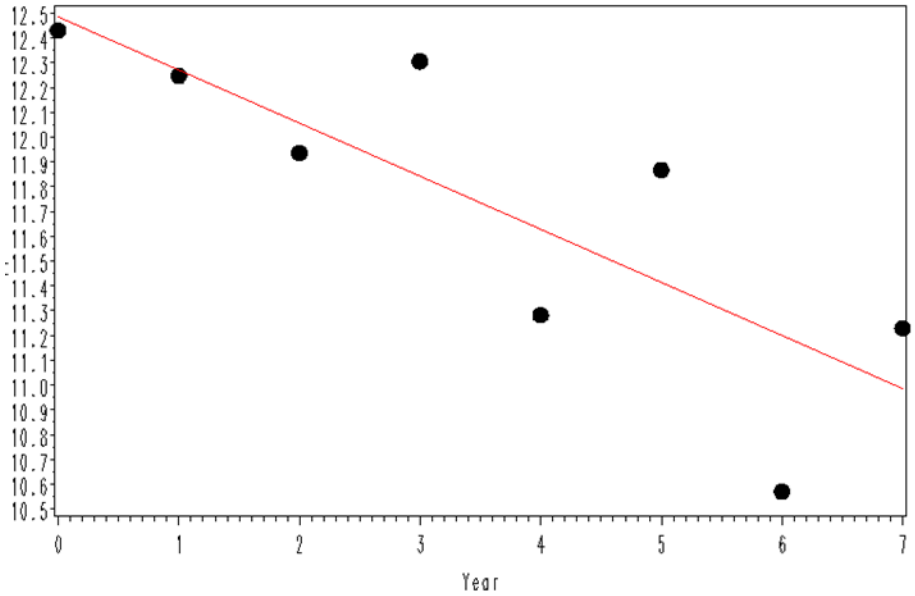

ression Equation:
?5 vr = 12.48451 - 0.214412*year index

Figure 11.7 PM2.5 Annual mean OLS trend, Deer Park C35, years since 2000

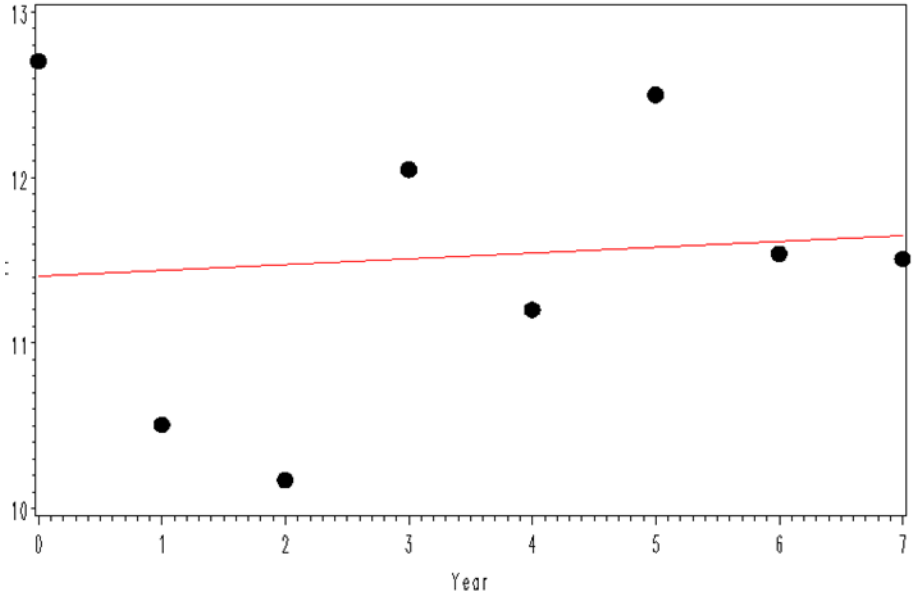

ression Equation:
5 yr = 11.40071 + 0.035064*year index

Figure 11.8 PM2.5 Annual mean OLS trend, Aldine C8, years since 2000

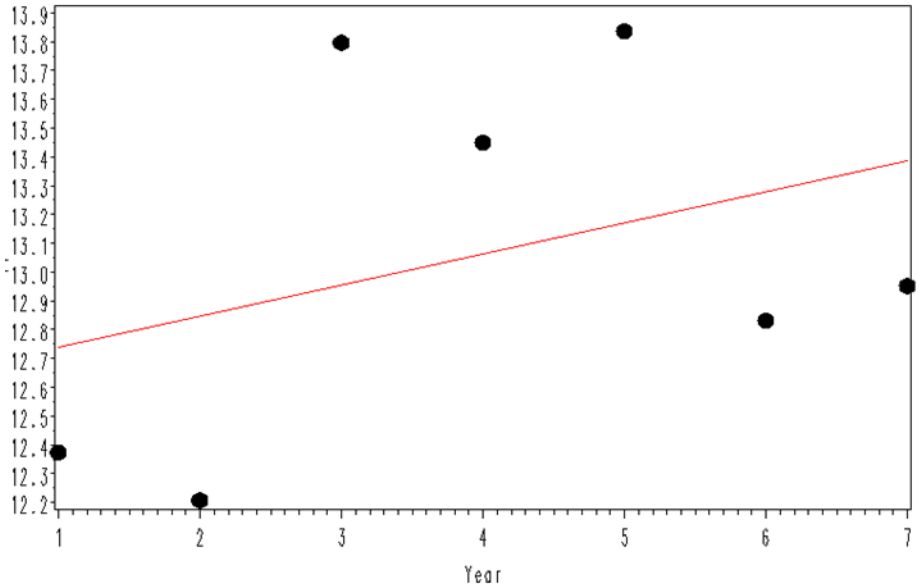

ression Equation:
5 yr = 12.63267 + 0.107931*year index

Figure 11.9 PM2.5 Annual mean OLS trend, Baytown, years since 2000

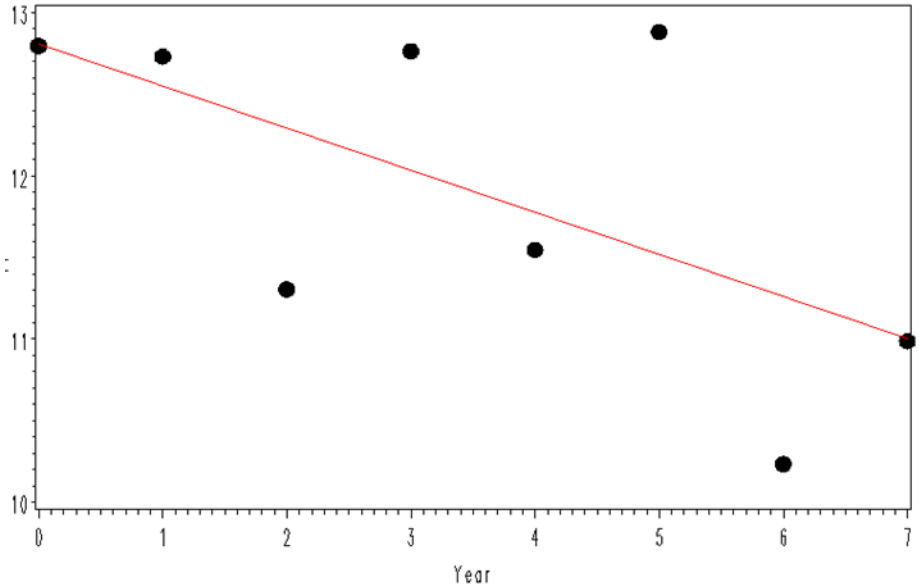

ression Equation:
25 yr = 12.80745 - 0.257469*year index

Figure 11.10 PM2.5 Annual mean OLS trend, Clinton Drive C403, years since 2000

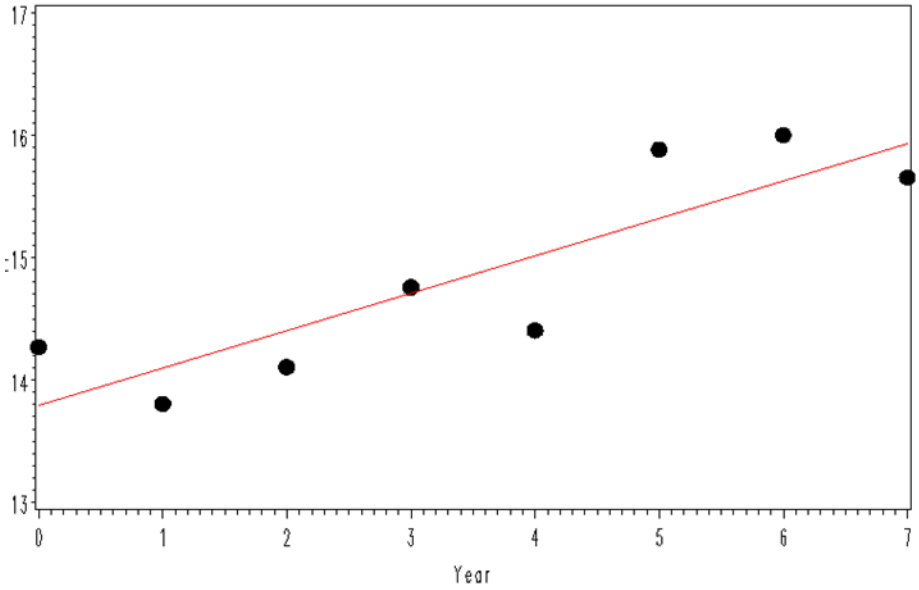

ression Equation:
25 yr = 13.79338 + 0.305247*year index

Figure 11.11 PM2.5 Annual mean OLS trend, Texarkana, years since 2000

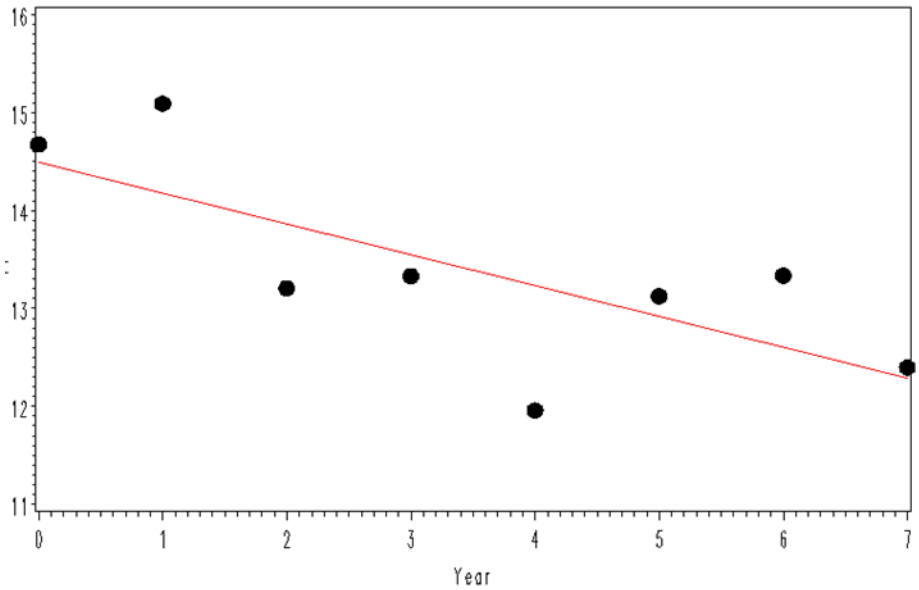

ression Equation:
25 yr = 14.48864 - 0.313456*year index

Figure 11.12 PM2.5 Annual mean OLS trend, Karnack C85, years since 2000

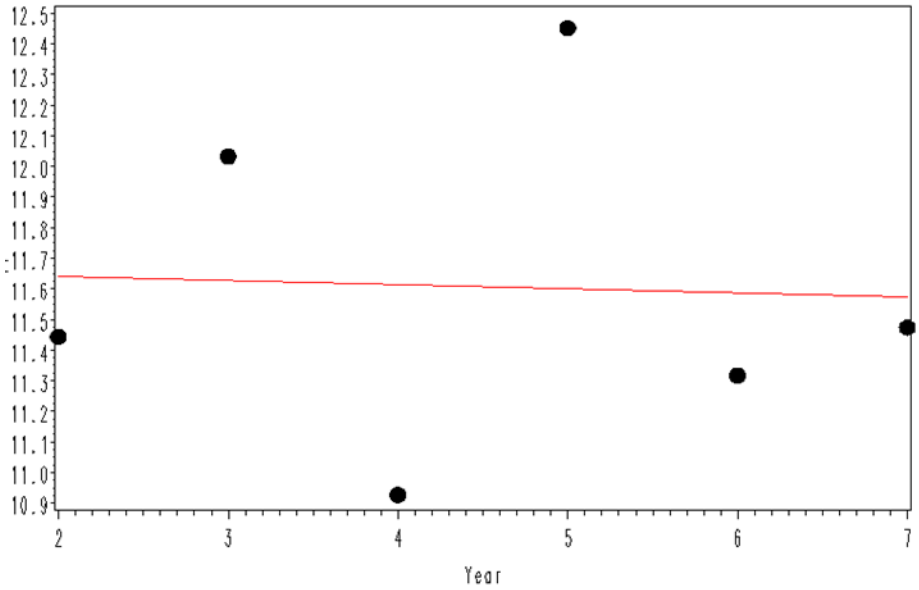

ression Equation:
25 yr = 11.66882 - 0.013473*year index

Figure 11.13 PM2.5 Annual mean OLS trend, West Orange C9, years since 2000

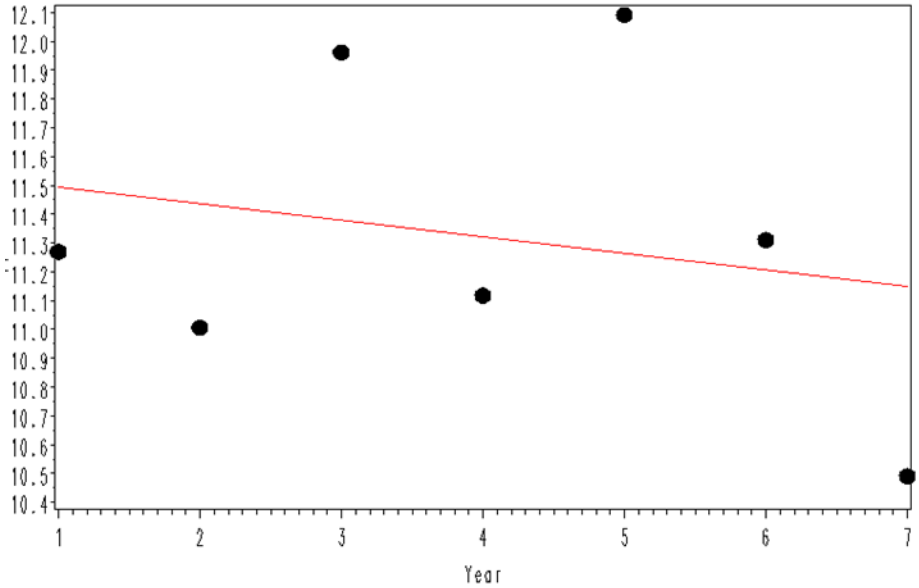

ression Equation:
25 yr = 11.5501 - 0.05705*year index

Figure 11.14 PM2.5 Annual mean OLS trend, Port Arthur Memorial School C303, years since 2000

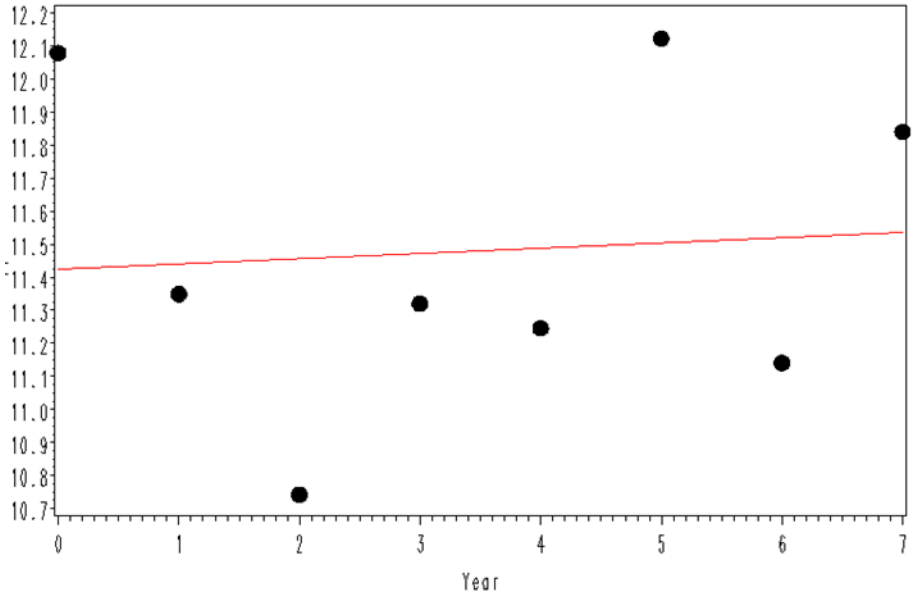

ression Equation:
25 yr = 11.42394 + 0.01606*year index

Figure 11.15 PM2.5 Annual mean OLS trend, Mission C43, years since 2000

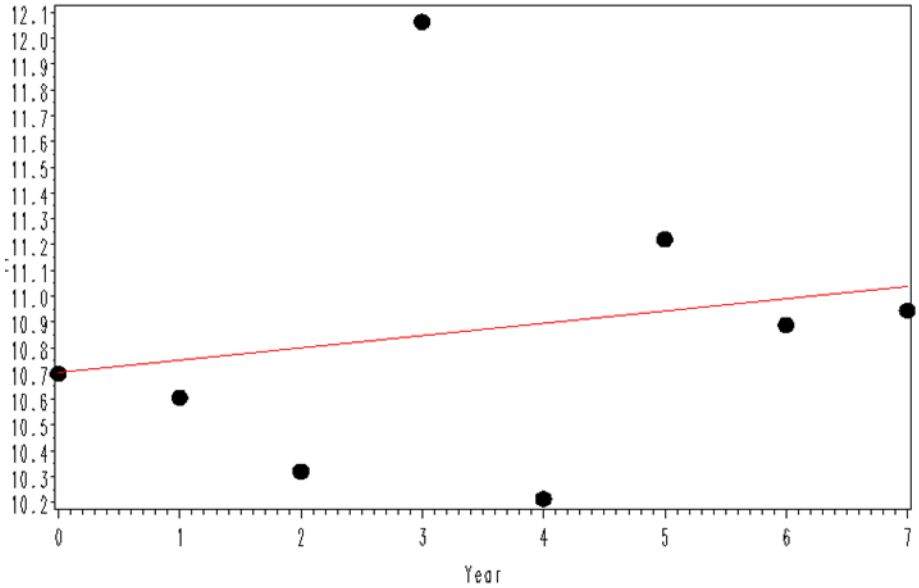

ression Equation:
25 vr = 10.70405 + 0.047383*year index

Figure 11.16 PM2.5 Annual mean OLS trend, Corpus Christi Dona Park C635, years since 2000

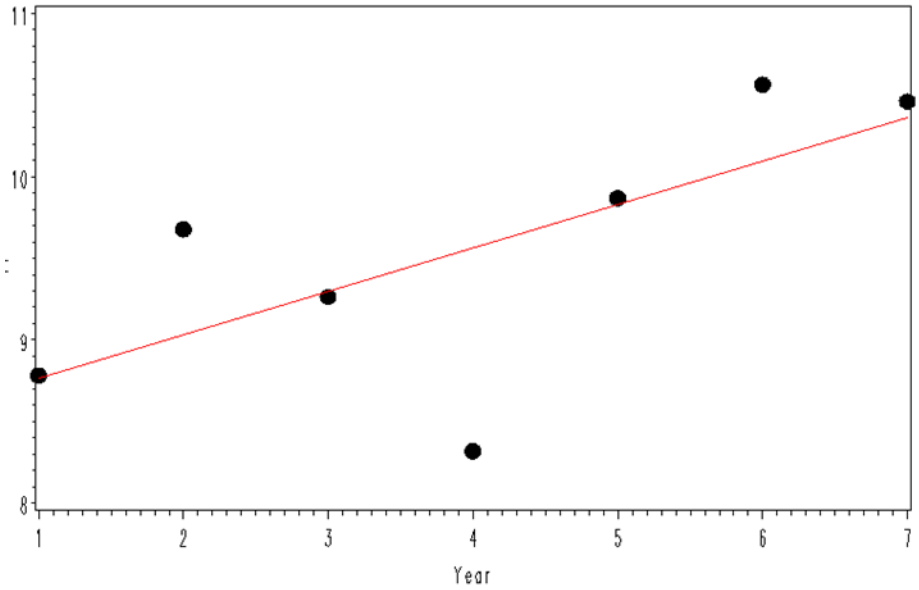

ression Equation:
25 vr = 8.503978 + 0.264773*year index

Figure 11.17 PM2.5 Annual mean OLS trend, Corpus Christi Huisache C98, years since 2000

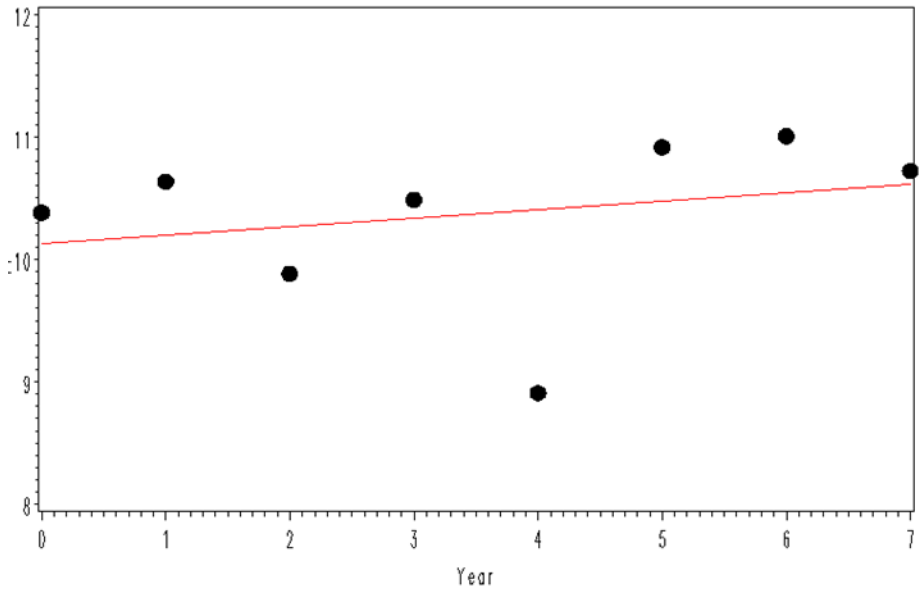

ression Equation:
5 yr = 10.12986 + 0.068467*year index

Figure 11.18 PM2.5 Annual mean OLS trend, El Paso UTEP C12, years since 2000

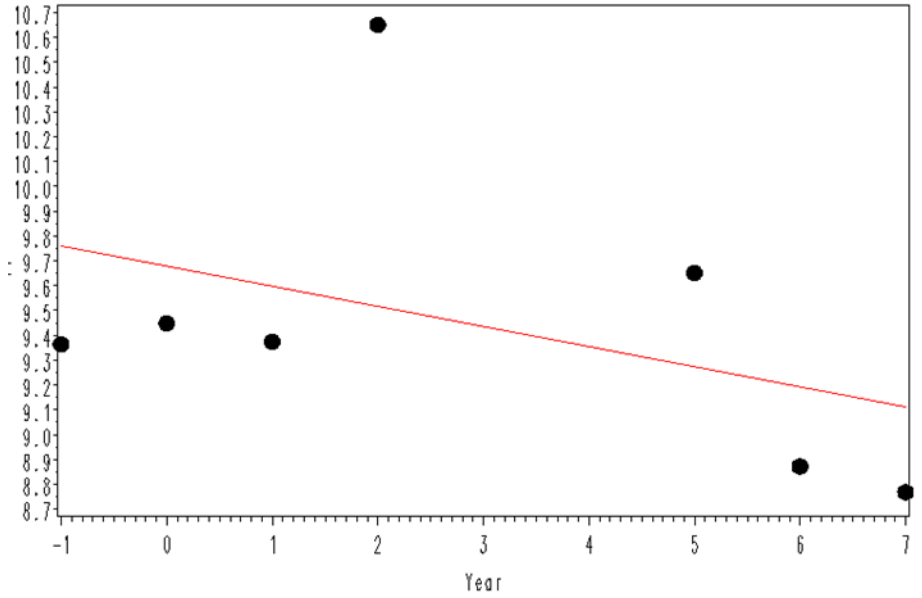

ression Equation:
5 yr = 9.67874 - 0.080871*year index

Figure 11.19 PM2.5 Annual mean OLS trend, Big Bend C67, years since 2000

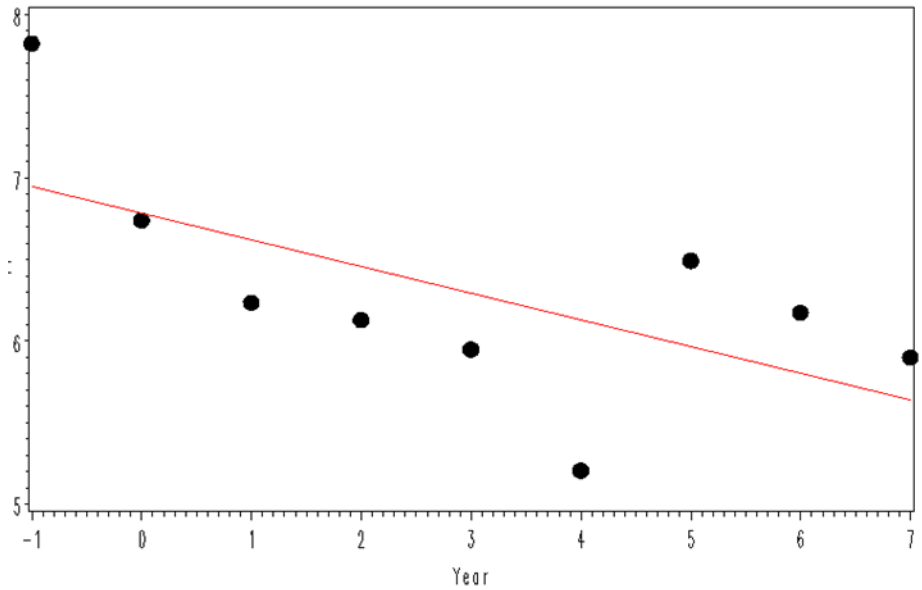

ression Equation:
25 yr = 6.784936 - 0.163333*year index

Figure 11.20 PM2.5 Annual mean OLS trend, El Paso Chamizal C41, years since 2000

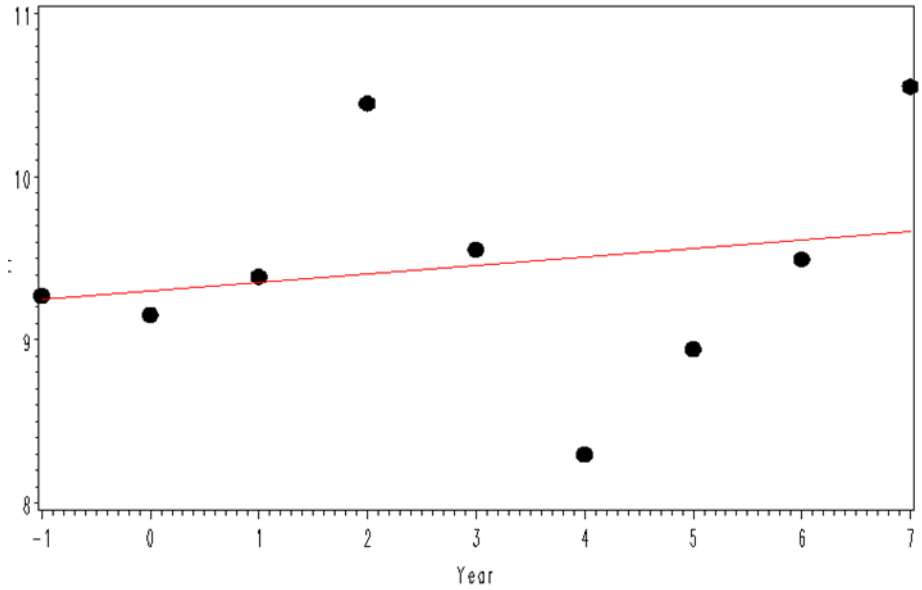

ression Equation:
25 yr = 9.301019 + 0.051729*year index

Figure 11.21 PM2.5 Annual mean OLS trend, Odessa Hays C47, years since 2000

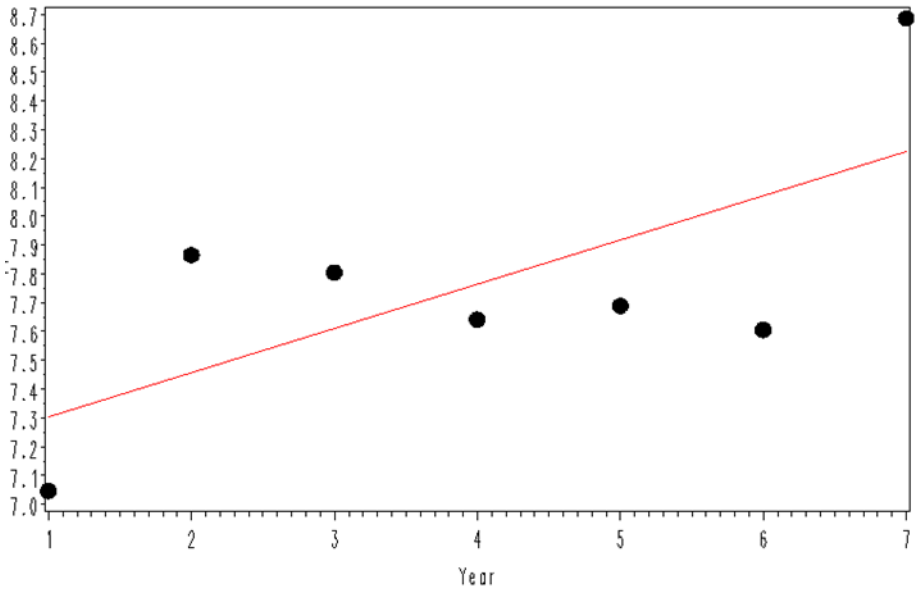

ression Equation:
25 yr = 7.15115 + 0.153057*year index

Figure 11.22 PM2.5 Annual mean OLS trend, El Paso Sun Metro C40, years since 2000

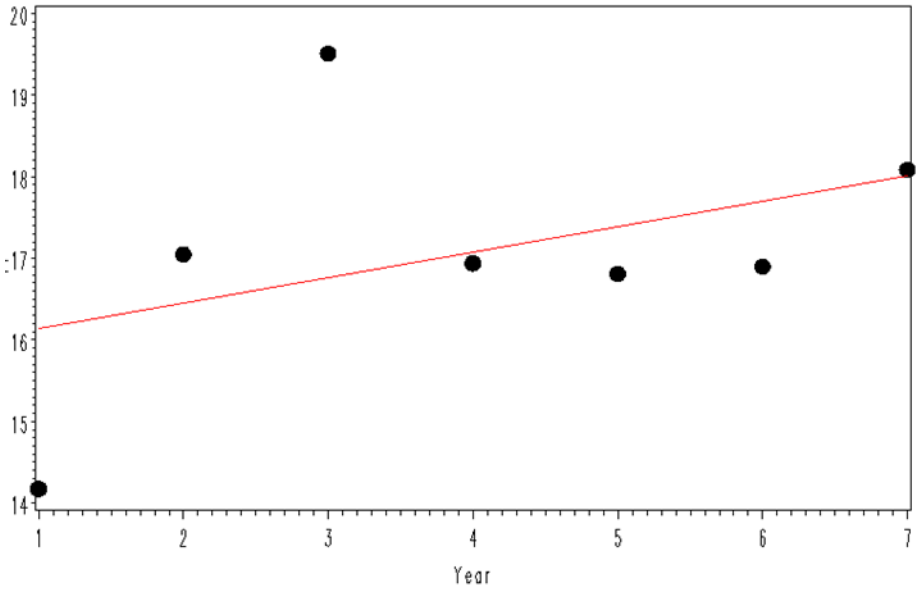

ression Equation:
25 yr = 15.82207 + 0.311518*year index

Summary

- Ozone coming down in Houston, DFW, inconclusive elsewhere
- SO2, CO generally coming down everywhere
- NOx in key industrial areas of Houston coming down
- VOCs coming down at 3 PAMS Type 2 sites (peak emissions locations) – weak trend at Deer Park!